FLUORESCENCE MICROSCOPY FOR THE IN SITU STUDY OF THE IBERIAN PYRITE BELT SUBSURFACE GEOMICROBIOLOGY

Cristina Escudero Parada

A dissertation submitted in partial fulfillment
of the requirements for the degree of
Doctor of Philosophy

Ph.D. Programme in Microbiology

Madrid, 2018

Agradecimientos

En primer lugar, como buena doctoranda y siguiendo el modelo de jerarquía establecido en los agradecimientos de una tesis, debo dar las gracias a mis directores. Tanto el Prof. Ricardo Amils como la Dra. Monike Oggerin apostaron por mí para realizar esta tesis, y agradezco muchísimo, aunque suene un poco "friki", la oportunidad que me han dado para estudiar un ambiente al cual muy pocas personas tienen acceso, me he sentido incluso VIP. Me gustaría agradecer su apoyo, tanto moral como profesional, así como el que me diesen alas para probar cosas "raras", como el Raman-FISH. Si se me considera investigadora "apta" tras esta tesis, es gracias a ellos.

En segundo lugar, a las personas que me han aguantado en el laboratorio: mis compañeros. En el fondo norte (CBM), no sé qué habría sido de mí sin Cati, Diego, Tania, Jose o Ting, que ya son más familia que amigos; sin Nuria Rodríguez, que es capaz de conseguir CUALQUIER cosa que necesites en tiempo record; o sin la gente que ha pasado por el lab a lo largo de estos años como Jose-CAB, Kary, Raquel, MariLu, Ana, Antonio o Delmo, con los que la risa ha estado a la orden del día. En el fondo sur (biológicas) debo destacar entre todos a Jose Luis y Mousta, por sus inestimables consejos, y mi Ana, que es una persona maravillosa. También debo un GRACIAS enorme a mis compañeros alemanes, sobre todo al ya Prof. Mario Vera y a Friede; a Adolfo del Campo, del ICV, que controla de Raman como nadie; y a los Profes. Carlos Sánchez y José Ramón Ares, del Departamento de Física de Materiales de la UAM, que han tenido la generosidad de ampliar mi pobre conocimiento de la pirita.

En tercer lugar, dar las gracias a la UAH (si, si, a la UAH). A mis compañeros de carrera, gracias a los cuales aprendí a jugar al mus (asignatura obligatoria), y al departamento de Microbiología, en especial a mis compañeros Ana, Topillo, Alba y Alberto, y mis profesores Enriqueta Arias y Manuel H. Cutuli (aunque sea del Atleti), que me contagiaron su pasión por la microbiología y son los principales responsables de que me decantara por el mundo "micro".

Y por último, a los más importantes, a los que me han aguantado CADA día: mi familia y amigos. A Charly, Miriam, Nuria y Laura, que son lo más grande que te puedes encontrar en el mundo; a mi primo Víctor, que ha estado ahí para vacilarme o abrazarme según mi cara al entrar en casa; a mi abuelo, mi gran referente en la vida; a mis padres, a los que se lo debo todo, ¡TODO!; y a ti Chikito, porque, gracias a ti, cada día es un gran día.

“Somewhere, something incredible is waiting to be known”

Carl Sagan

Table of contents

List of figures

List of tables

List of equations

Abbreviations

- AMD: Acid Mining Drainage
- ANNAMOX: ANaerobic AMMonium OXidation
- ANME: ANaerobic MEthanotrophic archaea
- AOM: Anaerobic Oxidation of Methane
- CARD-FISH: CAtalized Reporter Deposition-FISH
- CLSM: Confocal Laser Scanning Microscopy
- CRM: Confocal Raman Microscopy
- DAPI: 4 ',6-diamino-2-fenilindol
- DNRA: Dissimilatory Nitrate Reduction to Ammonia
- DOPE-FISH: Double labeling of Oligonucleotide Probes-FISH
- EDX: Energy Dispersive X-ray spectrometry
- EPS: Extracellular Polymeric Substances
- FISH: Fluorescence *In Situ* Hybridization
- FLBA: Fluorescence Lectin Binding Assay
- HRP: Horseradish Peroxidase
- IPB: Iberian Pyrite Belt
- IPBSL project: Iberian Pyrite Belt Subsurface Live project
- MARTE project: Mars Astrobiology Research and Technology Experiment
- mbs: meters below surface
- MIL-FISH: Multilabeled FISH
- NDFO: Nitrate-Dependent Fe Oxidation
- NGS: Next Generation Sequencing
- PAM: Prokaryotic Acidophile Microarray
- SEM: Scanning Electron Microscopy
- SLiMe: Subsurface lithoautotrophic microbial ecosystems
- SRB: Sulfate-Reducing Bacteria
- TSA: Tyramide Signal Amplification

1. Abstract

The subsurface is considered as an extreme environment characterized by a continuous darkness, anaerobiosis and oligotrophy where there is barely space for life. Despite the hostile conditions presented by the system, numerous studies have shown that life in the subsurface is diverse and is maintained by low energy anaerobic processes that, at first, are supported by the mineral geochemistry of the system. However, due to the difficulty of both sampling and analysis, our understanding of the functioning of these ecosystems is very limited.

The Iberian Pyrite Belt Subsurface Life (IPBSL) project and its predecessor, the Mars Astrobiology Research and Technology Experiment (MARTE) project, are drilling projects carried out for the characterization of the underground ecosystem of the Iberian Pyrite Belt (IPB), responsible for the peculiarities that the Río Tinto presents. Both projects have been developed by interdisciplinary teams and multiple complementary techniques have been applied to study the geomicrobiology of the IPB. Within the methodologies used for the study of the IPB subsurface microbiology, stands out Fluorescent *in situ* Hybridization (FISH), which allows not only to identify microorganisms but to analyze their distribution in the solid rock matrix.

Throughout this thesis, within the framework of the IPBSL project, the biodiversity of samples from drilling cores along borehole BH10 (613 meters below surface) has been characterized by means of several fluorescence microscopy techniques. To this end, new species specific probes have been designed, which have been used

together with probes already described for the study of the biodiversity distribution in the IPB subsurface through CAtalized Reporter Deposition fluorescence *in situ* hybridization (CARD-FISH). In addition, the presence of biofilms in native samples of the subsurface has been analyzed thanks to the use of fluorescent lectins and specific stains of DNA, lipids and proteins, as well as the optimization of the double labeling of oligonucleotide probes for fluorescence *in situ* hybridization (DOPE-FISH) protocol. On the other hand, the correlation between fluorescence microscopy and confocal Raman microscopy (CRM) allowed an *in situ* study of the microorganism-mineral interaction in these samples. Finally, the role of nitrate-reducing microorganisms, which are the most abundant in the IPB subsurface, has been analyzed.

Our results indicate that life in the IPB subsurface is diverse and is widely distributed along the BH10 column. The microorganisms that inhabit this environment live forming part of multi-species biofilms and are able, in principle, to survive thanks to metabolic interactions through which they can maximize the obtaining of energy and the biogeochemical cycles in the IPB subsurface can be maintained. In addition, mineralogy influences the distribution of life in the system, highlighting the nitrate-reducing microorganisms, which are candidates for the dissolution of metal sulfides in these anaerobic environment and, therefore, the high concentration of iron found in the Río Tinto basin.

2. Resumen

El subsuelo es considerado como un ambiente extremo caracterizado por una continua oscuridad, anaerobiosis y oligotrofia donde existe muy poco espacio para la vida. A pesar de las condiciones hostiles que presenta el sistema, numerosos estudios han mostrado que la vida en el subsuelo es diversa y se mantiene mediante procesos anaerobios de baja energía que, en un principio, se sustentan gracias a la geoquímica mineral del ecosistema. No obstante, debido a la dificultad tanto de la toma de muestras como de su análisis, nuestro entendimiento del funcionamiento de estos ecosistemas es muy limitado.

El proyecto Iberian Pyrite Belt Subsurface Life y su antecesor, el proyecto Mars Astrobiology Research and Technology Experiment, son proyectos de perforación llevados a cabo para la caracterización del ecosistema subterráneo de la Faja Pirítica Ibérica (FPI), responsable de las peculiaridades que presenta el Río Tinto. Ambos proyectos han sido desarrollados por equipos interdisciplinares y se han aplicado múltiples técnicas complementarias para el estudio tanto de las características geoquímicas del subsuelo de la FPI como de la vida que habita este sistema. Dentro de las metodologías utilizadas para el estudio de la microbiología del subsuelo de la FPI, destaca la Hibridación *in situ* Fluorescente, que permite analizar la distribución de la biodiversidad en sustratos sólidos minerales.

La aplicación de técnicas de fluorescencia en estudios del subsuelo, a pesar de su potencial, no ha sido utilizada debido a la dificultad que presentan los sustratos minerales, los cuales pueden emitir autofluorescencia. Para discernir las señales

provenientes de los fluoróforos empleados en este estudio, hemos recurrido al empleo de tinciones adicionales de DNA así como al uso del modo lambda disponible en microscopios de barrido laser confocal, el cual permite la caracterización del espectro de emisión de los fluoróforos a utilizar.

A lo largo de esta tesis, se ha caracterizado la biosfera presente a lo largo de la columna BH10, en el marco del proyecto IPBSL, mediante diversas técnicas de microscopía de fluorescencia, destacando técnicas de hibridación *in situ* fluorescente. Para ello, se han diseñado nuevas sondas para detectar miembros de los géneros *Tessaracoccus* y *Rhizobium*, las cuales se han empleado junto con sondas ya descritas para el estudio de la distribución de la biodiversidad en el subsuelo de la FPI mediante CARD-FISH. Los resultados obtenidos de este análisis indican que las bacterias son los microorganismos más distribuidos a lo largo de la columna BH10, destacando los phyla Proteobacteria, Actinobacteria y Firmicutes. El empleo de múltiples hibridaciones simultáneas ha permitido detectar la coexistencia de bacterias y arqueas así como la coexistencia de microorganismos relacionados con el ciclo del hierro y el azufre, los cuales podrían interconectar ambos ciclos a nivel de micronicho en el subsuelo de la FPI.

Además, se ha analizado la presencia de biopelículas íntegras en muestras nativas del subsuelo gracias al uso de lectinas fluorescentes y tinciones específicas de DNA, lípidos y proteínas, así como a la optimización del protocolo de DOPE-FISH. Estos análisis indican que la formación de biopelículas es un estilo de vida muy generalizado en ambientes subterráneos, a pesar del coste energético que supone tanto su producción como su mantenimiento.

Por otro lado, se han realizado cultivos, altamente representativos del subsuelo de la FPI, en los cuales se ha observado un aumento de la concentración de hierro en solución, lo que apoya la hipótesis del origen biológico del Río Tinto a partir del biorreactor subterráneo del sistema. Debido a que los microorganismos reductores de nitrato son muy abundantes en el pozo BH10, hemos analizado su posible papel en la disolución de sulfuros metálicos, minerales muy abundantes en el subsuelo de la FPI. Nuestros estudios muestran que microorganismos como *Acidovorax* o *Tessaracoccus* son capaces de oxidar hierro indirectamente a través de la producción de especies reactivas de nitrógeno, lo que apoya la teoría de que todos los microorganismos reductores de nitrato tienen la capacidad innata de generar hierro férrico. Dado que el Fe^{3+} es el principal oxidante de sulfuros metálicos como la pirita, presumiblemente todos los microrganismos reductores de nitrato tienen la capacidad de disolver estos minerales. Los estudios realizados a lo largo de este trabajo con *Acidovorax*, en los cuales se ha observado la disolución de pirita, apoyan esta hipótesis y supone la implicación de los microorganismos reductores de nitrato en la generación del alto contenido en hierro que presenta el Río Tinto.

Por otro lado, la correlación entre microscopía de fluorescencia y microscopía Raman confocal ha permitido estudiar *in situ* la interacción microorganismo-mineral. Estos estudios indican que la distribución de *Acidovorax* no solo está influenciada por la presencia de pirita a lo largo de la columna BH10, si no que *Acidovorax* produce cambios en el espectro Raman de la pirita, presumiblemente debido a la biooxidación del sulfuro metálico por parte del microorganismo.

Nuestros resultados indican que la vida en el subsuelo de la FPI es diversa y se encuentra muy distribuida a lo largo de la columna BH10. Los microorganismos

que habitan este ambiente viven formando parte de biopelículas multi-especie y son capaces, en principio, de sobrevivir gracias a interacciones metabólicas, gracias a las cuales los microorganismos podrían maximizar la obtención de energía y se mantendrían los ciclos biogeoquímicos en el subsuelo de la FPI. Además, la mineralogía influye en la distribución de la vida en el sistema, destacando los microorganismos reductores de nitrato, los cuales son candidatos para la disolución de sulfuros metálicos en el subsuelo y, por tanto, de la alta concentración de hierro que presenta el Río Tinto.

3. Introduction

3.1. The deep continental subsurface

3.1.1. The beginning of the deep biosphere study

Although almost two centuries ago Darwin predicted the possibility of life in the subsurface (Darwin, 1839), it was not until 1926, when the presence of sulfate-reducing bacteria (SRB) associated with an oil field was described (Bastin et al., 1926), that the first data about life at great depths were obtained. Shortly afterwards, in the 1930s, microbiological studies were initiated on marine sediments demonstrating the existence of life in the oceanic subsurface (ZoBell and Anderson, 1936; Zobell, 1938). However, advances in this field in subsequent years were limited due to the little credibility given by the scientific community (Lipman, 1931). In addition, after observing that the combined effect of low temperatures and high pressure inhibited the growth of microorganisms in the ocean depths, the possibility of finding active life in the deep subsurface was rejected (Jannasch et al., 1971).

The concept of life at great depths changed radically in 1979, when Corliss and coworkers revealed that, in deep oceanic hydrothermal vents, animal life existed sustained by the chemosynthesis produced by sulfur-oxidizing microorganisms, in an ecosystem completely independent of photosynthesis (Corliss et al., 1979).

Thanks to this discovery, the study of deep biosphere in the oceanic subsurface was promoted and included in the successful international programs: *Deep Sea Drilling Project* started in 1968, and its successors, the *Ocean Drilling Program* (ODP) in January 1985 and the *Integrated Ocean Drilling Program* (IODP) in 2004 (Oremland et al., 1982; Whelan et al., 1986; D Hondt et al., 2002).

However, the study of life in the continental subsurface was not seriously promoted until years after the discovery of the great biodiversity in the oceanic sediments and subsurface. In 1988, Ghiorse and Wilson denounced with their "*out of sight, out of mind?*" the indifference that had existed for the possible life existence in terrestrial subsurface environments (Ghiorse and Wilson, 1988). They pointed out that several studies had detected microorganisms in continental subterranean locations for decades, but they had been ignored and questioned due to the high risk of contamination that exists during the sampling (Lipman, 1931). For this reason, development and use of tracers were key in providing credibility to the study of life in subsurface environments, since they allow to control the main sources of microbiological and chemical contamination during sampling (Kieft, 2010).

Nevertheless, one of the first people to speculate about the existence of an ecosystem in the continental subsurface independent of photosynthesis was Thomas Gold. Gold not only considered the subsurface as a possible habitat for microorganisms, but also considered the possibility that this form of life could be found beyond our planet (Gold, 1992).

Finally, numerous studies showed unequivocally that, in fact, it exist a great microbial diversity in both oceanic and continental subsurface and, nowadays, we

can assure that life in these environments is ubiquitous and that it can represent a large percentage of earth's biomass.

3.1.2. Limitations of the continental subsurface study

Several research groups have carried out studies of the subsurface biosphere in different locations of the world and their methods of sampling and analysis of samples differ according to the geology of the studied area, the type of samples and the available technology (Table 1).

Nowadays, thanks to advances in drilling methodologies, samples can be extracted at great depths of the earth's crust, minimizing and quantifying their contamination by using tracers (Kieft, 2010). However, very few projects have performed devoted geomicrobiological drills from the surface to collect samples at different depths due to the difficulties, both mechanical and economic, that present (Zhang et al., 2005; Fernández-Remolar et al., 2008b; Gronstal et al., 2009; Itävaara et al., 2011b). Instead, many researchers have taken advantage of subterranean "windows", both natural and artificial, for deep sampling (Table 1). These include artesian wells (Stevens and McKinley, 1995; Chapelle et al., 2002), springs (Suzuki et al., 2013; Magnabosco et al., 2014; Probst et al., 2014a), underground locations for radioactive waste disposal (Pedersen, 1999), underground research facilities (Murakami et al., 2002; Momper et al., 2017a) or deep mines (Onstott et al., 2003; Sahl et al., 2008). In this last case, for example, instead of use a large surface drilling machinery, small equipment that can be deployed in limited spaces are

used and samples are taken from the walls of the tunnels that constitute the galleries of the mine.

Table 1. Examples of deep continental subsurface microbial studies and summary of their sampling and analytics methods. MPN=most probable number; PLFA= phospholipid fatty acid analysis; qPCR= quantitative PCR; DGGE= denaturing gradient gel electrophoresis; T-RFLP= terminal restriction fragment length polymorphism.

Location	Reference	Sampling depth	Sampling site	Samples	Count of microorganisms	Biodiversity analysis	Metabolic diversity analysis
Columbia River Flood Basalt (EEUU)	Stevens et al, 1993; Stevens and Mckiney, 1995; Fry et al., 1997	1270 mbs	Preexisting artesian well	Subsurface water	Acridine orange stain	Hybridization of RNA in nylon membranes, cloning	Enrichment cultures
Lidy Hot Springs (EEUU)	Chapelle et al., 2002	200mbs	Drilling and creation of artificial artesian well	Subsurface water	PCR-MPN, qPCR, FISH	Cloning	-
South Africa Gold Mines	Onstott et al., 2003	Up to 3000mbs	Subterranean mines	Fracture water and core rocks from small perforations made in the walls of the tunnels and chiselled rock from tunnel wall and floor.	PLFA	Cloning	Enrichment cultures
	Magnabosco et al., 2016			Fracture water from a drilled borehole in mine tunel	-	Metagenomic	Shotgun metagenomic
Dabie Sulu (China)	Zhang et al., 2005; Zhang et al., 2006	5000mbs	Drilling from surface	Rock cores and drilling water after use.	Acridine orange stain	Cloning and PLFA	Enrichment cultures
Chesapeake bay (EEUU)	Gronstal et al., 2009 Cockell et al, 2012	1766.3mbs	Drilling from surface	Rock cores	DAPI stain, MPN	Cloning, DGGE, FISH	Enrichment cultures
Outokumpu Deep Drilling Project (Finland)	Itävaara et al., 2011ab; Nyyssönen et al., 2013; Purkamo et al., 2013, 2015	2516mbs	Drilling from surface	Subsurface water	Baclight Bacterial Viability Kit, DAPI, qPCR (*dsrB* and *mcrA* genes)	DGGE, cloning, metagenomic and reverse transcription of RNA	Shotgun metagenomic, transcriptomic, qPCR and cloning of functional genes
Mt. Simon Sandstone (EEUU)	Dong et al., 2014a	up to 1800mbs	Drilling from surface	Subsurface water	FISH, TOPRO3 and Sybr Green I	Cloning, T-RFLP, metagenomic	Enrichment cultures, shotgun metagenomic
Regensburg (Germany)	Probst et al., 2013, 2014 a, b	?	Spring	Subsurface water and biofilm	qPCR, FISH	Microarrays, FISH, metagenomic, cloning	Metatranscriptomic
IPB (Spain)	Fernández-Remolar et al., 2008b; Puente-Sánchez et al., 2014b	164mbs	Drilling from surface	Rock cores	-	Microarray, cloning CARD-FISH	-
Mizunami Underground Research Laboratory (Japan)	Suzuki et al., 2014; Iwatsuki et al., 2015; Ino et al., 2016, 2017	300mbs	Subterranean laboratory	Subsurface water of preexisting and drilled artesian boreholes	Sybr green I	Pyrosequencing, clonación (16S, *dsrA* y *mcrA*)	Shotgun metagenomic
Samail Ophiolite (Oman)	Rempfert et al., 2017	up to 475mbs	Preexisting boreholes	Subsurface water	-	Metagenomic	-

It must be kept in mind, however, that the study of the subsurface biosphere through "artificial windows" is based on systems that have been previously modified by man (sometimes years before sampling) and, therefore, they are disturbed environments where microbial populations may not be representative of those existing in the subsurface. Perhaps a good example, among others (Moser et al., 2003), is represented by the work done by Sahl and collaborators (2008), who showed the great variation in the microbial composition of the water that flowed through wells drilled in the Henderson Mine after only two weeks of wells isolation, that is to say, after eliminating the aeration of the water (Figure 1).

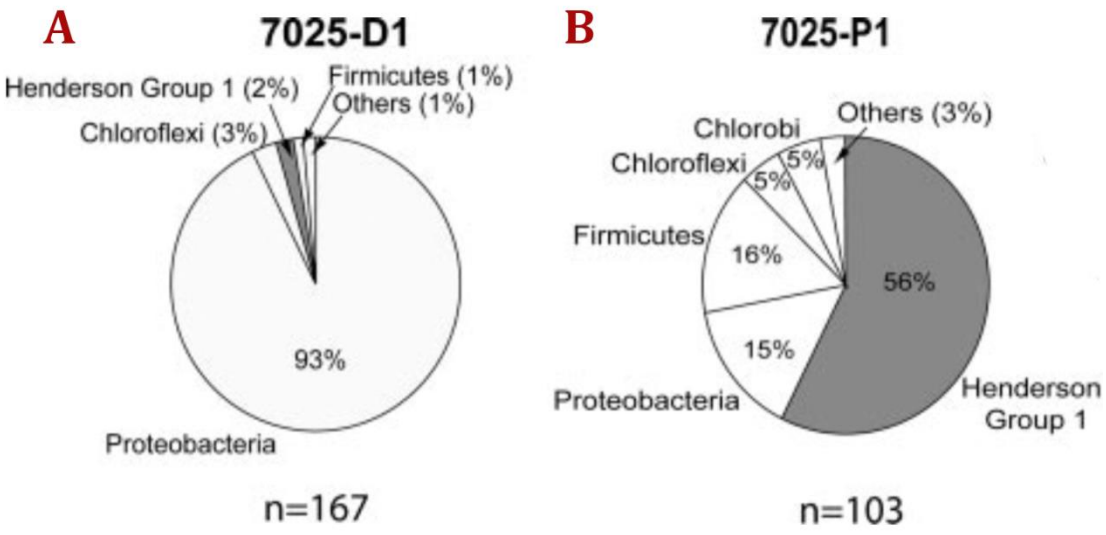

Figure 1. Subsurface water microbial composition in a deep mine before (A) and after two weeks (B) of packing a preexistent borehole in the wall. Figure taken from Sahl et al. (2008).

On the other hand, several studies confirmed that the microbial communities inhabiting the rocks show a different composition from those detected in the water (Lehman et al., 2004; Momper et al., 2017b). Hence, to obtain a true vision of

subsurface environment both types of samples should be analyzed in order to characterize the microorganisms associated to them. However, most of research groups have focused on the study of groundwater, since both sampling and analysis are easier than rocky samples (Table 1). Therefore, the data obtained from subsurface studies, up to now, corresponded mainly to planktonic life. If we consider that the number of microorganisms living attached to surfaces is up to three orders of magnitude higher than those microorganisms living unattached in subsurface environments (McMahon and Parnell, 2014), the great majority of microorganisms of the subsurface biosphere studied with this methodology is being underestimated.

3.1.3. Continental subsurface characteristics

According with Hoehler (2004), habitability of an underground environment on earth is defined by the presence of three basic requirements: energy availability, liquid water and clement temperature. Deep subsurface is considered an extreme environment characterized by darkness and anaerobiosis where the temperature and pressure increase with depth (Kieft, 2016). In these environments, geochemistry and geohydrology control nutrients and water availability and, therefore, the number and activity of microorganisms. Commonly, as buried organic matter is scarce or no longer profitable, the principal source of substrates is virtually limited to mineral dissolution or abiotic processes that release energy from minerals. Thus, the geological composition determinates the available electron donors and acceptors (Jones and Bennett, 2017; Rempfert et al., 2017), in

addition the main metabolisms operating in the deep subsurface are anaerobic and the energy obtained is low (Hoehler, 2004). On the other hand, growth of microorganisms is influenced by rock porosity and the presence of fractures or faults in the system. Fractured rocks or those with high porosity present an increase in water, nutrients flux and physical space, which promote microorganism colonization (Fredrickson et al., 1997a; Pedersen, 2000). In addition, geochemistry and geohydrology play an important role in the formation of heterogeneous and independent microniches, which would allow the coexistence of antagonist metabolisms such as sulfate reduction and methanogenesis (Jakobsen, 2007).

3.1.4. The deep biosphere

The number of "intraterrestrial" microorganisms reported varies markedly depending on the studied site. The values fluctuate between 10^2 and 10^7 cells/ml or gr (Pedersen, 2000; Zhang et al., 2005; Basso et al., 2009; Itävaara et al., 2011b) depending on the geology of the area, its physicochemical characteristics and the depth analyzed. Different studies have tried to calculate the percentage of biomass inhabiting subsurface environments, but their results differ greatly from each other (Whitman et al., 1998; Kallmeyer et al., 2012; McMahon and Parnell, 2014). However, if we consider the Earth's radius (c. 6300 km), the theoretical depth to which microorganisms could develop (5 - 10 km in most areas of the crust due to the temperature as limiting factor (Gold, 1992)) and the number of microorganisms detected in diverse studies, the percentage of prokaryotic life in subsurface has to be substantial.

It has been questioned that a large amount of prokaryotic biomass can live in the subsurface on the basis of the insufficient energy supply in several underground locations. To survive when energy is scarce or nonexistent many microorganisms are able to adopt a latent metabolic state, so it is believed that most microorganisms in the subsurface are in anabiosis (D'Hondt et al., 2002). Recent papers have shown that the number of active microorganisms increases when subsurface samples are incubated in enrichment media in the range of a few hours (Rajala et al., 2015; Rajala and Bomberg, 2017), which supports the hypothesis that microorganisms may not be metabolically active in this environments and that they are activated after an energy source is facilitated. However, according to Morita (1999), survival of DNA in a latent state is limited to 105 years at cold temperatures, but geological formations up to 250 million years old have been studied in which viable microorganisms have been recovered (Vreeland et al., 1998). Morita also offers a possible solution to this discrepancy by proposing that microorganisms could survive for long periods of time in starvation state if they are able to achieve a minimum of energy, called survival energy, to compensate the racemization of amino acids and the depurinization of DNA. This theory imply that subsurface microorganisms are metabolically active even though their growth rate is extremely low (Phelps et al., 1994), in such a way that we could even talk about geological times of duplication. In addition, several studies support the hypothesis of an active underground life, such as the discovery of biogeochemical signatures (Fernández-Remolar et al., 2008b), the measurements of microbial activity in different points of the subsurface (Pedersen, 2012; Wouters et al., 2013; Suzuki et al., 2014) or metatranscriptomic studies (Lau et al., 2016; Zinke et al., 2017).

The microbial populations that have been described in different subsurface locations vary widely, even at different depths of the same area, which may be due to the geological and physicochemical differences of the system studied as well as the origin of the water. This variability, together with the scarcity of samples studied and the different methodologies used, makes it difficult to correlate microbiological data and obtain general characteristics that are significant for this kind of environments. However, the presence of discrepancies between the different studied subsurface locations is an indicative of the heterogeneity of the system.

Recurrent data in all the studies carried out in continental subsurface indicate that when the depth increases, the number of microorganisms decreases (Moser et al., 2005; Itävaara et al., 2011a; Cockell et al., 2012; McMahon and Parnell, 2014) and there are less sequence similarity with the databases (Itävaara et al., 2011a), that is, it increases the number of unknown microorganisms, which is quite high. Even it has been found groups of sequences different of all known microbial groups, that could correspond to new divisions of both Bacteria (Gihring et al., 2006; Sahl et al., 2008) and Archaea (Takai et al., 2001; Probst and Moissl-Eichinger, 2015).

Although there are exceptions (Itävaara et al., 2011a), in most cases microbial diversity tends to decrease with increasing depth (Zhang et al., 2005; Lin et al., 2006b; Chivian et al., 2008). However, what kind of microorganisms is more numerous or diverse is not yet clear, since this variable depends directly on the geological characteristics of the area. Generally, diversity and abundance of bacteria is superior to archaea (Takai et al., 2001; Cockell et al., 2012; Ino et al., 2016; Lau et al., 2016; Rempfert et al., 2017). Within Bacteria, the most common

phyla reported in continental subsurface are Proteobacteria, Actinobacteria, Bacteroidetes and, above all, Firmicutes (Onstott et al., 2003; Moser et al., 2005; Zhang et al., 2005; Lin et al., 2006a; Dong et al., 2014a), which comprise, in some cases, up to 40% of the total population in the deepest layers (Basso et al., 2009). Nevertheless, it has been also detected others phyla less represented as Deinococcus-Thermus, Nitrospirae, Acidobacteria, Chloroflexi or the newly proposed phyla, which do not have cultivated members, as Candidate phylum Omnitrophica (OP3) or Candidate phylum Saccharibacteria (TM7) among others (Appendix 1).

One of the great surprises of the deep biosphere study has been the frequent appearance of sequences that belong to microorganisms that have the potential to carry out a photosynthetic metabolism. Members of the Cyanobacteria phylum have been found repeatedly in subsurface environments (Onstott et al., 2003; Zhang et al., 2005; Bomberg et al., 2014; Purkamo et al., 2015; Ino et al., 2017; Rempfert et al., 2017). These studies, however, do not offer a possible explanation about why this type of microorganisms has been detected hundreds of meters below the surface (mbs). Members of this phylum have the ability to carry out non-photosynthetic metabolism that allows them to grow in the absence of light (Mannan and Pakrasi, 1993; dos Santos et al., 2017) and, therefore, they may develop in the subsurface and be an active part of the system.

Finally, it should be noted that members of cultivated archaea found in the subsurface is very low (Takai et al., 2001). In general, members of the phylum Crenarchaeota are usually more abundant in the surficial layers of the subsurface, while members of the phylum Euryarchaeota are more common and diverse in

deeper layers (Takai et al., 2001; Zhang et al., 2006; Nyyssönen et al., 2014). Special attention should be given to the orders Methanobacteriales, Methanomicrobiales and Methanosarcinales, which are the cultivated archaea detected more often in the continental subsurface (Moser et al., 2005; Probst et al., 2014a; Purkamo et al., 2015; Rempfert et al., 2017).

In addition, not only microbial species have been detected in the subsurface. Several studies have shown the presence of viruses in subterranean environments (Kyle et al., 2008; Eydal et al., 2009; Lau et al., 2014; Nyyssönen et al., 2014), which could be involved in the horizontal transfer of genes between microbial populations of the subsurface (Labonté et al., 2015). However, perhaps one of the most surprising findings, due to the anaerobiosis of the system, has been the occasional detection of eukaryotic organisms in subsurface environments. Some studies have revealed the presence of fungal communities (Pedersen, 1997; Purkamo et al., 2013; Sohlberg et al., 2015) and even new species of nematodes (Borgonie et al., 2011). While in the latter case the survival of the nematodes could be explained by the presence of a minimum of oxygen in the water, there are authors who consider the possibility that the subterranean fungal communities can thrive in anaerobic conditions through collaboration between species (Sohlberg et al., 2015) or the existence of facultative anaerobic metabolism in these organisms (Kurakov et al., 2008). Even so, still few studies have paid attention to the non-prokaryotic communities and their role in the subsurface.

3.1.5. Energy sources and metabolism

Microorganisms are the only living beings capable of using almost any type of available energy. As previously mentioned, initially the mineralogy should control the availability of nutrients and the source of energy and, therefore, the operating metabolism at a given location and depth. In the subsurface, oxygen is rapidly consumed and anaerobic metabolisms, both autotrophic and heterotrophic, dominate in underground environments.

3.1.5.1. Primary production

One of the most controversial topics in the study of subsurface environments is whether the available metabolic energy sources are endogenous or, on the contrary, are partly dependent on products photosynthetically generated in the surface. The most purist authors affirm that only those microbial communities capable of developing independently of sunlight can be considered part of the subsurface biosphere (Orcutt et al., 2011; Momper et al., 2017b), that is, if they are part of lithoautotrophic microbial ecosystems. These ecosystems that operate in the absence of any influence of photosynthesis are called SLiMEs (Subsurface Lithoautrophic Microbial Ecosystem), name created by Stevens and Mckinley in 1995. As described by Nealson et al. (2005), a true SLIME system must be powered by the geosphere and both electron donors and acceptors should be renewed by geological processes continuously and, therefore, the microorganisms that form the basis of the ecosystem must be quimiolitoautotrophs. However, according to Hoehler (2004), to sustain life in underground environments, the mineral matrix

must not only store enough energy, but also have the potential to transfer it in a biologically accessible form.

Different studies have shown the capacity of microorganisms to use minerals as external electron donors or acceptors (Shock, 2009; El-Naggar et al., 2010) or to dissolve minerals such as biotite (Shelobolina et al., 2012), pyrite (Vera et al., 2013), chalcopyrite (Edwards et al., 2003) or feldspar (Rogers et al., 1998) among others (Dong et al., 2014a), releasing compounds that can be used as substrate and contribute to the production of biomass. However, in general, microorganisms need to produce extracellular agents to dissolve minerals, which imply an increase in the necessary energy to survive in an environment that is considered oligotrophic. Therefore, candidate environments to be considered SLiME are those in which energy is released and biologically accessible in an abiotic way.

One of the most abundant gases in the subsurface is hydrogen, which can be generated abiotically in many different ways (Apps and van de Kamp, 1993). H_2 is one of the most used molecules by chemolithoautotrophic microorganisms and is currently considered the main source of primary energy in environments considered SLIME. Both Stevens and McKinley (1995) and Pedersen (1997) suggested a similar model in which H_2 was the main driver of the underground biosphere in the Columbia River Basalt Group and the Äspö area respectively (Figure 2). According to this model, autotrophic methanogens and homoacetogenic microorganisms would conform the basis of the trophic chain through the consumption of H_2 and CO_2. Their metabolic products, as well as the biomass obtained by these communities, could serve as energy source for anaerobic heterotrophs and fermenters, closing the carbon cycle.

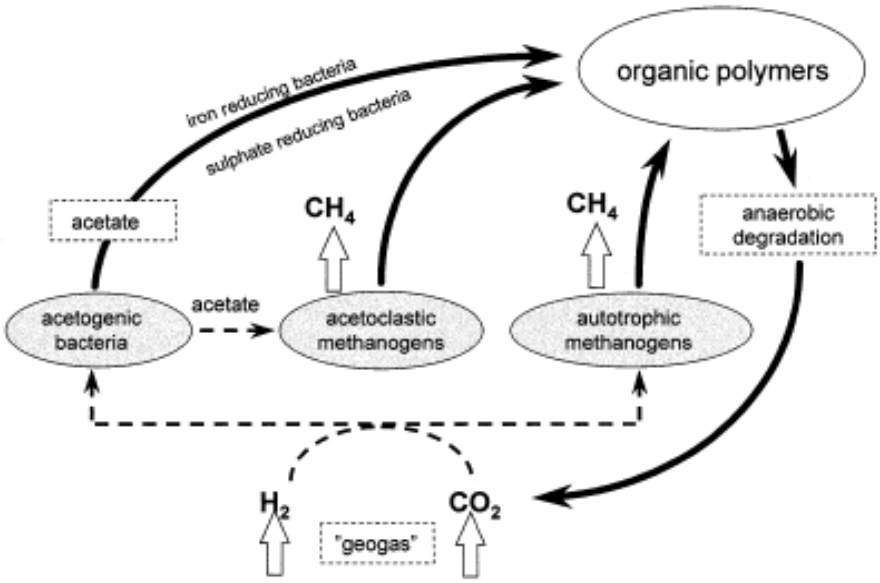

Figure 2. Proposed model in which hydrogen is the principal energy source for primary production in SLiMe environments. Figure taken from Pedersen (1997)

Several research groups defend the possibility that H_2 is the main source of energy for primary producers and, until now, it is the most accepted model that explains the survival of a subsurface biosphere independent to the surface (Chapelle et al., 2002; Nealson et al., 2005; Brazelton et al., 2012; Lau et al., 2016). Data obtained from several underground ecosystems reported the presence of H_2, CO_2 and CH_4, at least in micromolar concentrations, together with the presence, and sometimes dominance, of microorganisms whose metabolism is based on the oxidation of H_2 (Pedersen, 2000; Moser et al., 2005; Basso et al., 2009; Itävaara et al., 2011a), which support this hypothesis.

However, not all authors share the view that H_2 can be a significant source of abiotic energy and argue that underground life may be, at least in part, dependent on the flow of organic carbon and energy from the surface, that is to say on photosynthetic processes, for various reasons. One of them is that not all the

sources of energy available in the subsurface are inorganic compounds. The best examples are petroleum deposits or sedimentary rocks, where the presence of organic matter is indisputable (Fredrickson and Balkwill, 2006). On the other hand, subsurface is not a completely isolated system since the percolation of water through pores and fractures from the surface may contain small amounts of organic matter that can contribute in feeding the system. In addition, heterotrophy is a metabolism very represented in the subsurface and heterotrophic microbial populations are more diverse and, on occasions, more numerous than lithoautotrophic ones in these environments (Breuker et al., 2011; Purkamo et al., 2015). In this hypothetical case, the fermenting and heterotrophic microorganisms would be the primary producers of the system.

The reality is that, up to day, the existence of a truly SLiME community has not yet been unequivocally demonstrated in the continental subsurface.

3.1.5.2. Alternative sources of reducing power

In subsurface environments, other lithotrophic metabolisms have been detected that does not require H_2 or reduced organic compounds as an energy source. Among these are the oxidation of reduced sulfur compounds (Amend and Teske, 2005; Gihring et al., 2006; Lau et al., 2016), iron (Sahl et al., 2008; Swanner et al., 2011; Shelobolina et al., 2012) and nitrogen (Swanner and Templeton, 2011; Nyyssönen et al., 2014; Lau et al., 2016). In addition, other less common metabolisms have also been detected such as the oxidation of arsenic (Zhang et al., 2005; Sahl et al., 2008), manganese (Moser et al., 2005) or methane (Nyyssönen et al., 2012; Lau et al., 2016; Ino et al., 2017).

It is unknown if these alternative sources of reducing power could be sufficient to sustain an underground chemolithotropic ecosystem where H_2 levels are insufficient, but according to thermodynamic models these reactions could provide enough energy to maintain it (Amend et al., 2003; Osburn et al., 2014).

3.2. Iberian Pyrite Belt subsurface

3.2.1. Río Tinto

Río Tinto (Huelva, Southwestern of Spain), almost 100 km long, is one of the most extreme environments of the Iberian Peninsula in terms of its very low pH and high concentration of heavy metals in solution (López-Archilla et al., 2001; González-Toril et al., 2003). The characteristic red color of the river is given by ferric iron, which concentration is at least one or two orders of magnitude higher than the acidic rivers of the area, Odiel and Agrio (Amils et al., 2002), and which strong buffer capacity maintain an acidic constant pH of 2.3 along the river and the year (Figure 3, red arrows). Thus, at high pH values, dissolved Fe^{3+} precipitates as ferric hydroxide ($Fe(OH)_3$) and release protons while, at low pH, Fe^{3+} from ferric hydroxide precipitates dissolves, consuming protons and compensating the acidity (Amils et al., 2002).

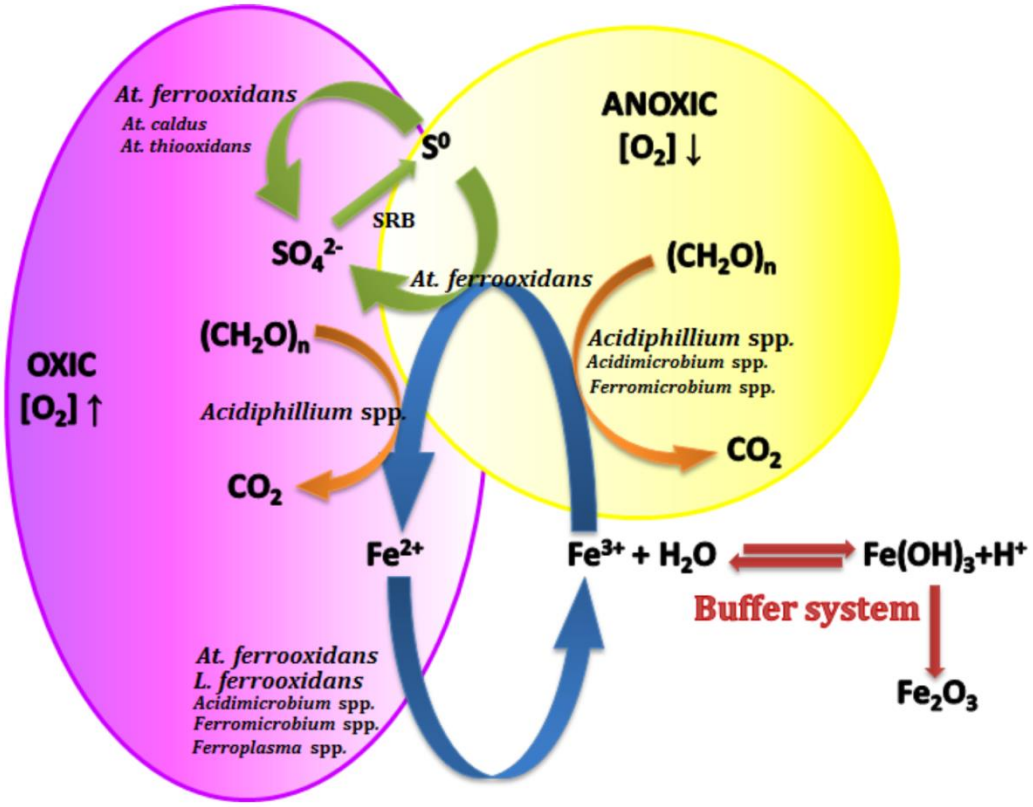

Figure 3. Geomicrobiological model coupling iron (blue arrows) and sulfur (green arrows) cycles that operate in Río Tinto water column. Ferric iron buffering system is indicated (red arrows). The type size of the microorganisms designation is proportional to their respective cell number in the river. Figure modified from Amils et al. (2011).

Fe^{3+} is produced essentially by the iron-oxidizing microorganisms *Acidithiobacillus ferrooxidans* and *Leptospirillum ferrooxidans*, that are very active and numerous in the aerobic part of the river (Figure 3). The resulting Fe^{3+} of their metabolism come in contact with the abundant metallic sulfides (MS) of the Iberian Pyrite Belt oxidizing the sulfide moiety of the mineral. Depending on the solubility of the mineral in acidic conditions, acid insoluble metal sulfides as pyrite (FeS_2) will be oxidized by the thiosulfate pathway (Rohwerder et al., 2003; Vera et al., 2013):

$$FeS_2 + 6Fe^{3+} + 3H_2O \rightarrow S_2O_3^{2-} + 7Fe^{2+} + 6H^+ \quad (1)$$

$$S_2O_3^{2-} + 8Fe^{3+} + 5H_2O \rightarrow 2SO_4^{2-} + 8\,Fe^{2+} + 10H^+ \quad (2)$$

or the polysulfide pathway if the massive sulfides are acid soluble (Rohwerder et al., 2003; Vera et al., 2013):

$$MS + Fe^{3+} + H^+ \rightarrow M^{2+} + 0.5\,H_sS_n + Fe^{2+} \ (n \geq 2) \quad (3)$$

$$0.5\,H_sS_n + Fe^{3+} \rightarrow 0.125\,S_8 + Fe^{2+} + H^+ \quad (4)$$

$$0.125\,S_8 + 1.5O_2 + H_2O \rightarrow SO_4^{2-} + 2H^+ \quad (5)$$

As a result, protons, sulfur compounds and ferrous iron, which are re-oxidized again by microorganisms, are released (Equation 1 and Equation 3). Protons can contribute to the oxidation of acid soluble metals sulfides (Equation 3) and sulfur compound can be oxidized chemically (Equation 2 and Equation 4) or biologically (Equation 5) by sulfur-oxidizing microorganisms to sulfuric acid, acidifying the system.

At. ferrooxidans and *L. ferrooxidans* are the principal drivers of metallic sulfides dissolution in the aerobic part of the river by the great increase of the oxidizing agent, the Fe^{3+}, which generation by microbial activity is up to five orders of magnitude higher than the Fe^{2+} oxidation carried out chemically by oxygen (Nordstrom and Alpers, 1999). These microorganisms along with the iron-reducing microorganism *Acidiphillium* spp. represent more than 80% of the prokaryotic diversity in the water column of Río Tinto (López-Archilla et al., 2001; González-Toril et al., 2003), maintaining an operative iron cycle (Figure 3), which

together with sulfur-oxidizing microorganisms such as *Acidithiobacillus thiooxidans and Acidithiobacillus caldus*, are essential to preserve Río Tinto's peculiarities (Amils et al., 2002). Other microorganisms involved in iron cycle have been detected in the Tinto basin such as members of the *Ferroplasma, Ferrimicrobium* and *Acidimicrobium* genera, but their low number suggests that they play a minor role in this cycle (González-Toril et al., 2003).

Río Tinto presents another singularity known as the eukaryotic paradox. Although the river presents a low prokaryotic diversity, which is consistent with what is expected from an extreme environment, it contains an unexpected great eukaryotic diversity (López-Archilla et al., 2001; Amaral-Zettler et al., 2002; Aguilera et al., 2006). Eukaryotic algae comprised 65% of the river biomass and support, together with chemolitotrophic microorganisms, the primary production of the system (López-Archilla et al., 2001). In addition to photosynthetic species, heterotrophic protists and decomposing fungi are also widely distributed along the river, showing the last ones a high abundance and diversity (Amaral-Zettler et al., 2002; López-Archilla et al., 2004). Most of these microorganisms form complex photosynthetic biofilms floating as macroscopic filaments or attached to the surface of rocks (Aguilera et al., 2007; García-Moyano et al., 2007; Souza-Egipsy et al., 2011).

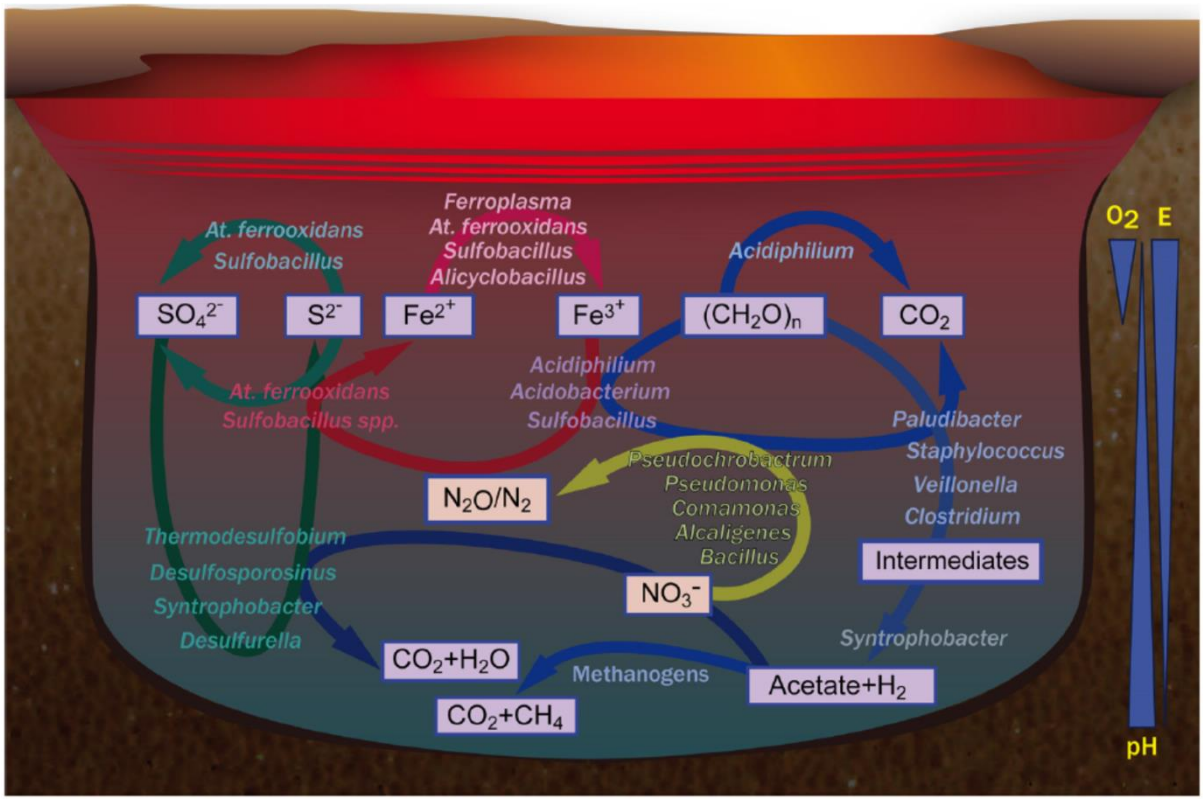

Figure 4. Geomicrobiological model of Río Tinto's sediments. Iron (red arrows), carbon (blue arrows), nitrogen (yellow arrows) and sulfur (green arrows) cycles are indicated. Figure taken from Sánchez-Andrea et al. (2011)

Regarding the sediments, of note is the detection of higher cell number and diversity, both microbial and metabolic, than the detected in Río Tinto's water column. Diverse studies have shown the presence of members of Proteobacteria, Bacteroidetes, Firmicutes, Actinobacteria, and Acidobacteria phyla as well as members of the archaeal Thermoplasmatales, Methanosarcinales and Methanobacteriales groups (Sánchez-Andrea et al., 2011; Sanz et al., 2011; García-Moyano et al., 2012). This biodiversity follow a differential pattern of distribution in the anoxic sediments of Río Tinto based on the microbial metabolism, and the redox potential and acidity parameters (Figure 4), which vary with depth. In the

upper layers, where the pH is low and the redox potential is positive, iron oxidation and reduction dominates. In the subsequent layers, where the conditions are less oxidizing, the predominant metabolism is fermentation, which is replaced by sulfate reduction or methanogenesis in the deepest layers, where the conditions became strongly reducing (Sánchez-Andrea et al., 2011; Sanz et al., 2011). Besides, nitrate or nitrite reducers have been also detected in the Río Tinto sediments (Sánchez-Andrea et al., 2011). Thus, contrary to the water column where the iron cycle dominates the whole system, in the sediments the carbon, nitrogen and, above all, sulfur cycles play a major role.

3.2.2. The origin of Río Tinto

Río Tinto springs up in Peña de Hierro, in the core of the IPB and flows into the Atlantic Ocean (Figure 5). The IPB is a 250 km long and 25– 70 km wide geological entity located in the South-Portuguese Zone of the Iberian Peninsula. With more than 80 known deposits, it contains over 1600 Mt of sulfide ore and is considered as one of the world's largest reserves of metallic sulfides (Tornos, 2006). The geology of the area is mainly composed of pyrite and chalcopyrite ($CuFeS_2$) and, to a lesser extent, other sulfides such as sphalerite (ZnS) and galena (PbS) (Tornos, 2006).

The geological characteristics of the IPB led to the exploitation of these giant sulfide deposits for 5000 years (Davis Jr et al., 2000; Leblanc et al., 2000) so, traditionally, it has been considered that the peculiarities of Rio Tinto waters are the product of the acid mining drainage (AMD) generated by the intensive mining

activity. Consequently, Río Tinto has been considered a polluted ecosystem that had to be remediated (Van Geen et al., 1997; Davis Jr et al., 2000; Nieto et al., 2007).

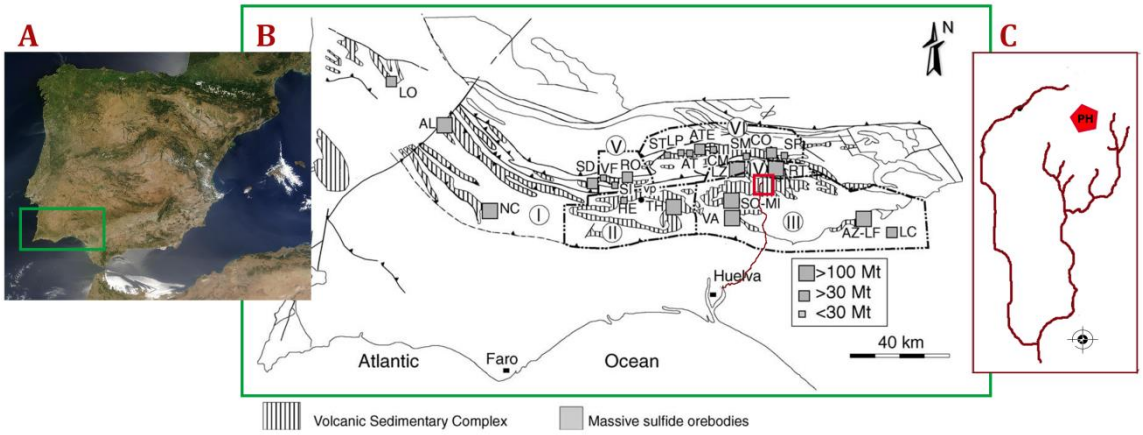

Figure 5. Location of the Iberian Pyrite Belt (A), the major massive sulfide deposits (B, gray squares) and Río Tinto's origin (red square). (C) Location of Peña de Hierro (PH) (red polygon) near Nerva town (black star). Figure modified from (Tornos, 2006).

However, studies performed by Fernandez-Remolar and co-workers (2003; 2005) showed that sedimentary iron-rich terraces located in the Río Tinto area, with different chronological ages, have the same mineralogical composition and evolution. In others words, old terraces, dated up to the end of Miocene, were originated under similar conditions to those observable today, with high concentration of ferric iron and low pH. Consequently, the acidic river system originated about seven million years ago (Essalhi et al., 2011), three orders of magnitude before than the oldest known mining activity. Today Río Tinto is considered one of the largest natural acidic ecosystems in the world (Fernández-Remolar et al., 2005) and, since December 2004, a Protected Natural Landscape by the Junta de Andalucía (BOJA, 2005).

Actually, Río Tinto is feeded by artesian springs located along faults at the southern end of Peña de Hierro, which waters already contains high ionic loads and low pH (Fernández-Remolar et al., 2005). In 2003, it was initiated the Mars Astrobiology Research and Technology Experiment project, a subsurface exploration of Peña de Hierro area by drilling boreholes that allowed to have access to the underground biosphere that interact with the mineral ores of the Iberian Pyrite Belt (Stoker et al., 2004). The fact of finding different microbial populations, including iron and sulfur cycle related microorganisms operating in this environment and their correlation with the geological and chemical features of the IPB led to the conclusion that Río Tinto's peculiarities may be the direct consequence of the existence of a subterranean bioreactor (Fernández-Remolar et al., 2008a; Fernández-Remolar et al., 2008b; Puente-Sánchez et al., 2014b). According with the authors, subsurface microorganisms would dissolve subsurface pyrite deposits through the generation of ferric iron by anaerobic iron-oxidizing metabolisms. This bioreactor, together with the bioleaching activity of the surface microorganisms described above, would originate the Río Tinto's characteristics.

3.2.3. Iberian Pyrite Belt Subsurface Life drilling project

IPBSL is a devoted interdisciplinary drilling project initiated for a deeper characterization of the IPB subsurface bioreactor in which geologist, chemist, engineers and microbiologists has been involved. Two boreholes, named BH10 and BH11, were drilled after a geophysical study determined the best locations to intersect the interaction of groundwater and the metal sulfidic ore bodies in Peña

de Hierro area (Gómez-Ortiz et al., 2014). Aseptic rock core samples were obtained from different depths (Amils et al., 2013), and different techniques have been applied to characterize the physicochemical, geological and microbiological features of the IPB subsurface.

3.2.3.1. Drilling and geological and physicochemical characterization of borehole BH10

The BH10 borehole (N37º 43' 45.74'', W6º 33' 22.37'') reached 613 mbs depth. It was drilled by rotary diamond-bit drilling producing 60 mm diameter cores. Tap water was used as drilling fluid to avoid overheating of the machinery and return cutting to the surface. Once in the surface, cores were inspected for sing of alteration. Selected cores where stored in bags under a nitrogen atmosphere and transferred to a nearby laboratory. Cores were placed in a sterile anaerobic chamber and subsamples were taken from inside the cores by using a drill with sterile bits. Temperature of the bits was controlled by an infra-red thermometer to not exceed 45°C.

Geological and chemical features of BH10 column was characterized by petrographic, mineralogical (X Ray Diffraction), elemental (Inductively Coupled Plasma Mass Spectrometry, Total reflection X-Ray Fluorescence) analysis of the rock samples and the mineral soluble composition by ion and gas chromatography (Figure 6).

As it is shown in Figure 6, BH10 intersects the Volcano-Sedimentary Complex (VSC) and the Culm Group (CG) (Gómez-Ortiz et al., 2014), two of the three geological sequences that summarize the stratigraphy of the IPB (Tornos, 2006).

Detailed information about the mineral composition and petrochemical analysis of each depth can be found in the Appendix 2. At the time of drilling, the water table was identified at 90mbs.

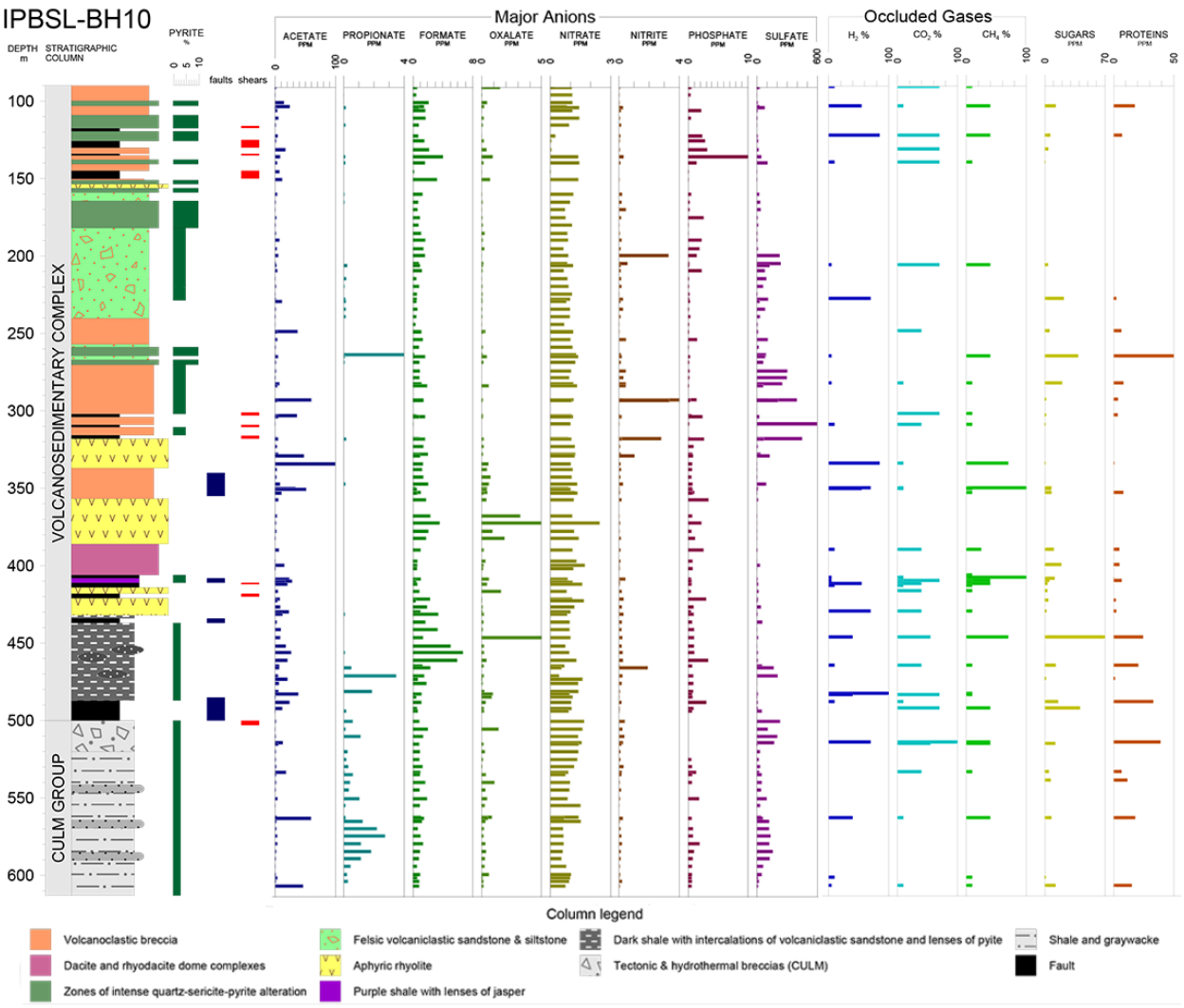

Figure 6. Stratigraphy and chemical composition of BH10 borehole. Taken from the IPBSL database.

As discussed above, contamination is one of the principal problems in subsurface sampling. In the IPBSL project, bromide added to the drilling fluid was used as

contamination tracer. The subsequent measurement of bromide concentration in the different samples indicated that drilling fluid was not in contact with them except for sample from 487.2mbs (data not shown). At this depth, the borehole intersected a fault and, as a result, drilling fluid could have access to the inner part of the core. However, most of the samples were considered no contaminated (absence or Br concentration much lower than the drilling fluid) and, therefore, representative of the native IPB subsurface.

Regarding the principal anions detected along the column, organic acids as acetate, oxalate, propionate and formate were present, being the last one the most abundant and distributed. These compounds could act as electron donors in heterotrophic metabolisms as fermentation or anaerobic respiration. In fact, putative electron acceptors for anaerobic respiration as nitrate and sulfate were also found. It is interesting to note the high concentration of nitrate detected at all depths analyzed. On the other side, litoautotrophic metabolisms could be maintained in the IPB subsurface by using hydrogen as electron donor and carbon dioxide as carbon source. In fact, at 400-550mbs there was a significant increase of these gasses together with methane, thus methanogenesis should be expected at these depths. Finally, sugars and proteins, which may be related with extant microbial presence, were irregularly detected along the column.

3.2.3.2. Microbial and metabolic diversity of BH10

Because all methodologies have limitations, to study the microbial diversity inhabiting the BH10 column, a multi-methodology approach was applied. Cultivation-independent methods such as immuno-detection with LDChip300 (Life

Detector Chip) (Blanco et al., 2012), oligonucleotide microarray analysis with the Prokaryotic Acidophile Microarray (PAM) (Garrido et al., 2008), cloning and Next Generation Sequencing (NGS) techniques were used for this purpose.

These analyses indicate that bacteria dominate the environment since few archaea sequences have been detected (Puente-Sánchez, 2016). Proteobacteria and Actinobacteria were the most abundant and diverse phyla identified.

Regarding to microbial metabolisms operating in the IPB subsurface, shotgun metagenomic and enrichment cultures to detect methanogenesis, methanotrophy, acetogenesis, nitrate reduction, sulfate reduction and iron oxidation and reduction were used. All metabolisms were detected in the IPB subsurface at different depths. In addition, metagenomic analyses were carried out to study the microbial diversity enriched in some selected cultures. On the other hand, several IPB subsurface microorganisms have been isolated from different enrichment cultures.

More information and the discussion about the microbial and metabolic diversity detected in the BH10 column will be provided along this work.

3.3. Microscopy techniques

As described, different sequencing techniques have been applied to determine the biodiversity of the IPB. However, the extraction of DNA of rock samples is not easy (Barton et al., 2006; Direito et al., 2012) and these techniques require large volume of sample to get a minimal DNA concentration for its study (Martino et al., 2012). Consequently, in spite of the high amount of bulk information that DNA methodologies offer, rock samples with low number of microorganisms cannot be

analyzed by these techniques. In the IPBSL project, only 12 of the 39 native rock samples available could be studied by NGS (Puente-Sánchez, 2016). In addition, the results obtained from sequencing techniques correspond to large areas of the subsurface and they don't provide a complete picture of the system, which is characterized by the presence of microniches that could be considered as isolated environments if the porosity of the rock is low.

To locate the microorganisms in the rock samples, microscopy techniques such as scanning electron microscopy (SEM) were also used. SEM, not only offer a great magnification and resolution of the microorganisms in their natural substrate but also the possibility of analyze the elemental composition of the mineral associated by energy dispersive X-ray spectrometry (EDX) (Goldstein et al., 2017). Actually, the study of the relation between microorganisms and minerals may be the key to understand the microbial distribution, mineral dissolution and biomineralization in the deep biosphere (Jones and Bennett, 2014). However, despite the presence of microorganisms hosted in the IPB rock samples have been detected by SEM, the identification of these microorganisms is beyond this technique.

3.3.1. Fluorescence *in situ* Hybridization

Fluorescence *in situ* hybridization (FISH) techniques are based on the use of oligonucleotide probes that match with rRNA sequences, mainly located in 16S rRNA, within the intact cell. The probes are usually labeled with fluorophores at the 5'-end, hence those microorganisms that have in their rRNA the sequence complementary to the probe will hybridize and emit fluorescence, which can be

detected and observed by fluorescence microscopy (Moter and Göbel, 2000) (Figure 7A).

The use of FISH techniques offer great advantages for the study of environmental microbiology (Amann et al., 1995; Moter and Göbel, 2000). First, as the samples are fixed immediately after the sampling and FISH is not a destructive technique, we can study the microorganisms in their natural environment. Second, as fluorescence emission intensity is directly proportional to the number of ribosomes, the detected microorganisms are alive and active, or at least they must have a high number of 16S rRNA (Poulsen et al., 1993). Third, FISH allows the study of the biodiversity and its quantification, cultivable or not, by using probes with different and complementary specificity, from high taxonomic level such as domain, phylum or class to genus and specie level. Actually, authors have named FISH "phylogenetic stain" (Kubota, 2013). Fourth, FISH offers the possibility of analyze the spatial distribution of the microorganisms in the sample, which is especially important in heterogeneous environments such as the subsurface. And, finally, it allows studying the interactions between microorganisms by multiple hybridizations. In resume, as Moter and Göbel (2000) stated: "*FISH combines the precision of molecular genetics with the visual information from microscopy to permit visualization and identification of individual microbial cells within their natural microhabitat*".

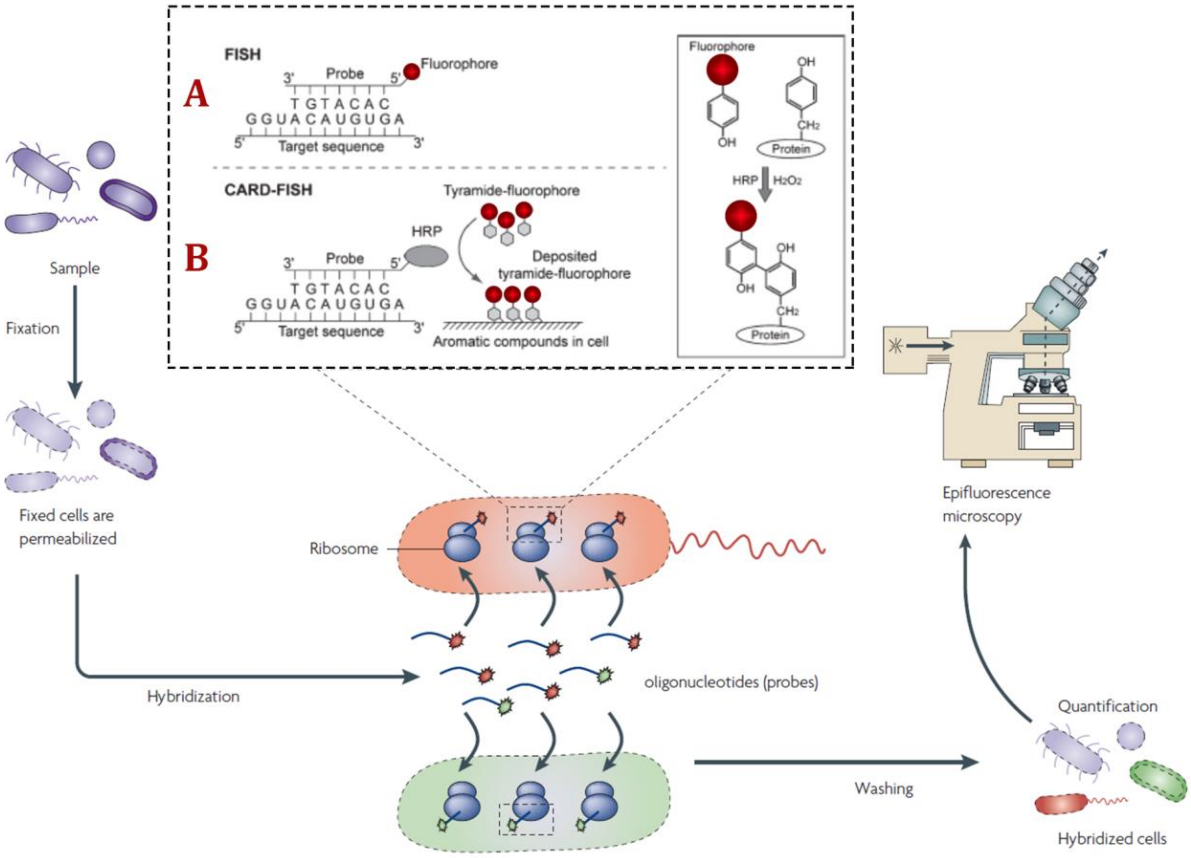

Figure 7. Principle of fluorescence in situ hybridization technique. In detail, main differences between FISH (A) and CARD-FISH (B). Figure modified from (Amann and Fuchs, 2008) and (Kubota, 2013).

3.3.1.1. Amplification of FISH signal

One of the principal problems that may arise when FISH is applied is the insufficient fluorescence signal intensity due to low rRNA content in slow-growing microorganisms (Poulsen et al., 1993), which may drive to false negative results. However, sensitivity of FISH can be increased by different methods. DOPE-FISH, with two fluorophores per molecule (Stoecker et al., 2010), or multilabeled oligonucleotides (MIL)-FISH (Schimak et al., 2015), with four fluorophores per molecule, have been described. Both amplification systems have been used with an increase in the intensity signal proportional to the number of fluorophores in the

probe. Another approach is the use of more than one probe to increase the number of fluorescent molecules per cell (Pernthaler et al., 2002), with which it can be detected even one single copy of the target sequence (Barrero-Canosa et al., 2017).

However, the most effective amplification system described so far is the called CARD-FISH or tyramide signal amplification (TSA) (Figure 7B), which results in an increase of more than 26 fold the signal intensity (Hoshino et al., 2008). In this case, the probe is labeled with horseradish peroxidase (HRP). Once the hybridization has been carried out, hydrogen peroxide and a high number of tyramide-conjugated fluorophore are added. The HRP, in the presence of hydrogen peroxide, converts the tyramide into a radical intermediate, which will react with aromatics compound as tyrosine and tryptophan located near the enzyme on a very short timescale. The result is the deposition of a great number of tyramine, and consequently of fluorophores, surrounding the HRP molecule, amplifying the fluorescence signal (Kubota, 2013).

3.3.1.2. Fluorescence hybridization techniques to study subsurface environments

Several studies have used fluorescence techniques to analyze subsurface environments. In fact, one of the most common methods applied in continental subsurface studies for enumeration of microorganisms is based on their direct count by DNA fluorescent staining and fluorescence microscopy (Table 1). However, the enumeration of microorganisms by fluorescence microscopy has been limited to subsurface water, which can be filtered and microorganisms concentrated in membrane filters (Stevens et al., 1993; Itävaara et al., 2011a; Ino et

al., 2017). The analysis of rocky samples by this method, due to the difficulties that present, has been avoided. Some minerals reflect the light at the same wavelength than the fluorophores and the background makes problematic the identification of true fluorescent signal. Instead, to count the microorganisms that inhabit the rocks, some research groups have detached the microorganisms of the solid substrate by sonication and filtration of the supernatant cell suspension, proceeding to the hybridization of the retained cells (Gronstal et al., 2009).

Regarding to FISH analysis, despite the great advantages that it offers, the number of studies that have applied this technique is much lower than those which applied general stains (Chapelle et al., 2002; Gronstal et al., 2009). The few research groups that used FISH techniques for the subsurface biosphere study only applied general probes to detect microorganisms at domain level. The use of general DNA stains or general probes as well as the exclusive analysis of fluid samples translates into a lack of information about the distribution of microorganisms in their natural environment in the subsurface: the solid substrate.

Nevertheless, the use of FISH techniques applied to subsurface environments should provide invaluable information not just about microbial diversity distribution, but about interactions and relationships between microorganisms using multiple hybridizations. Actually, thanks to FISH, a consortium between bacteria and archaea that mediate the anaerobic oxidation of methane (AOM) at more than 780m water depth in the sub-sea floor has been recently characterized (Jones and Bennett, 2017). In addition, the use of confocal laser scanning microscopy (CLSM) (Paddock, 1999) and the digital image analysis by image processing software result in a better resolution and interpretation of the

hybridized sample. The main advantage of CLSM is the restriction of the collected signal to a thin section trough a pinhole, which removes the out-of-focus fluorescence and improves the resolution of the image. The capacity of CLSM of take stacks of a specific field allows the three dimensional reconstruction of images, facilitating the visualization of the spatial distribution of the microorganisms.

3.3.2. Correlative microscopy

Microscopy based on fluorescence techniques has advanced in leaps and bounds in recent years, as reflected by the Nobel prize awarded to Eric Betzig, Stefan W. Hell and William E. Moerner in 2014 (Möckl et al., 2014). These researchers transgressed the optical limit of resolution of the traditional optical microscopes, allowing fluorescence to enter in the nanoworld. However, although fluorescence microscopy is one of the basic tools for the biological systems study, its utility in geological sciences is more limited.

As noted above, several studies have shown that the microbial diversity of a subterranean environment depends directly on the geological composition of the system (Jones and Bennett, 2014; Jones and Bennett, 2017; Rempfert et al., 2017). Therefore, the study of how the deep biosphere interacts with its environment, i.e. minerals, can be crucial to understand how the ecosystem works. The use of FISH techniques allows the visualization and identification of microorganisms in their natural environment, but the geological characterization of the sample is not possible through this type of microscopy. There are, however, other microscopy

techniques that allow the chemical analysis of the sample, such as the aforementioned SEM-EDX or the nanoscale secondary ion mass spectrometry (nanoSIMS) (Boxer et al., 2009), which are, on the contrary, limited in the identification of microorganisms. Therefore, the combined use of different types of microscopy could be of great interest for the *in situ* study of the subsurface microorganism-mineral interaction, since it could complement the information obtained by each of them.

Interest in correlative microscopy has grown in recent years. It stands out, for example, the correlation of light with electron microscopy (CLEM), which can combine the advantages of fluorescence microscopy and SEM-EDX. However, in subsurface studies, since the SEM is an analytical technique of surfaces, it would not be possible to access, without destroying the sample, to the area of interest of the microorganism-mineral interaction: its interphase.

3.3.2.1. Correlative fluorescence- Raman microscopy

Raman spectroscopy is an analytical technique based on the inelastic scattering, or Raman scattering, of monochromatic light when impacting on a molecule (Dieing et al., 2011; Smith and Dent, 2013). Briefly, when an electric field impact on a molecule disturbs the distribution of the electric charge of the molecule producing a dipole moment, after which the energy is quickly re-irradiated. Mostly, the scattered energy has the same frequency or wavelength as the incident light, which is known as Rayleigh scattering. However, because the different functional groups of the molecule absorb or lose energy, a small fraction of the photons is scattered at different wavelengths. The change in the frequency of these irradiated photons

is known as Raman scattering, which depends directly on the atoms, bonds, and structure of the molecule. Therefore, if Raman scattering is collected by spectroscopy, a characteristic vibrational spectrum of the molecule is obtained.

Because the identification and study of the Raman spectrum is quite complicated, especially in complex molecules, this analytical technique has been applied mainly to material sciences, including mineralogy and petrography since it allows rapid and non-destructive identification of the mineral (Dieing et al., 2011). In fact, the European Space Agency has designed a miniature Raman instrument for missions landed on Mars, which not only identify and characterize the mineral phases of the planet but also identify organic compounds and look for biological signatures (Escudero-Sanz et al., 2008). The application of Raman spectroscopy to the life sciences, however, is quite recent. The complexity of biological systems produces complex Raman spectra, which makes their analysis challenging. However, since the combination of Raman spectroscopy with confocal laser microscopy began in the 90s, allowing the analysis of a micrometric area of the sample and the generation of images of its chemical composition, the number of reports on the application of confocal Raman microscopy (CRM) to biology has increased exponentially (Dieing et al., 2011).

Since both CRM and fluorescence microscopy are non-destructive techniques and both complement the information that can be obtained by each of them, the correlation between both techniques offers great advantages. In fact, the combination of fluorescence microscopy and Raman microscopy has been described previously, emerging the term Raman-FISH (Huang et al., 2007). Thanks to the Raman-FISH, combination of the phylogenetic and chemical analysis of

individual microorganisms has been possible and allowed the analysis of isotopically labeled substrates utilization by specific microorganisms. However, until now, Raman-FISH has never been applied to geomicrobiological samples. Using Raman-FISH for subsurface studies could be very useful since it would allow not only the identification of the microorganism and the associated mineral in its natural environment, but also the analysis of the interphase between them, which would shed light about their interaction.

4. Objectives

The Iberian Pyrite Belt subsurface biosphere arouses great interest because it can be the key to understand the origin of the largest natural acidic river of the world, Río Tinto. Despite the abundant work performed to characterize this bioreactor, up to now no information about microbial distribution, microorganism-microorganism or microorganism-mineral interactions has been obtained. This data, would offer an invaluable picture of the geomicrobiological processes operating in the IPB subsurface.

The work developed in this thesis aimed to characterize the geomicrobiology of the Iberian Pyrite Belt subsurface by means of fluorescent *in situ* hybridization and microscopy techniques.

This thesis has been focused on accomplishing the following objectives:

- Adaptation of fluorescence *in situ* hybridization protocols to the study of microorganisms associated with solid mineral substrates
- Use of probes of complementary specificity, already designed, to identify the microorganisms corresponding to different phyla, classes, orders and genera and analyze their distribution
- Design of new specific probes from data obtained by other techniques applied in the IPBSL project
- Study and characterization of biofilms in the IPB subsurface
- Study the role of nitrate-reducing microorganisms in the IPB subsurface

- Identification of minerals associated with selected species of microorganisms
- Establishment of a geomicrobiological model of the operating IPB subsurface ecosystem

5. Materials and methods

5.1. IPB subsurface samples

Samples consist in splinters and dust from inside the cores obtained during BH10 drilling within the framework of the IPBSL project described in the introduction (Amils et al., 2013). Only samples below 90mbs were included as the first 90 meters were drilled using destructive techniques, which precluded the retrieval of intact cores. Samples were fixed in the laboratory field with 4% formaldehyde in Mackintosh minimal media ($(NH_4)_2SO_4$ 132mg/l, KH_2PO_4 27mg/l, $MgCl_2*6H_2O$ 53mg/l, $CaCl_2*2H_2O$ 147mg/l, pH 1.8) for 2h at 4 °C. After fixation, samples were washed with Mackintosh minimal media to remove the fixation agent, PBS (NaCl 8g/l, KCl_2 0.2g/l, Na_2HPO_4 1.44g/l, KH_2PO_4 0.24g/l) to neutralize the pH and, finally, they were stored in ethanol:PBS (1:1) at -20 °C until further processing.

5.1.1. Sample processing

5.1.1.1. Membrane filters

Samples were sonicated by 3 cycles of 20 seconds with one pulse per second at 20% intensity. 100µl of supernatant were filtered in black membranes 0.22 µm (Millipore, Germany) in aseptic conditions. Filters were washed with PBS and absolute ethanol and air dried. Once the filters were dried, they were covered with

agarose at 0.2%, dried at 37°C, dehydrated with absolute ethanol and stored at -20°C.

5.1.1.2. Rocks

Rocks were grounded in sterile conditions with a mortar until sand grains size, covered with agarose at 0.2% (Conda, Spain), dried at 37°C, dehydrated with absolute ethanol and stored at -20°C.

As controls, subsurface rocks of the same depths of the samples studied were used. Rock controls were previously cleaned and sterilized as described (Harneit et al., 2006) and processed as indicated above.

5.2. Fluorescence *in situ* Hybridization

5.2.1. Probe design

Three probes were designed for fluorescence *in situ* hybridization. S-G-Tess-681-a-A-21 (TESS681) was designed to detect members of *Tessaracoccus* genus, S-S-Tlap-1449-a-A-18 (Tlap1449) for the detection of the specie *Tessaracoccus lapidicaptus* and S-G-Rhi-124-a-S-22 (RHI124) to detect members of *Rhizobium* genus, in which are included the species *R. selenitirreducens* and *R. naphthalenivorans*. All probes were designed as described in (Hugenholtz et al., 2002) with the PROBE DESING tool of ARB software (Ludwig et al., 2004).

5.2.1.1. Determination of Probe Hybridization Conditions

To determine the optimal formamide concentration for FISH with Tlap1449, TESS681 and RHI124 probes, several control microorganisms were used (Table 2).

Tessaracoccus profundi T2-5-50, *Rhizobium selenitirreducens* T2-30D-1.1 and *Rhizobium naphthalenivorans* T2-26MG-112.2, all isolated from enrichment cultures carried out in the IPBSL project, were generous provided by Tania Leandro (University of Coimbra, Portugal). The rest of microorganisms were purchased from the Leibniz Institute DSMZ-German Collection of Microorganisms and Cell Cultures (Braunschweig, Germany). All microorganisms were grown in liquid media as Table 2 indicates.

Table 2. Summary of control microorganisms used in this work and their culture conditions

<table>
<tr><th>Microorganisms</th><th>Culture media</th><th>Tª (˚C)</th><th>pH</th></tr>
<tr><td>Tessaracoccus lapidicaptus IPBSL-7</td><td rowspan="6">Tryptic Soy Broth (TSB) 30g/l (Difco)</td><td rowspan="2">37</td><td rowspan="6">7.3</td></tr>
<tr><td>Tessaracoccus profundi T2-5-50</td></tr>
<tr><td>Tessaracoccus profundi DSM21240</td><td rowspan="4">30</td></tr>
<tr><td>Tessaracoccus oleiagri DSM22955</td></tr>
<tr><td>Tessaracoccus lubricantis DSM19926</td></tr>
<tr><td>Tessaracoccus flavescens DSM18582</td></tr>
<tr><td>Deinococcus radiodurans DSM20539</td><td>Casein peptone, tryptic digest 10g/l, yeast extract 5g/l, glucose 5g/l, NaCl 5g/l</td><td>30</td><td>7.2-7.4</td></tr>
<tr><td>Aeromicrobium ginsengisoli DSM22238</td><td>TSB 30g/l and yeast extract 3g/l</td><td>28</td><td>7-7.2</td></tr>
<tr><td>Rhizobium selenitirreducens T2-30D-1.1</td><td rowspan="2">Yeast extract 0.5g/l, protease peptone 0.5g/l, casaminoácids 0.5g/l, glucose 0.5g/l, soluble starch 0.5g/l, sodium piruvate 0.3g/l, K_2HPO_4-$2H_2O$ 0.36g/l, $MgSO_4$ 0.05 g/l</td><td rowspan="2">Room temperature</td><td rowspan="2">7.2</td></tr>
<tr><td>Rhizobium naphthalenivorans T2-26MG-112.2</td></tr>
<tr><td>Rhizobium rosettiformans DSM26376</td><td>TSB 30g/l (Difco)</td><td></td><td>7.3</td></tr>
</table>

Microorganisms were fixed with 4% of formaldehyde in PBS for 2h at 4°C and filtered, processed and stored as described in 5.1.1.1 section.

Designed probes were synthetized and labeled with CY3 fluorophore (Biomers, Germany). Specificity and optimal astringency conditions of the probes were determined by FISH as described in (Hugenholtz et al., 2002) in triplicate experiments using EUB338-I probe (see Table 3) labeled with FITC fluorophore as positive control.

5.2.2. CARD-FISH

CARD-FISH experiments were performed in filters and rock samples as previously described in detail (Pernthaler et al., 2004) with minor modifications. Endogenous peroxidases were inactivated as described (Ishii et al., 2004). For cell wall permeabilization, samples were treated with lysozyme and achromopeptidase solutions. Hybridization was performed with 5´-HRP-labeled oligonucleotide probes (Biomers, Ulm, Germany) for 2h at 46°C and then samples were washed at 48°C for 10 min. Stringencies were regulated for each probe by adjusting formamide (FA) and NaCl concentration in hybridization and washing buffer respectively (Table 3). TSA was carried out for 45min at 46°C. In multiple CARD-FISH experiments, an additional inactivation of peroxidases was done between hybridizations.

Table 3. Summary of probes used in this study and their specificity. FA and NaCl optimal concentration in hybridization and washing buffer respectively are indicated.

Probe	Sequence (5' - 3')	Specificity	FA (%) / NaCl (mM)	Reference
ACD840	CGACACTGAAGTGCTAAGC	*Acidiphilium* spp.	10/450	(Bond and Banfield, 2001)
ACI145	TTTCGCTTCGTTATCCCC	*Acidovorax* spp.	35/80	(Schulze et al., 1999)
ACI208	CGCGCAAGGCCTTGC	*Acidovorax* spp.	20/225	(Amann et al., 1996)
ALF968	GGTAAGGTTCTGCGCGTT	α-Proteobacteria	20/225	(Neef, 1997)
AMX368	CCTTTCGGGCATTGCGAA	all ANAMMOX bacteria	15/318	(Schmid et al., 2003)
ARC915	GTGCTCCCCCGCCAATTCCT	Archaea	20/225	(Stahl and Amann, 1991)
[a]BET42a	GCCTTCCCACTTCGTTT	β-Proteobacteria	35/80	(Manz et al., 1992)
CF319a	TGGTCCGTGTCTCAGTAC	Bacteroidetes	35/80	(Manz et al., 1996)
CFX109	CACGTGTTCCTCAGCCGT	*Chloroflexi* (subdivision 3)	30/112	(Björnsson et al., 2002)
CFX1223	CCATTGTAGCGTGTGTGTMG	Chloroflexi	35/80	(Björnsson et al., 2002)
CREN537	TGACCACTTGAGGTGCTG	Crenarchaea	20/225	(Teira et al., 2004)
CYA361	CCCATTGCGGAAAATTCC	Cyanobacteria	35/80	(Schönhuber et al., 1999)
DSS658	TCCACTTCCCTCTCCCAT	*Desulfosarcina-Desulfococcus*	60/14	(Manz et al., 1998)
EUB338-I	GCTGCCTCCCGTAGGAGT	Bacteria	35/80	(Amann et al., 1990)
EUB338-II	GCAGCCACCCGTAGGTGT	Planctomycetales	35/80	(Daims et al., 1999)
EUB338-III	GCTGCCACCCGTAGGTGT	Verrucomicrobiales	35/80	(Daims et al., 1999)
EURY806	CACAGCGTTTACACCTAG	Euryarchaea	20/225	(Teira et al., 2004)
[b]GAM42a	GCCTTCCCACATCGTTT	γ-Proteobacteria	35/80	(Manz et al., 1992)
GNSB-941	AAACCACACGCTCCGCT	Chloroflexi	35/80	(Gich et al., 2001)
HGC69a	TATAGTTACCACCGCCGT	Gram+ high G+C content (*Actinobacteria*)	25/159	(Roller et al., 1994)
LF655	CGCTTCCCTCTCCCAGCCT	*L. ferrooxidans* Groups I, II, III.	35/80	(Bond and Banfield, 2001)
LGC354a	TGGAAGATTCCCTACTGC	Gram+ low G+C content (*Firmicutes*)	35/80	(Meier et al., 1999)
LGC354b	CGGAAGATTCCCTACTGC			
MC1109	GCAACATAGGGCACGGGTCT	Methanococcaceae	45/40	(Raskin et al., 1994)
MEB859	GGACTTAACAGCTTCCCT	Methanobacteriales but Methanothermaceae	25/159	(Boetius et al., 2000)
MG1200	CGGATAATTCGGGGCATGCTG	most Methanomicrobiales	20/225	(Crocetti et al., 2006)
MSSH859	TCGCTTCACGGCTTCCCT	Methanosarcinales	35/80	(Boetius et al., 2000)
NON338	ACTCCTACGGGAGGCAGC	Negative Control	0/900	(Wallner et al., 1993)
RHI124	GTAGGGTACGGTAGATTCCCAC	*Rhizobium* spp.	50/28	This study
SBR385	GTTCCTCCAGATATCTACGG	Sulfate-reducing bacteria	35/80	(Amann et al., 1990)
SS_HOL1400	TTCGTGATGTGACGGGC	Acidobacteria	20/225	(Meisinger et al., 2007)
SUL228	TAATGGGCCGCGAGCTCCC	*Sulfobacillus* spp.	30/112	(Bond and Banfield, 2001)
THIO1	GCGCTTTCTGGGGTCTGC	*Acidithiobacillus* spp.	35/80	Stoffels (unpublished)
THIO820	ACCAAACATCTAGTATTCATCG	*Acidithiobacillus* spp.	10/450	(Peccia et al., 2000)
[c]TESS681	ACGCATTCCACCGCTTCACCA	*Tessaracoccus* spp.	50/28	This study
TESS681c	ACGCATTCCACCGCTMCACCA	*Tessaracoccus* spp. competitor	50/28	This study
Tlap1449	AGCTCCCCCCGCAAACGG	*Tessaracoccus lapidicaptus* sp.	10/450	This study

Table 3 (continuation)
[a]Unlabeled probe Gam42a was used in equal amounts as a competitor to enhance specificity.
[b]Unlabeled probe Bet42a was used in equal amounts as a competitor to enhance specificity.
[c] Unlabeled competitor TESS681c was used in equal amounts to enhance specificity.

5.2.3. FISH and DOPE-FISH

CY3 single and double labeled EUB338-I probes (Biomers, Germany) were compared using *Escherichia coli* DH5α pure-cultures. *E.coli* was grown in tryptone 10g/l, yeast extract 5g/l, NaCl 5g/l (Luria-Bertani medium), for 4h at 37°C, fixed at 4% formaldehyde for 2h at 4°C and filtered in 0.2µm membrane filters (Millipore, Germany). FISH and DOPE-FISH were carried out with identical hybridization and washing buffers (Glöckner et al., 1996) as well as identical hybridization (2h, 46°C) and washing (10min, 48°C) conditions. To decrease background intensity in DOPE-FISH experiments, FISH and geneFISH hybridization buffers were compared. GeneFISH buffer was prepared as described (Moraru et al., 2010). An additional incubation with geneFISH buffer was carried out without probe for 1h at 46°C previous to the hybridization. All experiments were carried out in triplicate.

FISH and DOPE-FISH experiments were then performed in subsurface rock samples using fluorophore single or double labeled probes (Biomers, Germany). For DOPE-FISH hybridizations, samples were previously permeabilized with lysozyme for 1h at 37°C and geneFISH buffer was used for pre-hybridization and hybridization step.

5.2.4. Biofilm detection

5.2.4.1. Lectin Binding Assay

Polysaccharides were visualized by Fluorescence Lectin Binding Assay (FLBA), using lectins conjugated with fluorescein isothiocyanate (FITC) fluorophore (Vector Laboratories, USA, Table 4). Lectins were diluted using the proper buffer as suggested by the manufacturer. Samples were washed with lectin specific buffer and stained as was described by Zhang et al. (2015). Lectins were employed alone or in combination as described (Neu et al., 2001).

Table 4. Summary of lectins and their specificity used in this study

Name	Abbreviation	Source	Specificity
Concanavalin A	ConA	Jack beam (*Canavalla ensiformis*)	Glucose, Mannose
***Aleuria aurantia* lectin**	AAL	*Aleuria aurantia*	Fucose
Peanut agglutinin	PNA	Peanut (*Arachis hypogea*)	Galactose
***Ulex europaeus* I**	UEA I	Furze gorse (*Ulex europaeus*)	Fucose

5.2.4.2. Specific proteins and lipids stains

Proteins were stained with SYPRO ruby (Thermo Fisher, USA) prior to FLBA. Sample was incubated with the stain for 30min and washed three times with filter-sterilized milliQ water. Lipids were stained adding Nile red (Merck, Germany) 1:1000 in the Vectashield: Citifluor mixture.

5.2.5. Ferric iron detection

Samples were stained with 2µM Ferrum 430™ (Ursa BioScience, USA) diluted in ethanol/H_2O 90/10 (%Vol/Vol) for 10min. Samples were washed with ethanol/H_2O 90/10 (%Vol/Vol) and let air dry in darkness.

5.2.6. Counterstaining and mounting

Filters and rock samples were counterstained with DAPI (4´,6-diadimino-2-phenylindole) or Syto9 (Thermo Fisher Scientific, USA) as manufacturer recommended and covered with a mix of 1:4 Vectashield (Vector Laboratories, USA): Citifluor (Citifluor, United Kingdom). Filters were mounted onto glass slides and rock samples were mounted onto µ-slides 8-well glass bottom (Ibidi, Germany).

5.3. Fluorescence Microscopy and image processing

5.3.1. Confocal laser scanning microscopy

To compare the fluorescence signal intensities in the determination of optimal hybridization conditions of the new designed probes and the fluorescence intensity comparison between FISH and DOPE-FISH probes, images were taken with the same confocal microscope settings using a confocal laser scanning microscope LSM510 coupled with an inverted microscope AxioObserver (Carl

Zeiss, Germany) equipped with argon (488/514 nm) and helium and neon (543 and 633 nm) lasers. Images were collected with a 63x/1.4 oil immersion lens.

Subsurface samples were imaged using a confocal laser scanning microscope LSM710 coupled with an inverted microscope AxioObserver (Carl Zeiss, Germany) and equipped with diode (405 nm), argon (458/488/514 nm) and helium and neon (543 and 633 nm) lasers. Images were collected with a 63x/1.4 oil immersion lens.

Lambda mode was used to characterize individually the emission spectra of every fluorophore and dye used in the experiments and employed to assure the source of the fluorescence signal in the rock hybridizations. Because every fluorophore has a singular spectrum, only the signals that matched with the spectrum of the fluorophore used were accepted as positive signals.

5.3.2. Image processing

All images were processed using Fiji software (Schindelin et al., 2012). To compare fluorescence, at least 3000 individual cells were analyzed on each experiment. The net fluorescence in FISH VS DOPE-FISH controls was considered as the result of the mean fluorescence of the microorganisms less the mean fluorescence of the background.

Biofilms images were further processed using Imaris 7.4 software (Bitplane AG, Switzerland).

5.4. Log D calculations

Log D and log P values of each fluorophore and dye were calculated in MarvinSketch 16.9.12 (Chem Axon, United Kingdom) using the structure of hydrolyzed reactive group as described (Hughes et al., 2014).

5.5. Natural rock samples incubation

Rock samples consist in splinters and dust from inside the cores obtained during the BH10 drilling of the IPBSL project. Samples from 102.6, 139.4 and 228.6mbs were placed in sterile bottles after sampling under a nitrogen atmosphere. As control, subsamples from the same depths were sterilized at 120°C overnight and stored at the same conditions.

MilliQ water was boiled, gassed with N_2 during cooling and sterilized under N_2 atmosphere at 121°C for 20min. 5ml of sterile milliQ water was added to the rock containing bottles with sterile syringes and they were incubated for 10months at 37°C in darkness.

Total iron concentration was monitored in duplicates by the α,α-dipyridyl method (Malki, 2003) with minimal modifications. Briefly, 10µl of sample were mixed with 40µl of hydroxylamine hydrochloride (10% in 1M HCl), a reducing agent, and 100µl of 40mM sulfamic acid (in 1M HCl), which remove the NO_2^- of the solution (Schaedler et al., 2017). After 30min, it was added 150µl of ammonium acetate (28%) to neutralize the pH to 5.5 and, after 5min, 200µl of α,α-dipyridyl (0.5% in absolute ethanol). Sterile 0.2 µm-filtered milliQ water was added until a final

volume of 2ml. Absorbance was measured at 520nm with a U-2000 spectrophotometer (Hitachi, Japan). Ferrous iron concentration was determined without adding the hydroxylamine hydrochloride solution. Ferric iron concentration was determined as the difference between total iron and ferrous iron.

pH was measured by using Test Strips 4.5-10 (Sigma, USA)

5.6. Anaerobic iron oxidation by nitrate-reducing microorganisms

5.6.1. Microorganisms and culture conditions

Acidovorax BoFeN1 (Kappler et al., 2005), kindly provided by Prof. Andreas Kappler (University of Tübingen, Germany), and *Tessaracoccus lapidicaptus* IPBSL-7 were grown in free-oxygen liquid media in triplicate. Basal media contained 0.4g/l KH_2PO_4, 0.3g/l NH_4Cl, 0.5g/l $MgSO_4 \cdot 7H_2O$ and 0.2g/l $CaCl_2 \cdot 2H_2O$ and was autoclaved under N_2/CO_2 atmosphere (80:20) for 20 min at 121°C.

The medium was then buffered at pH 6.8 with 22mmol/l $NaHCO_3$. 1ml/l trace elements solution (Tschech and Pfennig, 1984), 1ml/l selenate–tungstate solution (0.5g/l NaOH, 3mg/l $NaSeO_3 \cdot 5H_2O$ and 4mg/l $Na_2WO_4 \cdot 2H_2O$) and 1ml/l vitamin solution (Widdel and Pfennig, 1981) were added. Basal medium was then amended with 10mM $NaNO_3$ and 5mM acetate for *Acidovorax* and 10mM $NaNO_3$, 1g/l glucose and 1g/l yeast extract for *T. lapidicaptus*. The stock solutions of all of the compounds added to basal medium were autoclaved separately under a

N_2/CO_2 atmosphere for 20min at 121°C, but vitamin solution, which was sterilized by filtration (0.2µm).

This medium was used to grow microorganisms in presence or absence of Fe^{2+}. As ferrous iron source, 4mM $FeCl_2$ was added dissolved in anoxic milliQ water (boiled and flushed with N_2 during cooling). After 48h, medium was filtered (0.2µm) to eliminate vivianite and siderite precipitates, leaving a clear solution with ~3-3.5 mM of dissolved Fe^{2+}. In non-inoculated controls, no further vivianite and siderite precipitation was observed during the incubations.

15ml of media were transferred into sterile 33ml serum bottles that were closed with butyl rubber stoppers, crimped and flushed with N_2/CO_2 (80:20). Bottles were inoculated with 1ml of *Acidovorax* BoFeN1 or *T. lapidicaptus* in an exponential phase (~$6x10^6$ microorganisms) which were grown in non-iron-containing medium. *Acidovorax* cultures were incubated at 28°C and *T. lapidicaptus* cultures at 37°C.

Number of microorganisms and iron oxidation were measured daily or every few days (see below).

5.6.2. Growth curve and iron oxidation quantification

0.5ml of liquid media was fixed, stored and filtered in 0.2 µm membrane filters as described before (see section 5.2.1.1). Membrane filters were stained with SYBR® Gold (Thermo Fisher, USA) (final concentration 4×) at room temperature for 15 min in the dark and washed three times with sterile 0.2 µm-filtered milliQ

water. Counting of microorganisms was performed in an epifluorescence microscope Axioskop (Zeiss, Germany).

Total iron, Fe^{2+} and Fe^{3+} concentration was determined in duplicates as described in section 5.5.

5.7. *In vitro* dissolution of pyrite

5.7.1. Pyrite preparation and characterization

A pyrite cube (La Rioja, Spain) was cut parallel to {100} face in 1mm thick slides with a miter saw. Pyrite slides were cut in small pieces with a mean size of 0.5x0.5cm. Pyrite was sonicated until powder attached was removed and cleaned and sterilized as described (Schippers et al., 1996).

Pyrite composition was determined using a JEOL JSM-5600V scanning electron microscope coupled to an Oxford INCA X-sight EDAX Energy Dispersive X-ray Microanalysis Probe. The pyrite atomic composition was 48.57 at.% of S and 35.3 at.% of Fe with impurities of Ni (0.31at.%), Ti (0.30 at.%), Al (0.41 at.%), Si (0.24 at.%) and C (14.87 at.%).

5.7.2. Culture conditions and growth curve

Acidovorax BoFeN1 was grown in triplicate in different media conditions to determine its ability to dissolve pyrite (Table 5). Basal medium and acetate, NO_3^-

and $FeCl_2$ stock solutions were prepared as described in section 5.6.1. Non-inoculated controls and controls in which NO_3^- was replaced by 10mM NO_2^- were carried out.

~0.5gr of pyrite coupons were placed in 120ml serum bottles and 50ml of media was added. Bottles were flushed with N_2/CO_2 (80:20), inoculated with 1ml of *Acidovorax* BoFeN1 in an exponential phase (~$6x10^6$ microorganisms) which was grown in non-iron-containing medium, and incubated at 28°C.

Table 5. Growth conditions in which were tested pyrite dissolution by Acidovorax BoFeN1. Non-inoculated controls are included.

	Carbon source	Electron acceptor	$FeCl_2$	Inoculum
Pyrite	Acetate	NO_3^-	-	*Acidovorax* BoFeN1
	Acetate	NO_3^-	+	*Acidovorax* BoFeN1
	Acetate	NO_3^-	-	-
	Acetate	NO_3^-	+	-
	Acetate	NO_2^-	-	-
	Acetate	NO_2^-	+	-

5.7.3. Analytical methods

pH was measured as described in section 5.5.

Ferrous and ferric iron in solution was determined as described before in section 5.5 with an exception. In those culture media that were not amended with iron, iron measurement was performed with 50µl of sample and milliQ water was added until a final volume of 1ml. To determine the final iron amount, in two of the three replicas of the experiment, media was removed and the remained pyrite in the

flask was washed with sterile milliQ water. Then, pyrite and flask were washed with 5ml of 40mM sulfamic acid (in 1M HCl) in a shaker overnight to recover the precipitated iron attached to them. Attached iron, dissolved in sulfamic acid/HCl, was measured as described before. Final iron quantification was calculated as the sum of the iron amount in solution and the precipitated iron amount recovered from the acidic washing realized with sulfamic acid.

Iron released from pyrite was calculated by the difference between initial total iron and final total iron amount.

Nitrite and nitrite concentrations were determined by ion chromatography in the Servicio Interdepartamental de Investigación (SIdI) of the Universidad Autónoma de Madrid (Spain) with a Dionex DX-600 ion chromatograph.

The pyrite of the third replica of the experiment was used to characterize it by means of CRM and CLSM. Pyrite was fixed at 4% formaldehyde in PBS for 2h, washed with PBS and stored in PBS:Ethanol (50:50 (vol:vol)) under anaerobic conditions until analysis. Pyrite coupons were characterized before and after *Acidovorax* incubation by CRM (see below in section 5.8.2) mapping several areas of 25μm^2 and 2μm^2 in individual cells.

5.8. Correlative fluorescence- Raman microscopy

5.8.1. CARD-FISH and confocal microscopy

Rock samples were processed as described in section 5.1.1.2 and CARD-FISH was performed as described in section 5.2.2. However, samples were not immobilized in agarose or covered with antifade mounting medium to avoid the interference of both agarose and Vectashield:citifluor mixture with Raman spectroscopy. Samples were mounted onto a glass Micro-Slide Field Finder, in which a rectangular-coordinate grid pattern was drawn (EMS, United Kingdom).

Samples were imaged using a confocal laser scanning microscope LSM710 coupled with an vertical microscope AxioObserver (Carl Zeiss, Jena, Germany) and equipped with diode (405 nm), argon (458/488/514 nm) and helium and neon (543 and 633 nm) lasers. Images were collected with a 50x/1.4 air lens.

5.8.2. Confocal Raman Microscopy

Raman analyses were performed by using a confocal Raman microscope Witec alpha-300RA (Witec, Germany). Raman spectra were obtained using a 532 nm excitation laser and a 100X/0.95 air objective lens. The incident laser power was 2 mW and the acquisition time for a single Raman spectrum was 1 s.

Collected spectra were analyzed by using Witec Control Plus software (Witec, Germany). Features such as Raman peak intensity or Raman shifts to compare

spectra and represent the derived Raman image were analyzed using Lorenzian peak curves to fit the Raman peaks (Equation 6):

$$y = y_o + \frac{2}{\pi}\sum_{i=0}^{n-1}\frac{A_i W_i}{(4(x-x_i)^2 + W_i^2)} \quad (6)$$

Where Y_0 is the offset, A is the peak area, W is the full width at half maximum of the peak and X the peak center.

Reference organic materials and several fluorophores labeled tyramide were analyzed on glass slides. Glucose, starch, cellulose, trypsin and lysozyme were analyzed in powder form. *E. coli* and *Staphylocuccos aureus* Raman spectra were provided by Dr. Adolfo del Campo (Instituto de Cerámica y Vidrio, CSIC, Spain).

In correlation experiments, once the cells were located in the coordinate system by CLSM, samples were analyzed by confocal Raman microscope after bleaching the fluorophore as described (Huang et al., 2007). Raman images consist of the resulting analysis of several planar sections in the cells location. The acquisition time for a single Raman spectrum was 1 s (1 pixel, 1μm^2).

6. Results and discussion

6.1. CARD-FISH to study the biodiversity distribution of the IPB subsurface

Fluorescence techniques are a useful tool to analyze environmental samples. Specifically, FISH offers the possibility of studying the distribution of microorganisms by means of specific probes, which is of special importance in heterogeneous environments such as the subsurface (Moter and Göbel, 2000). Today, FISH is widely used in research and a countless number of probes to detect different groups of microorganisms are available. Otherwise, it is possible to design new probes for the identification and study of microorganisms based on data of the 16S rRNA obtained by sequencing techniques, whether the microorganisms are cultured or not. In the IPBSL project, thanks to the use of several complementary techniques such as NGS, cloning or isolation of new microorganisms, new probes have been designed to detect groups of microorganisms that inhabit the IPB subsurface and have been applied, together with already designed probes, to characterize the distribution of the deep biosphere of this environment.

6.1.1. Fluorescence *in situ* hybridization on mineral substrates

The principal problem when applying fluorescence techniques in rock substrates is the presence of minerals. On the one hand, because their intrinsic fluorescence can hinder the detection of true signals and, on the other hand, because, as in any other substrate, probes and dyes can bind unspecifically. Thus, the correct choice of fluorophores and dyes is essential for each rock sample.

Because not all the minerals reflect light or present fluorescence at the same wavelength, each rock sample was checked by fluorescence microscope to select suitable fluorophores to be used in further experiments, avoiding mineral fluorescence interference. To make sure that the observed fluorescence signal in hybridization experiment was biological, additional criteria were taken into account: the use of DNA-binding dyes DAPI or Syto-9 as counterstaining as well as the form, size and emission spectrum of the signal. In this last case, spectrum fingerprint of each fluorophore used in this study (Table 6) was measured by lambda mode of the CLSM and only signals that matched exactly with the spectrum of the used fluorophore were accepted as positive signals.

The use of lambda mode was especially useful in those samples in which DAPI general stain was applied due to the weak staining and yellowish fluorescence that this dye showed in some samples. Actually, it has been already reported difficulties in the detection of cells stained with DAPI in natural samples, as those from sea sediments (Llobet-Brossa et al., 1998). Among the reasons that can explain the weak signal of the DAPI at 461nm, its maximum emission, are the absorption of its emission by other fluorophore (Llobet-Brossa et al., 1998) or its spectrum

emission shifts to higher wavelength due to the formation of DAPI-RNA or DAPI-polyphosphate complexes (Kapuscinski, 1995; Omelon et al., 2009). In this last case, DAPI maximum emissions are at 500nm and 520nm respectively and its quantum yield is about 1/5 of the DAPI-DNA complex, which can explain the low yellowish fluorescence observed in the IPB subsurface samples. For this reason, DAPI staining was avoided as much as possible in this work and it was exclusively used in those experiments in which the use of additional fluorophores with green emission didn't allow the DNA staining with Syto9.

Table 6. Summary of dyes and fluorophores used in this study. Net charge and LogD were calculated using the molecular structure of the fluorophore with hydrolyzed reactive group. The molecular structure of Syto9 and Sypro ruby is not public available.

Fluorophore	Ex	Em	Technique	Net charge pH 7,4	LogD at pH7,4
Pacific Blue	410	455	CARD-FISH/DOPE-FISH	-1,96	-3,37
FITC	490	525	FLBA	-1,99	-1,48
Alexa 488	490	525	CARD-FISH	-2,99	-10,13
Alexa 594	590	617	CARD-FISH	-2,99	-7,04
CY3	550	570	FISH/DOPE-FISH	0,00	4,69
DAPI	350	461	DNA stain	2,00	-4,68
SYTO9	485	500	DNA stain	-	-
Nile red	552	636	Lipids stain	0,00	3,83
Sypro ruby	280/450	610	Proteins stain	-	-

An additional potential problem when applying FISH techniques to rocks substrates is the unspecific binding of the probe or dye to the inorganic surface resulting in high background or false positive signal. The principal sorption-driving forces described are hydrophobicity, electron donor-acceptor interactions or complementary charges between inorganic surface and organic molecule

(Schwarzenbach et al., 2005). In BH10 borehole, each depth present a different mineralogy (see Appendix 2) in which each mineral may show a dissimilar surface charge. Additional controls were carried out with NON338 probe with different fluorophores and with each dye in clean and sterilized rocks in which no organic matter was detected by Raman spectroscopy (data not show). In this case, any detected signal must be due to unspecific binding of the probe to the mineral substrate. Each selected dye and fluorophore showed some degree of nonspecific binding in some of the samples. This heterogeneous unspecificity of the probes may be due to the different charge or hydrophobicity that each probe presents, resulting in a differential sorption to the varied minerals of the samples.

To check this hypothesis, net charge and distribution-coefficient (logD) values of each fluorescent molecule were calculated at neutral pH, in which FISH is carried out (Table 6). On one hand, net charge is defined as the sum of all atom charges in a molecule, in such a way that those molecules with negative values will be attracted by positive charged mineral surfaces and vice versa. On the other hand, the logD value is the calculation of the equilibrium partition coefficient of the molecule between octanol and water, i.e. the logarithm of the ratio of the concentrations of the compound in hydrophilic and hydrophobic phases. LogD calculation is a common method to predict hydrophobicity (Hughes et al., 2014): logD values > 0 indicate hydrophobicity, while logD values 0<indicate hydrophilic properties. Most of the fluorophores analyzed are hydrophilic and showed negative net charge except DAPI, which presents a positive net charge that explains the preference of this dye for negative electrostatic A-T regions in DNA (Kapuscinski, 1995). Only CY3 fluorophore and Nile red dye, a lipid stain, showed net charge cero and

hydrophobicity. Thus, the chemical properties of the fluorescent molecules could explain their dissimilar non-specific binding with the array of minerals in the native samples due to diverse Van der Waals or hydrophobic interactions (Schwarzenbach et al., 2005).

All dyes or fluorophores used on each rock sample in this study was chosen to avoid both the non-specific binding with the mineral substrate and the mineral fluorescence interference.

6.1.2. Design and evaluation of new Oligonucleotide Probes

By sequencing methods it was detected at different depths, among others, two interesting genera of microorganisms in IPB subsurface samples, *Tessaracoccus* and *Rhizobium*. *Tessaracoccus* spp. was one of the most abundant microorganisms detected in the IPB subsurface by the different techniques applied in the IPBSL project and it was possible to isolate two species of this genus through enrichment cultures, the newly described *Tessaracoccus lapidicaptus* (Puente-Sánchez et al., 2014a) and *Tessaracoccus profundi* T2-5-50. Concerning the genus *Rhizobium*, two species were isolated from strict anaerobic enrichment cultures: *Rhizobium selenitirreducens* T2-30D-1.1 and *Rhizobium naphthalenivorans* T2-26MG-112.2, which interest lies in the fact that, as far as we know, only the ecology of the genus *Rhizobium* in soils has been studied, mainly associated with plants (Carareto Alves et al., 2014).

While no probes for *Tessaracoccus lapidicaptus* or *Tessaracoccus profundi* T2-5-50 have been designed up to now, there are some probes already designed for the

genus *Rhizobium*. Of these, only one, RHIRA7 (Kyselkova et al., 2009), could detect the isolated species *R. selenitirreducens* or *R. naphthalenivorans*. However, this oligonucleotide was designed for its use in an oligonucleotide microarray and, as FISH probe, its accessibility to the 16S rRNA target region was not suitable for *in situ* hybridization (Behrens et al., 2003). Thus, to study the distribution of *Tessaracoccus* and *Rhizobium* species along the BH10 column, three new probes were designed: TESS681, to detect microorganisms that belong to the genus *Tessaracoccus*; Tlap1449, designed to detect specifically the specie *Tessaracoccus lapidicaptus*; and RHI124, complementary to some species of the genus *Rhizobium* among which *R. selenitireducens* T2-30D-1.1 and *R. naphthalenivorans* T2-26MG-112.2 are found. Selected parameters of the new probes are detailed in Table 7.

Table 7. New FISH probes designed in this work and their optimized conditions.

Probe	ODP[a] designation	Sequence (5'-3')	*E. coli* position	Length (nt)	Tm (°C)[b]	G+C (%)	FA(%)	Positive control	Negative control (nº mismatch)
TESS681	S-G-Tess-681-a-A-21	ACGCATTCCACCGCTTCACCA	681	21	58,22	57,1	50	*T. lapidicaptus* *T. profundi* *T. oleiagri* *T. lubricantis* *T. flavescens* *T. profundi* T2-5-50	*D.radiodurans* (1)
TESS681[c]	-	ACGCATTCCACCGCTMCACCA[d]			57,6-59,3	57-62			
Tlap1449	S-S-T.lap-1449-a-A-18	AGCTCCCCCCGCAAACGG	1449	18	57,19	72,2	10	*T. lapidicaptus*	*A. ginsengisoli* (2)
RHI124	S-G-Rhi-124-a-S-22	GTAGGGTACGGTAGATTCCCAC	124	22	52,74	54	50	*R. selenitirreducens*	*R. rosettiformans* (1)
RHI124[c]	-	GTAGGGCACGGTAGATTCCCAC			55,55	59		*R. naphthalenivorans*	

[a] Oligonucleotide Probe Database (Alm et al., 1996)
[b] Determined by nearest-neighbour method and calculated using 50mM NaCl and 50nM oligonucleotide.
[C] Probes competitors
[d] M= C+A nucleotides

The designed oligonucleotide probes showed a perfect match with the sequences of the desired microorganisms (Figure 8). TESS681 probe covers 79.1% of all available 16S rRNA gene sequences of the genus *Tessaracoccus* within the SILVA

database (Quast et al., 2012) and it was also complementary with two sequences of uncultured microorganisms, a member of Planctomycetales and a Propionibacteraceae bacterium. *Deinococcus radiodurans* was chosen as negative control for this probe since it has the most abundant mismatch detected in the target region (Figure 8A). Tlap1449 was only complementary to *Tessaracoccus lapidicaptus*. As negative control was chosen *Aeromicrobium ginsengisoli*, with two mismatches, as the three sequences detected with one mismatch belong to uncultured microorganisms (Figure 8B). RHI124 covers 9.3 % of the *Rhizobium* group, among which we can find some *Agrobacterium* species that had been reordered in the *Rhizobium* genus (Young et al., 2001). All the complementary sequences to this probe belong to the *Agrobacterium*/*Rhizobium* cluster as well as those sequences with a weakly destabilizing T-G misparing. As representative of the last ones it was chosen *Rhizobium rosettiformans* to be used as negative control for the RHI124 probe (Figure 8C).

Using the FISH protocol, the hybridization conditions for stringency were determined for each probe with positive and negative control microorganisms (Figure 9). The difference in the FISH signal intensity between the positive and negative control cells was obvious for Tlap1449, which optimal percentage of formamide was 10% and no hybridization was detected with *A. ginsengisoli* (Figure 9A). However, that was not the case for TESS681 and RHI124 probes. With the aim of improve the difference of fluorescence between positive and negative controls, competitors were designed to block nontarget probe binding sites for both probes (Table 7). The competitor of TESS681 improved considerably the discrimination of single mismatches (Figure 9B) and an optimal percentage of

formamide of 50% was determined. Conversely, RHI124c didn't enhance the probe specificity since it was not observed a greater difference between the signal intensity of the negative and positive controls used (data not shown). Moreover, it influenced negatively the probe sensitivity, which showed lower signal intensity in the target microorganisms.

A

Organism name	TESS681
	TGGTGAAGCGGTGGAATGCGT
Tessaracoccus bendigoensis	UGGAAUUCC-==========-AGAUAUCAG
Tessaracoccus profundi T2-5-50	UGGAAUUCC-==========-AGAUAUCAG
Tessaracoccus profundi	UGGAAUUCC-==========-AGAUAUCAG
Tessaracoccus flavescens	UGGAAUUCC-==========-AGAUAUCAG
Tessaracoccus lubricantis	UGGAAUUCC-==========-AGAUAUCAG
Tessaracoccus oleiagri	UGGAAUUCC-==========-AGAUAUCAG
Tessaracoccus lapidicaptus	UGGAAUUCC-==========-AGAUAUCAG
Tessaracoccus flavus	UGGAAUUCC-==========-AGAUAUCAG
uncultured Propionaceae bacterium	UGGAAUUCC-==========-AGAUAUCAG
Deinococcus radiodurans	UGGAAUUCC-=====U==========-AGAUACCAG
uncultured Planctomycetales bacterium	UGGAACUUG-=====g==========-UGAUAUCAC
Aestuariimicrobium kwangyangense	UGGAAUUCC-=====g==========C-AGAUAUCAG

B

Organism name	Tlap1449
	CCGTTTGCGGGGGGAGCT
Tessaracoccus lapidicaptus	UGGCCUAAC-==========-GUCGAAGG
uncultured BRC1 bacterium	CUUAACCUU-==========C=====-ACGGUGUGG
uncultured Legionellaceae bacterium	AGUCUAACC-g==========-ACGGUGUGG
uncultured Hydrogenophilaceae bacterium	AGCCUAACC-g==========-ACGGUGAGU
Aeromicrobium ginsengisoli	GUGGCCCAA-======A===A=======-GUCGAAGGU

C

Organism name	RHI124
	GTGGGAATCTACCGTACCCTAC
Rhizobium selenitireducens	GAGUAACGC-==========-GGAAUAACG
Rhizobium naphthalenivorans	GAGUAACGC-==========-GGAAUAACG
Rhizobium vitis	GAGUAACGC-==========-GGAAUAGCU
Rhizobium daejeonense	GAGUAACGC-==========-GGAAUAACG
Rhizobium radiobacter	GAGUAACGC-==========-GGAAUAACG
Rhizobium ipomoeae	GAGUAACGC-==========-GGAACAACA
Rhizobium taibaishanense	GAGUAACGC-==========-GGAAUAGCU
Agrobacterium albertimagni	GAGUAACGC-==========-GGAAUAGCU
Rhizobium rosettiformans W3	GAGUAACGC-==========g======-GGAAUAGCU
Rhizobium aggregatum	GAGUAACGC-==========g======-GGAAUAGCU
Agrobacterium sp. IrT-JG14-14	GAGUAACGC-==========g======-GGAAUAGCU

Figure 8. rRNA sequence alignments showing target regions of probes for a selection of reference strains. Nucleotides are only identified for mispairings; pairings are indicated by double lines. A. TESS681 probe, B. Tlap1449 probe and C. RHI124 probe.

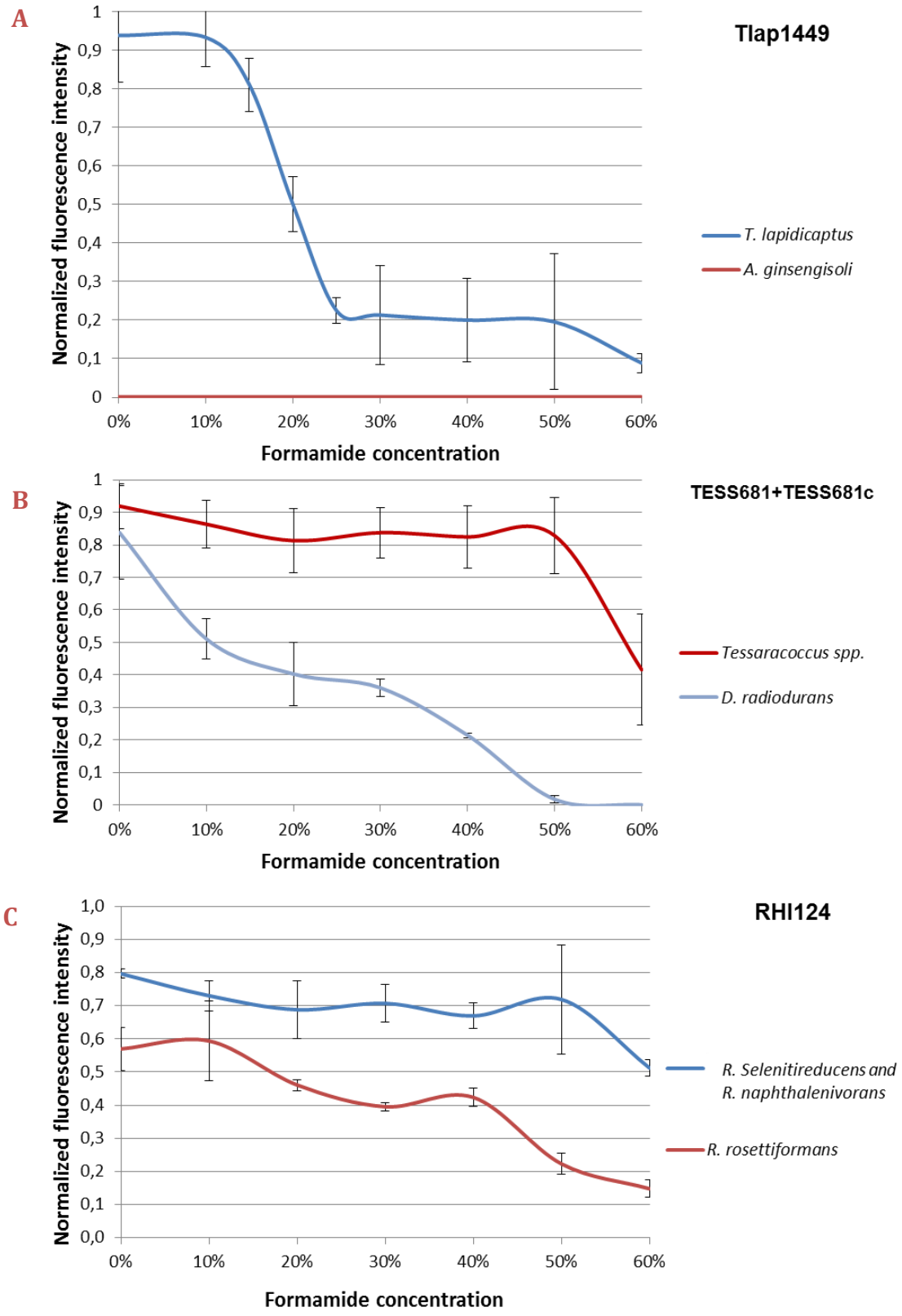

Figure 9. Optimal formamide concentration for (A) Tlap1449 probe, (B) TESS681 probe (with competitor) and (C) RHI124 probe. For TESS681 and RHI124 is represented the mean value of the normalized fluorescence intensity of all positive controls used.

This fact may be explained by the very weak mismatch (0.2 mismatch weight calculated with SILVA TestProbe tool) between the probe and *R. rossetiformans* as well as between the competitor and *R. selenitireducens* and *R. naphthalenivorans,* which binding affinity and position in the probe could not allow to enhance the discrimination of these microorganisms even at high formamide concentrations.

Nevertheless, as RHI124 only present one or two mismatches with *Agrobacterium*/*Rhizobium* cluster members, we applied this probe without competitor using the maximum percentage of formamide in which it showed positive hybridization with *R. selenitireducens* T2-30D-1.1 and *Rhizobium naphthalenivorans* T2-26MG-112.2, that is to say, 50% (Figure 9C). Further experiments need to be carried out to test the competitor as a probe and its use together RHI124 in a mix to detect a higher group of members of the *Rhizobium* genus using a new negative control.

The probes were then applied to BH10 subsurface samples to detect and analyze the distribution of *Tessaracoccus* and *Rhizobium* communities in the IPB subsurface (see 6.1.3 section).

6.1.3. Biodiversity distribution in the IPB subsurface

With the aim to detect and identify the maximum amount of microorganisms and study its distribution, CARD-FISH was chosen as fluorescence hybridization technique to apply in deep subsurface samples. The amplification of the probe signal by CARD-FISH allows the detection of living microorganisms even though their number of ribosomes is rather low (Pernthaler et al., 2004), which may be

expected in deep subsurface environments due to the limited energy supply and low microbial metabolic rates (Hoehler and Jorgensen, 2013).

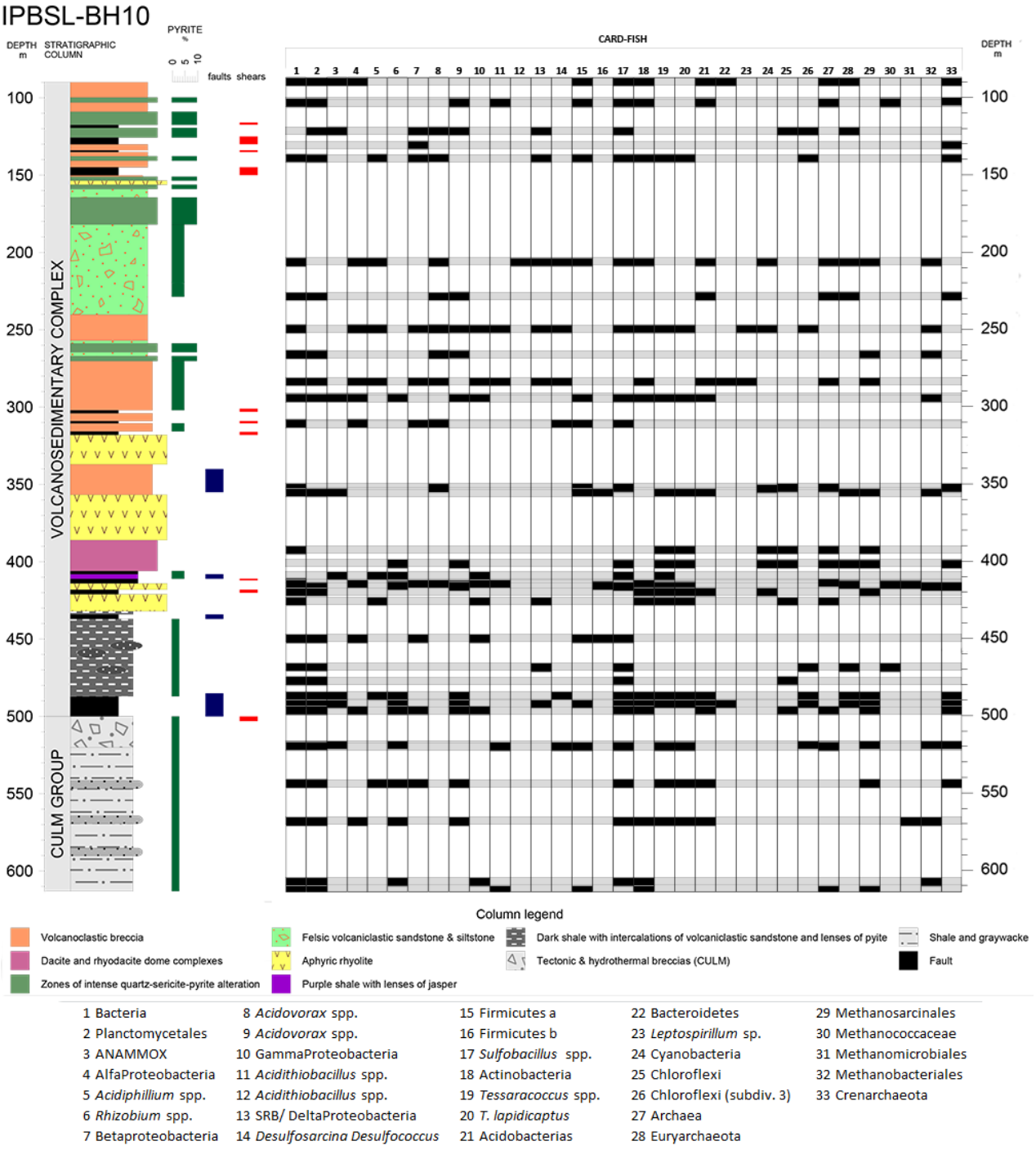

Figure 10. Distribution of subsurface microbial diversity along BH10 column analyzed by CARD-FISH. Black and grey squares indicate presence or absence of microorganisms at a determined depth respectively.

CARD-FISH was carried out with several probes with various ranges of specificity in the so-called top to bottom approach (Amann et al., 1995), from phyla to species level, in sonicated and filtered samples (Figure 10). CARD-FISH analysis showed that microorganisms are widely distributed in the IPB subsurface, being at fractures and more porous zones, as between 487.2-496.8 mbs, where more microorganisms, bigger colonies and different phylogenetic groups were detected, as expected due to the bigger space and higher nutrient flow (Fredrickson et al., 1997a).

6.1.3.1. Bacteria diversity and distribution

CARD-FISH results corroborate most of the biodiversity data obtained by others techniques carried out in the IPBSL project as immuno-detection, oligonucleotide microarrays, NGS (Figure 11), cloning and enrichment cultures (data not shown). The bacteria number and biodiversity detected was higher than archaea, as reported previously in other subsurface environments (Cockell et al., 2012; Purkamo et al., 2015; Ino et al., 2016). Proteobacteria, Firmicutes and Actinobacteria were the most distributed phyla along the IPB subsurface (Figure 10), which agree with the results shown by other subsurface studies (Appendix 1). Accordingly, these phyla seem to be well adapted to the conditions of this environment.

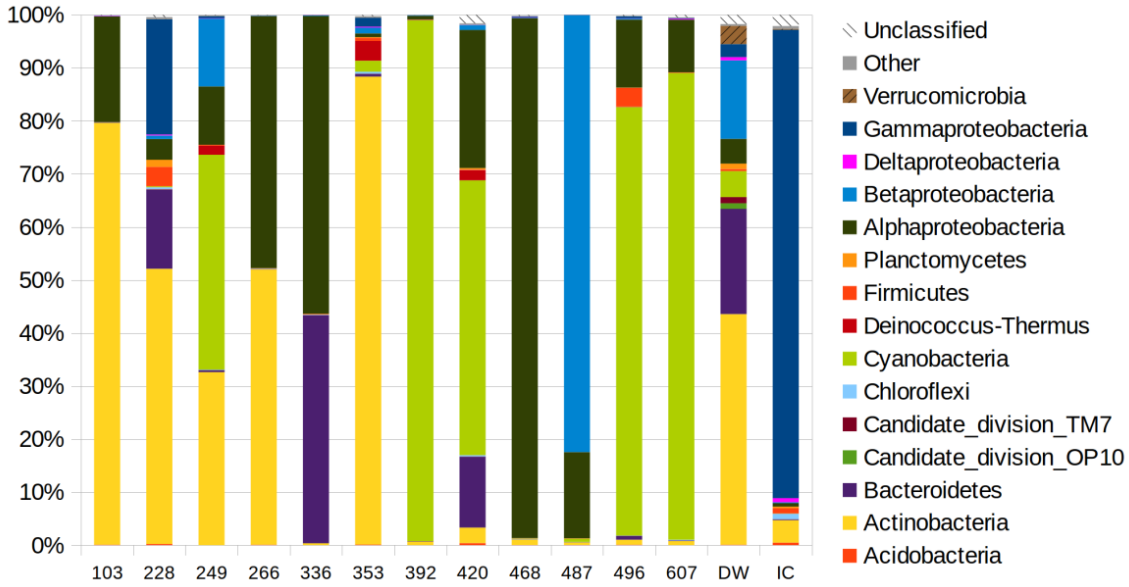

Figure 11. Taxonomic composition at phylum level (with Proteobacteria expanded into classes) of BH10 samples by means of NGS. Sample names indicate sampling depth, except in DW (drilling water control) and IC (internal laboratory control). Image provided by Dr. Fernando Puente Sánchez (Puente-Sánchez, 2016).

6.1.3.1.1. Proteobacteria phylum (and Leptospirillum spp.)

Concerning the Proteobacteria phylum, members of the classes Alfa, Beta, Gamma and Delta-Proteobacteria classes were detected (Figure 12).

Within Alfa-Proteobacteria members of the genera *Acidiphillium* (Figure 13A and B) and *Rhizobium* (Figure 13C and D) were the most prominent. *Acidiphillium* is an iron-reducing microorganism that is abundant in the anoxic zone of Río Tinto water column (González-Toril et al., 2003) and, in fact, it was detected at several depths in the BH10 column where iron-reducing metabolisms in enrichment cultures were also detected together with the presence of iron, which may support its growth using organic matter as electron donor and carbon source (Figure 12).

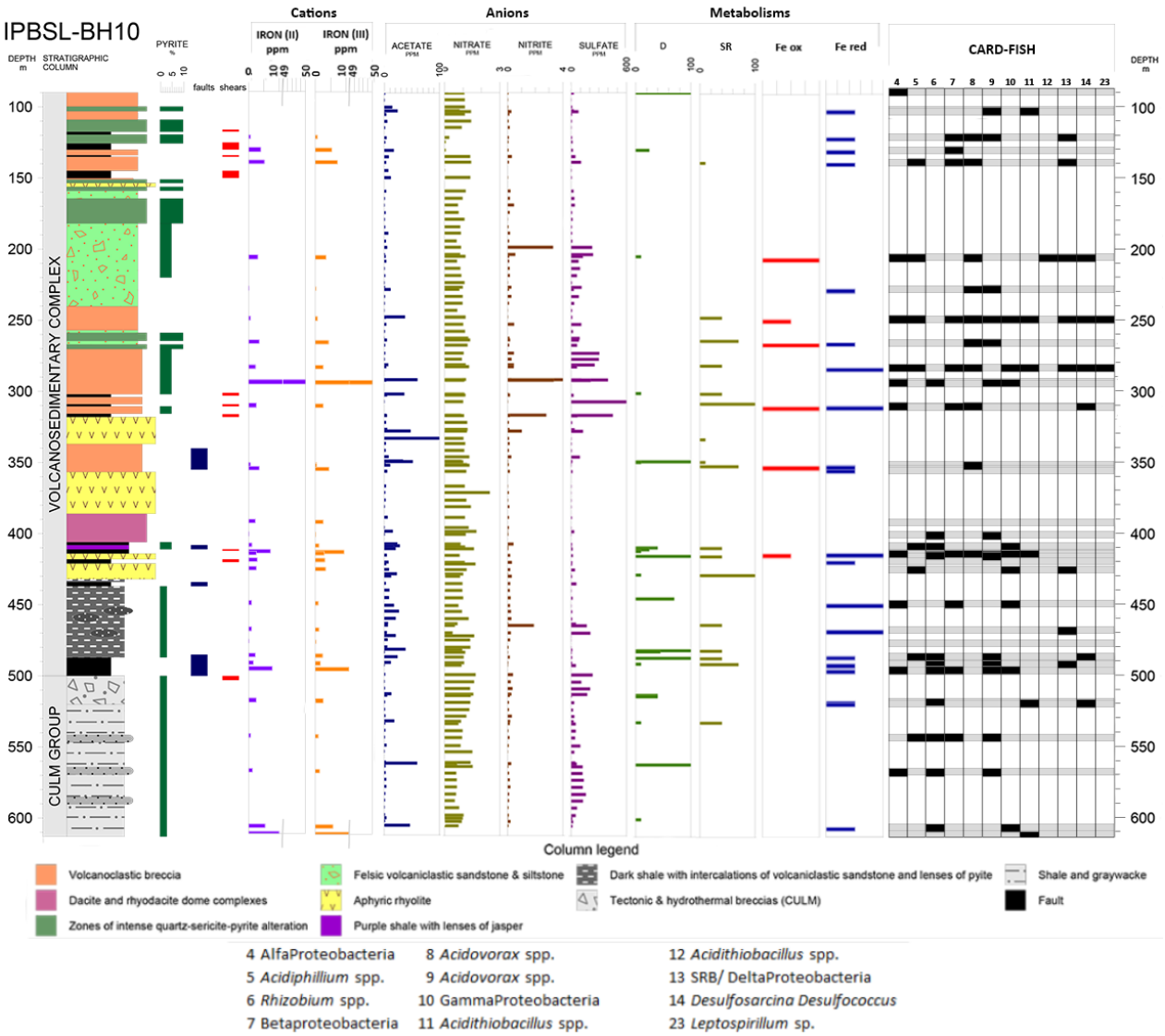

Figure 12. Proteobacteria phylum and Leptospirillum spp. distribution along BH10 column analyzed by CARD-FISH. Black and grey squares indicate presence or absence of microorganisms at a determined depth respectively. Data about identified compounds and metabolisms of interest obtained during the development of the IPBSL project are shown. D= denitrification; SR=sulfate reduction; Fe ox and Fe red= iron oxidation and reduction respectively.

Regarding the genus *Rhizobium*, most of the studies carried out on this group of microorganisms have focused exclusively on its importance to establish symbiotic relationships with plants (Zahran, 1999; Carareto Alves et al., 2014) and their possible role in alternative environments has been ignored. Nevertheless, in the

1980s several studies unequivocally demonstrated that members of the genus *Rhizobium* are able to grow in anaerobiosis using nitrate as electron acceptor (Zablotowicz et al., 1978; Daniel et al., 1982; O'hara and Daniel, 1985), which would allow them to grow in a wider range of habitats. But the ecology of these microorganisms in anaerobic environments, as far as we know, has never been analyzed.

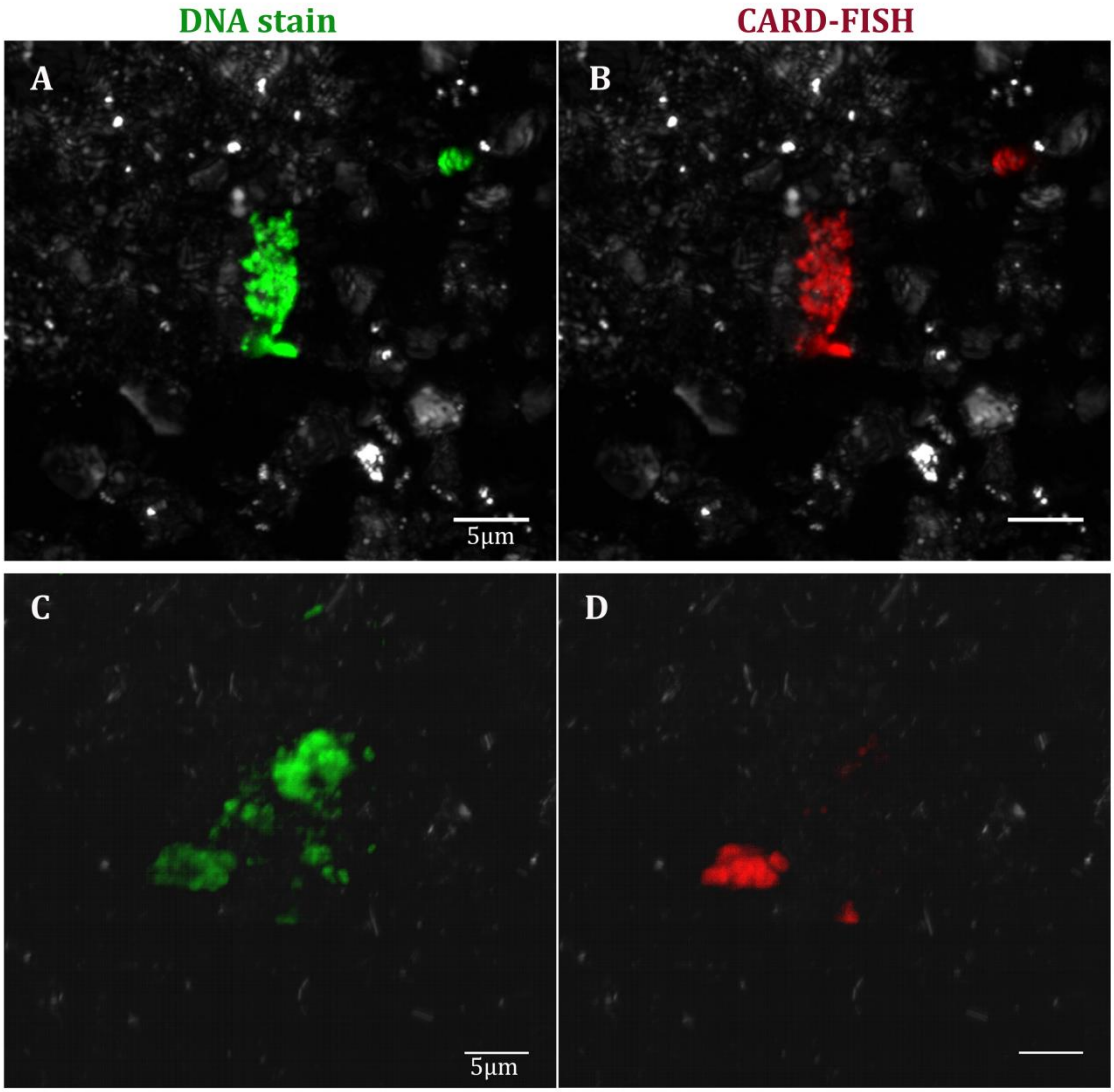

Figure 13. α-Proteobacteria members detected by CARD-FISH in the IPB subsurface . A-B, Acidiphillium sp. at 206.6 mbs; C-D, Rhizobium sp. at 496.8 mbs. In green, Syto9 stain. In red, CARD-FISH signal. In grey, reflection. Scale bars, 5µm.

As mentioned, two species of the genus *Rhizobium*, *Rhizobium selenitireducens* T2-30D-1.1 and *Rhizobium naphthalenivorans* T2-26MG-112.2, were isolated from strictly anaerobic enrichment cultures in the IPBSL project. While *R. selenitireducens* T2-30D-1.1 was isolated from an anaerobic enrichment culture for denitrifying microorganisms using a sample from 538.5mbs, *R. naphthalenivorans* T2-26MG-112.2 was isolated from an anaerobic enrichment culture for methanogens using a sample from 492.6mbs. Currently a whole genome sequencing analysis of *Rhizobium selenitireducens* T2-30D-1.1 and *Rhizobium naphthalenivorans* T2-26MG-112.2 is being carried out in our laboratory and preliminary results show the presence in both *Rhizobium* species of the ArcA/B system. ArcA/B is a two-component signal transduction system that acts as an oxygen sensor and mediates adaptive responses to changing respiratory conditions (Georgellis et al., 2001). The existence of this system in both *Rhizobium* strains indicates that they could also grow by using an alternative anaerobic metabolism as was demonstrated in others *Rhizobium* species (Daniel et al., 1982).

To evaluate the distribution of these members of the genus *Rhizobium* in the IPB subsurface, CARD-FISH analysis was carried out by using the probe RHI124 designed in this work (see section 6.1.2). Results showed the presence of these microorganisms at several depths along the BH10 column, mostly concentrated in a fault zone (487.2-496.8 mbs) (Figure 12). In addition, as shown in Figure 13 (C and D), the DNA stain signals are more abundant than RHI124 probe signals, which might indicate the interaction between different microorganisms (see section 6.3). As a result, a metabolic association of *Rhizobium* with other microbial species

could promote, somehow, its growth in this anaerobic environment or facilitate the development of the unidentified neighbors.

On the other hand, the presence of members of the genus *Rhizobium* in underground environments is not exclusive to the IPB subsurface. This genus has been detected in other studies of anoxic subsurface environments as those carried out in the South Africa Gold mines (Lau et al., 2014; Magnabosco et al., 2016) or the drilling projects of Mt. Simon Sandstone (Dong et al., 2014a) and Outukumpu (Nyyssönen et al., 2014; Purkamo et al., 2015). Hence it cannot be rejected the possibility that the subsurface, together with the soil, is a natural habitat in which the members of the genus *Rhizobium* can be found.

Acidovorax genus is one of the few members of Beta-Proteobacteria identified in the BH10 column, but it has been detected by every technique used to determine the microbial diversity in the IPBSL project. By metagenomic analysis of native rock samples, it was showed that *Acidovorax* was the most abundant microorganism at 487.2 mbs (Amils et al., in preparation) and it has been identified in several enrichment cultures and cloning analysis from several depths (data not shown). *Acidovorax* is of special interest in the IPBSL project because, up to now, is the only microorganism identified in the BH10 column that has been described as an iron oxidizer in anaerobic conditions using nitrate as electron acceptor (Kappler et al., 2005), the main metabolism that, in principle, could explain the generation of high concentrations of iron in the subsurface bioreactor, giving rise to the extreme conditions detected in Río Tinto (see section 3.2.2). Therefore, a CARD-FISH study was performed to analyze the distribution of these microorganisms in the subsurface of the IPB. Two different probes were used,

ACI145 and ACI208, to include the largest number of members of the *Acidovorax* genus, since both probes complement each other (Amann et al., 1996; Schulze et al., 1999). Results indicated that *Acidovorax* is one of the genera with higher distribution along the BH10 column (Figure 12 and Figure 14A and B), supporting the data obtained by the rest of techniques. Moreover, *Acidovorax* was detected by CARD-FISH at depths were iron, acetate and nitrite showed higher concentrations, being the nitrite the metabolic product of nitrate reduction. This data together with the observation of a high distribution of *Acidovorax* in the MARTE project (Puente-Sánchez et al., 2014b), performed also in the IPB subsurface, strongly suggest that this genus must play an important role in the iron and nitrogen cycles of this ecosystem and, therefore, in the solubilization of the subsurface sulfide ores of the IPB (see section 6.5.2).

Gamma and Delta-Proteobacteria, detected by GAM42a and SRB358 probes respectively, are the Proteobacteria classes that seem to be less distributed in the BH10 column. It stands out the genus *Acidithiobacillus*, which is one of the main microorganisms detected in the water column of Río Tinto (González-Toril et al., 2003). CARD-FISH analysis showed a higher distribution of *At. thiooxidans* and *At. ferrooxidans* by using the THIO820 probe (Figure 14C and D), an oligonucleotide that detect specifically both species (Peccia et al., 2000). These *Acidithiobacillus* species use inorganic reduced sulfur compounds or hydrogen as electron donors and ferric iron as electron acceptor in anaerobic conditions (Vera et al., 2013).

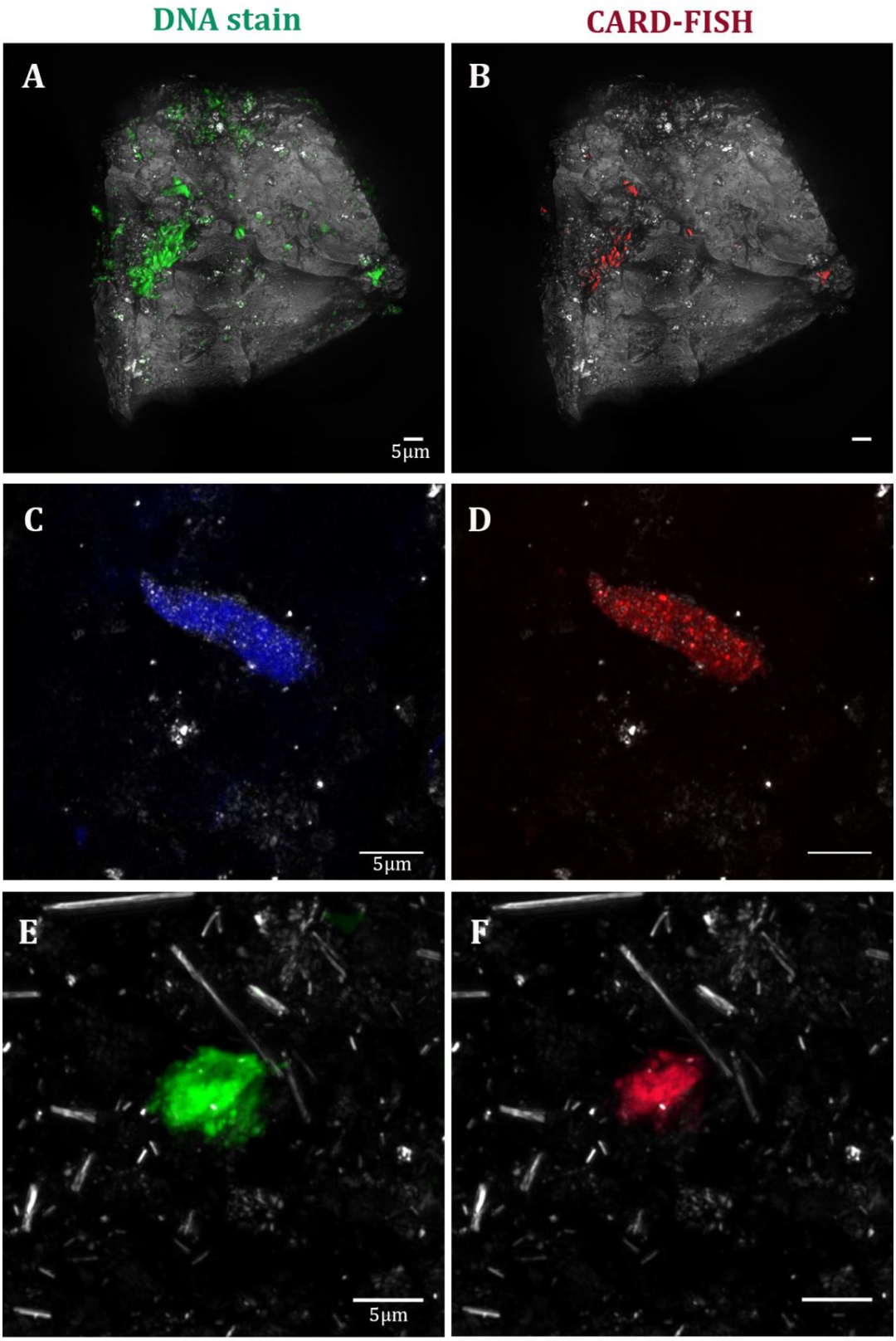

Figure 14. β, γ and δ- Proteobacteria members detected by CARD-FISH in the IPB subsurface. A-B, Acidovorax sp. at 206.6 mbs; C-D, Acidithiobacillus sp. at 414.8 mbs; and E-F, Desulfosarcina sp. or Desulfococcus sp. at 520 mbs. In green, Syto9 stain. In blue, DAPI stain. In red, CARD-FISH signal. In grey, reflection. Scale bars, 5µm.

Due to the observation that the genera *Acidiphillium* and *Acidithiobacillus,* abundant in Río Tinto's water column, are present in the IPB subsurface, we proceeded to analyze the presence of *Leptospirillum* genus, the third most abundant genus in the river. However, this genus was only detected at two depths by CARD-FISH, 249.8 and 284mbs (Figure 12). The low distribution of the genus *Leptospirillum* in the BH10 column could be attributed to its strictly aerobic metabolism. Nevertheless, this genus has also been detected in the IPB subsurface in the MARTE project framework (Puente-Sánchez, 2016) and in other anaerobic environments, such as in the Río Tinto's sediments (García-Moyano et al., 2009; García-Moyano et al., 2012), or in microaerobic environments, such as biofilms developed at 60cm deep in an abandoned mine in Wales (Hallberg et al., 2006). Genomic analysis of *Leptospirillum* species have shown that these microorganisms carry genes related with an anaerobic metabolism as the formate-hydrogen lyase clusters or anaerobic cobalamin biosynthesis pathway, which have been found only in known anaerobes (Goltsman et al., 2009). However, although the possible existence of an anaerobic metabolism is contemplated in some species of this genus (García Moyano, 2007; Goltsman et al., 2009), as far as we know, it has not yet been possible to demonstrate unequivocally whether *Leptospirillum* is capable of using alternative electron acceptors to oxygen. Therefore, the presence of *Leptospirillum* in the IPB subsurface could be due to its resistance for long periods of time in anaerobic conditions, as indicated in studies carried out in our laboratory in which members of this genus could be isolated from long-term anaerobic enrichment cultures (González Toril, 2002), but their role in the IPB subsurface does not seem to be substantial.

Sulfate-reducing bacteria belonged to Delta-proteobacteria have been detected also in the IPB subsurface, highlighting species as *Desulfosarcina* and *Desulfococcus* detected by DSS658 probe (Figure 14E and F). Specific enrichment cultures to detect SRB showed a significant presence of this metabolism between 250-350mbs and 400-500 mbs (Figure 12), which correspond with the location of these microorganisms along the BH10 column. The growth of these microorganisms may be supported, together with sulfate, by the organic matter or H_2 and CO_2 (Barton, 2013) present in the IPB subsurface.

6.1.3.1.2. Firmicutes and Actinobacteria phyla

Regarding Firmicutes and Actinobacteria phyla, the distribution of the genera *Sulfobacillus* and *Tessaracoccus* was analyzed (Figure 15).

Sulfobacillus spp. have been detected in the IPB subsurface by using LD300chip and PAM oligonucleotide microarray in both the MARTE (Puente-Sánchez, 2016) and the IPBSL projects. To check the distribution of this genus in the BH10 column, CARD-FISH with SUL228 probe was carried out (Figure 15 and Figure 16A and B). SUL228 probe, used as well in the LD300chip, hybridize mainly with *S. thermosulfidooxidans* and *S. benefaciens* (Bond and Banfield, 2001; Quast et al., 2012), which have been described as members of the microbial communities that accelerate sulfide mineral dissolution (Watling et al., 2008). These microorganisms are metabolically versatile and can utilize a broad range of energy substrates including organic matter, diverse species of reduced sulfur and hydrogen by using Fe^{3+} as electron acceptor in anaerobic conditions (Justice et al., 2014). Our results

show that *Sulfobacillus* spp. are widely distributed along the entire column, being highly represented from 450 to 607.6 mbs, where the presence of iron, sulfur compounds, organic matter or even hydrogen may support the growth of these microorganisms (Figure 15).

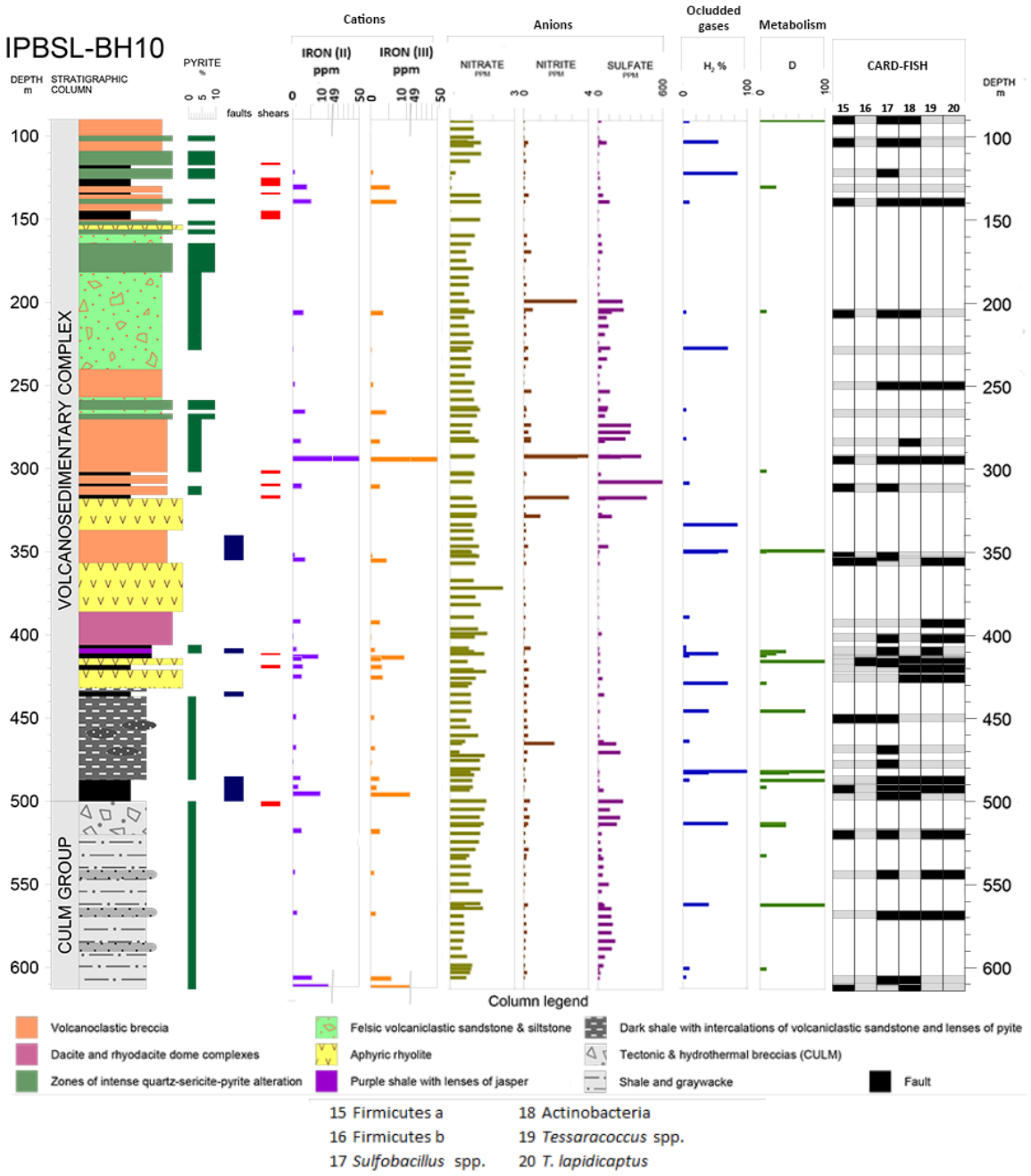

Figure 15. Firmicutes and Actinobacteria phyla distribution along the BH10 column analyzed by CARD-FISH. Black and grey squares indicate presence or absence of microorganisms at a determined depth respectively. Data about identified compounds and metabolisms of interest obtained during the development of the IPBSL project are shown. D= denitrification.

Within the Actinobacteria phylum, highlights the genus *Tessaracoccus*, which has been detected at several depths by metagenomic analysis of native samples as well as in different enrichment cultures for acetogens, methanogens, sulfate-reducing and nitrate-reducing microorganisms (Puente-Sánchez, 2016; Leandro, personal communication). As discussed, two species belonging to *Tessaraccocus* genus has been isolated in the IPBSL project, *T. lapidicaptus,* described in the framework of this project (Puente-Sánchez et al., 2014a), and *Tessaracoccus* T2-5_50*,* specie related to *T. profundi*, which was described for the first time in another deep subsurface environment (Finster et al., 2009). While *Tessaracoccus* T2-5_50 was only isolated from an specific enrichment culture for methanogenic microorganisms from a 139.4mbs sample, *T. lapidicaptus* has been isolated anaerobically using nitrate as electron acceptor (Puente-Sánchez et al., 2014a) from cores sampled at 206.6 and 297m depth as well as through enrichments cultures for methanogenic microorganisms from cores sampled at 139.4 and 284mbs (Leandro, personal communication). Therefore, the distribution of members of the *Tessaracoccus* genus, and specifically *Tessaracoccus lapidicaptus*, was analyzed by the new designed probes TESS681 and Tlap1449 respectively (see section 6.1.2). In this case, double hybridizations with both probes were used to determine the percentage of members of the *T. lapidicaptus* species in the IPB subsurface in relation to the total number of members of the *Tessaracoccus* genus (Figure 16C-E).

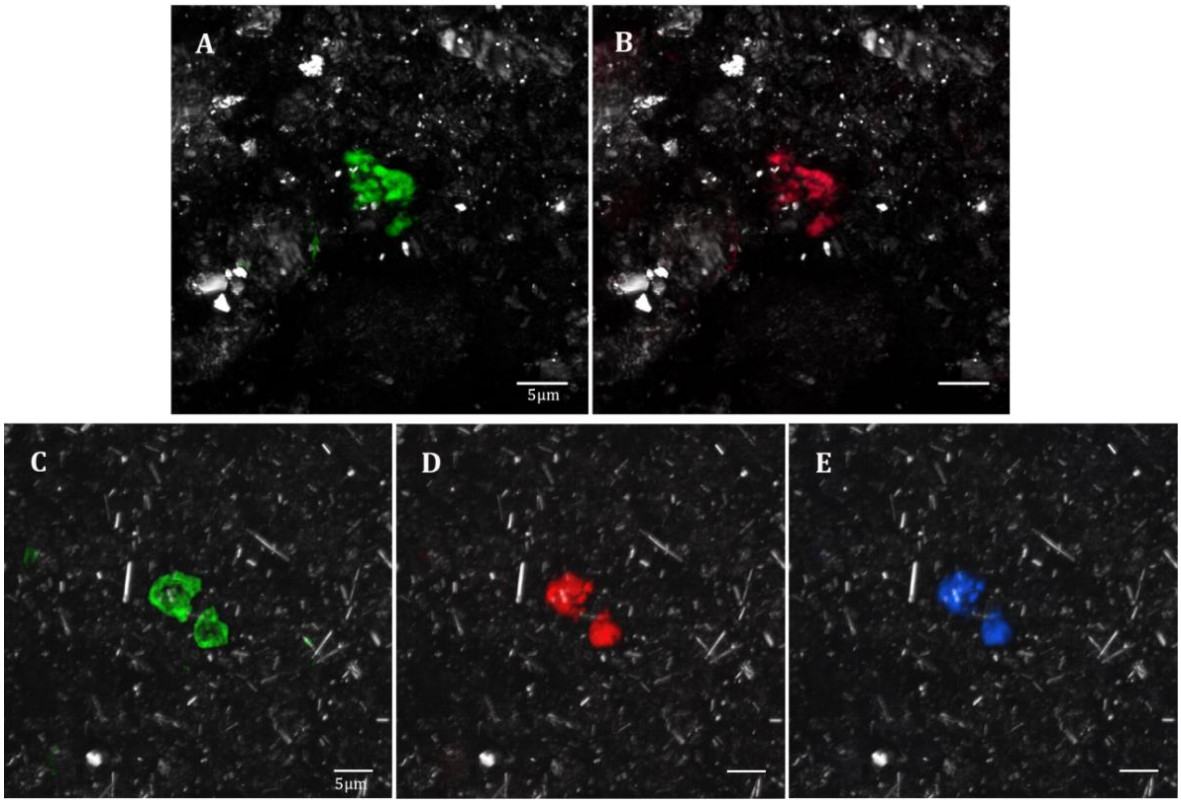

Figure 16. Firmicutes and Actinobacteria phyla in the IPB subsurface detected by CARD-FISH. A-B, Sulfobacillus (red) at 401.9mbs; and C-E, Tessaracoccus genus probe signal (red) and T. lapidicaptus probe signal (blue) at 544 mbs. In green, Syto 9 stain. In grey, reflection. Scale bars, 5µm

The CARD-FISH study showed that *Tessaracoccus* is one of most distributed genus along the BH10 column. All members detected along the column belonged to the specie *T. lapidicaptus* except at 409.7mbs, where no Tlap1449 probe signal could be visualized (Figure 15). This result implies that *T. lapidicaptus* is the main specie of *Tessaracoccus* genus inhabiting IPB subsurface. Of note is the preference of IPB subsurface *Tessaracoccus* species to grow in minimal media (Leandro, personal communication), an extreme oligotrophic condition, which may explain the presence and high distribution of these species in the IPB subsurface.

6.1.3.1.3. Planctomycetes and Chloroflexi phyla

Other Bacteria that were also vastly represented were members of Planctomycetes and Chloroflexi phyla (Figure 17). Although by metagenomic it was only detected members of the phylum Planctomycetes at 228mbs, mainly members of the family Isosphaeraceae (Puente-Sánchez, 2016), CARD-FISH results revealed that this phylum is highly distributed along the column, especially in the deepest areas. Planctomycetes phylum is widely distributed in marine, terrestrial and even in subsurface environments (Fuerst and Sagulenko, 2011). This group of microorganisms involves unusual bacteria due to their lack of peptidoglycan and their intracellular compartmentalization (Fuerst, 2005), which may be related with the origin of the eukaryotic cell (Fuerst and Sagulenko, 2013). Within this group, it is of special interest the anaerobic ammonium-oxidizing (ANAMMOX) bacteria, microorganisms that can oxidize ammonium in anaerobic conditions using nitrite as electron acceptor and generating N_2. To do that, they have a special intracellular compartment called anammoxosome (Neumann et al., 2011). In the IPB subsurface, putative ANAMMOX bacteria were detected at different depths in the BH10 column by using AMX368 probe (Figure 17 and Figure 18A and B).

Despite no others techniques applied in the IPBSL project confirmed the presence of ANAMMOX bacteria in the IPB subsurface, their growth may be supported by the ammonium and nitrite founded along the column, underlining the deepest borehole areas where the amount of ammonium detected was higher. Besides, ANAMMOX bacteria species capable to reduce nitrate to overcome the shortage of ammonium, as well as ANAMMOX species that are able to use alternative energy source as organic matter or ferrous iron as electron donors and oxidized iron or

manganese as electron acceptor, have been described (Neumann et al., 2011), which could be also present along the BH10 column. This group of microorganisms has been previously detected in terrestrial subsurface environments (Lau et al., 2016; Kumar et al., 2017; Momper et al., 2017a) where they have an important role in the nitrogen cycle.

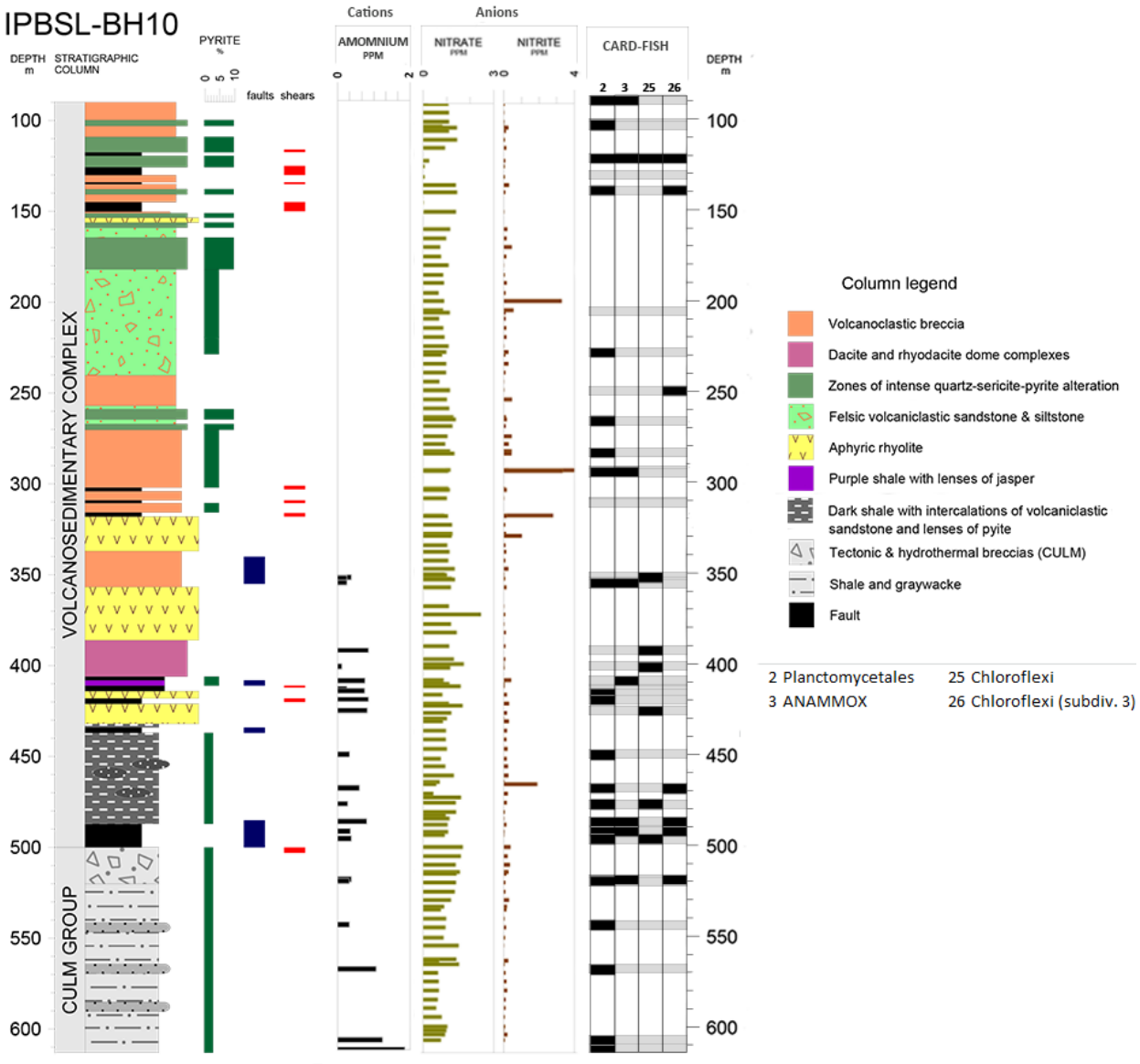

Figure 17. Planctomycetales and Chloroflexi phyla distribution along the BH10 column analyzed by CARD-FISH. Black and grey squares indicate presence or absence of microorganisms at a determined depth respectively. Data about identified compounds and metabolisms of interest obtained during the development of the IPBSL project are shown.

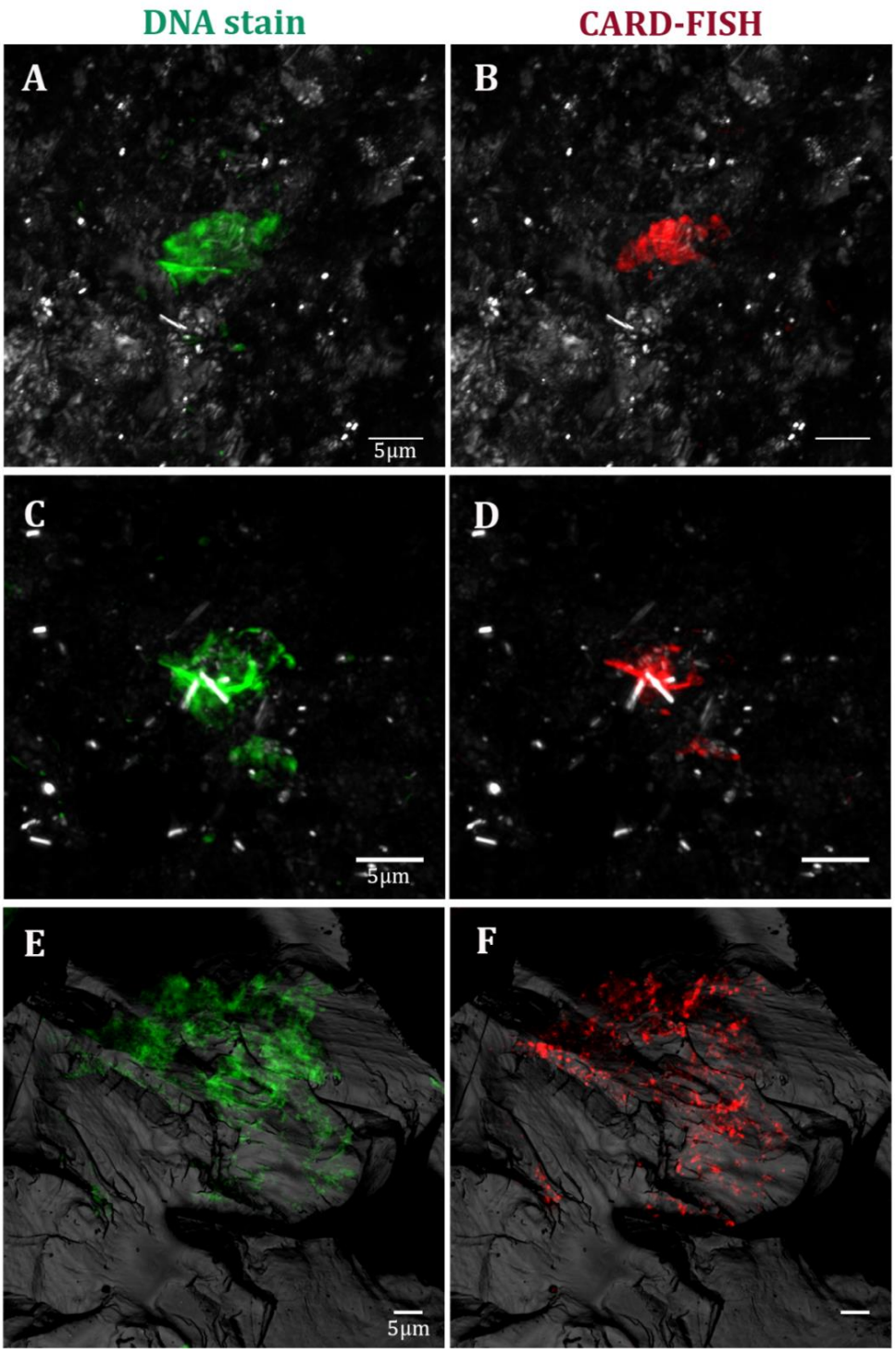

Figure 18. Planctomycetes and Chloroflexi phyla in the IPB subsurface detected by CARD-FISH. A-B, ANAMMOX bacteria at 355.7 mbs; C-D, Chloroflexi: CFX1223 and GNSB941 probes signal at 568.6 mbs; and E-F, Chloroflexi: CFX109 probe signal at 228.6 mbs. In green, Syto9 stain. In red, CARD-FISH signal. In grey, reflection. Scale bars, 5µm

Regarding Chloroflexi, known before as green non-sulfur bacteria, is a large phylum that contains diverse metabolic features. Chloroflexi is a widespread group of bacteria found in a range of microbial habitats, including sub-seafloor (Fry et al., 2008) and continental subsurface environments (Chivian et al., 2008; Breuker et al., 2011; Purkamo et al., 2015; Ino et al., 2016). In the IPBSL project, sequences belonged to the classes Anaerolineae, which englobe filamentous bacteria, and Thermomicrobia has been detected in specific enrichment cultures for methanogens growth (Amils et al, in preparation). Three complementary probes have been used in CARD-FISH experiments to detect members of the Chloroflexi phylum along the BH10 column (Figure 17). CFX1223 and GNSB941 probes, used as a mix, are complementary to most of the Chloroflexi sequences in the SILVA database (Quast et al., 2012), including the Anaerolineae and Thermomicrobia classes. On the other hand, CFX109 probe is able to detect members of the subdivision 3, mostly the class Chloroflexia (Björnsson et al., 2002). CARD-FISH results indicate that members of the Chloroflexi phylum are part of the microbial community of the IPB subsurface. Filamentous colonies as those described in the Anaerolineales order by CFX1223 and GNSB941 probes (Figure 18 C and D) as well as coccoid morphologies with the CFX109 probe have been identified along borehole BH10 (Figure 18E and F).

6.1.3.1.4. Bacteroidetes, Acidobacteria and Cyanobacteria phyla

Using CARD-FISH other phyla less distributed along the column as Bacteroidetes and Acidobacteria have been detected (Figure 19A-E). In spite that metagenomic

analysis corroborated a low biodiversity and number of Acidobacteria phylum in native samples, it was not the case for Bacteroidetes phylum, which was found as one the predominant phyla at 228.6mbs, 336mbs and 420mbs (Figure 11). However, it must be considered that the probe used, CF319a, only detect around 44% of the Bacteroidetes sequences of the SILVA database (Quast et al., 2012). Thus, several microorganisms that belong to this phylum may escape detection by the used CARD-FISH probe as most of the members of the family Cytophagaceae, which has been detected by NGS of native samples (Puente-Sánchez, 2016) and in enrichment cultures (Leandro, personal communication). For that reason, additional probes should be tested, to cover the groups of Bacteroidetes phylum detected by others techniques that are not complementary to the CF319a probe and analyze the real distribution of this phylum in the IPB subsurface.

Surprisingly, especially after the possibility that sample contamination was discarded, Cyanobacteria were detected at some depths of the BH10 column (Figure 19A, F and G). By metagenomic it was shown that this phylum represented the most abundant OTUs at 249, 392, 420, 496 and 607 mbs (Figure 11), being corroborated the presence of these microorganisms in most of this depths by CARD-FISH analysis. As discussed above (see section 3.1.4), far from be an exception, Cyanobacteria phylum has been detected in several subsurface environments (Suzuki et al., 2013; Lau et al., 2014; Nyyssönen et al., 2014; Osburn et al., 2014; Ino et al., 2016). Nonetheless, the role of these organisms in dark environments is still unknown.

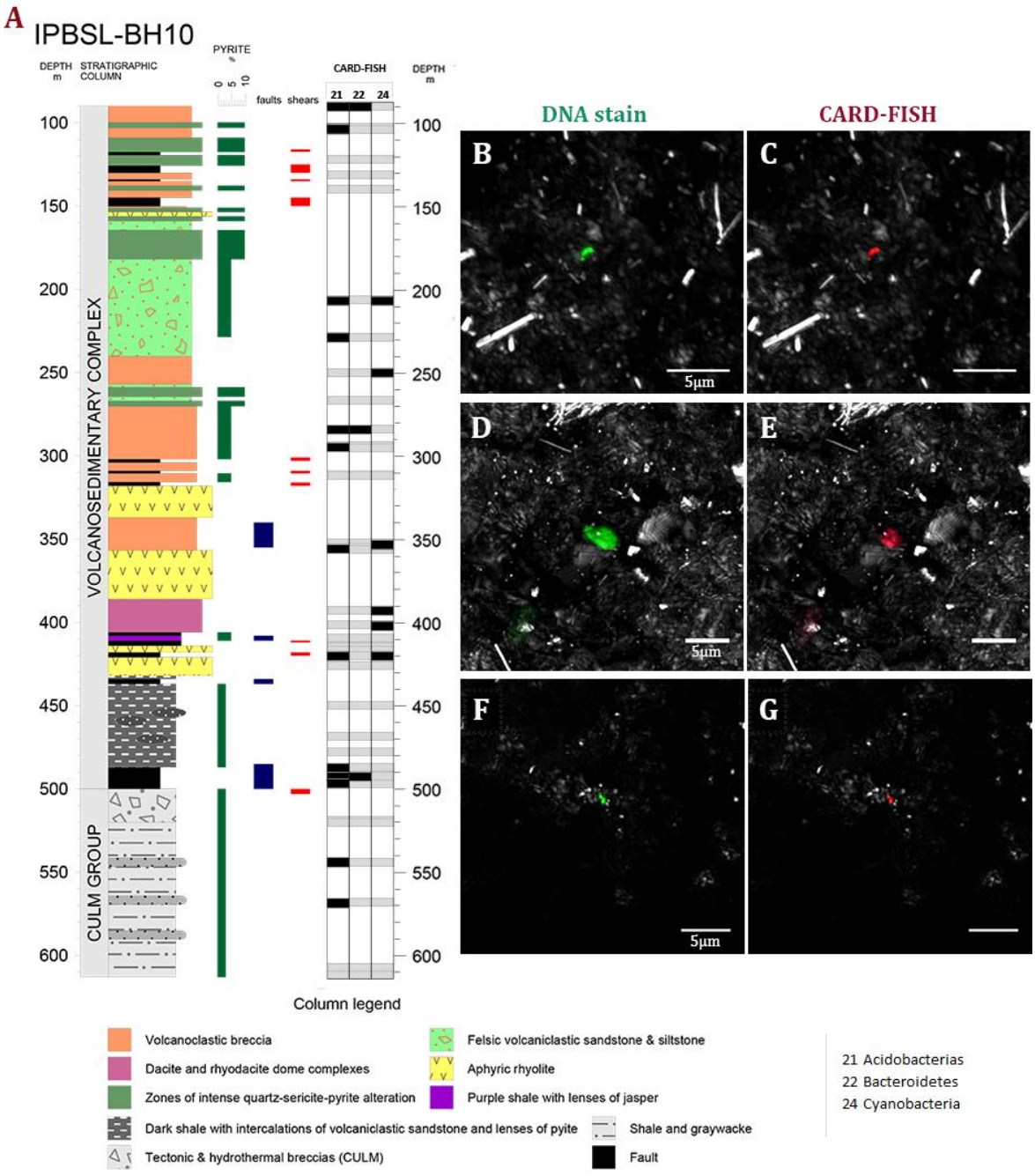

Figure 19. Acidobacteria, Bacteroidetes and Cyanobacteria phylum in the IPB subsurface. A, Distribution along the BH10 column analyzed by CARD-FISH, black and grey squares indicate presence or absence of microorganisms at a determined depth respectively; B-C, Bacteroidetes at 492.6 mbs; D-E, Acidobacteria at 102.6 mbs; and F-G, Cyanobacteria at 206.6 mbs. In green, Syto9 stain signal. In red, CARD-FISH signal. In grey, reflection. Scale bars, 5µm.

6.1.3.2. Archaea diversity and distribution

Of note is the detection of archaea through CARD-FISH (Figure 20) when 16S rRNA metagenomic or cloning techniques have not detected them in the native samples (Figure 11). This incongruence may be due to low number of Archaea showed by CARD-FISH and its difficult detection by sequencing methods, which are techniques that need a large amount of sample for their analysis and in which primers designed specifically to amplify archaeal 16S rRNA gene sequences also amplify bacterial sequences (Bohorquez et al., 2012). Members of the phylum Euryarchaeota were only detected in native rock samples by shotgun metagenomic analysis of sample 420mbs, corresponding only to 0.21% of the sequences (Puente-Sánchez, 2016). At this depth, members of Methanosarcinales order were detected by CARD-FISH.

Nevertheless, different methodologies imply an active archaeal population in IPB subsurface as the detection of CH_4, and H_2 and CO_2 along the column (Figure 20), which may support the growth of autotrophic methanogens; and the observed methane production in specific enrichment cultures for methanogenic microorganisms at different depths, which can be attributed exclusively to the members of the Archaea domain. In addition, by sequence analyses of enrichment cultures from 450.3 and 492.6mbs the presence of members of the *Methanosarcina* genus were identified, while members of the *Methanobacterium* genus were detected in cultures from 139.4mbs (Leandro personal communication). CARD-FISH experiments support the methane production in the IPB subsurface by the detection of members of the archaeal orders Methanosarcinales (Figure 21A and B), Methanobacteriales (Figure 21C and D) and Methanomicrobiales and the family

Methanococcaceae, mainly in those depths where methane and methanogenic activity were detected. Members of the Crenarchaeaota phylum has been detected using CARD-FISH in the IPB subsurface too, although they have not been identified by other techniques applied in the IPBSL project.

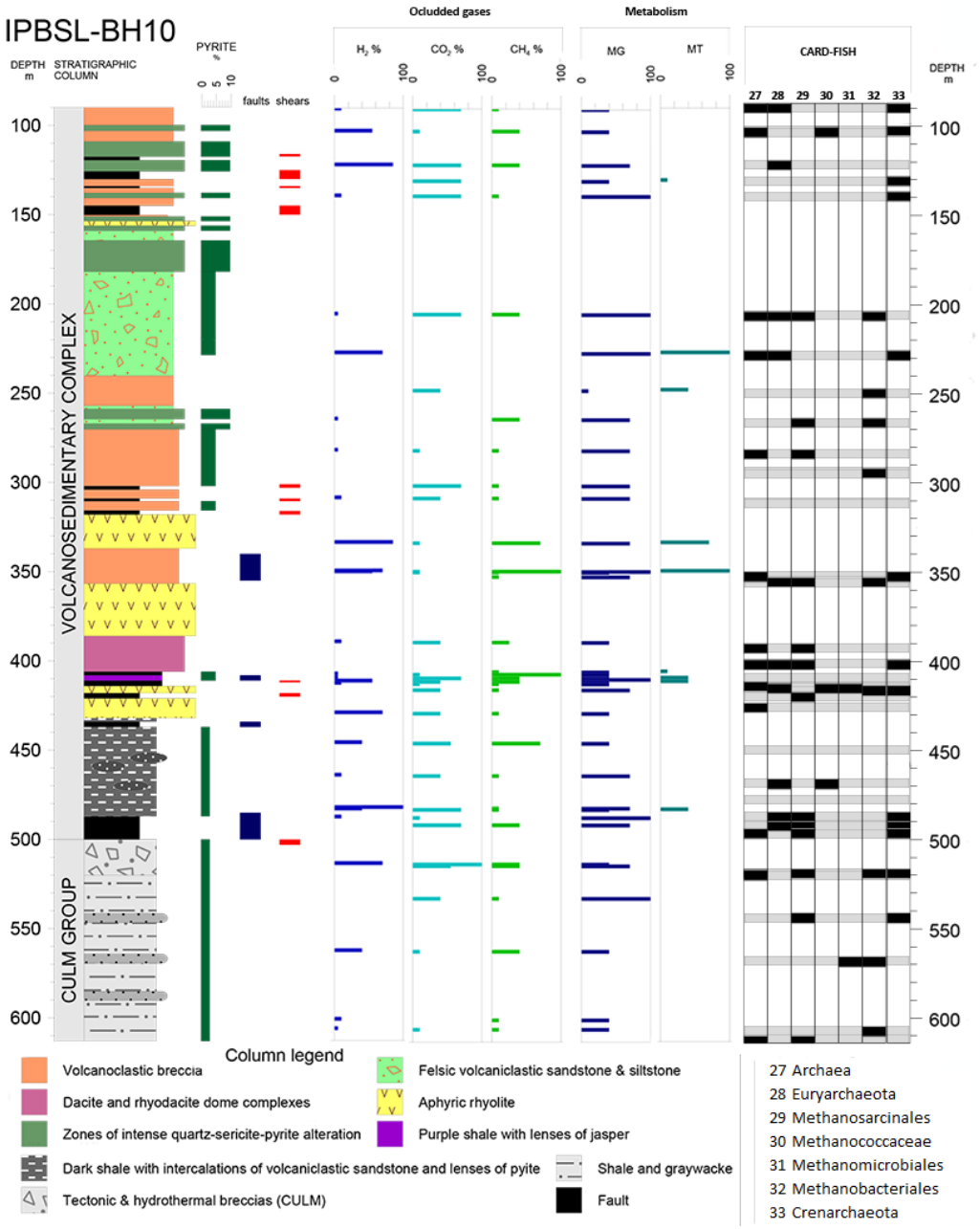

Figure 20. Archaea distribution along the BH10 column analyzed by CARD-FISH. Black squares indicate presence of the microorganisms; white squares indicate absence of the microorganisms. Data about identified compounds and metabolisms of interest obtained during the development of the IPBSL project are shown. MG=methanogenesis; MT= methanotrophy.

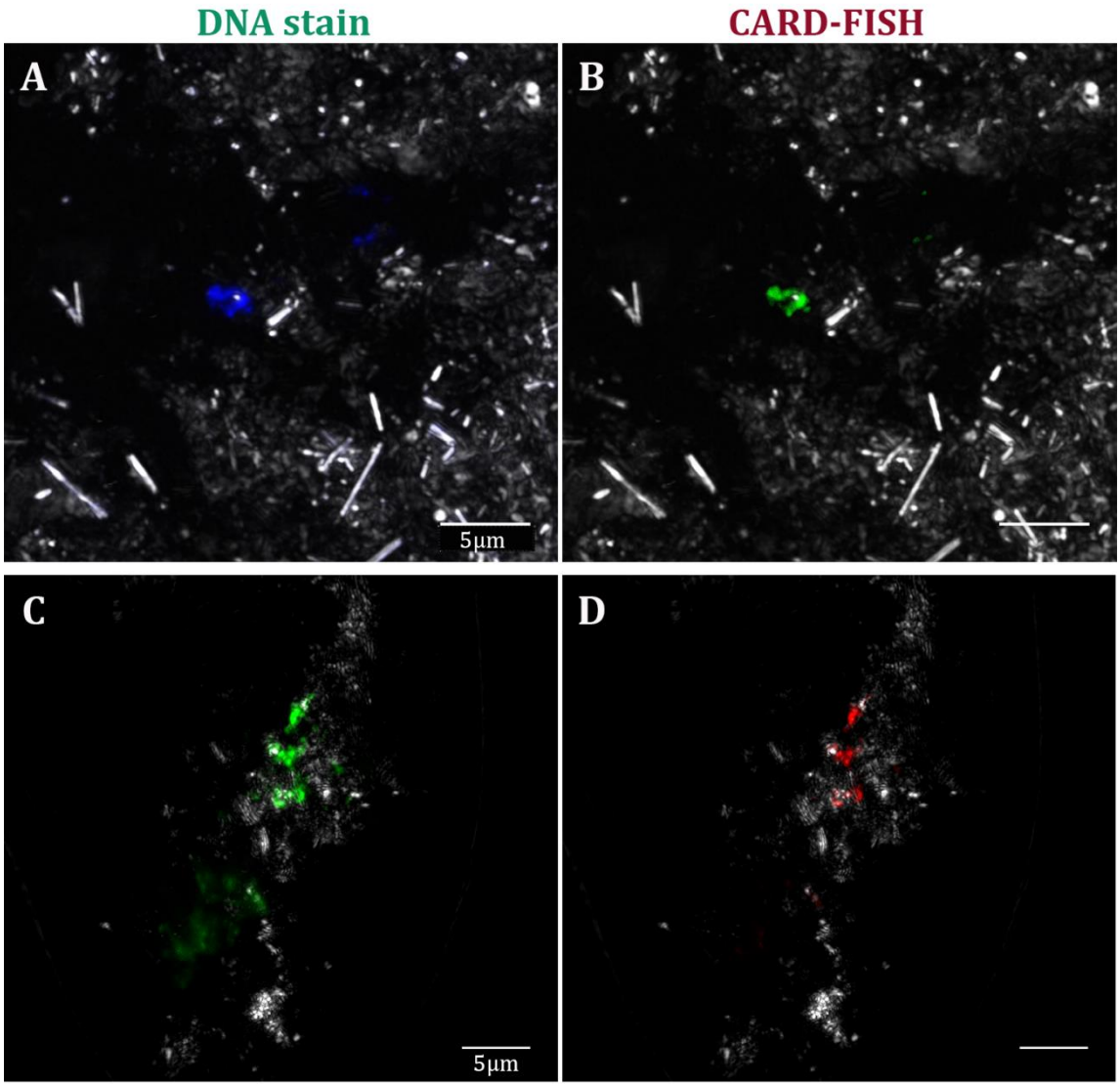

Figure 21. Methanogenic archaea detected at different depths in the IPB subsurface. A-B, Methanosarcinales order at 544mbs (green), in blue DAPI stain; C-D, Methanobacteriales order at 355.7mbs (red), in green, Syto9 stain. In grey, reflection. Scale bars, 5µm.

6.1.4. Limitations of CARD-FISH analysis

Despite the important information that CARD-FISH offered in the analysis of the microbial distribution in the subsurface of the IPB, as any technique, it has limitations. Maybe the main one is the selection of probes to apply. Unless previous

data about microbial diversity are available, CARD-FISH became a “try and failure” assay. Besides, the lack of information about microbial composition of the sample hinders the selection of appropriates protocols to permeabilize the cells (Kubota, 2013), which may translates in a lower rate of microbial detection. Fortunately, as planned in the IPBSL project, microbial diversity data, conveniently complemented with the MARTE project data, was available before hybridizations were started. Thus, most of probes were chosen in consequence. This multi-methodological approach favored to gain a better knowledge of the IPB subsurface biosphere.

Other limitation observed in the use of CARD-FISH to analyze the microbial distribution in subsurface environments should be mentioned. At some depths, there is no correlation between the different complementary probes used. An example is the probe EUB338 I-III, which signal should be detected at all depths since more specific probes at phylum, order, genus or specie level showed the presence of different bacterial members along the entire column (for a complete picture, see Figure 10). This discordance could be due to the low number of microorganisms that are detached from the rock sample after sonication (see below) as well as to the small amount of sample analyzed in each CARD-FISH, which translates in an extremely low number of microorganisms per filter section examined. Nevertheless, the amount of sample per filter couldn’t be increased due to the presence of small mineral particles, which completely cover the surface of the filter, not allowing the correct visualization of the sample by fluorescent microscopy.

6.2. Improving microorganisms detection by microscopy techniques in subsurface environments

To evaluate the number of microorganisms that inhabit subsurface environments, some research groups have recurred to fluorescence microscopy techniques. However, most of these studies have focused their efforts in subsurface water samples, which analysis is far easier than the analysis of rock samples (see section 3.1.2). The projects that studied the number of microorganisms in rock samples tried to detach the microorganisms from the rock and let them in an easily filtered suspension (Zhang et al., 2005; Cockell et al., 2009), as we did using sonication for the study of the microbial distribution in the IPB subsurface. However, we realized that, when we detected microorganisms in our filtered samples, part of the fluorescence remained attached to the rock particles. This observation was indicating that sonication and the subsequent filtration might not be the best protocol for the detection of all microorganisms. In order to check if microorganisms persist habitually attached to the rocks after sonication we tried CARD-FISH on the rock sample itself. Our results show that an important fraction of the microorganisms remain attached to the rock particles even after the sonication step (Figure 22). Thus, when analyzing the number of microorganisms in a rock sample using this protocol, it should be taken into account that the total number of microorganisms could be underestimated, since a high percentage of microorganisms remain attached to the substrate. Instead, a direct count of microorganisms in the substrate could provide more reliable data regarding the

biomass present in these environments, despite the difficulty of working directly with rock substrates.

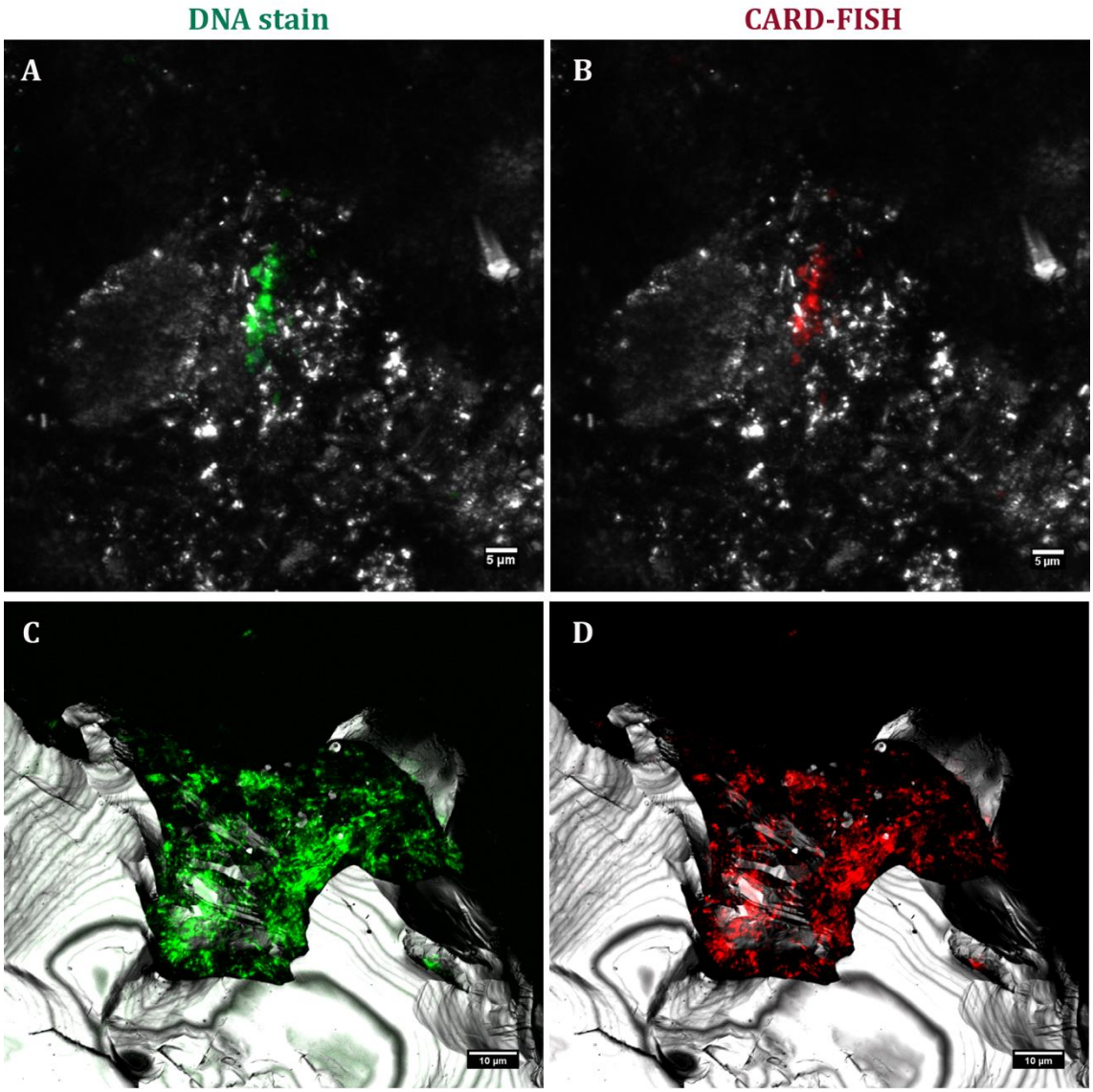

Figure 22. Comparison of microorganisms detected by CARD-FISH by using filters (A-B) or rocks (C-D) in a sample from 139.4 mbs after sonication. In green, Syto9 stain. In red, bacteria detected with EUB338 I-III probe. In grey, reflection. Scale bar 5 µm (A-B) and 10 µm (C-D).

Due to this observation, the rest of the reported experiments were performed directly on the rock substrates. Nevertheless, no counting of microorganisms was

done in the IPB subsurface due to the limited amount of fixed samples and the high volume of samples that would be needed to obtain a statistically confident result.

6.3. Microbial interactions in IPB subsurface

Several studies have shown that the metabolic cooperation between species seems to be critical for the survival of the microorganisms in oligotrophic environments maximizing the energy obtaining (Morris et al., 2013). In fact, it has been proposed the existence of an interconnected network of activities that supports the subsurface biosphere in which the metabolic products from some of these microorganisms are utilized by others (Hug et al., 2016). However, the low number of cultured syntrophic microorganisms limits our understanding of their association (Orphan, 2009).

One of the greatest advantages of FISH techniques is the possibility of study interactions between microorganisms, cultured or uncultured, through multiple hybridizations. As mentioned, in some IPB subsurface samples, DNA stain signals were more abundant than total probe signals (Figure 23), which can be related with the existence of mixed colonies of different types of microorganisms and the detection of only one of those microbial groups by the specific probe used. To corroborate if different species of microorganisms are interacting in the IPB subsurface, double CARD-FISH analysis with different probes were carried out.

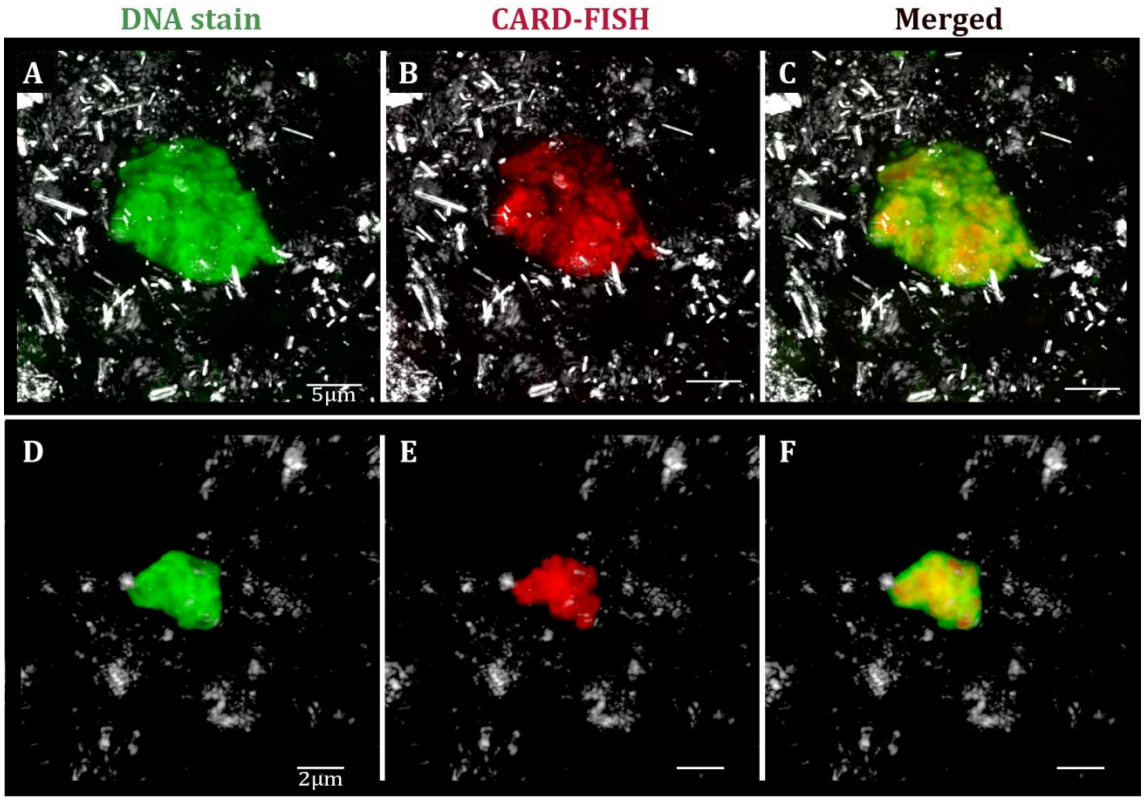

Figure 23. Detection of bacteria (A-C) and archaea (D-F) in subsurface rock samples at 420mbs and 496.8mbs respectively. In green, Syto9 stain. In red, CARD-FISH signal. In gray, reflection. Scale bars, 5µm (A-C) and 2 µm (D-F)

6.3.1. Bacteria and Archaea interaction in IPB subsurface

As it is shown in Figure 23, both bacteria and archaea probe signals were lower than total DNA stain at some depths. Consequently, we tried double hybridizations with general EUB338 I-III and ARC915 probes to verify if mixed colonies of bacteria and archaea were present in the IPB subsurface. Figure 24 shows the existence of bacteria and archaea mixed colonies at some depths, which may be related with a metabolic association between microorganisms from both domains.

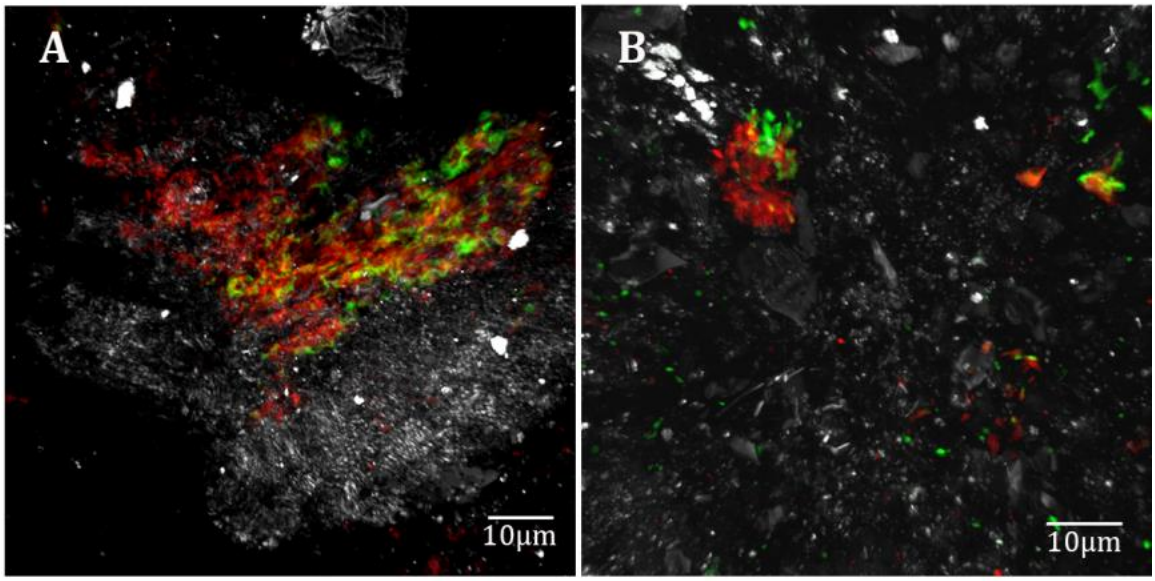

Figure 24. CARD-FISH detection of bacterial and archaeal mixed colonies in drilled samples from different depts. Double CARD-FISH with bacteria probe (green) and archaea probe (red) at (A) 139.4mbs and (B) 284mbs. Scale bars: 10 µm.

Actually, FISH analysis of enrichment cultures designed to grow methanogenic archaea showed the presence of mixed colonies even after successive transfers in fresh media (Leandro, personal communication). A probably obligatory syntrophic association between bacteria and archaea could explain this observation as well as the failure, up to now, to isolate archaea from the IPB subsurface. Actually, 16S rRNA metagenomics of these cultures showed the presence of microorganisms from both domains, represented by *Methanosarcina* and *Methanocella* as archaeal members and *Syntrophomonas* and *Acetobacterium* as bacterial members. On one hand, it has been showed that members of the genus *Syntrophomonas*, which consume fatty acids and produce acetate or H_2, grow in co-culture with methanogens as *Methanosarcina* (Beaty and McInerney, 1989) and members of the genus *Methanocella* (Li et al., 2015), which consume the metabolic products generated by the bacteria. On the other hand, a metabolic consortium may exist

between *Acetobacterium*, an acetogenic microorganism, and *Methanosarcina* spp., which may use the produced acetate by *Acetobacterium* as energy source (Winter and Wolfe, 1979). Associations of this nature could be operating not only in the enrichment cultures but also in the IPB subsurface.

Furthermore, previous studies had described syntrophic consortiums of bacteria and archaea in anoxic sediments promoting the AOM (Knittel and Boetius, 2009; Briggs et al., 2011) and the existence of these syntrophic consortiums in continental subsurface environments has been proposed (Lau et al., 2016). Despite that the existence of this type of consortium has not been confirmed in the IPB subsurface, the fact of finding methane-oxidizing metabolisms along BH10 column by enrichment cultures (Figure 20) and the detection of ANME2c microorganisms in the MARTE project framework (Puente-Sánchez, 2016) as well as members of the *Desulfosarcina/Desulfococcus* group (see section 6.1.3.1.1), which can be partners of anaerobic methanotrophs of the ANME-2 clade (Schreiber et al., 2010), could be an indication of the presence of an AOM association in the IPB subsurface.

In addition, other studies have shown the co-occurrence of microorganisms from both domains in a broad range of habitats which are important for the maintenance of biogeochemical cycles such as the iron, sulfur, nitrogen or carbon cycles (Edwards et al., 2000; Koch et al., 2006; Weidler et al., 2008; Justice et al., 2012; Probst et al., 2013). Unfortunately, in most cases the structural relationship between both kinds of microorganisms is still unknown.

Futures studies should be conducted to identify these microorganisms and the nature of their metabolic association in the IPB subsurface.

6.3.2. Operative iron and sulfur cycles in the IPB subsurface

As mentioned, one of the most common microorganisms inhabiting the IPB subsurface belongs to the genus *Acidovorax*. As discussed before, *Acidovorax* spp. have been described as an iron-oxidizing bacteria (Kappler et al., 2005; Chakraborty and Picardal, 2013) and, consequently, they are putative microorganisms involved in the massive sulfide dissolution through the generation of ferric iron in anaerobic conditions (see section 6.5).

In the IPB subsurface, usually general DNA stain of different samples show a higher number of microorganisms than those corresponding to *Acidovorax*. This might imply that different species of microorganisms in the subsurface are co-inhabiting with these species. Different combinations of probes were used to identify possible *Acidovorax* partners. As metabolic associations are usual between microorganisms, we first tried double hybridizations with *Acidovorax* probes and complementary probes to identify known iron-reducing microorganisms, which could take advantage of the ferric iron produced by *Acidovorax*. Actually, members of the genus *Acidovorax* have been previously described showing anaerobic cycling of iron in co-culture with iron-reducing bacteria (Straub et al., 2004). In the IPB subsurface, two of the main co-inhabitants of *Acidovorax* belong to the genera *Acidithiobacillus* (Figure 25A-C) and *Acidiphillium* (Figure 25D-F), both capable of an anaerobic respiration using ferric iron (Osorio et al., 2013; Vera et al., 2013). The interaction between these living microorganisms, iron-oxidizers and iron-reducers, corroborates the importance of cooperation between species in

underground environments to maximize the energy obtaining, implying the existence of an operative iron cycle in the IPB subsurface at microniche level.

In addition, members of *Sulfobacillus* genus are commonly found in the IPB subsurface intimately associated with *Acidovorax* (Figure 25G-I) forming intricate mixed colonies (Figure 25J). In spite that several kind of metabolisms has been described for *Sulfobacillus* spp., under anaerobic conditions these microorganisms are able to reduced iron using organic matter or CO_2 as carbon source and $S_4O_6^{2-}$, S^0 or H_2 as electron donors (Justice et al., 2014). Although the nature of the relationship between *Acidovorax* and *Sulfobacillus* is unknown, we estimated that if *Acidovorax*, as iron oxidizer, is able to enhance metal sulfides dissolution, as pyrite, *Sulfobacillus* would be able to use reduced sulfur compounds as electron donors and/or ferric iron as electron acceptor, the main products of this reaction (Vera et al., 2013). In fact, it has been shown that *Sulfobacillus* species are able to enhance the metallic sulfide bioleaching in co-cultures with iron oxidizers, at least in aerobic conditions (Watling et al., 2008).

On the other hand, it has been found that *Acidovorax* is not the only supposed collaborator of *Sulfobacillus*. Previous studies have shown the co-ocurrence of sulfur-oxidizing and sulfate-reducing microorganisms in subsurface environments maintaining an operative a sulfur cycle (Lau et al., 2016). Thus, due to the co-occurrence at several depths of SRB and *Sulfobacillus* detected by CARD-FISH (Figure 26), both related with sulfur metabolism, we thought that these microorganisms could be interacting in the IPB subsurface. To test it, double hybridizations with *Sulfobacillus* specific probe and SRB probe were performed and mixed colonies of both microorganisms were detected (Figure 25K-M) at

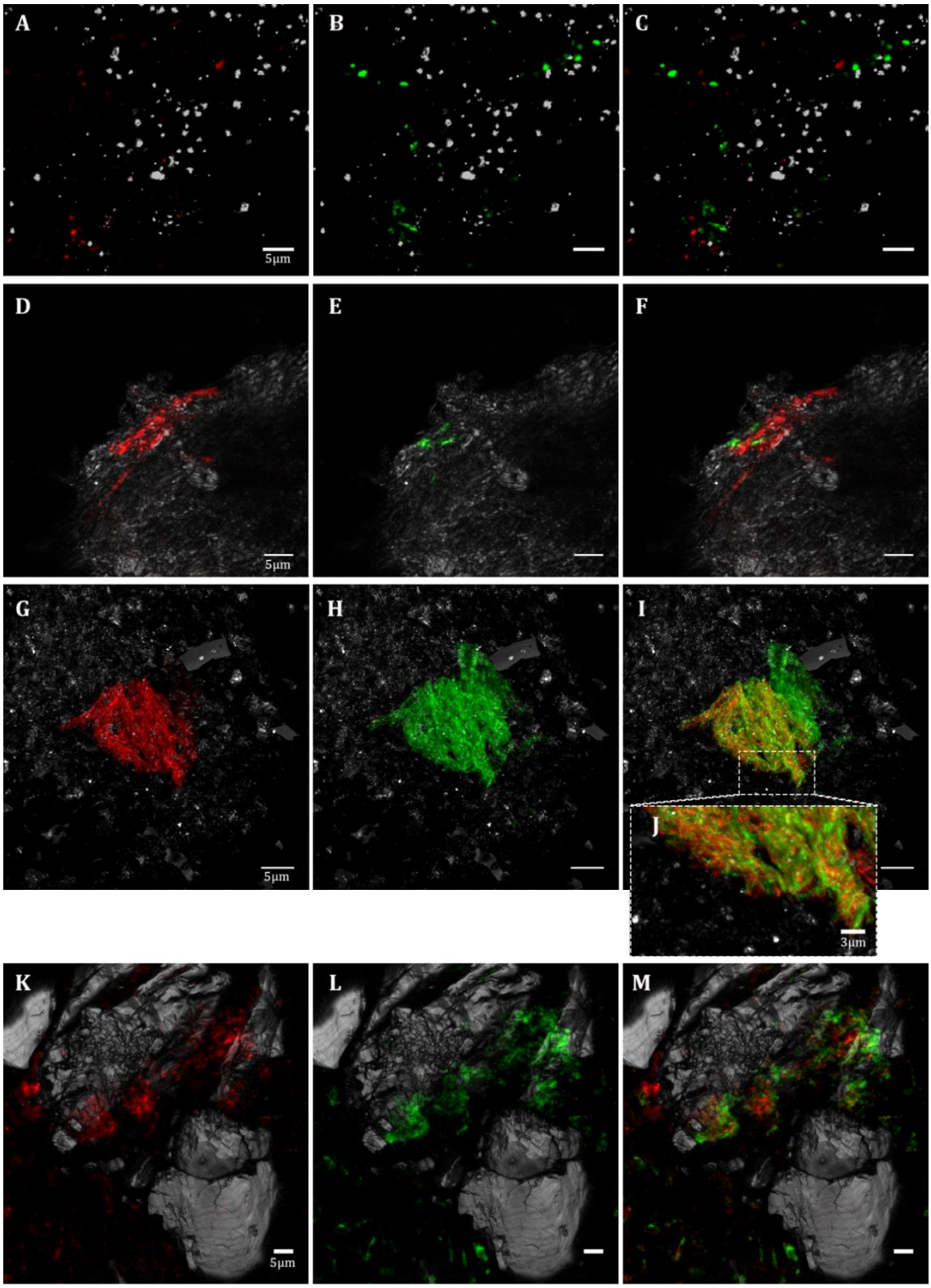

Figure 25. Putative iron and sulfur cycles in the IPB subsurface. A-C, interaction of Acidovorax (red) and Acidithiobacillus (green) at 414.8mbs; D-F, interaction of Acidovorax (red) and Acidiphillium (green) at 414.8mbs; G-J, interaction of Acidovorax (red) and Sulfobacillus (green) at 249.8mbs; K-M, interaction of Sulfobacillus (red) and SRB (green) at 139.4mbs;. In grey, reflection. Scale bars 5µm except J, 3µm.

several depths, which is a strong indication of the existence of an active sulfur cycle in IPB subsurface.

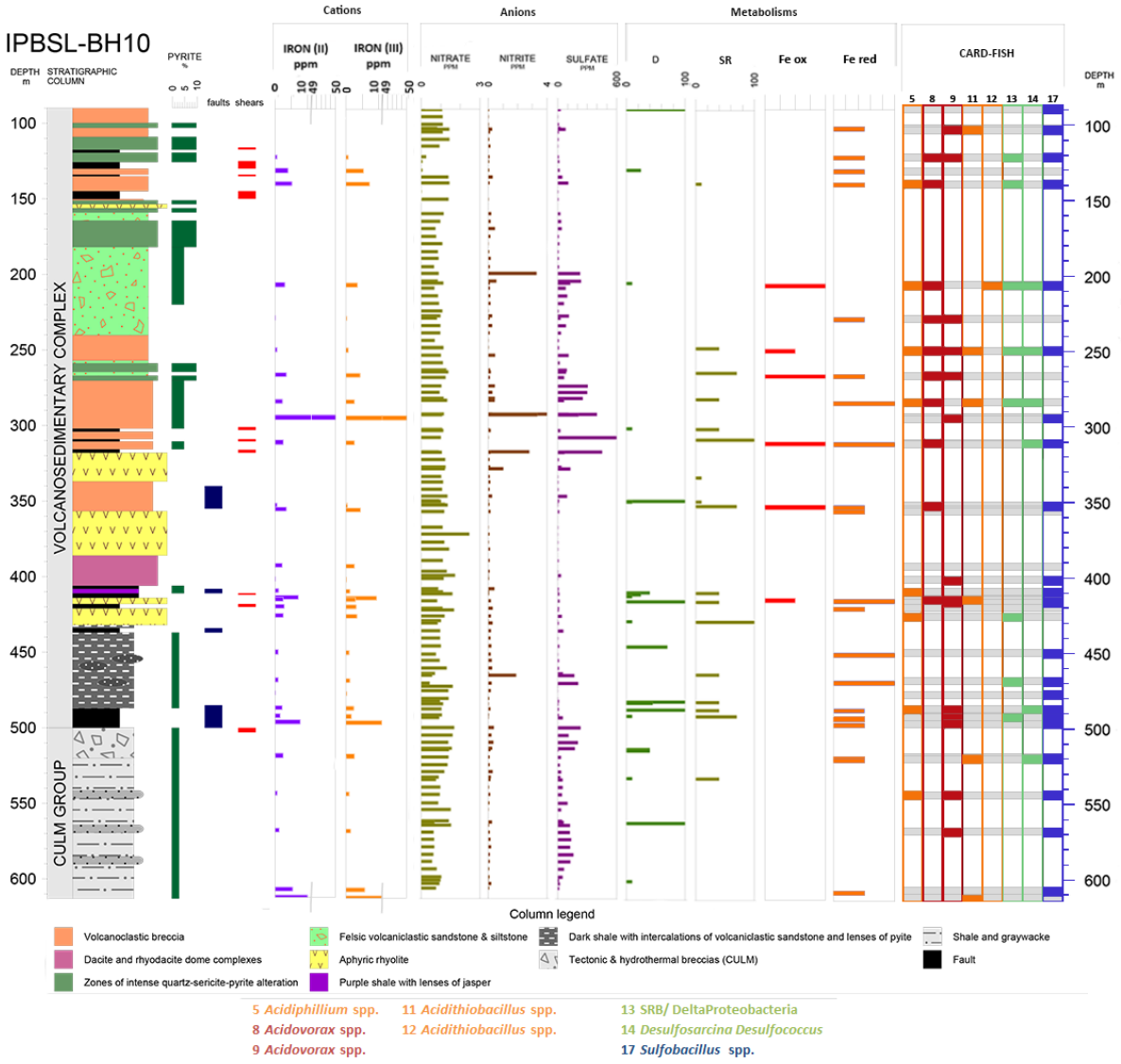

Figure 26. Distribution of iron-oxidizing (red), iron-reducing (orange), sulfur-oxidizing (blue) and sulfate-reducing (green) microorganisms along BH10 column analyzed by CARD-FISH. Grey squares indicate absence of microorganisms at a determined depth. Data about identified compounds and metabolisms of interest obtained during the development of the IPBSL project are shown.

In addition, due to the observed relationship between *Acidovorax* and *Sulfobacillus*, we inferred that iron and sulfur cycle might be interconnected. Actually, the presence of iron and sulfur metabolism related microorganisms have been observed frequently at the same depths along the BH10 column (Figure 26). As a consequence, we tried a quadruple CARD-FISH with *Acidovorax*, *Acidiphillium*, *Sulfobacillus* and SRB probes, representing iron oxidation, iron-reduction, sulfur oxidation and sulfate reduction respectively.

Figure 27 shows the interaction between these four types of microorganisms. The occurrence of both oxidizers and reducers of iron and sulfur compounds at the same microniche, in an environment where the metal sulfides are the main minerals of the system, raises the possibility that the dissolution of these ores is the key to understanding their collaboration. Actually, this interaction was observed at different depths (139.4mbs, 206.6 mbs and 249.8 mbs) in which, in addition, weathered pyrite has been reported (Figure 26), farther supporting this hypothesis.

However, their association is quite intriguing because the optimal pH described for the characterized strains, as well as the redox potentials described for their metabolisms, are quite different. On the one hand, *Acidiphillium* and *Sulfobacillus* are acidophilic microorganisms (Johnson, 1998), whereas *Acidovorax* and SRB generally grow at circumneutral pH (Barton and Tomei, 1995; Willems, 2014). However, it must be borne in mind that, so far, no representative of these genera has been isolated of the IPB subsurface and, therefore, the native strains of this environment may show a wider range of tolerance to pH. In fact, acidophilic SRB have been isolated from Río Tinto‘s sediments (Sánchez-Andrea et al., 2013) and

members of the genus *Acidovorax* have been detected in acid mine drainages environments (Méndez-García et al., 2015) and recently in the acidic anaerobic sediments of Río Tinto (Kappler, personal communication), so the optimum pH of each of these microorganisms may not be an impediment to their association. On the other hand, the presence of these microorganisms in the same microniche does not fit with the thermodynamic models. Sulfate reduction occurs at negative redox potentials (Barton and Tomei, 1995), while both the nitrate reduction, carried out by *Acidovorax*, and the Fe^{3+} reduction require a positive redox potential (Thauer et al., 1977; Weber et al., 2006). Generally, the underground systems show a redox stratification in which the different metabolisms are distributed, as have been observed in wetlands and sediments (Amend and Teske, 2005; Sánchez-Andrea et al., 2011) and, as far as we know, an association of this type has never been described before. Therefore, the thermodynamic explanation of this association remains, as the pH, an open question. Further studies, that are beyond this work, are needed to determine how the redox potential influences the cooperation between these microorganisms as well as the possible influence of the presence of biofilms (see below) in the distribution and management of the redox potential.

Nevertheless, although much more data is needed to interpret the results obtained through CARD-FISH, the fact that these microorganisms are present in the same depths as well as their co-localization in the same colonies at some of those depths is a strong indication that the iron cycle and the sulfur cycle could be operating jointly in the IPB subsurface, possibly at a microniche level.

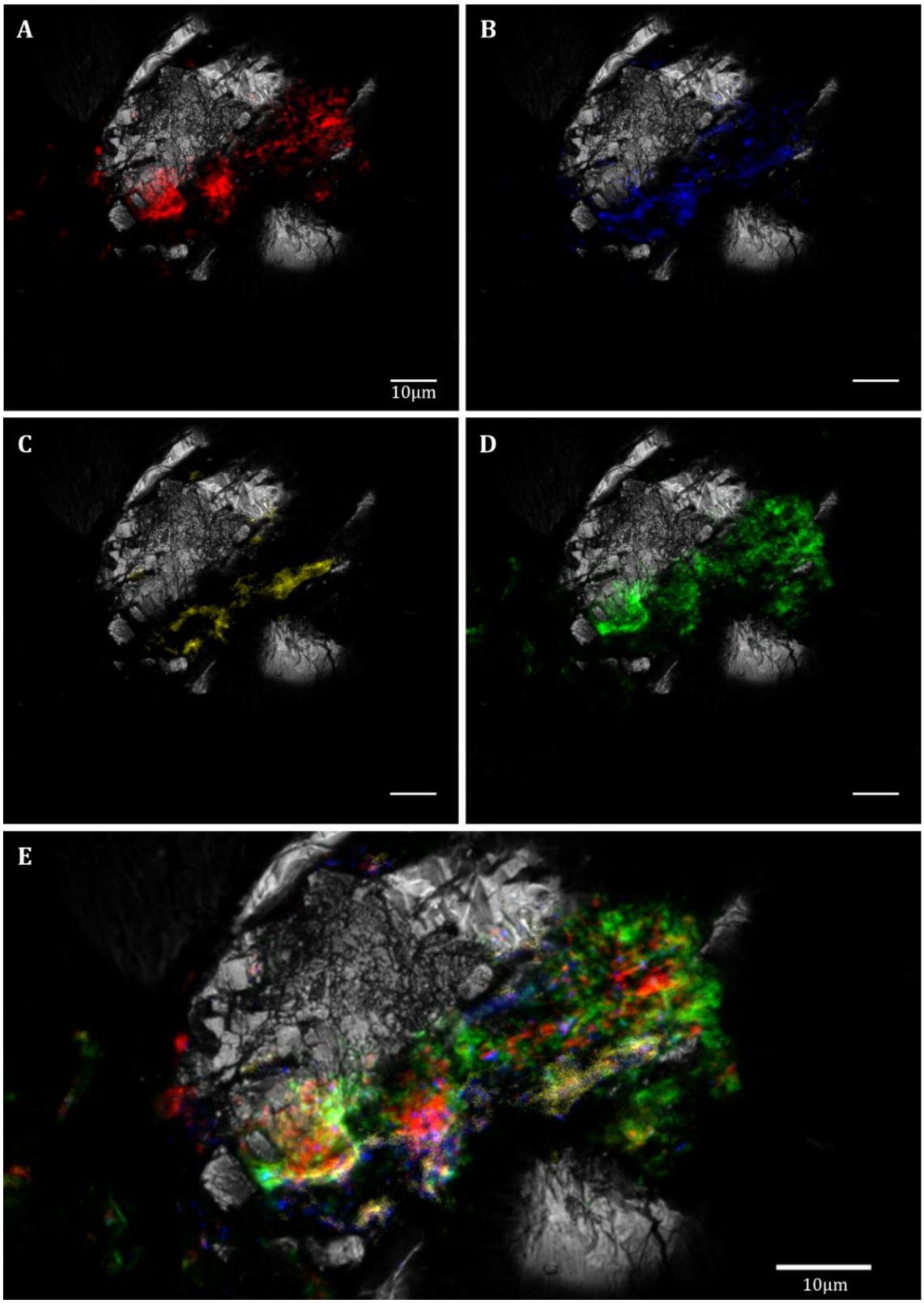

Figure 27. Putative iron and sulfur cycle interconnection in the IPB subsurface at 139.4mbs. A, Acidovorax (red); B, Sulfobacillus (blue); C, Acidiphillium (yellow); D, sulfate-reducing bacteria (green); and E, merged. In grey, reflection. Scale bars, 10µm

6.4. Biofilms

Natural microbial communities most often live attached to surfaces or interfaces forming biofilms, defined as the coexistence of one or more species of microorganisms sharing space in a self-produced matrix. The matrix is a three-dimensional structure mostly composed of extracellular polymeric substances (EPS) such as polysaccharides, proteins, nucleic acids, lipids and, above all, water (Flemming and Wingender, 2010; Flemming, 2011). Therefore, the development of biofilms implies a change in genetic regulation and the consumption of energy to generate its components and maintain biofilm integrity (Stoodley et al., 2002; Sauer, 2003; Saville et al., 2011). However, biofilm lifestyle provides an ideal microenvironment where microorganisms can survive and grow even when external conditions are adverse. Some of the functions associated to biofilms are: adhesion to surfaces, retention of water, structuration of biomass, sorption of organic and inorganic compounds, enzymatic activity, nutrient source, redox regulation, or quorum sensing among others (Flemming, 2011; Flemming et al., 2016).

It is considered that in deep subsurface environments, where geochemistry and geohydrology control nutrient and water availability, most microorganisms show very low metabolic rates or remain in a dormant state in poor porous matrix rocks (Fredrickson et al., 1997b). Consequently, it has been suggested that in these conditions microbial biofilms may not exist due to the high energetic cost required for their formation and maintenance (Coombs et al., 2010). Still, the ability of isolated subsurface microorganisms to form biofilms has been demonstrated *in*

vitro (Sakurai and Yoshikawa, 2012) as well as the formation of biofilms through *in situ* colonization experiments on added glass and rock surfaces in natural subsurface environments (Anderson et al., 2006a; Anderson et al., 2006b). In addition, a few studies have shown that microbial biofilms are formed in native rock matrixes at least in fracture zones, where the flux of water and nutrients is higher, or near the surface, where oxygen is present (Pfiffner et al., 2006; Wanger et al., 2006; Jagevall et al., 2011). But up to now, there has been no information about the formation of native biofilms in deep poor porous rock matrix, where there is no oxygen, water is limited and life is supported mainly by anaerobic low energy metabolisms.

Fluorescence microscopy techniques are useful tools to study the three-dimensional structure of biofilms, but, as was discussed above, they have been discarded to study subsurface samples because the reflection and autofluorescence of some minerals in rock samples make very difficult to distinguish them from true positive signals (Jagevall et al., 2011). Instead, other microscopy techniques such as SEM have been applied, but no information about microbial or EPS composition of the biofilms was obtained (Anderson et al., 2006a; Wanger et al., 2006; MacLean et al., 2007).

FISH techniques combined with FLBA and other specific stains offer valuable information about biofilms (Neu and Lawrence, 2014). While FISH allows the identification of a particular living microorganism present in a sample due to the use of specific 16S RNA probes (Amann and Fuchs, 2008), lectins labeled with fluorophores used in combination with other specific stains for DNA, proteins and lipids can provide data about the biofilm composition (Neu and Lawrence, 2014).

6.4.1. Improving microbial biofilms detection

CARD-FISH combined with FLBA was applied to deep subsurface samples of the IPB to determine the presence of natural microbial biofilms in the rock matrix. Different lectins were tested (see Table 4, materials and methods) and parallel hybridizations were carried out in clean rock controls with no signal detection. CARD-FISH and FLBA analysis revealed the presence of living bacterial and archaeal microcolonies surrounded by traces of polysaccharides at all checked depths (Figure 28 A-B). It was detected the presence of α-linked fucose residues and galactosyl (β-1,3) N-acetylgalactosamine residues in some of the biofilms visualized through AAL, UEA I or PNA lectins respectively. Nevertheless, Concanavalin A (Con A), which specifically binds internal and non-reducing α-D glucosyl and α-D mannosyl residues, was the lectin that revealed broader biofilm surface, which is consistent with previous results that indicated that both monosaccharides were the most abundant sugars in the subsurface of the IPB (Parro, unpublished data). However, the lectin signal was poor and scarce, even when more than one lectin was used to reveal the biofilm structure. This fact may suggest that either i) the existence of certain glycoconjugates unrecognized by the lectin used; ii) that in the subsurface, EPS production may be reduced in response to low nutrient levels (Stanley and Lazazzera, 2004); or iii) the signals correspond to the remains of the exopolysaccharides which were consumed by microorganisms, since the EPS matrix can serve as a reservoir of nutrients to maintain the geobiochemical cycles (Pinchuk et al., 2008; Neu and Lawrence, 2016). Furthermore, because CARD-FISH requires a large and aggressive sample

preparation protocol, the low and sparse lectin signals observed could be also due to the numerous washing steps, the inactivation of peroxidases or the cell permeabilization steps required by this technique.

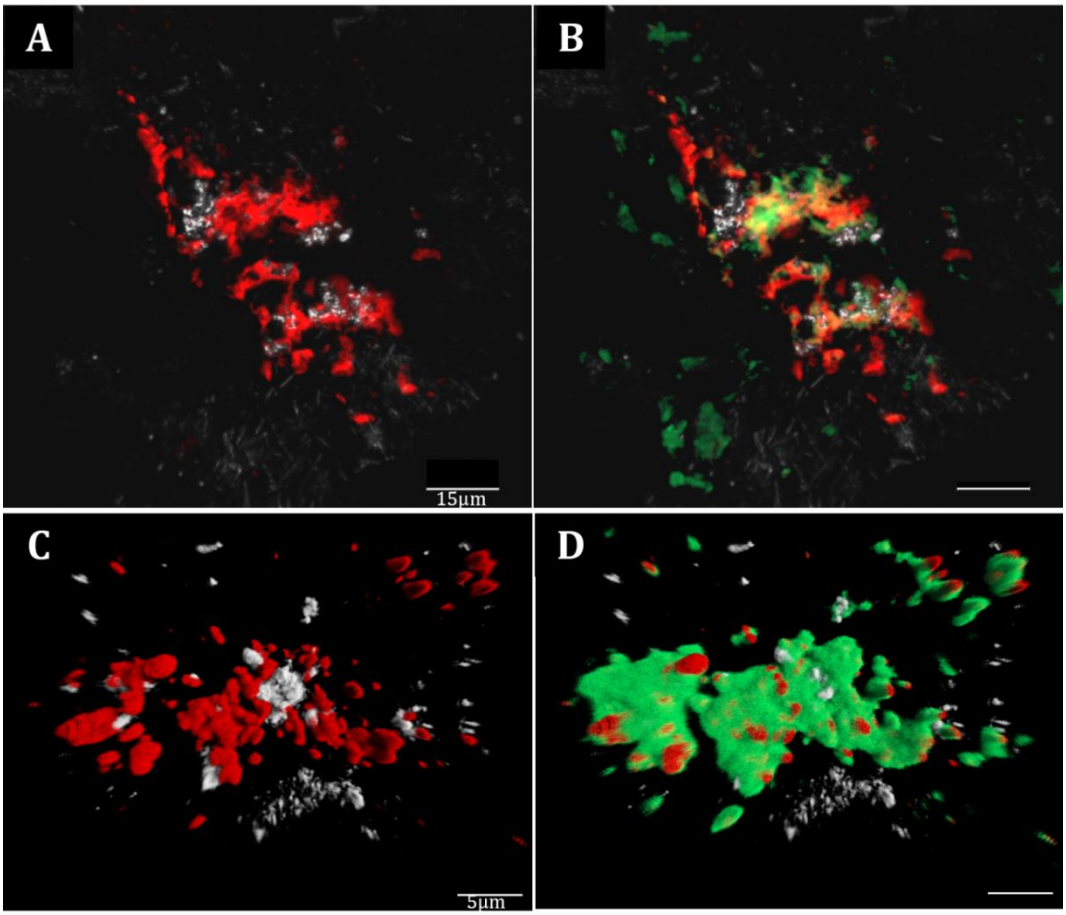

Figure 28. Bacterial biofilms detected at 414.8mbs by CARD-FISH (A and B) and FISH (C and D). In red, EUB338 I-III probe signal. In green, FITC-ConA lectin signal. In gray, reflection. Scale bars: A and B, 15 µm; C and D, 5 µm.

To avoid the influence of the CARD-FISH protocol on the integrity of the biofilms, we repeated the experiment using FISH for microorganism detection. The FISH-FLBA hybridization showed the existence of well conserved and mature biofilms on the subsurface rock matrix (Figure 28C and D). However, the number of colonies visualized by FISH was lower, as expected, than by CARD-FISH. This

reduction in the number of microorganisms detected in comparison to CARD-FISH may be due to the low metabolic rate that some microorganisms present in the subsurface, since FISH signal intensity is directly proportional to the number of ribosomes present in the cells (Pernthaler et al., 2001). Consequently, the microorganisms that comprise these biofilms detected by FISH are not in a dormant state but are metabolically active, which corroborates the concept of a living and functional subsurface biosphere.

In order to visualize as many microorganisms as possible without compromising the integrity of biofilms, DOPE-FISH (Stoecker et al., 2010) was checked as an alternative signal amplification method. The signal intensity of DOPE-FISH was compared with FISH signal using *E. coli* in laboratory control experiments (Figure 29). These results showed that the fluorescence signal using DOPE-FISH was almost twice that of FISH, in accordance with Stoecker et al. (2010). However, DOPE-FISH background was 3.7 times higher than that of FISH, resulting in a final increase of just 1.2 times in net fluorescence signal compared to FISH, defined here as cell fluorescence minus background fluorescence, when the hybridization was carried out in the same conditions. To increase the signal-noise ratio, alternative hybridization buffers were tested. It has been stated that the CARD-FISH buffer, which contains blocking reagent and dextran sulfate, increase the signal up to 20% (Schimak et al., 2015). In this work, geneFISH hybridization buffer (Moraru et al., 2010), which contains extra blocking reagents such as salmon sperm DNA and yeast RNA to decrease the background, was tested. Our results indicate that the use of geneFISH buffer in a pre-hybridization incubation as well as in the hybridization not only decreased the background intensity but increased the cell

signal intensity, yielding an increase of net fluorescence signal in DOPE-FISH of 2.4 times over that of FISH (Fig. 3). Other methods for signal amplification such as MIL-FISH (Schimak et al., 2015) were tested but no remarkable improvement was achieved in our samples (data not shown).

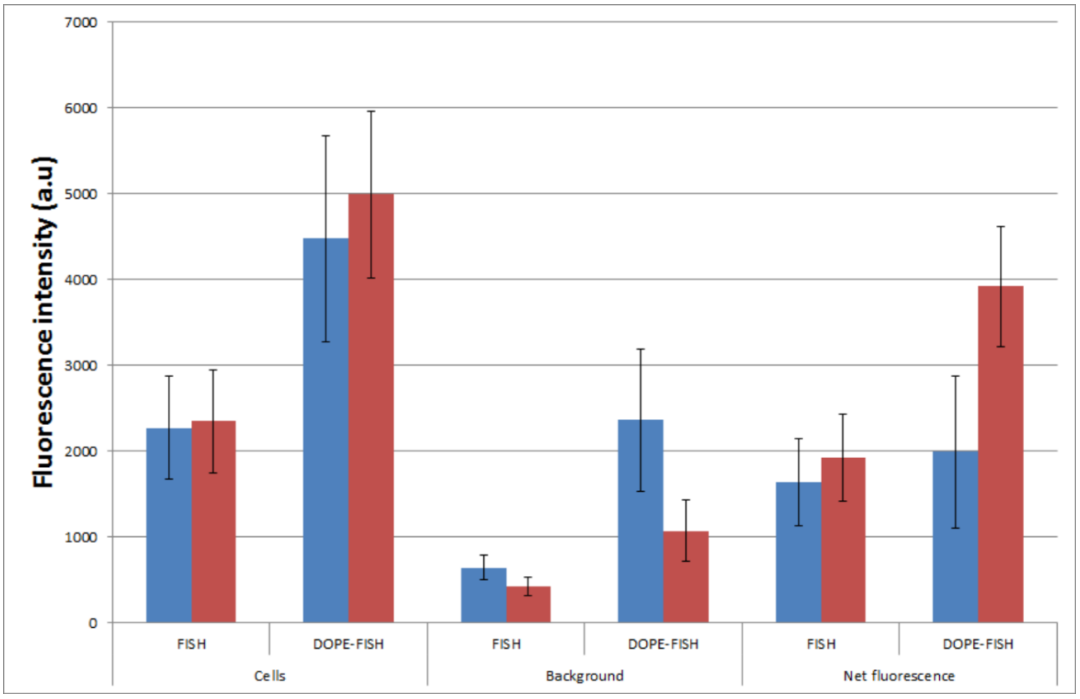

Figure 29. Comparison of FISH and DOPE-FISH mean fluorescence intensity of cells, background and net fluorescence efficiencies in E. coli. Hybridizations were carried out with FISH buffer (blue) or geneFISH buffer with pre-hybridization step (red).

6.4.2. Biofilms in deep subsurface rock matrix

DOPE-FISH and FLBA were then applied to subsurface rock samples showing a greater number of detected microorganisms than FISH hybridizations with a similar degree of biofilm integrity (Figure 30). Proteins and lipids are also present in the subsurface biofilms. In most of the detected biofilms, the main detected components were polysaccharides and proteins (Figure 30B-C), with some exceptions where lipids seemed to be more abundant than proteins (Figure 30A).

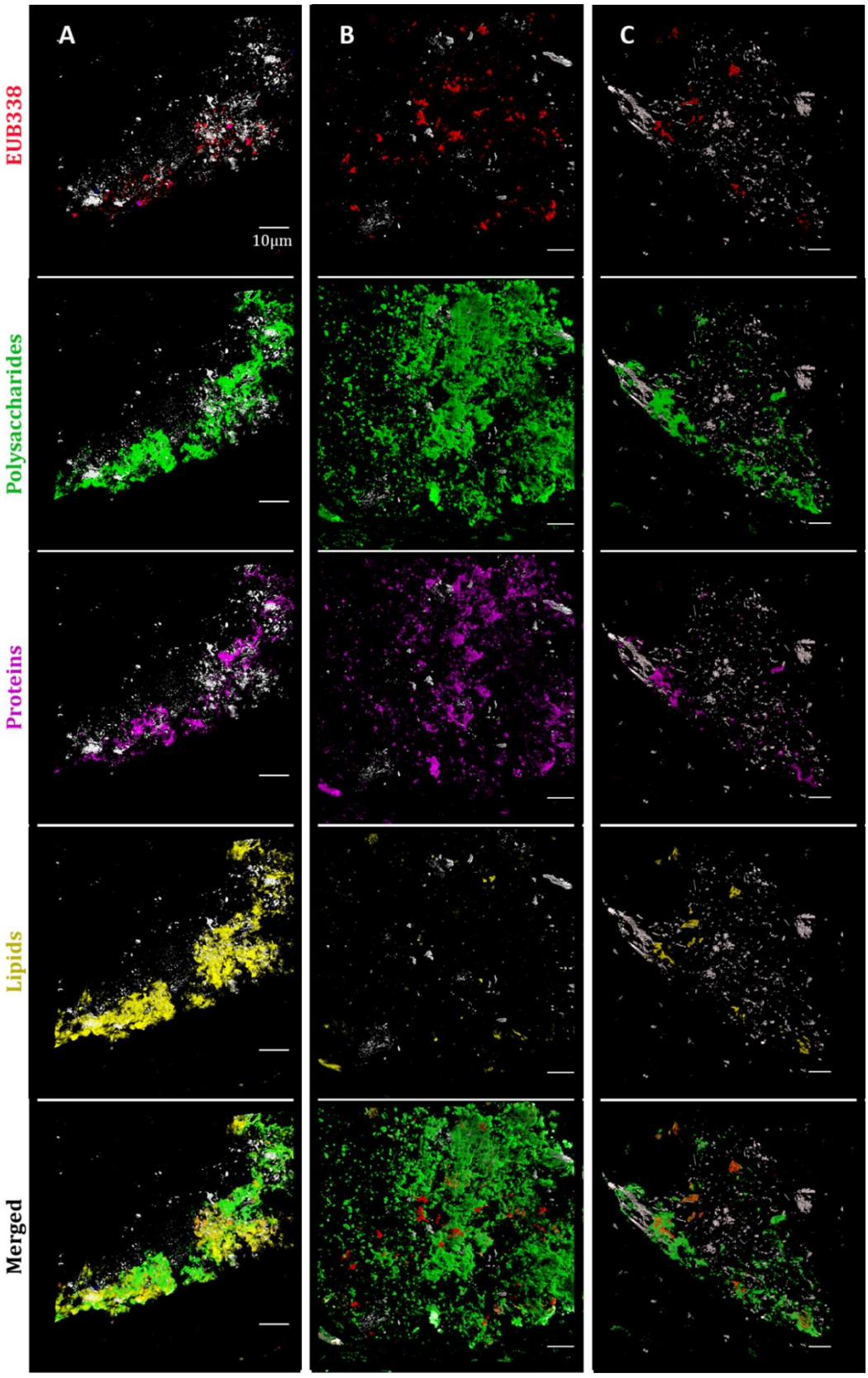

Figure 30. Bacterial biofilm detection in subsurface hard rock samples from different depths. DOPE-FISH of bacteria (red), FITC-ConA (green), Sypro Ruby (violet) and Nile red (yellow) at 355.7mbs (A), 420mbs (B) and 519.1mbs (C). Scale bars 10 µm.

All colonies exhibited, at least, traces of EPS surrounding them. In fact, it is noticeable that biofilms were detected in samples from all checked depths, even in poor porous rocks. This indicates that the biofilm lifestyle is common in the subsurface despite being considered an oligotrophic environment along with the energetic cost of biofilm production and maintenance (Sauer, 2003; Saville et al., 2011). In an environment where water and nutrients are limited and energy must be obtained from inorganic sources, the derivation of energy to biofilm production underlines its importance not only in the retention of nutrients and water (Coyte et al., 2016) but also in efficiency in the generation of energy (Vera et al., 2013).

6.4.3. Multi-species biofilms in deep subsurface rock matrix

Because bacterial and archaeal mixed colonies were detected in some of the samples from different depths, double DOPE-FISH and FLBA were used to determine whether these microorganisms were able to produce biofilms. Figure 31 shows the existence of native subsurface biofilms with a mixture of microorganisms from both domains. The existence of these multidomain biofilms is indicative of the advantage of bacterial and archaeal collaboration (Zelezniak et al., 2015) which may be extremely critical on the subsurface.

It is interesting to note that usually the EPS signal is not concentrated in only one single colony but extends along the rock matrix, interconnecting more than one cluster of cells (Figure 30 and Figure 31), separated by a substantial distance. Gantner et al. (2006) showed that “calling distance” of quorum sensing can extend up to 78 μm by single species biofilms. However, cooperation between different

microorganisms seems to need their co-aggregation (Nielsen et al., 2000; Egland et al., 2004; Zelezniak et al., 2015). Yet, in subsurface environments, where confined space can limit the aggregation of cells, the possibility of communication and cooperation by diffusion of metabolites between different microcolonies, even when the distance is significant, cannot be discarded.

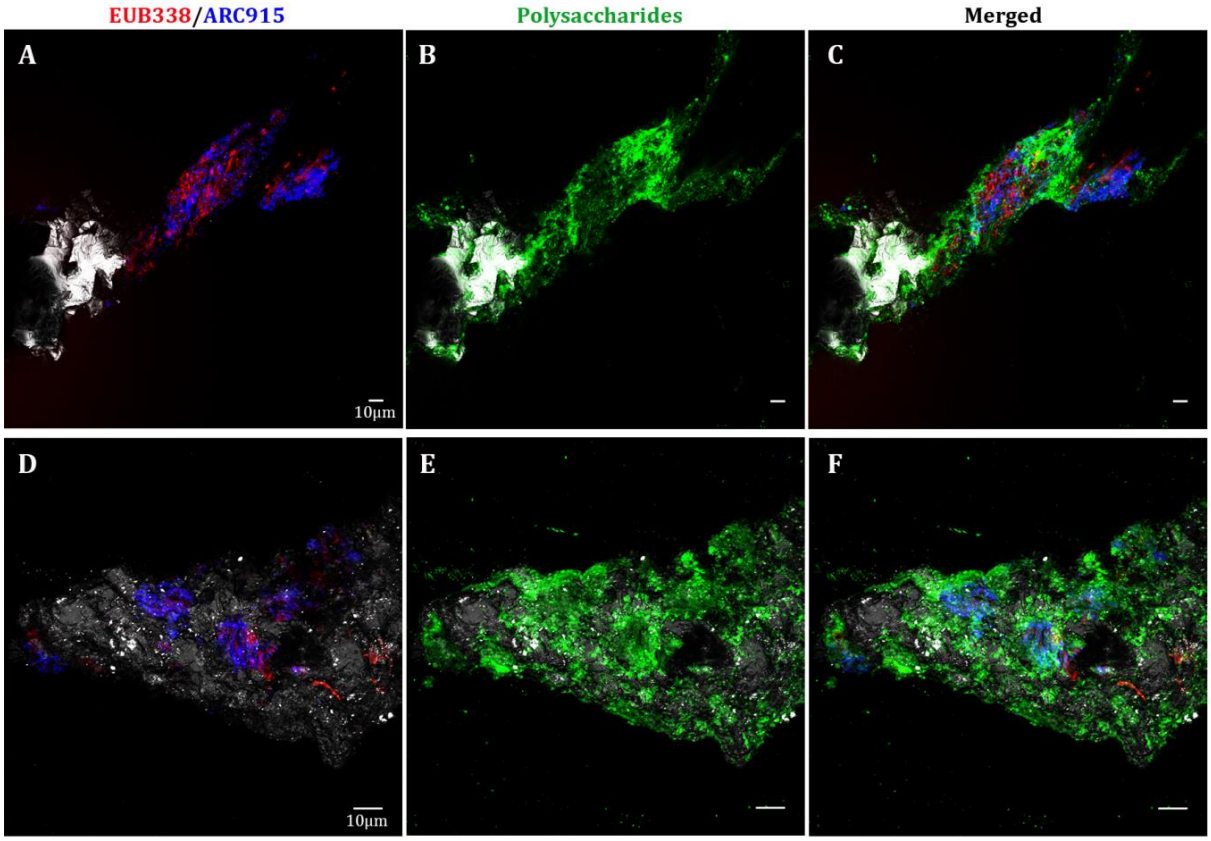

Figure 31. Detection of bacterial and archaeal mixed biofilms using double DOPE-FISH and FLBA at 139.4mbs. A and D, DOPE-FISH with bacteria (red) and archaea (blue) probes. B and E, FLBA with ConA, AAL and PNA lectins (green). C anf F, merged. Scale bars 10 µm.

6.5. Testing the anaerobic subsurface bioreactor hypothesis of Río Tinto origin

As mentioned in the introduction, the natural origin of Río Tinto was demonstrated after the study of the mineralogy of ancient sedimentary terraces, which were formed under the same conditions that the river presents today: an extraordinary concentration of ferric iron and low pH on its waters (Fernández-Remolar et al., 2003). This observation discarded the anthropological origin of the river's features by mining activity, which would not begin until millions of years later. An anaerobic underground bioreactor located in the Peña de Hierro area was proposed as the natural origin of Río Tinto's characteristics (Fernández-Remolar et al., 2008a; Fernández-Remolar et al., 2008b). The microorganisms inhabiting the IPB subsurface would dissolve the metallic sulfides that are abundant in this region through anaerobic iron-oxidizing metabolisms.

To carry out an exhaustive study and demonstrate the existence of the mentioned bioreactor, two drilling projects have been carried out in the IPB subsurface, the MARTE and the IPBSL projects. Thanks to both projects, great information has been obtained about its underground biosphere as it has been detailed throughout this work. The mineralogical composition and the energy sources available for this bioreactor are today well characterized. We also know that the deep biosphere of the IPB is active, the main microbial populations of the ecosystem and the metabolisms that are being carried out at different depths. However, up to now, we are missing the explicit demonstration that the microorganisms inhabiting the IPB subsurface can dissolve the metal sulfides that comprise this geological unit generating the high iron content and acidic pH that Río Tinto presents.

6.5.1. Generation of Río Tinto features from native samples of the IPB subsurface

To check if the interaction of water, native microorganisms and substrates of the IPB subsurface could generate an increase of the iron in solution and a low pH at natural conditions, a simple experiment was performed. Three samples from different depths: 102.6, 139.4 and 228.6mbs, were chosen in base of their high pyrite content: 10.6%, 8.5% and 8.5% respectively (Appendix 2 and Figure 32D). Samples were stored after sampling the drilling cores in sterile bottles under nitrogen atmosphere and subsamples of the same depths were sterilized and stored in the same conditions, which would serve as abiotic controls. In both cases, only sterile and anoxic milliQ water was added at the beginning of the experiment and iron production and pH was followed for ten months.

Figure 32 (A- C) shows the generation of iron in solution at all tested depths, being the cultures of samples from 102.6mbs and 139.4mbs where more soluble iron production was observed. At these depths, 4.6g/l and 6.2g/l of total iron in solution was measured respectively after ten months of incubation. All controls also showed some increase of iron in solution, but the great difference of iron production between cultures and sterilized controls indicates that most of the iron solubilization is the consequence of the microbial activity present in the samples, although a minimal abiotic production is taking place.

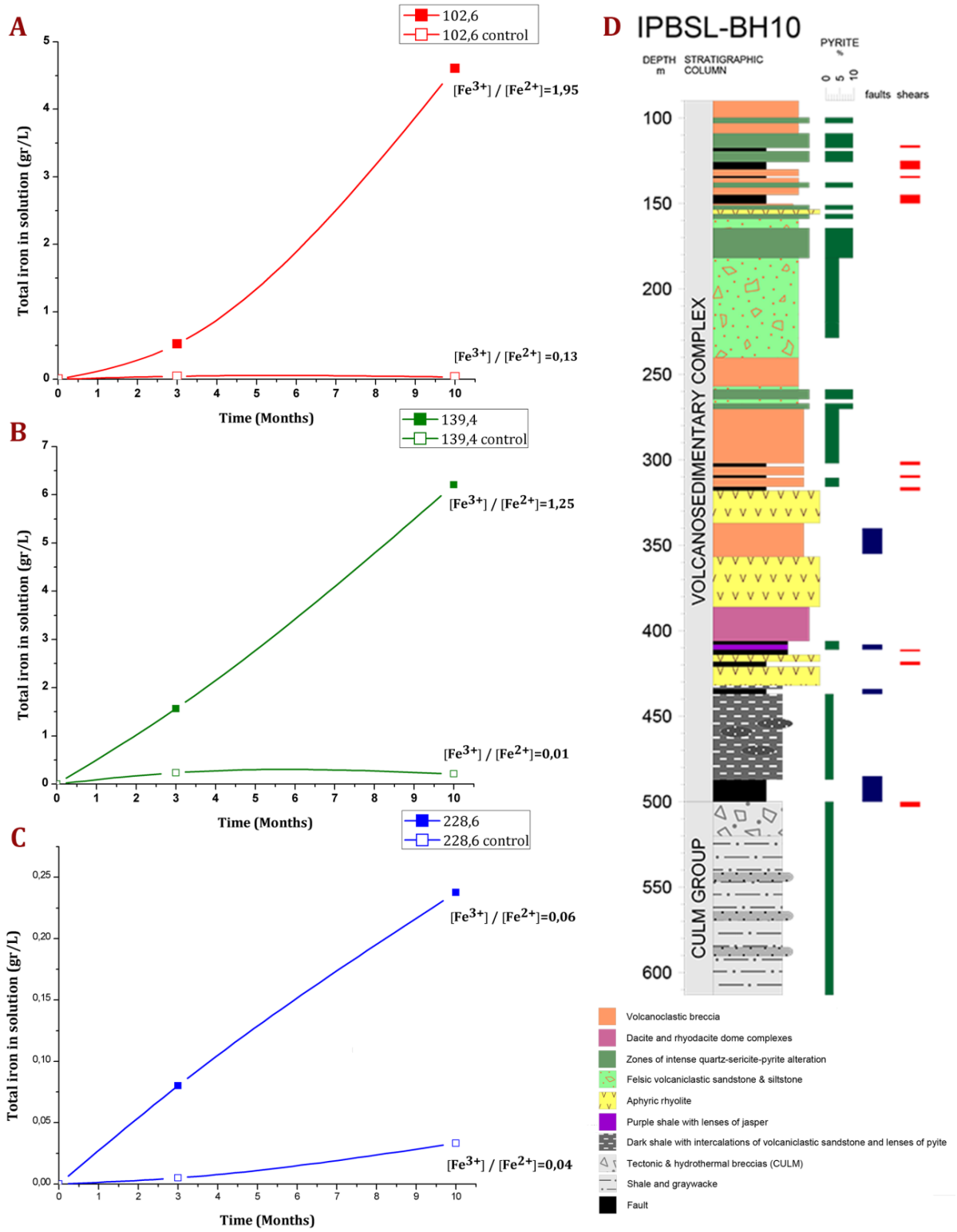

Figure 32. Total iron production by microbial activity (filled squares) or abiotic processes (open squares) in natural samples from 102.6 mbs (A), 139.4mbs (B) and 228.6mbs (C) of the IPB subsurface. Final Fe^{3+}/Fe^{2+} ratio of each culture is indicated. In D, BH10 stratigraphic column in which pyrite content and depths were pyrite alteration was detected are indicated.

Must be taken into account that these cultures are representatives of the IPB subsurface since only native samples were present and no microbial inoculum or additional compounds were added. Hence, native microorganisms of the rocky substrates are active, their metabolism is maintained by the natural resources of the samples and, as a consequence, dissolution of the iron-bearing minerals is been carried out. However, the nature of the minerals that are being dissolved is not clear since, at those depths, a diverse mineralogical composition was identified, including iron-bearing minerals as pyrite, illite or clinochlore (Appendix 2). Nevertheless, at 102.6mbs and 139.4mbs signs of weathered pyrite were noticed in the BH10 column, while at 228.6mbs, the culture in which a much lower total iron solubilization was detected, pyrite alteration was not observed (Figure 32D). This correlation might indicate that pyrite, the massive iron sulfide of the IPB, is the main mineral dissolved at those depths and, therefore, in these cultures. If we consider that Fe^{3+} is the chemical oxidant of pyrite (Chandra and Gerson, 2010), even at neutral pH (Moses and Herman, 1991), it is feasible to associate the large difference in total iron release detected in active cultures to the generation of Fe^{3+} mediated by microorganisms, which would not be produced in sterile cultures. Actually, while in the sterile controls the Fe^{2+} was the dominant iron specie, in the active cultures that showed a high iron solubilization, the Fe^{3+} concentration was higher than the concentration of Fe^{2+} (Figure 32A and B). At all analyzed depths, iron-oxidizing microorganisms as *Acidovorax* have been detected by CARD-FISH (see section 6.1.3.1), which would support the hypothesis of a putative pyrite dissolution mediated by the biological generation of Fe^{3+}. The maintenance of Fe^{2+} over time in all non-sterile cultures may indicate the presence of an iron-reducing

metabolic activity carried out by microorganisms such as *A. ferrooxidans* or *Acidiphillium* spp., which were also detected by CARD-FISH at these depths and would reverse the iron oxidation state.

In relation the pH, instead an acidification of the water as was expected due to the pyrite oxidation, a neutral pH was maintained (data not shown). The dissolution of pyrite generates protons (Vera et al., 2013), to which should be added the protons released by the ferric ion hydrolysis (Langmuir and Whiitemore, 1971). However, pH might be maintained neutral due to the operation of additional biological processes as sulfate reduction (Blodau, 2006; Koschorreck, 2007), the generation of NH^{4+} or the presence of neutralizing minerals. Thus, the solution remains neutral if the iron produced is not sufficient to acidify the pH. Consequently, since most of Fe^{3+} precipitates at neutral pH and in this experiment only iron in solution was measured, it is possible that, in both sterile and active cultures, the real total iron produced has been underestimated.

Interestingly enough, as shown in these cultures the pH measured in the water column of borehole BH10, which has been selected for being in the origin of the underground bioreactor, few months after drilling was circumneutral, although the pH measured in the downgradient borehole BH11 (400m away from borehole BH10) was very acidic (pH~3). This suggests that the groundwater plume becomes acidic as it flows through the metal sulfides of the IPB due to the interaction of an increasing concentration of ferric iron with these ores (Gómez-Ortiz et al., 2014).

At present, these cultures are still operational and will be monitored in the coming months to verify if the pH varies after a higher production of ferric iron. Nevertheless, this experiment allows to explain the natural origin of the high

concentration of iron detected in the Río Tinto basin as a consequence of the operation of a subsurface bioreactor in the IPB, as proposed.

6.5.2. The nitrate-reducing microorganism's case

The subterranean origin of Río Tinto implies that anaerobic iron-oxidizing microorganisms are operating in the IPB subsurface. However, in both the MARTE and the IPBSL projects, only members of the genus *Acidovorax*, described in the literature as anaerobic iron oxidizers, have been detected.

Acidovorax is a genus of the family Comamonadaceae of the Beta-proteobacteria phylum that, in general, is divided into two clusters. In the first, only pathogenic plant species are included, while the second comprises environmental species (Willems, 2014), including species isolated from sediments and underground environments (Huang et al., 2012; Chakraborty and Picardal, 2013; Lee et al., 2015). Although different metabolisms have been attributed to members of the genus *Acidovorax* under anaerobic conditions, such as the oxidation of H_2 or arsenite (Huang et al., 2012; Lee et al., 2015), habitually have been described as mixotrophic microorganisms, which use acetate as carbon source, ferrous iron as electron donor and nitrate as electron acceptor at circumneutral pH (Straub et al., 2004; Kappler et al., 2005; Chakraborty and Picardal, 2013).

$$10Fe^{2+} + 2NO_3^- + 18H^+ \rightarrow 10Fe^{3+} + N_2 + 6H_2O \quad (7)$$

The circumneutral nitrate-dependent Fe^{2+} oxidation (NDFO) (Equation 7) has generated great interest since this metabolism was first described twenty years ago in an enrichment culture (Straub et al., 1996) from which members of the genus *Acidovorax* were isolated (Straub et al., 2004). Until then, only the anaerobic iron oxidation carried out by anoxigenic photosynthetic microorganisms was known (Hedrich et al., 2011). In the following years, it was shown that numerous microorganisms of diverse phylogenetic groups and isolated from a wide range of habitats could carry out this metabolism (Hafenbradl et al., 1996; Benz et al., 1998; Lack et al., 2002; Kumaraswamy et al., 2006; Weber et al., 2009), and it was suggested that the oxidation of iron through the reduction of nitrate could be very relevant in the iron and nitrogen cycles on a global scale (Straub et al., 2001).

However, all the microorganisms that carry out the NDFO, including the members of the genus *Acidovorax*, require an organic co-substrate and, although the presence of iron favors their growth, it does not seem indispensable (Muehe et al., 2009; Chakraborty et al., 2011). This observation, together with the failure in the detection of proteins or genes related to the enzymatic oxidation of iron in NDFO microorganisms (Carlson et al., 2013), led to question the energy benefits of iron oxidation through this metabolism.

Subsequent research, focused mainly on members of the genus *Acidovorax*, suggested an indirect iron oxidation by these microorganisms through the reactive nitrogen species produced by nitrate respiration (Picardal, 2012; Klueglein and Kappler, 2013; Klueglein et al., 2015). Nitrite and nitric oxide, which are produced transiently during denitrification, are strong oxidants in aqueous solutions (Van Cleemput and Baert, 1983). Different experiments have shown that under anoxic

and neutral conditions NO_2^- (Equation 8), and the subsequent produced NO (Equation 9), are able to oxidize iron at neutral pH, with N_2O being the main product of this reaction (Equation 10) as is indicated in equation 11 (Moraghan and Buresh, 1977; Yan et al., 2015).

$$NO_2^- + Fe^{2+} + 2H^+ \rightarrow Fe^{3+} + NO + H_2O \quad (8)$$

$$NO + Fe^{2+} + H^+ \rightarrow Fe^{3+} + HNO \quad (9)$$

$$2HNO \rightarrow N_2O + H_2O \quad (10)$$

Overall reaction: $NO_2^- + 2Fe^{2+} + 3H^+ \rightarrow 2Fe^{3+} + {}^1/_2\, N_2O + {}^3/_2\, H_2O \quad (11)$

Far from being a slow oxidative reaction, Klueglein and Kappler (2013) showed that, during an anoxic incubation, 14% of 1 mM Fe^{2+} solution was oxidized by 1mM NO_2^- within the first minute and almost completely after twenty minutes, being even faster the oxidation rate at acidic pH. These authors demonstrated that the presence of nitrate reduction products leads to an overestimation of the iron oxidation rate of NDFO microorganisms such as *Acidovorax*, and questioned the existence of an enzymatic oxidation of iron coupled to the reduction of nitrate that was proposed in previous studies of this microorganism.

Based on these data, several authors defended that all nitrate-reducing microorganisms have the innate ability to catalyze the oxidation of iron through the generation of reactive nitrogen species (Carlson et al., 2013). The observation

that microorganisms such as *E. coli* or *Pseudomonas* spp. can oxidize iron when they use nitrate as electron acceptor, supports this hypothesis (Brons et al., 1991; Li et al., 2017). Nowadays, more than a gain of electrons, the improvement of growth observed in nitrate-reducing species such as *Acidovorax* in the presence of iron is attributed either to its high demand as a nutrient (Klueglein and Kappler, 2013) or to the detoxifying effect that can lead to the elimination of both Fe^{2+} and the reactive nitrogen species product of its metabolism (Carlson et al., 2013). However, a possible enzymatic oxidation of iron has not been completely ruled out and both processes, biotic and abiotic, are accepted today (Carlson et al., 2013; Schaedler et al., 2018).

6.5.2.1. Fe oxidation by nitrate-reducing microorganisms of the IPB

Since NO_2^- oxidizes Fe^{2+} at neutral and anaerobic conditions (Yan et al., 2015), we considered the possibility that, in addition to *Acidovorax*, other nitrate-reducing microorganisms that inhabit the IPB can also carry out an indirect iron oxidation and, consequently, facilitate the dissolution of metallic sulfides in the subsurface. To verify this hypothesis we compare the iron oxidation ability of two of the most abundant nitrate-reducing microorganisms detected in the IPBSL project, *Acidovorax* and *Tessaracoccus lapidicaptus*. Because no member of the genus *Acidovorax* has been isolated so far from the IPB subsurface, we used instead *Acidovorax* BoFeN1, one of the closest species to the 16S rRNA sequences of *Acidovorax* genus obtained by non-culture-dependent techniques in the IPBSL project (data not shown).

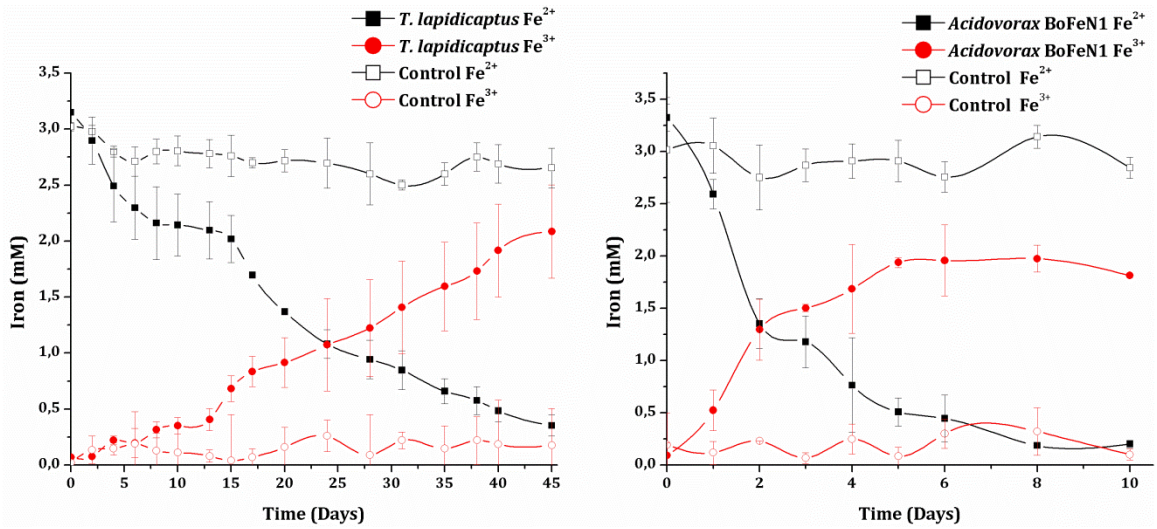

Figure 33. Comparison of iron oxidation rate of T. lapidicaptus (A) and Acidovorax BoFeN1 (B).

As shown in Figure 33, both microorganisms are capable of oxidize iron. While *Acidovorax*, as described before for this genus (Chakraborty and Picardal, 2013; Klueglein et al., 2014), showed a total iron oxidation after 8 days, the iron oxidation rate of *T. lapidicaptus* was much lower, showing an almost total conversion of ferrous iron to ferric iron after 45 days.

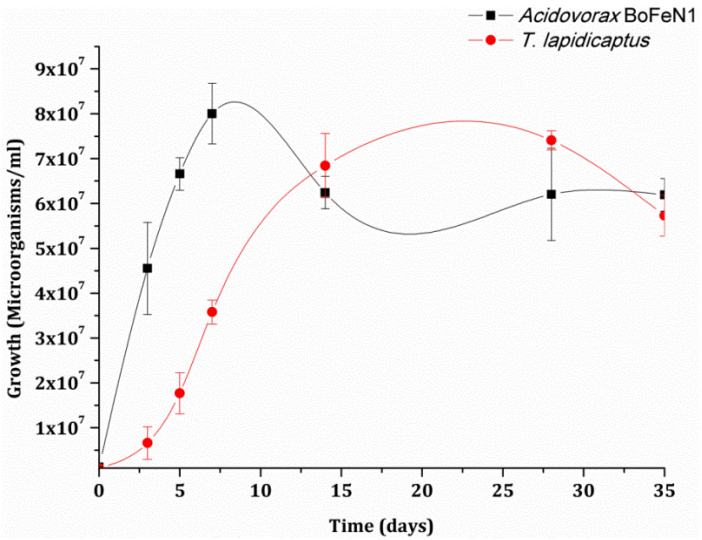

Figure 34. Comparison of microbial growth of Acidovorax BoFeN1 and T. lapidicaptus in heterotrophic cultures amended with NO_3^- and Fe^{2+}.

Even though the difference in the Fe^{2+} oxidation rate between both microorganisms could be due to the lower growth rate of *T. lapidicaptus* (Figure 34), the lack of periplasmic space in gram-positive bacteria and the pathway used by each bacteria to reduce nitrate should be considered. *Acidovorax* BoFeN1 is a gram-negative bacteria that carry out a respiratory denitrification (Kappler, personal communication), in which nitrate reduction takes place in the cytoplasm and the nitrite produced is transported to the periplasm, where it can be further reduced to N_2 (Tiedje, 1988). Thus, the interaction of nitrogen oxidative species and the Fe^{2+} that penetrates into the periplasmic space or is retained in the outer membrane can be enhanced (Carlson et al., 2013; French et al., 2013). On the contrary, members of the genus *Tessaracoccus* are gam-positive bacteria that carry out a dissimilatory nitrate reduction to ammonia (DNRA), as shown in the preliminary results obtained from their whole-genome sequencing (Leandro et al., 2017). In this case, the reduction of nitrate to nitrite is produced by transmembrane proteins and may be associated with energy conservation. However, the nitrite can be reduced to ammonium by a cytoplasmic protein (Tiedje, 1988), resulting into a lower probability of interaction between nitrite and Fe^{2+}, which would be mainly retained by the thick cell wall of the gram-positive bacteria (French et al., 2013).

Nevertheless, the observation of Fe^{3+} production by *T. lapidicaptus*, genus in which iron-oxidizing activity has never been described before, supports the hypothesis of an innate ability to catalyze the oxidation of iron through nitrate respiration.

6.5.2.2. Fluorescence microscopy to detect Fe oxidation by nitrate-reducing microorganisms in the IPB

As shown above, both *Acidovorax* and *T. lapidicaptus* can oxidize iron under anaerobic conditions. However, while only a nitrate-reducing metabolism has been attributed to *Acidovorax* in the absence of oxygen (Kappler et al., 2005; Huang et al., 2012; Lee et al., 2015), *T. lapidicaptus* is able to carry out alternative metabolisms such as fermentation (Puente-Sánchez et al., 2014a). To verify that an operative iron-oxidizing metabolism, direct or indirect, is being carried out in the IPB subsurface by both *Acidovorax* and *T. lapidicaptus*, we make use of a specific Fe^{3+} fluorescent metal probe.

The use of fluorescent sensors is a viable approach to visualize the presence of specific metal ions (Hao et al., 2013; Yin et al., 2015). Nowadays, a high variety of fluorescent metal probes are available to detect metals specifically, including zinc, cadmium, copper or iron among many others (Hao et al., 2016). In recent years, numerous studies have applied these probes to analyze both intracellular and extracellular locations of a wide range of metal ions by fluorescence microscopy, which have been useful to understand physiological and pathological processes occurring in living systems (Domaille et al., 2008).

Therefore, we applied fluorescent ferric iron sensor in combination with CARD-FISH using *Acidovorax* and *T. lapidicaptus* specific probes to determine if the presence of these microorganisms correlate with the product of iron-oxidizing metabolisms in the IPB subsurface. Samples from several depths were analyzed and, as Figure 35 shows, both microorganisms were detected in direct contact with Fe^{3+} in the IPB subsurface.

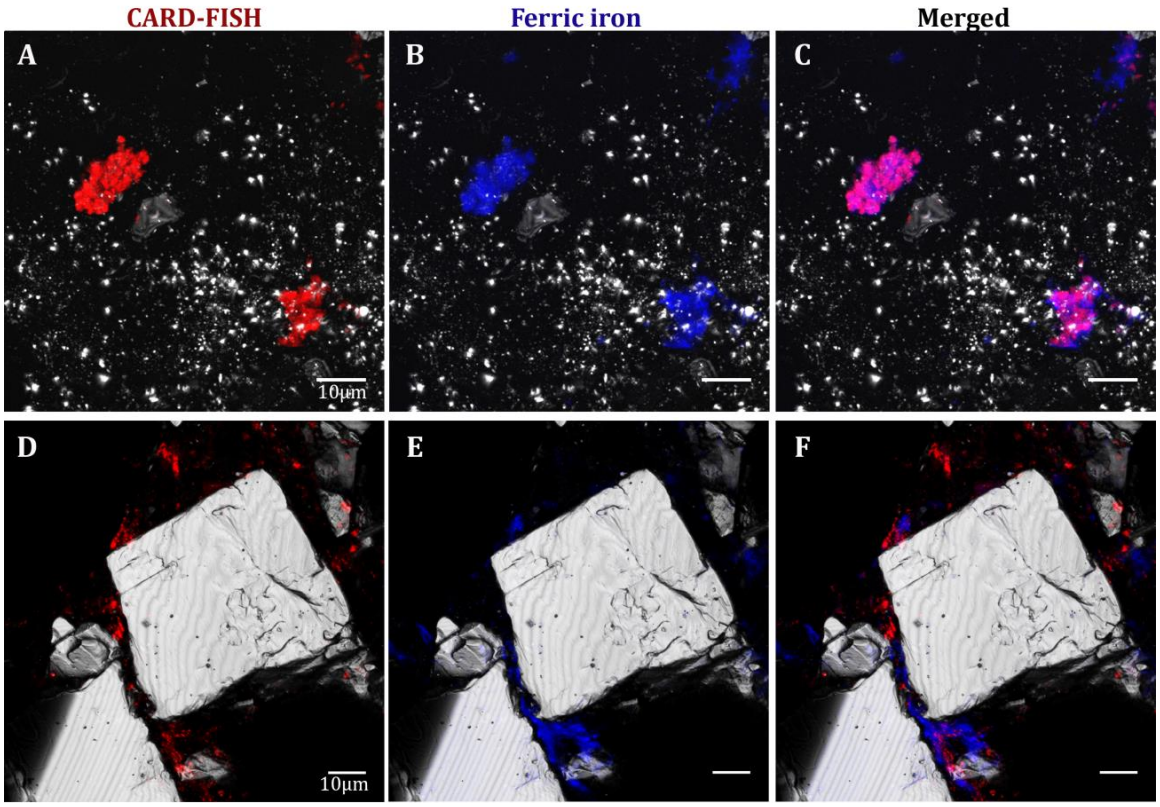

Figure 35. Ferric iron and microorganisms co-localization in the IPB subsurface. A-C, Acidovorax at 414.8mbs. D-F, T. lapidicaptus at 228.6 mbs. In red, CARD-FISH signal. In blue, ferric iron fluorescence signal. In grey, reflection. Scale bars, 10µm.

Regarding the members of the genus *Acidovorax*, in some cases the fluorescent Fe^{3+} probe signal was exactly co-localized with the CARD-FISH signal (Figure 35A-C). This phenomenon was previously described by Schmid et al. (2014), who attributed the co-localization of Fe^{3+}- *Acidovorax* to the cell encrustation, both intracellular and extracellular, as consequence of Fe^{3+} precipitation at neutral pH, which finally causes the death of the microorganism (Miot et al., 2015). However, in our case, a high percentage of colonies did not show signs of biomineralization (Figure 36A). Previous studies carried out with members of this genus revealed that, in continuous flow incubation systems in which the amount of Fe^{3+} is low, the encrustation of the cells is minimized and the culture remains active for longer

periods of time than in batch cultures (Chakraborty et al., 2011). Accordingly, those *Acidovorax* colonies that didn't show cell encrustation could be located in subsurface areas where there was a greater flow of water than those areas where *Acidovorax* presented signs of encrustation. This flow would decrease local Fe^{3+} concentration and, consequently, avoid *Acidovorax* encrustation.

On the other hand, while most *Acidovorax* colonies were surrounded by Fe^{3+}, some *T. lapidicaptus* colonies which didn't show a positive signal for the fluorescent metal sensor were found. This observation correlates with a possible alternative anaerobic metabolism for this microorganism. Thus, at those locations where organic matter is available but no nitrate, *T. lapidicaptus* could grow by using a fermentative metabolism, not producing the oxidation of iron. The fact of finding ferric iron surrounding some colonies is indicative of iron oxidation by *T. lapidicaptus* in this environment, probably through the production of nitrite.

The observation of Fe^{3+} surrounding colonies of both, members of the genus *Acidovorax* and members of the specie *T. lapidicaptus*, indicates that these microorganisms are carrying out a direct or indirect iron-oxidizing metabolism in the IPB subsurface, supporting the hypothesis of an operative metallic sulfide dissolution by nitrate-reducing microorganisms in this environment if they are in contact with these ores. Actually, these microorganisms were detected associated to biofilms, which are essential to enhance the biooxidation of metallic sulfides (Rohwerder et al., 2003; Sand and Gehrke, 2006). Unlike the biofilms in which *Acidovorax* was found (Figure 36A and B), it was not possible to reveal the complete biofilm structure in which members of *T. lapidicaptus* are located (Figure 36C and D), probably because the exopolysaccharides that surround them are not

recognized by the fluorescent lectins used. However, in both cases the Fe^{3+} signal is mostly co-localized with the exopolysaccharide signal, which is in accordance with the fact that EPS are commonly responsible for metal ions binding, like ferric iron (Sand and Gehrke, 2006).

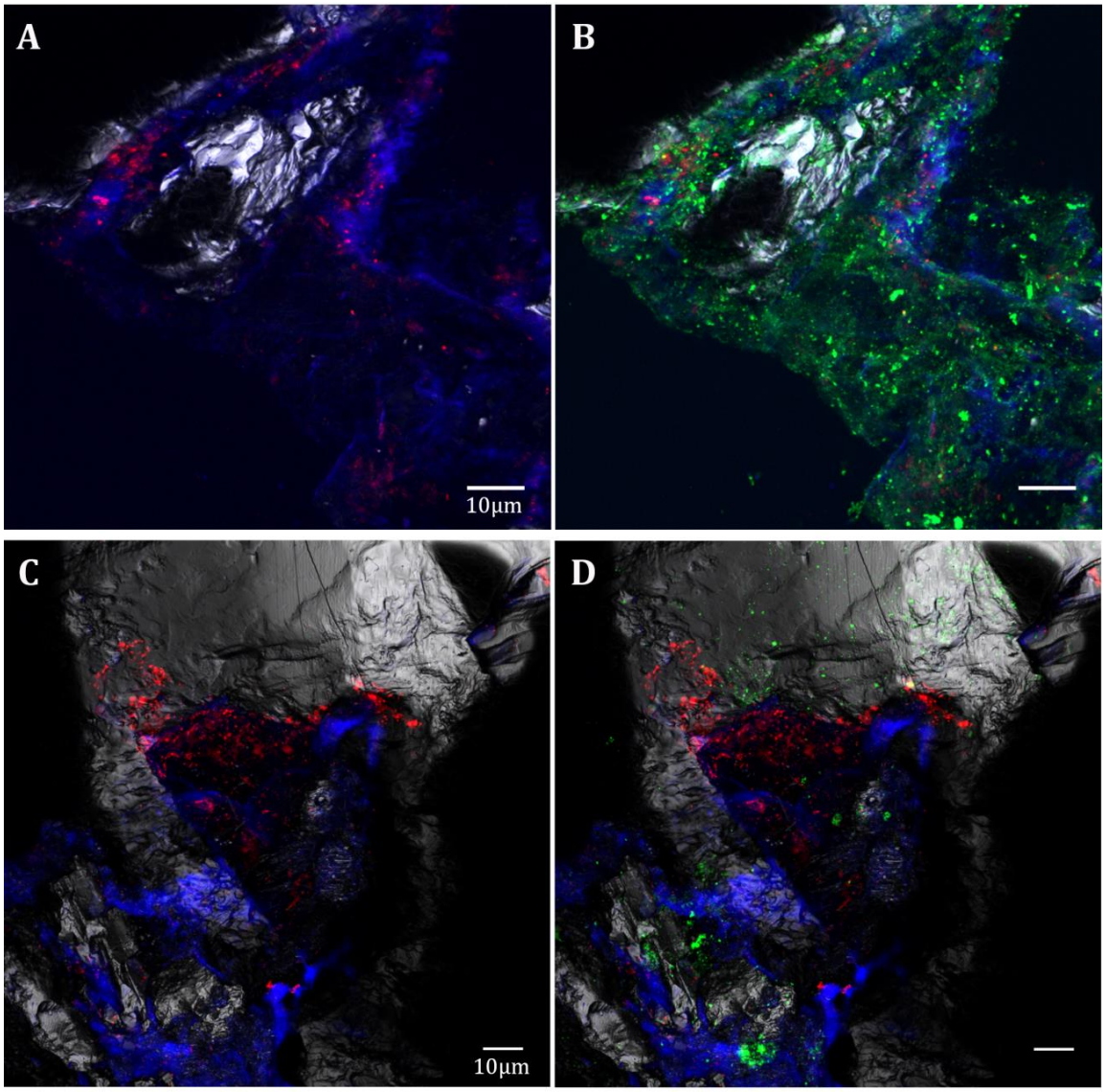

Figure 36. Microorganisms-Fe^{3+}-EPS co-localization in the IPB subsurface. A and B, DOPE-FISH with Acidovorax probe (red) at 139.4mbs; C and D, DOPE-FISH with T. lapidicaptus probe (red) at 228.6mbs. In blue, Fe^{3+} signal. In green, ConA lectin signal. In grey, reflection. Scale bars 10µm.

6.5.3. Pyrite dissolution by nitrate-reducing microorganisms

The biological dissolution of metal sulfides through the generation of Fe^{3+} has raised great interest in recent decades, mainly due to its possible application in biomining (Brierley and Brierley, 2013). Several microbial groups, which present different physiologies in terms of their response to oxygen (aerobic, facultative and anaerobic) or optimal pH of growth (neutrophiles, moderate and extreme acidophiles), have the capacity to oxidize iron (Hedrich et al., 2011) and, therefore, to induce the dissolution of metal sulfides such as pyrite following the equation 1 (see list of equations in page 17).

$$FeS_2 + {}^{7}/_{2}\, O_2 + H_2O \rightarrow 2SO_4^{2-} + Fe^{2+} + H^+ \qquad (12)$$

$$Fe^{3+}_{(aq)} + 3H_2O \rightarrow Fe\,(OH)_{3(s)} + 3H^+ \quad (\text{pH} > 2.5) \qquad (13)$$

However, most of the studies have focused their efforts on analyzing the biooxidation of these minerals at acidic conditions since it was traditionally assumed that the pyrite oxidation at neutral pH was mainly produced by oxygen (Equation 12) due to the low solubility of Fe^{3+} at pH higher than 2.5 (Equation 13) (Nordstrom, 1982). Hence, as pyrite oxidation rate by Fe^{3+} is higher than by oxygen, most of the available data about pyrite biooxidation refer to acidophilic microorganisms, which oxidize iron using oxygen as electron acceptor (Rohwerder et al., 2003; Vera et al., 2013), and pyrite biooxidation at circumneutral and anaerobic conditions using Fe^{3+} has been ignored. In any case, the few studies

dedicated to the analysis of the chemical oxidation of pyrite at neutral pH have indicated that the pyrite oxidation mediated by Fe^{3+} is possible, showing oxidation rates one order of magnitude higher under these conditions than the rate observed in saturated oxygen media, in which the critical element will be the maintenance of a high concentration of Fe^{3+} (Moses et al., 1987; Moses and Herman, 1991). Therefore, an anaerobic oxidation of pyrite at neutral pH is possible if the generation of high Fe^{3+} concentration is produced by microorganisms capable of oxidize iron in these conditions.

Curiously, several bioremediation field studies have shown that nitrate-reducing microbial activity in underground environments, operating in anaerobiosis and neutral pH, is always associated with an increase in SO_4^{2-} and iron in solution if pyrite is present in the system (Postma et al., 1991; Schwientek et al., 2008; Zhang et al., 2009). These studies, which were initiated to analyze aquatic underground systems contaminated with NO_3^- due to the excessive use of fertilizers in agriculture, have shown that the groundwater, in addition, is enriched with trace metals, whose concentration depends directly on its content in pyrite (Houben et al., 2017). Since the organic matter in these systems is mostly recalcitrant, it was suggested that pyrite could be the main electron donor used by denitrifying chemolithotropic microorganisms (Equation 14) (Postma et al., 1991). As a result, the pyrite would dissolve and SO_4^{2-}, iron and trace metals released while the NO_3^- concentration would decrease. The isotopic composition of nitrogen and sulfur compounds carried out in these environments supported this hypothesis (Schwientek et al., 2008; Zhang et al., 2012).

$$5FeS_2 + 14NO_3^- + 4H^+ \rightarrow 7N_2 + 10SO_4^{2-} + 5Fe^{2+} + 2H_2O \qquad (14)$$

Nevertheless, there is controversy about whether chemolithotropic denitrifying microorganisms, or any other microorganisms, have the ability to use pyrite as direct electron donor. Several studies have been carried out in the last decades but the results obtained are totally contradictory. Schippers and Jørgensen (2001, 2002) observed that, in marine sediments, the oxidation of pyrite was carried out chemically by manganese oxide and found no evidence of biological oxidation. These researchers observed that only iron sulfide (FeS) is susceptible of oxidation in the presence of nitrate-reducing microorganisms via the polysulfide-mechanism.

$$FeS + H^+ \rightarrow Fe^{2+} + HS^- \qquad (15)$$

In this case, Fe^{2+} could be oxidized by NDFO microorganisms, resulting in the precipitation of Fe^{3+} and the generation of H^+ (Equation 13), being the latter the main oxidant of acid-soluble minerals as FeS (Equation 15) (Rohwerder et al., 2003; Vera et al., 2013). Studies on wetland soils carried out by Haaijer et al. (2007), in which the addition of FeS to bioreactors induced the release of SO_4^{2-} in the media, while in bioreactors amended with pyrite no change in anion composition was observed, corroborated these data. According to these authors, the oxidation of the FeS and not the pyrite would explain the increase of SO_4^{2-} and

iron and the decrease of nitrate in underground environments (Schippers and Jørgensen, 2002; Haaijer et al., 2007).

On the other hand, subsequent studies contradicted these results and showed that the addition of pyrite to reactors with natural sediment samples does enhance the growth of nitrate-reducing microorganisms and increases the concentration of SO_4^{2-} in solution (Jørgensen et al., 2009; Torrentó et al., 2011). Studies carried out with different species of *Thiobacillus*, mainly *Thiobacillus denitrificans*, corroborated the capacity of these chemolithotropic denitrifying microorganisms to grow in cultures in which pyrite was the only electron donor available (Torrentó et al., 2010; Bosch et al., 2012; Vaclavkova et al., 2015). Since the influence of NO_3^-, NO_2^- or Fe^{3+} as pyrite oxidants is discarded at neutral pH, the only pathway currently contemplated is the direct oxidation of pyrite. However, the mechanism by which the pyrite dissolves and the chemolithotropic nitrate-reducing microorganisms get the energy is not yet clear. In fact, up to now, no study has verified that, in incubations with nitrate-reducing microorganisms, the proposed stoichiometry for the direct dissolution of pyrite (Equation 14) is fulfilled, although the possibility of an incomplete denitrification process (NO_3^- to NO_2^-, NO or N_2O) has also been considered (Torrentó et al., 2010). Since iron precipitates at neutral pH, only the measures of $SO_4^{2-}$and nitrate in solution have been taken into account to analyze pyrite dissolution, which, generally, show that the SO_4^{2-}produced is not sufficient to explain the amount of NO_3^- consumed. According to different authors, the possibility of generating diverse chemical sulfur species such as thiosulfate or tetrathionate, which would underestimate the total amount of total sulfur produced (Bosch et al., 2012), as well as the presence of a heterotrophic

respiration of NO_3^- or a NDFO metabolism, which would overestimate the amount of nitrate reduced by oxidation of pyrite (Torrentó et al., 2010; Vaclavkova et al., 2015), would be the cause of this discrepancy.

Nevertheless, due to the low solubility of the Fe^{3+} at neutral pH, all the bioleaching studies carried out so far have obviated its possible role in pyrite dissolution, although its oxidizing potential in these conditions was shown decades ago (Moses et al., 1987; Moses and Herman, 1991). In addition, the role of reactive nitrogen species in the maintenance of a high Fe^{3+} concentration has not been considered either in this scene. Consequently, the possibility that pyrite dissolution can occur through the indirect generation of Fe^{3+} by any nitrate-reducing microorganism has never been contemplated.

6.5.3.1. Pyrite dissolution by microorganisms inhabiting the IPB

Based on the results obtained so far, nitrate-reducing microorganisms are candidates to dissolve metallic sulfides such as pyrite in the IPB subsurface due to its ability to generate Fe^{3+}. However, since up to now a pyrite dissolution mediated by Fe^{3+} produced biologically at neutral pH has not been reported, to determine if the pyrite biooxidation under anaerobic and neutral conditions by nitrate-reducing microorganisms such as *Acidovorax* is possible, batch experiments were carried out for 45 days in which the dissolution of pyrite was analyzed under different culture combinations: presence or absence of microorganisms as well as initial presence or absence of ferrous iron (Table 8). Furthermore, additional controls

were carried out with NO_2^- in the presence or absence of ferrous iron to determine its importance in the chemical regeneration of Fe^{3+}.

Table 8. Experimental culture conditions to determine if Acidovorax is able to dissolve pyrite at neutral and anoxic conditions.

Culture		Carbon source	Electron acceptor	Iron source	Inoculum
1	Pyrite	Acetate	NO_3^-	Fe^{2+}	*Acidovorax* BoFeN1
Control 2		Acetate	NO_3^-	Fe^{2+}	-
Control 3		Acetate	NO_2^-	Fe^{3+}	-
Control 4		Acetate	NO_3^-	-	*Acidovorax* BoFeN1
Control 5		Acetate	NO_3^-	-	-
Control 6		Acetate	NO_2^-	-	-

As Figure 37A shows, in those cultures in which *Acidovorax* grew in the presence of Fe^{2+} (culture 1) complete iron oxidation was observed after seven days. The fact of not finding nitrite in the medium indicates that iron oxidation was, at least in part, chemically produced (Figure 38B). In this culture, the total iron concentration in solution decreased according to the oxidation of Fe^{2+} (Figure 37A), possibly due the precipitation of the Fe^{3+} at neutral pH in the form of $Fe(OH)_3$ as indicated in equation 12 (Moses and Herman, 1991; Bonnissel-Gissinger et al., 1998). However, the precipitation of Fe^{3+} seems to reach equilibrium since its concentration in solution remains constant after the tenth day. In fact, from this day, the concentration of Fe^{2+} and total iron in solution are also constant, increasing slightly in the last phase of the experiment. This balance between the different iron oxidation states could be a sign of the generation of Fe-oxide cell encrustations as

previously observed in this specie in batch cultures (Kappler et al., 2005; Schmid et al., 2014; Miot et al., 2015). As discussed (see section 6.5.2.2), the precipitation of Fe^{3+} in the periplasmic space and around the membrane of *Acidovorax* produce the death of the microorganism, which could explain the non-reduced NO_3^- that remains in the medium at the end of the experiment (Figure 38B), and, therefore, the oxidation of Fe^{2+} ceases. Yet, as shown in Figure 38A, a total iron increase of 6.54 mg was observed in the presence of *Acidovorax*, being 7.15 times higher than the iron released in the non-inoculated controls with initial Fe^{2+} and NO_3^- (control 2). In control 2 (Figure 38A), the small amount of ferric iron produced could be due to a slight oxidation of Fe^{2+} either by some undetermined oxidant present in the culture media or the entry of a minimum amount of oxygen into the system. This minimal production of Fe^{3+} could oxidize the pyrite, which would explain the 0.91mg of extra iron (Figure 38A) as well as the slight fluctuations of Fe^{2+} and Fe^{3+} detected in this control (Figure 37B). Nevertheless, the great difference in iron released between inoculated and non-inoculated cultures (Figure 38A) is a strong indication that *Acidovorax* is capable of promoting the dissolution of pyrite through the oxidation of Fe^{2+}, which does not occur in the non-inoculated control (Figure 37A and B).

On the other hand, additional non-inoculated controls were carried out in which the NO_3^- was replaced by NO_2^- (control 3) to evaluate its importance in the oxidation of Fe^{2+} and the subsequent oxidation of pyrite at neutral pH. In this control, Fe^{2+} oxidation is chemically produced by NO_2^-, which is confirmed by the decrease of this compound in solution (Figure 38B).

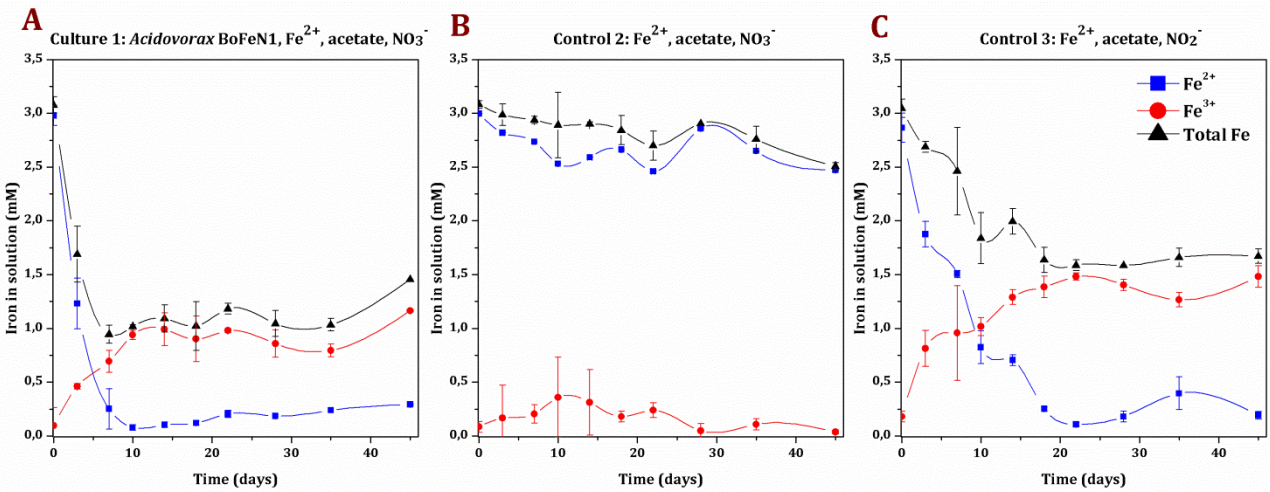

Figure 37. Changes in the iron oxidation state observed in (A) cultures inoculated with Acidovorax in the presence of Fe^{2+}; (B) controls with initial $Fe^{2+}$and NO_3^-; and (C), controls with initial Fe^{2+} and NO_2^-.

In the presence of NO_2^-, like in culture 1 in which *Acidovorax* was present, a total oxidation of Fe^{2+} was observed accompanied by a total iron decrease in solution due to the possible formation of precipitates in the form of $Fe(OH)_3$ (Figure 37C). However, the iron oxidation rate in this control was much slower than that shown in the presence of *Acidovorax* (Figure 37A and C). Recently, Schaedler and colleagues (2018) observed this same phenomenon in microcosms, in which the Fe^{2+} oxidation rate mediated by microorganisms was much higher than the chemical oxidation mediated by NO_2^-. They also observed that the addition of Fe^{2+} stimulated the expression of genes related to nitrate reduction, indicative of a direct influence of Fe^{2+} on microbial metabolism. Consequently, the authors suggested that, in addition to a chemical oxidation mediated by nitrite (indirect), a biological Fe^{2+} oxidation (direct) could also be operating in their system. Accordingly, in spite that a direct iron oxidation by *Acidovorax* BoFeN1 has been questioned (Klueglein and Kappler, 2013), the fast Fe^{2+} oxidation rate observed in

the presence of *Acidovorax* in our experiments strongly suggest the existence of both chemical and biological Fe^{2+} oxidation in inoculated cultures as suggested (Schaedler et al., 2018). On the other hand, since no NO_2^- was detected in cultures where *Acidovorax* grew while a small amount remained in the chemical control (Figure 38B), another plausible explanation for the fast Fe^{2+} oxidation rate observed could be that, as discussed above (see section 6.5.2.1), the microorganism also favors the interaction between Fe^{2+} and NO_2^- in the periplasm and, therefore, the chemical generation of Fe^{3+}. Thus, both a biological and a chemical enhanced Fe^{2+} oxidation would explain the 2.9 times higher pyrite dissolution observed in *Acidovorax* cultures in relation to the controls with initial Fe^{2+} and NO_2^- (Figure 38A).

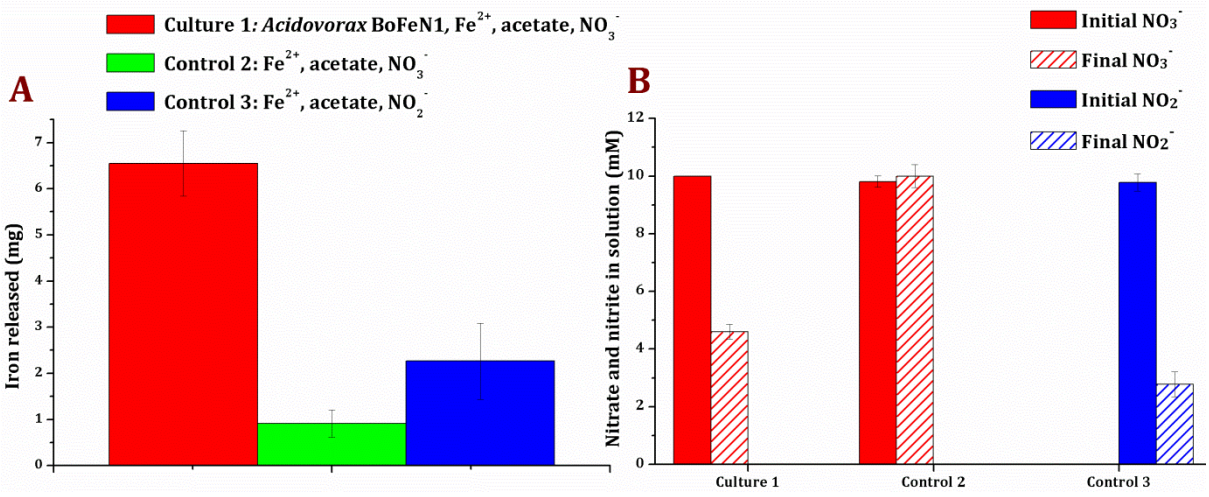

Figure 38. Iron released after pyrite dissolution (A) and nitrate and nitrite concentration (B) detected in the cultures carried out in presence of initial ferrous iron.

The fact that both culture 1 and control 3, in which Fe^{2+} oxidation has been observed (Figure 37A and C), showed a higher final iron production than those controls in which iron oxidation has not occurred (control 2, Figure 37B) or in which initial Fe^{2+} was not added (Figure 39A, see below) corroborates that Fe^{3+} is the main oxidant of pyrite even at neutral pH (Moses et al., 1987; Moses and Herman, 1991). Therefore, despite its low solubility, the role of Fe^{3+} in the dissolution of metal sulfides in neutral underground systems cannot be ruled out as proposed earlier (Schippers and Jørgensen, 2002; Jørgensen et al., 2009; Bosch et al., 2012). In fact, the possible contribution of Fe^{3+} in the pyrite oxidation in neutral underground environments has been previously contemplated (Bottrell et al., 2000; Schwientek et al., 2008). But the absence of chemical oxidation of pyrite at neutral pH in the presence of amorphous iron oxide discarded this idea (Schippers and Jørgensen, 2002). Still, Luther III (1987) suggested that if Fe^{3+} is in direct contact with pyrite, the local generation of H^+ could favor the Fe^{3+} mobilization and, therefore, the dissolution of the mineral at neutral pH.

In addition, in spite that biological Fe^{2+} oxidation may be produced by *Acidovorax*, the role of NO_2^- in the oxidation of Fe^{2+} (Figure 37C) and the subsequent pyrite dissolution (Figure 38A) is indisputable, as shown in control 3. Hence, the influence of heterotrophic nitrate-reducing microorganisms on the dissolution of metal sulfides should not be ruled out either. Actually, in most of the studies carried out so far, both field studies and under controlled laboratory conditions, NO_2^- in solution has not been detected (Schwientek et al., 2008; Jørgensen et al., 2009; Torrentó et al., 2010). However, the absence of NO_2^- has been attributed to its conversion to N_2 by denitrifying microorganisms and its iron oxidant capacity

has not been considered, resulting in a possible overestimation of the direct pyrite oxidation rate by denitrifying chemolitotrophic microorganisms (Bosch et al., 2012) as suggested by Yan et al. (2015).

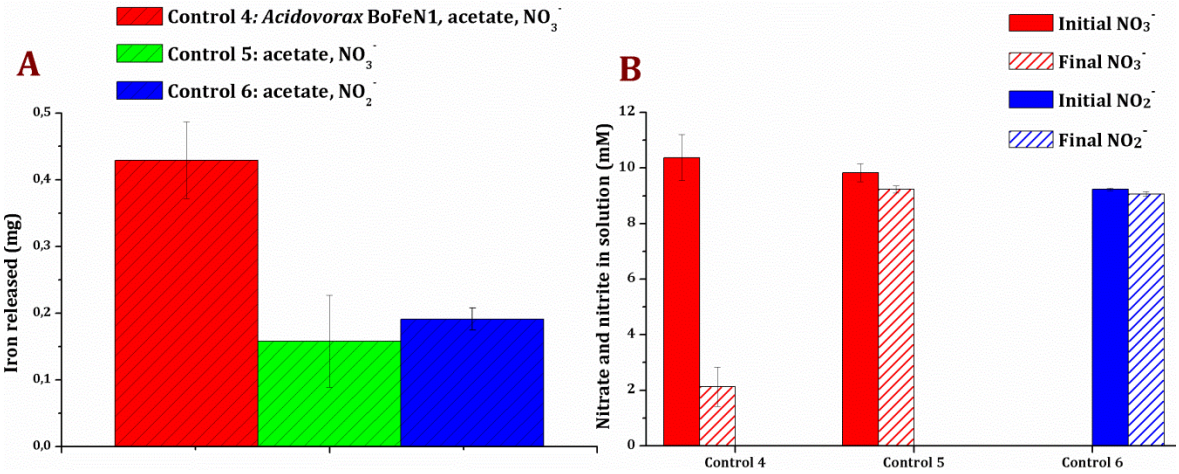

Figure 39. Iron released after pyrite dissolution (A) and nitrate and nitrite concentration (B) detected in the cultures carried out in absence of initial ferrous iron.

Interestingly, a slight iron generation was also observed in those inoculated cultures in which no initial iron was added (Figure 39A). As no Fe^{2+} was added, no Fe^{3+} production should take place and, therefore, no pyrite dissolution should be observed. Although the amount of iron detected was small, the difference between inoculated (control 4) and non-inoculated (controls 5 and 6) cultures was significant (Figure 39A). Since the possibility of a direct pyrite biooxidation by heterotrophic nitrate-reducing microorganisms is today discarded, we can assume that pyrite, upon contact with the culture medium, released small number of iron molecules, which could explains the presence of iron in these controls. Thus, in those cultures inoculated with *Acidovorax* (control 4), this small amount of iron could be susceptible of being part of the oxidation-reduction cycle mediated by the

pyrite and the NO_2^- produced by the microorganism, resulting in a higher production of iron than the observed in the non-inoculated control 5 (Figure 39A). Actually, no NO_2^- was observed in this culture at the end of the experiment (Figure 39B), which suggest that NO_2^- has been consumed either due to its reaction with Fe^{2+} (Equation 8, see list of equation in page 17) or due to a complete denitrification carried out by *Acidovorax*. However, if we consider than the iron released in control 4 was due to the chemical oxidation of Fe^{2+} by NO_2^- and the subsequent attack to pyrite by the Fe^{3+}, accordingly, the NO_2^- added to control 6 (Figure 39B) should have been able to produce the oxidation of Fe^{2+} and show a similar iron release than the controls carried out in presence of *Acidovorax*. Instead, the final iron production in *Acidovorax* cultures (control 4) was 2 times higher than those non-inoculated control carried out with NO_2^- (control 6), which showed a final iron increase similar to the control with initial NO_3^- (control 5) (Figure 39A).

Furthermore, the analysis carried out by fluorescence microscopy of the pyrite resulting from these experiments, both in the presence and absence of iron, showed that *Acidovorax* is attached to the mineral (Figure 40). If we discard a direct pyrite oxidation, these observations indicate that *Acidovorax*, in addition to increasing the iron oxidation rate, could increase the local concentration of Fe^{3+} in the mineral-microorganism interface, resulting in a higher pyrite dissolution rate in inoculated cultures than in non-inoculated cultures. In fact, co-localization of iron and cells was observed by fluorescence microscopy (Figure 40), which would support this hypothesis. Thus, the microorganism-mineral interaction could be

crucial for the metallic sulfides dissolution mediated by nitrate-reducing microorganisms, as has been observed in bioleaching studies mediated by acidophilic iron-oxidizing microorganisms such as *At. ferrooxidans* (Sand and Gehrke, 2006).

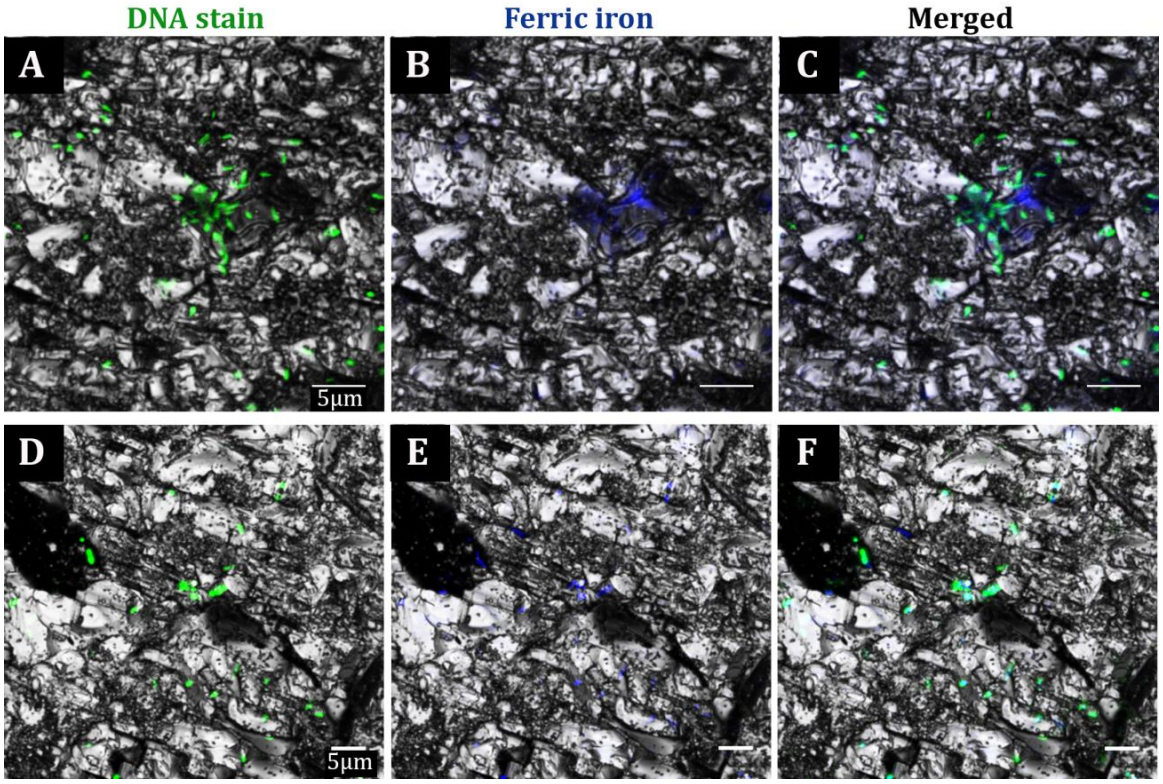

Figure 40. Acidovorax attachment to pyrite resulting of cultures carried out in the presence (A-C) or absence (D-F) of initial iron. In green, Acidovorax stained with SybrGold. In blue, Fe^{3+} stain. In gray, reflection. Scale bars 5µm.

Interestingly, in those cultures in which no initial ferrous iron was added, the number of microorganisms attached to pyrite was higher than in cultures in which initial ferrous iron was added (Figure 41). While in the first case the number of cells was $2.9x10^7 \pm 3.94x10^6$ microorganisms/mm^2, in the presence of iron a lower number of cells, $9.83x10^6 \pm 2.79x10^6$ microorganisms/mm^2, was observed. This result strongly suggests that *Acidovorax* could attach to the pyrite in search of an

iron source, either because it is used as energy source, because its high demand as a nutrient or its detoxifying effect as Klueglein and Kappler (2013) and Carlson et al. (2013) suggested respectively.

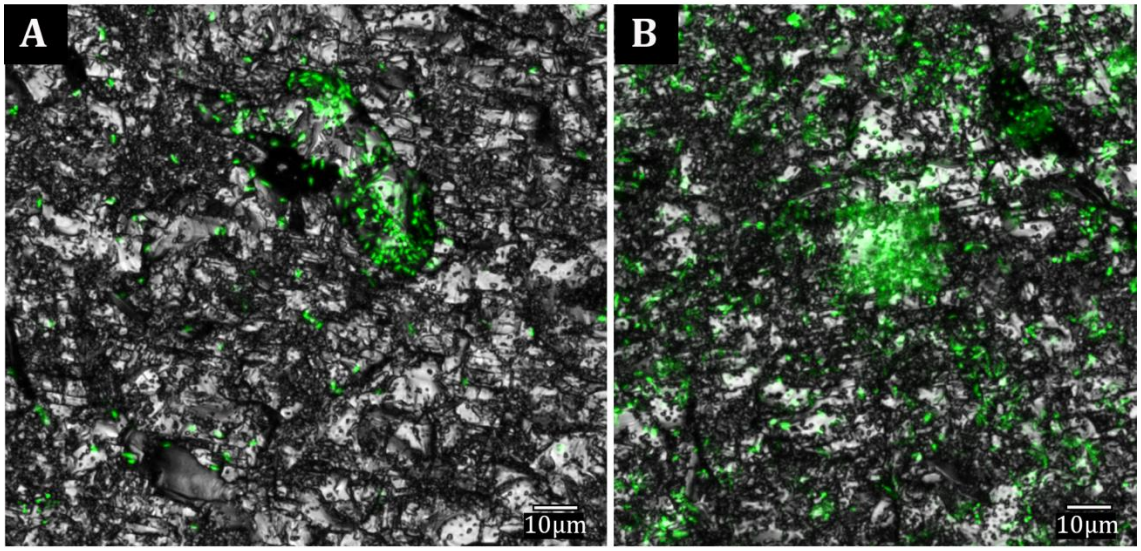

Figure 41. Comparison between the number of Acidovorax cells attached to pyrite after culturing in the presence (A) and absence (B) of initial ferrous iron. In green, Acidovorax stained with SybrGold. In gray, reflection. Scale bars 10µm.

Regarding the pH, while the cultures inoculated with *Acidovorax*, in the presence or absence of initial Fe^{2+}, showed a slight pH increase, the sterile controls did not show any variation (data not shown), which suggests that the consumption of H^+ is higher than the H^+ release due to the precipitation of $Fe(OH)_3$. Although oxidation of pyrite is generally accompanied by acidification of the medium (Bonnissel-Gissinger et al., 1998), in some studies carried out to determine the oxidant capacity of Fe^{3+} under anaerobic and neutral conditions, an increase in pH was also observed in the absence of any buffer in the medium (Moses et al., 1987). However,

no hypothesis has been advanced that explains the basification of the medium during the dissolution of pyrite under these conditions.

Unfortunately, because these experiments were designed exclusively to determine if *Acidovorax* had the ability to biooxidate pyrite, the data necessary to calculate its dissolution rate, such as the specific surface area of the pyrite used, were not calculated. Therefore, it is not possible at this moment to compare the ability of *Acidovorax* to lixiviate pyrite with the available dissolution rates of acidophilic and aerobic microorganisms such as *At. ferrooxidans,* which has been extensively studied in the last decades (Fowler et al., 2001; Rojas-Chapana and Tributsch, 2001; Rohwerder et al., 2003; Sand and Gehrke, 2006). In addition, the generation of cellular encrustations makes it difficult to obtain real values of pyrite dissolution by these microorganisms in cultures in which initial Fe^{2+} was added. In natural environments, such as the subsurface, the concentration of local iron could be much lower, which could prevent the inactivation of these microorganisms due to the precipitation of $Fe(OH)_3$, as discussed in section 6.5.2.2. In this case, the dissolution of pyrite might not be affected by the formation of growth-limiting cell encrustations. Therefore, additional experiments with continuous flow systems are necessary to determine the real rate of pyrite biooxidation mediated by *Acidovorax* at neutral pH and anaerobic conditions.

Nevertheless, these data confirm that an anaerobic oxidation of pyrite at neutral pH by nitrate-reducing microorganisms such as *Acidovorax* is possible. Actually, in the IPBSL project, 30% of microorganisms identified by at least two different techniques (Amils et al, unpublished results) are able to use nitrate as electron acceptor, including members of the genera *Tessaracoccus*, *Rhizobium*,

Hymenobacter, *Propionibacterium, Aquabacterium* or *Pseudomonas*, reducing nitrate to nitrite (Kaspar, 1982; Straub et al., 2004; Buczolits et al., 2006; Li et al., 2017). If we consider that these microorganisms can potentially induce iron oxidation through the generation of nitrogen reactive species, as was demonstrated for members of the genus *Tessaracoccus* (see section 6.5.2.1) or *Pseudomonas* (Li et al., 2017), and consequently able to promote pyrite dissolution as shown for *Acidovorax* BoFeN1, they are, together with *Acidovorax*, putative candidates to dissolve metallic sulfides in anaerobic and neutral conditions. Thus, those microorganisms with the ability to directly oxidize iron may not be the only ones involved in the generation of the high concentration of Fe detected in the Tinto basin, which means that nitrate-reducing microorganisms should be also considered. Accordingly, nitrogen and iron cycles could be the key biogeochemical cycles that can explain the subsurface origin of the high concentration of iron in Río Tinto.

6.5.4. Correlative Fluorescence-Raman microscopy

One of the main unknowns that must be solved to understand the functioning of underground ecosystems is how mineralogy affects the distribution of the microbial populations or, on the contrary, how a specific microbial population affects the mineralogy of the system. Several studies have shown that deep subsurface biodiversity depends directly on the mineralogical composition of the subsurface. Minerals, being considered the main sources of electron donors and acceptors in these ecosystems, would determine which chemolithotropic

metabolisms can be carried out and, therefore, the microorganisms that inhabit a certain microniche (Jones and Bennett, 2014; Rempfert et al., 2017). However, up to now, hardly any studies have been carried out to relate the presence of a determined metabolism to the presence of a specific type of mineral (Jones and Bennett, 2014) and no study has analyzed how the microorganism-mineral interaction can affect the ecosystem.

In the IPB subsurface, this issue acquires even greater relevance. As we have shown before, the generation of the characteristics detected in the Tinto basin is consequence of the metabolic activity of the microorganisms that inhabit this environment, interacting with the minerals of the IPB subsurface. As discussed above, nitrate-reducing microorganisms seems to be involved in the dissolution of metal sulfides, mainly pyrite, giving rise to the high concentrations of ferric iron detected in the river. In addition, as discussed, this process is more effective if the microorganisms are attached to the metal sulfide (Sand and Gehrke, 2006; Vera et al., 2013).

To determine if nitrate-reducing microorganisms are in contact in the subsurface with metallic sulfides, we make use of the correlation between fluorescence and confocal Raman microscopy. On the one hand, fluorescence microscopy allows the identification of a specific microorganism by using specific probes (Amann et al., 1995) and, on the other hand, confocal Raman microscopy allows the analysis of the composition and molecular structure of the mineral substrate (Smith and Dent, 2013). Thus, while FISH will provide the location of a specific microorganism, the mineral to which it is attached can be identified by means of Raman spectroscopy.

6.5.4.1. Avoiding fluorescence interference

The main problem of correlating fluorescence microscopy and confocal Raman microscopy lies in the need of fluorophores. Both fluorescence and Raman spectroscopy are based on the same principle: the incidence of a monochromatic light source on a molecule will cause changes in its wavelength, which will be recorded in a detector (Paddock, 1999; Smith and Dent, 2013). Since the fluorescence phenomenon is considerably more efficient than the Raman scattering, it can mask the Raman signal, to such an extent that fluorescence is considered the natural enemy of Raman spectroscopy (Dieing et al., 2011). To avoid the interference of fluorescence in Raman spectroscopy, it is possible to make use of fluorophores that are not excited by the laser line used for the acquisition of the Raman spectrum. However, the use of fluorophores that are excited with the same wavelength is also possible if, prior to the Raman analysis, the fluorophore is photobleached (Read et al., 2010). Photobleaching is a light-induced process resulting in the permanent photochemical destruction of the fluorophore, thus photobleached molecules will lose the ability of emit fluorescence and will not interfere in the Raman analysis (Song et al., 1995).

To choose in our study the most suitable fluorophores for the FISH-Raman correlation, several fluorophores were analyzed by CRM, whose excitation laser line was 532nm.

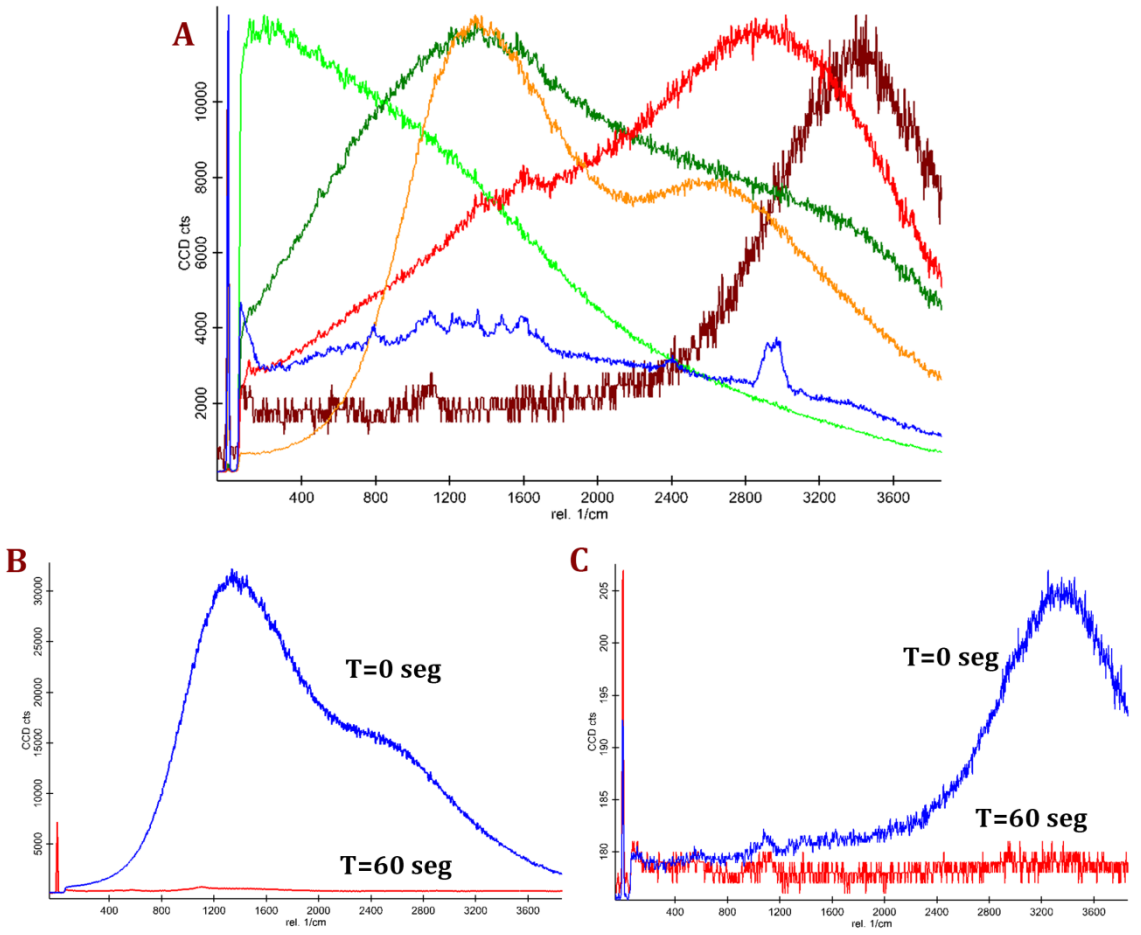

Figure 42. Raman spectra of the different fluorophores tested in this study. A, Raman spectra of Pacific Blue (blue), FITC (light green), Alexa 488 (green), CY3 (orange), Alexa 594 (red) and Alexa 633 (brown). B, Laser induced photobleaching of Cy3 fluorophore after 60s of laser incidence. C, Laser induced bleaching of Alexa633 fluorophore after 60s of laser incidence.

Figure 42A shows that, by confocal Raman microscopy, the fluorescence signal were detected for all the fluorophores analyzed, even in those whose excitation does not coincide with the incident wavelength, which can be explained by the wide excitation spectrum that they present. Although in this case the intensity of fluorescence detected was lower, as shown for the Pacific Blue fluorophore (excitation max at 410nm), it could not be seen clearly the Raman signal of the molecule, which was hidden by the emitted fluorescence signal. However, all fluorophores were susceptible to photobleaching, showing fluorophores CY3 and

Alexa 633 the highest fluorescence loss after only one minute of laser incidence (Figure 42B and C). In fact, CY3 fluorophore has been previously used in Raman-FISH analysis showing a similar photobleaching rate (Huang et al., 2007). Therefore, the subsequent Raman-FISH experiments for the IPB subsurface samples were carried out using one of these fluorophores, CY3 or Alexa 633, whose choice in each sample was made based on the data obtained in the non-specific binding controls of the fluorescent molecules detailed in section 6.1.1.

6.5.4.2. Organic material reference

Since it is expected that the area to be studied by CRM in native subsurface samples contain organic matter due to the presence of microorganisms, several different organic compounds and polymers were analyzed to serve as a reference in the interpretation of their Raman spectra (Figure 43). The materials analyzed included: proteins, such as lysozyme and trypsin; polysaccharides, such as starch and cellulose; and sugars, such as glucose. In addition, the Raman spectra of the bacteria *S. aureus* and *E. coli* were included as reference material, which were obtained in the same Raman equipment in which all the measurements of this work were made.

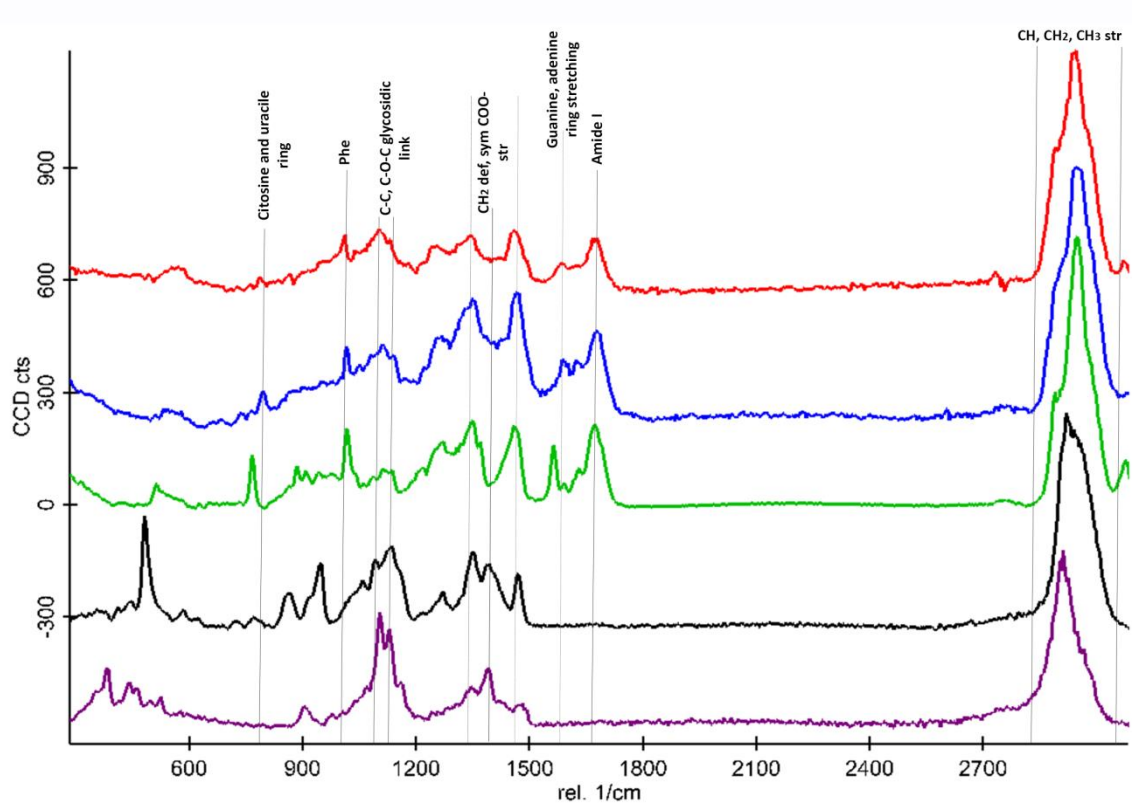

Figure 43. Raman spectra of selected organic reference material. From top to bottom: E. coli spectrum (red), E. aureus spectrum (blue), lysozyme spectrum (green), starch spectrum (black) and cellulose spectrum (purpura). The characteristic bands of each spectrum are shown.

Table 9 summarizes the assignment of the Raman bands to characterize the reference material. All the spectra of the organic matter analyzed were characterized mainly by the presence of prominent bands in the range of 2800-3020 cm^{-1}, which are typical of the stretching mode of the CH bond, probably originated from the functional groups $-CH_3$, $-CH_2$ and -CH of the different molecules (Figure 43). Polysaccharides, both starch and cellulose, present bands of great intensity at 1127 cm^{-1}, which can be assigned to the C-C stretching bond and the C-O-C glycosidic link, and between 1400-1420 cm^{-1}, assigned to the vibration of the COO^- group. Regarding the Raman spectrum of proteins, the characteristic peaks of tryptophan (770cm^{-1}), phenylalanine (1014cm^{-1}), and the amide III (1270cm^{-1})

and amide I (1670cm^{-1}) bonds were observed. Finally, both the spectra of *E. coli* and *S. aureus* showed characteristic peaks of carbohydrates, lipids and proteins, the main constituents of the microbial cells, as well as a series of low intensity bands that were assigned to the DNA/RNA nucleotide rings vibration (at 785cm^{-1} for uracil and cytosine and at 1580cm^{-1} for adenine and guanine).

Table 9. Assignment of Raman bands. Str= stretching, def=deformation, breath=breathing, asymm= asymmetric, symm=symmetric, G= guanine, A=adenine, C=cytosine, U=uracil, Phe=phenylalanine, Trp=tryptophan.

Raman band or band range (cm^{-1})	Assignment				Reference
	Carbohydrates	DNA/RNA	Lipids	Proteins	
2800-3020	CH, CH_2 and CH_3 str		CH, CH_2 and CH_3 str	CH, CH_2 and CH_3 str	b, f, g
1670-1680				Amide I	e, h
~1580		G and A ring str			c, d, e
1400-1420	symm COO- str				e, f, j
1350-1475	CH and CH_2 def		CH and CH_2 def	CH and CH_2 def	a, c, f, h
1270				Amide III	c, h
1160	C–C, C–O ring breath, asymm				e, j
1127	C-C str and C-O-C glycosidic link		C-C str	C-C str	e, j
1092		Phosfate ester str, symm	Phosfate ester str, symm		c, e
1014			Phe		h
785		C and U ring str			c, d, f
770				Trp	h
530-540	C-O-C glycosidic link				e, I, j
306-480	Skeletal mode carbohydrates				e, j

a- Cael et al. (1973)
b- Czamara et al. (2015)
c- Dieing et al. (2011)
d- Harz et al. (2005)
e- Ivleva et al. (2009)
f- Lin-Vien et al. (1991)
g- Maquelin et al. (2002)
h- Rygula et al. (2013)
i- Schuster et al. (2000)
j- Wagner et al. (2009)

6.5.4.3. Raman-FISH for IPB subsurface native samples

The selected microorganism for the study using Raman-FISH was *Acidovorax*. The members of the genus *Acidovorax* are able to oxidize iron by reducing nitrate (Straub et al., 2004; Kappler et al., 2005) and, as showed in section 6.5.3.1, are able to promote pyrite dissolution. Therefore, *Acidovorax* is one of the genera that could be involved in the dissolution of metal sulfides in the IPB subsurface.

CARD-FISH was performed with the specific probes to detect members of the genus *Acidovorax* in selected rock samples from several depths. Once microorganisms were located by means of fluorescence in the coordinate system used, an analysis of the area was performed using CRM. In our studies, Raman analyses were carried out by mapping different focal planes (z-stack) of each studied area, in which a single spectrum/μm^2 was acquired. As a result, for each analyzed area thousands of spectra were obtained that provided information on the structure and chemical composition of the sample in three dimensions at high resolution.

The thousands of spectra obtained from each analyzed area could be classified into three representative spectra, called spectrum A, spectrum B and spectrum C, which were repeated throughout the Raman mappings (Figure 44A and B). Both spectrum A and spectrum B (Figure 44A) showed the characteristic peaks of the CH stretching bond of organic matter in the range 2800-3020 cm^{-1}. However, unlike spectrum B, spectrum A presents Raman bands representative of different organic compounds such as proteins at 1014 cm^{-1} and 1672 cm^{-1}, assigned to the presence of Phe and to the amide I bond respectively; and DNA and phospholipids at 1092 cm^{-1}, assigned to the phosphate ester bonds. On the contrary, the spectrum

B is characterized by the presence of bands in the range of 530-540 cm^{-1} as well as 1160 cm^{-1}, which are representative of carbohydrates. Thus, we could determine that spectrum A corresponds to bacteria, that is to say to members of the genus *Acidovorax*, and spectrum B corresponds to polysaccharides.

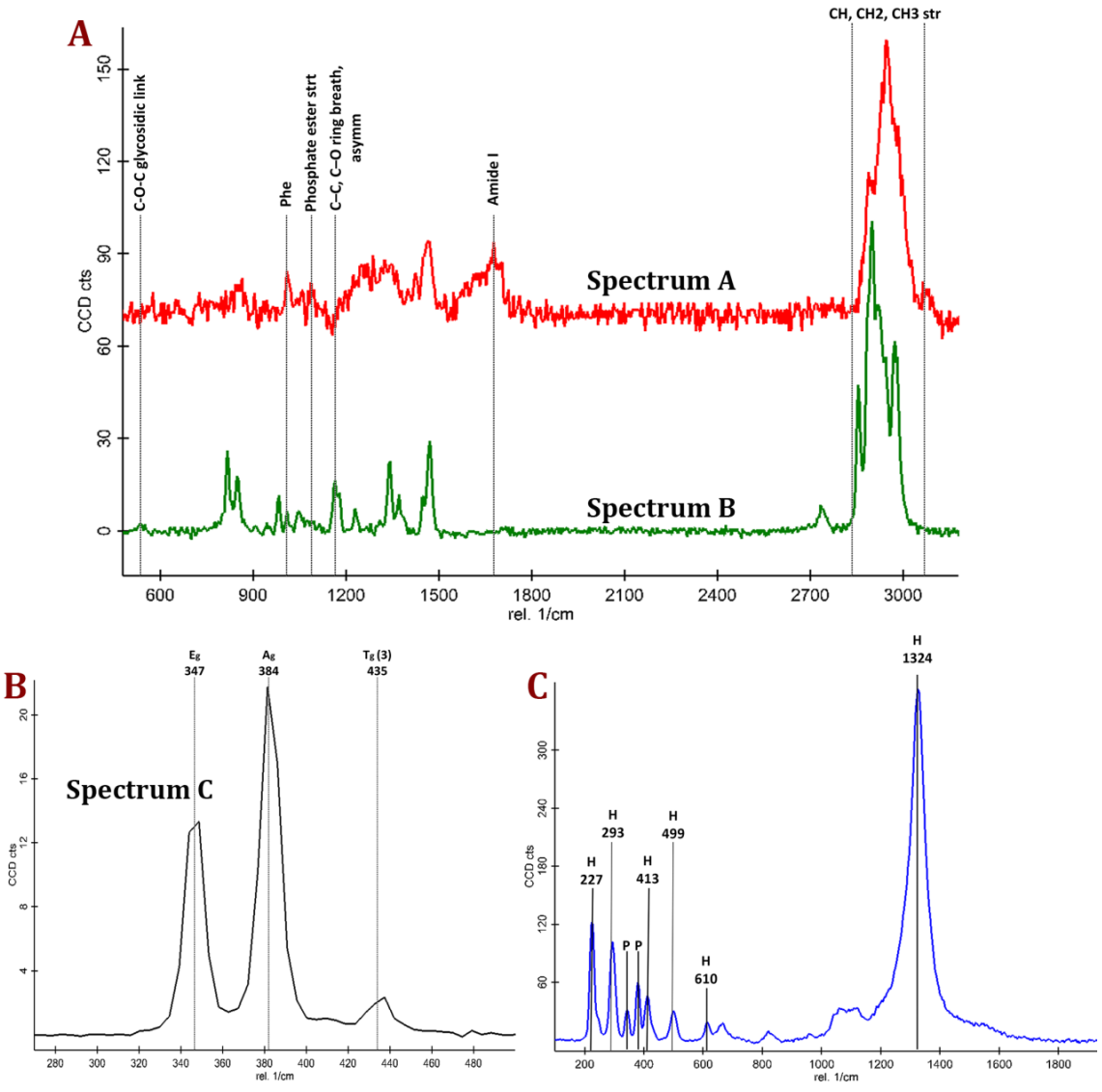

Figure 44. Representative Raman spectra detected by CRM in areas where members of the genus Acidovorax were located by CARD-FISH. A, Raman spectra assigned to organic matter: in red, spectrum A/Acidovorax; in green, spectrum B/polysaccharides. B, Raman spectrum assigned to pyrite (spectrum C); and D, Raman spectrum assigned to hematite. The characteristic bands of each spectrum are indicated.

Figure 45 is a two-dimensional representation of the position of both spectra in the analyzed area of a sample taken at 228.6mbs showing the presence of polysaccharides surrounding the cells. This observation corroborates the data presented above which indicated that members of the genus *Acidovorax* are included in biofilms (Figure 36B). As shown before, iron was present in *Acidovorax*-containing biofilms, which would enhance the metallic sulfides dissolution.

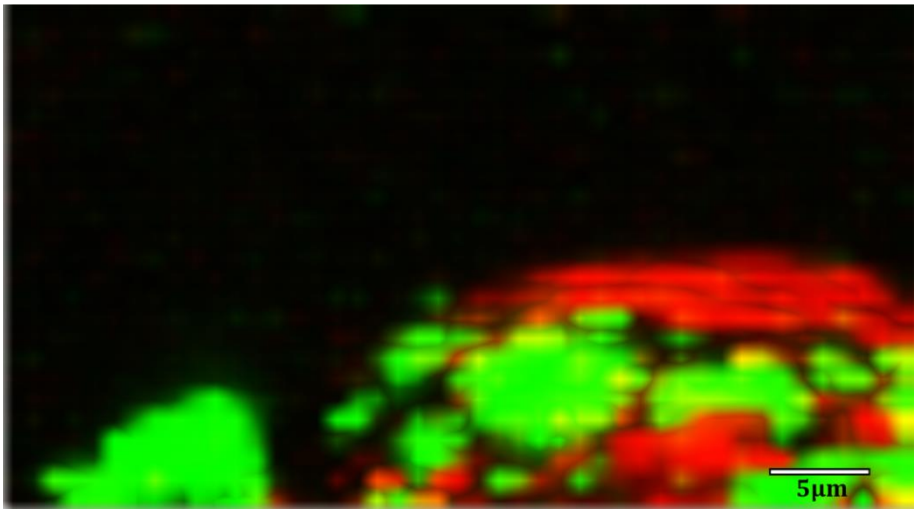

Figure 45. Maximum intensity projection of organic matter Raman maps of a native sample of the IPB subsurface from 228.6 mbs. In red, location of the spectra assigned to Acidovorax. In green, location of the spectra assigned to polysaccharides. Scale bar, 5µm.

On the other hand, spectrum C corresponds to the average spectra of the mineral substrate on which the microorganisms are attached (Figure 44B). The spectrum C shows two peaks of high intensity at 347 and 384 cm^{-1} and a less intense band at 435 cm^{-1}, which are characteristic of the Raman-active modes of pyrite (Ushioda, 1972; Vogt et al., 1983; Bryant et al., 2018). The first corresponds to the S2 dumbbell libration (Eg), the second to the symmetric stretching of the S-S link in

phase (Ag) and the third to the coupling of the libration and stretch modes (Tg (3)) (Blanchard et al., 2005). All the *Acidovorax* colonies detected were attached to pyrite in each of the samples analyzed in this study. In some cases the presence of hematite was detected in the studied area. The hematite spectrum (Figure 44D) is easily recognizable due to the presence of bands at 227 cm^{-1}, 246 cm^{-1}, 293 cm^{-1}, 412 cm^{-1} , 498 cm^{-1}, 610 cm^{-1} and, above all, the strong band at 1322 cm^{-1}, whose intensity varies with the applied intensity of the incident laser (De Faria et al., 1997; De Faria and Lopes, 2007). Hematite is a ferric iron oxide whose appearance has been observed after the dissolution of pyrite at alkaline pH as a secondary mineral (Caldeira et al., 2003). In addition, hematite has been observed in the terraces formed in Río Tinto basin, as a final product of iron hydroxides evolution (Fernández-Remolar et al., 2005).

Interestingly, the pyrite Raman spectrum varies in different samples and even within the same analyzed area in each sample. Variations in the relative intensity of the Eg and Ag bands were observed as well as changes in the pyrite bands positions (Figure 46). In fact, both parameters of the pyrite Raman spectrum vary greatly from one study to another (Ushioda, 1972; Vogt et al., 1983; Blanchard et al., 2005; Cavalazzi et al., 2012). Recently, this variability has been analyzed in depth by Bryant and collaborators (2018), who determined that both the crystalline orientation of the pyrite and laser heating are the main causes of the differences in the pyrite Raman spectra. On the one hand, the changes in the relative intensity of the Eg and Ag bands were attributed to the crystalline orientation of the pyrite with respect to the polarization plane of the incident laser, which, in addition, may be affected by the laser power. Actually, the intensity ratio

of the Ag band relative to the Eg band vary from 0.9 to 3.5 in different studies in which different pyrite size and morphologies were analyzed using different laser power. Bryant and collaborators showed variations in the range of 0.22-1.3 in centimeter scale cubic pyrite while in pyritohedral pyrite (12 faces) varied from 0.81 to 2.01 due to the differential excitation of the bands of the different analyzed pyrite faces. However, in the Raman spectra obtained from the natural pyrite of the IPB subsurface samples, variations of the intensity ratios of the Ag relative to Eg band in the range of 0.6-3.5 have been observed in the same pyrite grain, which, to our knowledge, never has been described before (Figure 46A and B).

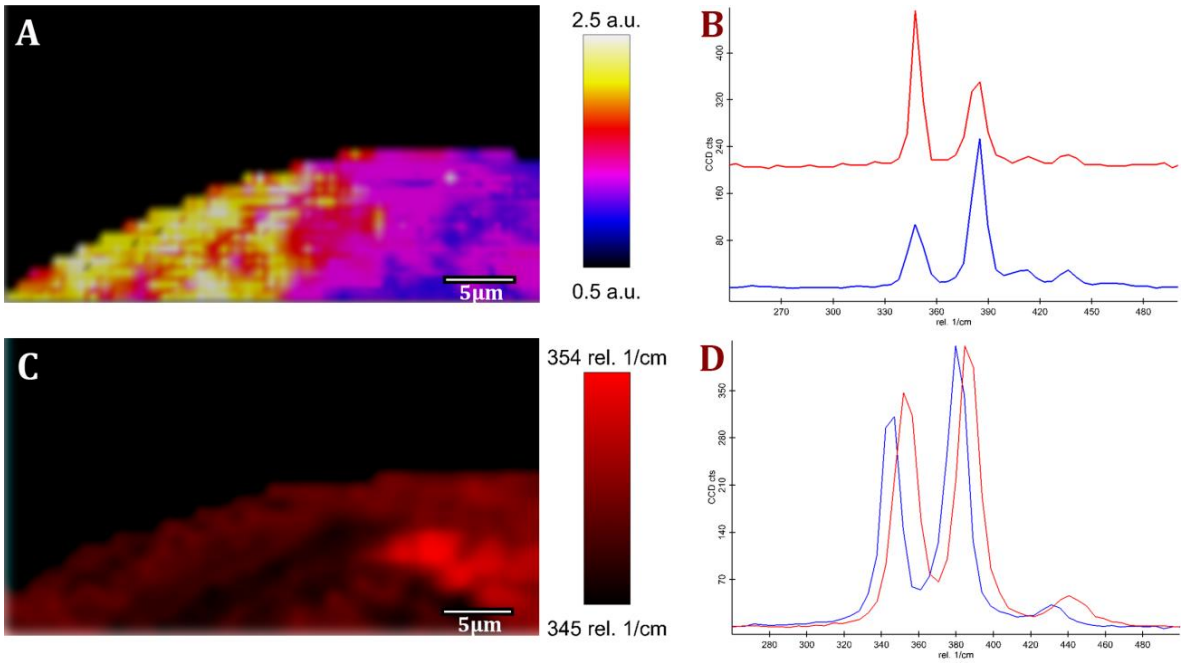

Figure 46. Variations detected in the pyrite Raman spectrum in which Acidovorax was attached (see Figure 45) in a sample from 228.6mbs of the IPB subsurface. A, Raman map of the variations in the intensity ratio of the Ag band relative to Eg band. B, Raman spectra showing the minimum and maximum intensity ratio of the Ag band relative to Eg band. C, Raman map of the Eg band displacement. D, Raman spectra showing the minimum and maximum Raman shift detected in the pyrite bands. Scale bar, 5µm.

On the other hand, the displacement of the position of the pyrite bands towards lower wavelengths has been attributed either to an effect of laser heating or to the presence of trace elements such as copper, zinc or lead among others (Bryant et al., 2018). While in the latter case the variation of the position of the bands is minimal (up to ~ 1cm^{-1}), downshifting of the pyrite bands up to 12.7 cm^{-1} due to the laser heating has been observed (Bryant et al., 2018). However, these extreme variations in bands position have only been detected modifying the laser power in pyrite which grain size was below 10μm. In our analyzes, variations up to 10cm^{-1} in the position of the pyrite bands have been detected in the same grain (Figure 46 C and D), which in all cases had at least 150μm. In addition, a low laser power has been used in our experiments, which was held constant throughout the analysis. Hence, the observed Raman shifts in those pyrite grains where *Acidovorax* was present may not be a consequence of the laser heating.

In the native pyrite of the IPB subsurface in which *Acidovorax* is attached, both the range of relative intensity of the Eg and Ag bands and the range of displacement of the observed bands do not conform the variations in the Raman spectra of the pyrite due to the effects of the crystalline orientation or laser heating described above. However, there is no data available about pyrite Raman spectra and its variability in a lateral micrometer scale since all measurement made up to now where carried out with macroscopic techniques which provide only averaged information (Bryant et al, 2018 and references therein). Actually, natural pyrite may be found in a varied combination of crystal orientations due to the microscopic alteration of growth faces (Chandra and Gerson, 2010). In addition, spatially resolved surface characterization of pyrite performed with alternative

microanalytical methods as scanning photoelectron microscopy (SPEM) or X-ray photoemission electron microscopy (PEEM) revealed a very heterogeneous pyrite surface, both topographically and chemically (Chandra and Gerson, 2010). Hence, the resolution of the Raman equipment applied in other studies may be not sufficient to detect the surface variability observed in our microanalysis.

On the other hand, no Raman analysis of pyrite performed so far has included the effect that microorganisms can cause on the mineral and, therefore, in their Raman spectra. In fact, in Figure 45 and Figure 46 (A and C), which show Raman maps of the microorganisms and the variations of the pyrite Raman spectrum of the same analyzed area, a correlation between both is detected. To determine if the presence of *Acidovorax* influences the relative intensity of the Eg and Ag bands or their position displacement, the variations of both parameters were analyzed in the presence or absence of the microorganism in each mapping performed in this study.

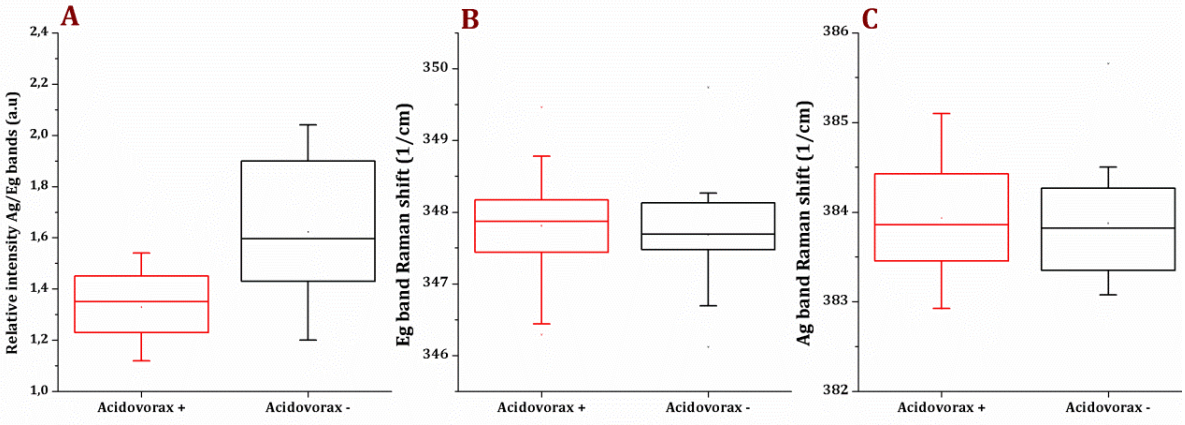

Figure 47. Average values of the intensity ratio of the Ag band relative to Eg band (A), the position of the Eg band (B) and the position of the Ag band (C) of pyrite Raman spectra in presence (red) or absence (black) of Acidovorax resulting from Raman analysis of the IPB subsurface native samples.

As shown in Figure 47, it is clearly observed that in the presence of *Acidovorax* the ratio of the intensity of the Ag band relative to Eg band is considerably lower than the values determined in the absence of the microorganism (Figure 47A). In the presence of *Acidovorax*, the values fluctuate between 1.11-1.54, with an average value of 1.34 while in the absence of *Acidovorax*, the values fluctuate between 1.19 and 2.03, showing an average value of 1.60. As discussed above, the difference in the ratios of the intensity of the Ag and Eg bands are attributed to the crystalline orientation of the mineral (Bryant et al., 2018). Therefore, these data could indicate that *Acidovorax* attach preferentially to those faces of pyrite in which the band Eg, which represents the S2 dumbbell libration of the pyrite structure, shows a greater intensity. However, the possibility that *Acidovorax*, in some way, could affect the pyrite structure cannot be ruled out due to the great range of relative intensity Ag/Eg observed in the same pyrite grain.

Regarding the Raman displacement of the Ag and Eg bands, the minimum difference in the average position of both bands in the presence and absence of the microorganism seems to indicate that there is no correlation between the location of *Acidovorax* and this displacement (Figure 47B and C). However, the results obtained indicate that the presence of *Acidovorax* seems to extend the range of displacement of both bands, being its average value slightly displaced at longer wavelengths, which is the opposite to what has been described before, since changes in pyrite position bands tent to downshift due to the laser heating or the presence of trace metals (Bryant et al., 2018).

In addition, many studies have shown that the formation of biofilms enhance the dissolution of metal sulfides since ferric iron is concentrated in the

microorganism-mineral interface due to the presence of exopolysaccharides, such as those containing uronic acid (Sand and Gehrke, 2006; Vera et al., 2013). As *Acidovorax* biofilms contain a considerable amount of iron (see section 6.5.2.2), the possibility that the presence of iron-exopolysaccharides could affect the Raman spectrum of pyrite was also analyzed. However, our analysis did not show a correlation between the presence of exopolysaccharides and the variations in the Raman spectrum of pyrite in the native samples of the IPB subsurface (data not shown).

To determine if *Acidovorax* is responsible of the changes observed in the pyrite Raman spectra in native samples of the IPB subsurface, the surface characterization of the biooxidated pyrite by *Acidovorax* resulting from the experiment described above (section 6.5.3.1) is being carried out at this moment and only the preliminary results of the pyrite obtained from control 4 and control 5, the cultures in which initial ferrous iron was no added, are included in this memory.

Preliminary results of the pyrite obtained from the control 4, in which *Acidovorax* was grown in absence of initial ferrous iron, indicate that, although there seems to be no co-localization of *Acidovorax* with the variation of the Raman position of the Ag and Eg bands (data not shown), as observed in native subsurface samples, *Acidovorax* is co-localized in the areas where the pyrite shows a minor intensity ratio of the band Ag relative to the Eg band (Figure 48).

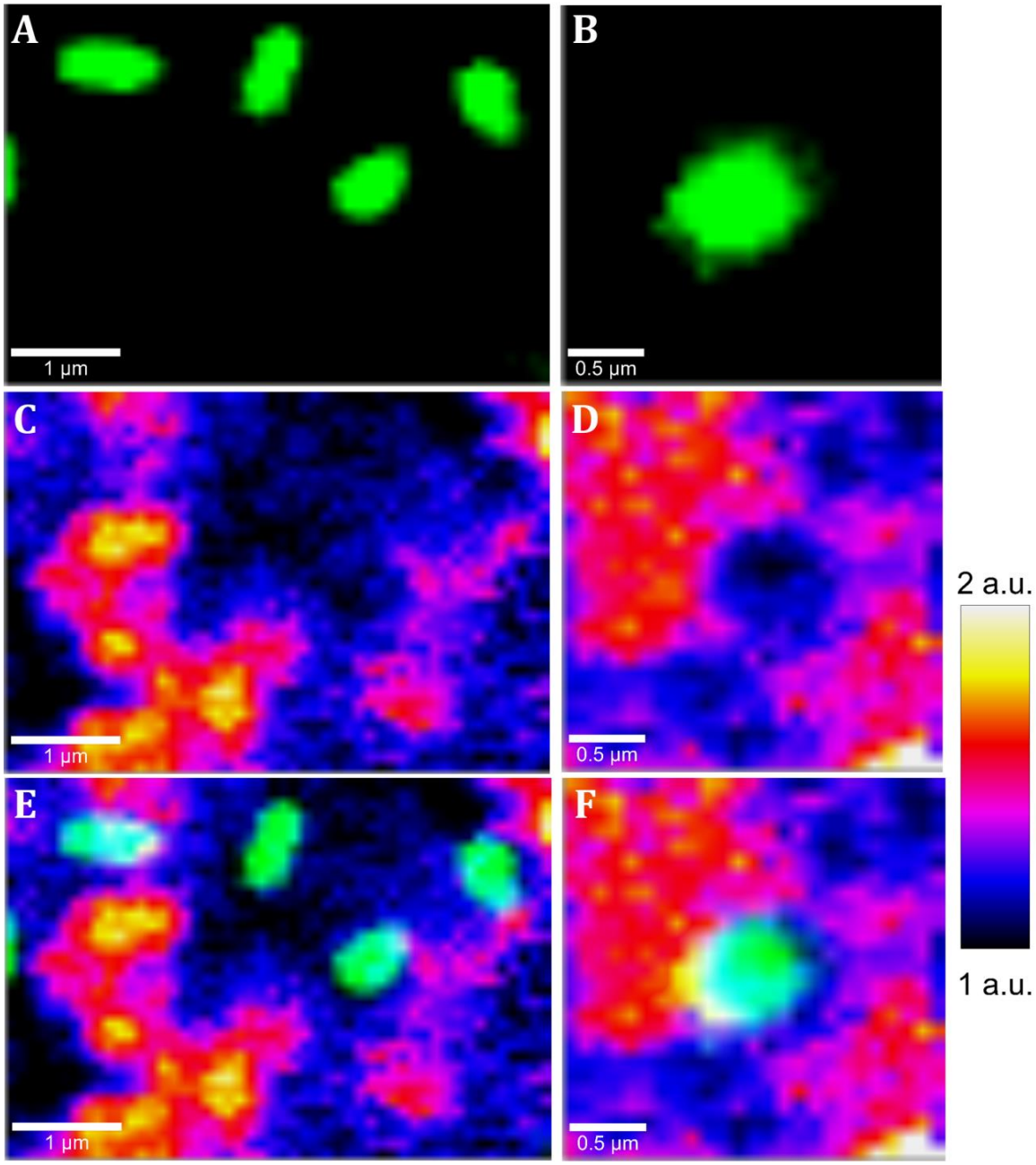

Figure 48. Raman map of the biooxidized pyrite by Acidovorax (control 4) showing the co-localization of cells and pyrite areas which showed a low intensity ratio of Ag band relative to Eg band. A and B, location of the Raman spectra assigned to Acidovorax. C and D, Raman map of the variations in the intensity ratio of the Ag band relative to Eg band. E and F, merged.

In the experiment carried out to determine if *Acidovorax* was able to oxidize pyrite, pyrite coupons cut in parallel to {100} face of the mineral were used. However,

since the coupons were not polished, the pyrite surface was not completely smooth and presented different crystal orientations due to the presence of cracks and imperfections. The existence of these dissimilarities, both topographic and orientation, on the surface of the starting mineral could indicate that *Acidovorax* attach preferentially either to areas where the ratio of the intensity of the band Ag in relation to the band Eg tends to 1 or to areas where there are imperfections. In fact, several studies have shown that both parameters can influence the adhesion of microorganisms to pyrite. It has been observed that *At. ferrooxidans* preferentially attach to pyrite, in addition to areas where there are imperfections, to areas with low degree of crystallization (Sanhueza et al., 1999) or oriented along the crystallographic axes (Edwards and Rutenberg, 2001). Furtermore, it has been observed that members of the genera *Leptospirillum* and *Acidithiobacillus* attach preferentially to electronegative areas (Gehrke et al., 1998; Schippers et al., 2013). While adhesion to areas that show imperfections can be attributed to an increase in the area of contact between microorganism-mineral, preferential adhesion to certain crystallographic orientations or to electronegative zones remains as an open question.

However, although the starting pyrite presents variations, the analysis of Raman mappings performed in the biooxidated and control pyrite show clearly that *Acidovorax*, indeed, does influence the pyrite Raman spectrum. Figure 49 shows the comparison of the average pyrite Raman spectra of several planes obtained from cultures in which *Acidovorax* grew in the absence of initial iron (control 4, see section 6.5.3.1) and the average pyrite Raman spectra of its respective non-inoculated control (control 5). These preliminary results show that, in cultures

where *Acidovorax* grew, the average pyrite Raman spectra present changes in the ratio of the intensity of the band Ag relative to Eg band, which tends to be lower, as well as displacements of both bands at higher wavelengths.

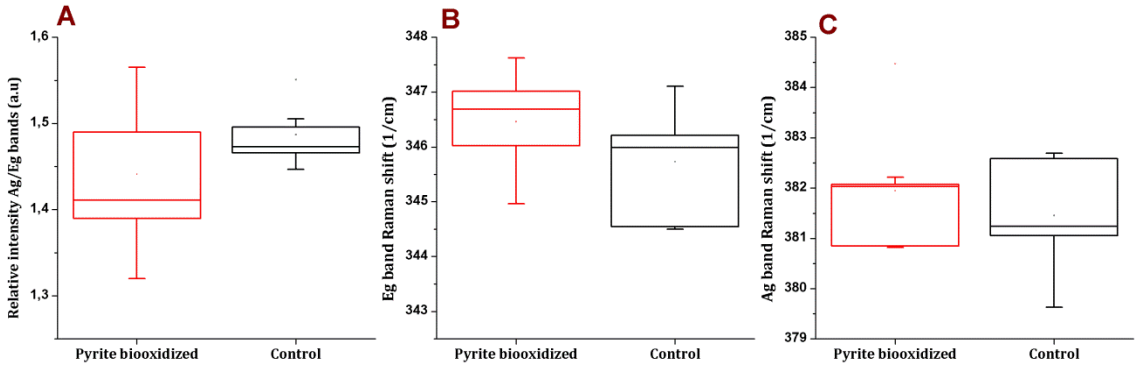

Figure 49. Pyrite Raman spectra comparison between biooxidized and control pyrite. A, intensity ratio of the Ag band relative to Eg band; B, Raman position of Eg band; C, Raman position of Ag band.

If we consider that in this culture an increase of final iron was observed (Figure 39A), that is, pyrite dissolution, it is reasonable to relate the variations of the average pyrite Raman spectra with the activity of *Acidovorax*. However, more in-depth analysis is needed to determine why *Acidovorax* attach to specific areas of pyrite and how it produces these modifications in the mineral.

Nevertheless, the repeated observation of *Acidovorax* attached to pyrite in the IPB subsurface at different depths being part of iron-containing biofilms as well as the presence of hematite, together with the data present above in which it was proved that this microorganism is able to promote the pyrite dissolution, supports the hypothesis that nitrate-reducing microorganisms such as *Acidovorax* are, at least in

part, responsible for the dissolution of this mineral at neutral pH and, therefore, of the subsurface origin of the high concentration of iron found in Río Tinto.

6.6. Overall discussion

Thanks to the IPBSL project and its predecessor, the MARTE project, it has been possible to characterize in depth both the geochemical characteristics and the microbial diversity dwelling in the IPB subsurface. To determine both microbial and metabolic diversity, several complementary methodologies have been implemented, ranging from the use of more traditional techniques such as cloning or enrichment cultures to the use of state-of-the-art techniques such as NGS. The results obtained from both projects have shown that life in the IPB subsurface is (relatively) abundant and diverse, even though the hard rock subsurface systems are considered extreme oligotrophic environments.

The subsurface is considered an extreme environment, fundamentally, due to the low energy availability (Kerr, 2002; Hoehler, 2004; Jørgensen and Boetius, 2007). This is the reason why it has traditionally considered that most of the microorganisms that inhabit these systems are in a dormant state (Hoehler and Jorgensen, 2013). However, in the IPB subsurface, energy availability does not seem to be a limiting factor. The presence of both organic acids and putative inorganic electron donors and acceptors that can be used by microorganisms in their metabolism has been detected. Although the concentration of these compounds is not very high, many of the microorganisms that inhabit the IPB

subsurface seem to be not only alive, or simply "surviving" as has been proposed (Kerr, 2002; Jørgensen and Boetius, 2007; Hoehler and Jorgensen, 2013), but also active, as shown by the hybridizations carried out with FISH probes, which indicate the presence of a considerable amount of ribosomes in the hybridized microorganisms. The oligotrophy, therefore, does not seem to be an impediment to life in the IPB subsurface, as it is not in other underground environments (Zinke et al., 2017). Actually, some of the microorganisms isolated in this system, such as *Tessaracoccus* T2-5-50, showed a higher growth rate under oligotrophic conditions than in the presence of high concentrations of organic matter, hence they seem to be very well adapted to conditions of low availability of nutrients (Leandro, personal communication).

In addition, not only many of the microorganisms appear to be active, but they also obtain the necessary amount of energy to produce and maintain biofilms, which entails a high energy cost. However, the investment of energy to produce these structures could be a long-term benefit for microorganisms in the subsurface, since it implies greater retention of water and nutrients as well as the provision of an energy reservoir (Flemming, 2011; Flemming et al., 2016; Neu and Lawrence, 2016). In fact, biofilms seem to be a fairly widespread lifestyle in the IPB subsurface.

On the other hand, the complete set of data obtained in the IPBSL project indicates that in this system there is a great diversity, both microbial and metabolic. In fact, the biosphere detected in the IPB subsurface is much more diverse than the prokaryotic biodiversity detected in the Río Tinto basin, both in the water column (González-Toril et al., 2003) and in the sediments (Sánchez-Andrea et al., 2011;

García-Moyano et al., 2012). The IPB subsurface is not an isolated case since it has been shown that the majority of underground locations, although with exceptions (Moser et al., 2005; Dong et al., 2014b), show a high degree of biodiversity (Lau et al., 2014; Nyyssönen et al., 2014; Probst et al., 2014a; Ino et al., 2016) (Appendix 1).

Among the techniques used for the characterization of the IPB subsurface biosphere, FISH techniques stand out. As discussed throughout this work, FISH is the only technique, so far, that allows to analyze the distribution of microbial biodiversity at a micrometer scale (Moter and Göbel, 2000), which can become especially relevant in heterogeneous environments such as the subsurface. Thus, we have been able to verify that phyla such as Proteobacteria or Actinobacteria, which showed to be very numerous by means of NGS techniques (Puente-Sánchez, 2016), are widely distributed in the IPB subsurface. On the contrary, thanks to CARD-FISH analysis reported in this work, it has been possible to verify that members of other phyla, with much less evidences for their presence using other techniques, could play a more important role than it can be expected due to its high level of distribution along borehole BH10. For instance members of the Archaea domain or the Chloreflexi and Planctomycetales phyla detected by fluorescence *in situ* hybridization all along BH10 column.

On the other hand, the metabolic cooperation between species seems to be crucial for life in underground environments, since it allows maximizing the energy obtaining by microorganisms (Morris et al., 2013). Thanks to the analyzes carried out by CARD-FISH, it has been possible to verify that the majority of the colonies observed could be formed by more than one type of microorganism, as indicated

by the existence of a greater quantity of microorganisms detected by general DNA staining in relation to the number of microorganisms detected with specific probes. Actually, the presence of several different microorganisms has been also detected in the analysis of individual colonies isolated from enrichment cultures (T. Leandro, personal communication). This observation suggests that obligatory collaborations have been established in the IPB subsurface, which has made difficult to isolate a greater number of microorganisms in this project. By means of double hybridizations, we have also been able to determine some of the microbial interactions that are taking place in the IPB subsurface. Among the associations detected, the interaction between members of the iron and the sulfur cycle stand out. Although we cannot determine the nature of the association between bacteria and archaea until a deeper study is made, the association between *Acidovorax*, *Acidiphillium*, *Sulfobacillus* and SRB induces to consider a metabolic collaboration thanks to which the iron and the sulfur cycles are functionally active and interconnected in the ecosystem.

The co-localization of *Acidovorax* with Fe^{3+} and pyrite, along BH10, strongly suggests that this microorganism is one of those responsible for the dissolution of this mineral in the IPB subsurface, releasing both Fe^{2+} and $S_2O_3^{2-}$. In addition, the presence of acetate and nitrate throughout the entire column suggests that the activity of this microorganism is not limited by the lack of nutrients. The reduced Fe generated can be oxidized again by *Acidovorax*, re-generating the main pyrite oxidant. However *Acidiphillium* and *Sulfobacillus* can also benefit from Fe^{3+}, which can use it as an electron acceptor (Küsel et al., 1999; Johnson and Bridge, 2002; Justice et al., 2014). On the other hand, the sulfur species present in these

microniches will depend mainly on the local pH. At pH close to neutrality, it has been observed that the reservoir of sulfoxy intermediates product of the pyrite dissolution is higher than at acidic pH (Bonnissel-Gissinger et al., 1998). In the presence of an oxidizing agent, such as Fe^{3+} or NO_2^- produced by *Acidovorax*, $S_2O_3^{2-}$ can be further oxidized to $S_4O_6^{2-}$, which is quite stable at pH less than 7 (Nordstrom, 1982). $S_4O_6^{2-}$ could be used by *Sulfobacillus* as an electron donor coupling it to the reduction of Fe^{3+} (Bridge and Johnson, 1998), producing SO_4^{2-}, which will be used as an electron acceptor by the SRBs (Barton and Tomei, 1995).

Although this described cooperation is completely theoretical, the metabolic collaboration between these species could be essential for their performance in the IPB subsurface. In fact, it has been observed the presence of iron oxidizers and reducers as well as sulfur oxidizers and reducers at the same depth along the BH10 column, although not sharing the same microniche. However, the interconnection of microniches by flowing water and the presence of biofilms, which can interconnect different clusters of cells (Escudero et al., 2018), could facilitate the flow of soluble electron donors and acceptors between different microorganisms. Indeed, the great majority of microorganisms detected in the IPBSL project are able to use as energy source the metabolic products of co-inhabitants of the IPB subsurface, thus maintaining the main biogeochemical cycles (Figure 50).

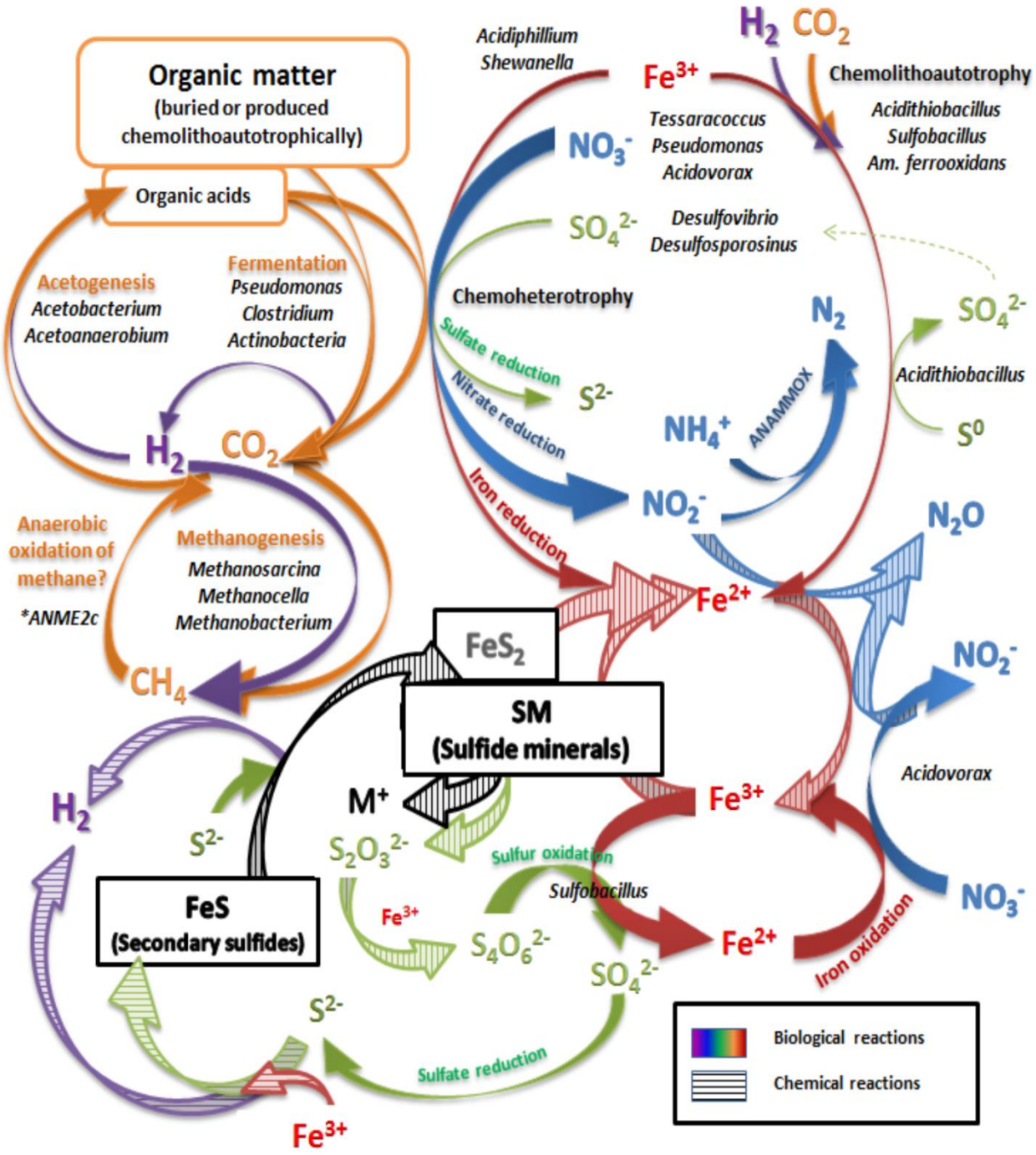

Figure 50. Putative biogeochemical cycles operating in the IPB subsurface. In blue, nitrogen cycle: in red, iron cycle; in green, sulfur cycle; in orange, carbon cycle. Close arrows indicate reactions carried out by microbial metabolism; open arrows indicate chemical reactions. Microbial representatives of each metabolism, detected in the IPB subsurface by the array of techniques applied in the IPBSL project, are indicated. *Based on MARTE project data.

The iron cycle can be sustained by iron oxidizers, both direct (*Acidovorax*?) and indirect through the generation of reactive nitrogen species (Carlson et al., 2013) by members of the genera *Acidovorax* (Klueglein and Kappler, 2013), *Tessaracoccus* (Puente-Sánchez et al., 2014a), *Rhizobium* (Daniel et al., 1982) or *Pseudomonas* (Li et al., 2017) among others, and iron-reducing microorganisms, such as *Acidiphillium* (Johnson and Bridge, 2002), *Sulfobacillus* (Bridge and Johnson, 1998) or *Acidithiobacillus* (Osorio et al., 2013). The activity of denitrifying microorganisms would produce reduced nitrogen compounds such as NO_2^- which, together with NH_4^+ produced by dissimilatory nitrate reduction to ammonium and released by decomposer microorganisms, can be used by the ANAMMOX bacteria, generating N_2. On the other hand, the decomposer microorganisms, that is to say fermenters, such as *Clostridium* (Udaondo et al., 2017), and anaerobic respirators, produce CO_2 and H_2. Both compounds can be used by acetogenic microorganisms as *Acetobacterium* (Müller, 2003) or methanogenic archaea such as *Methanobacterium* (Zinder, 1993) or *Methanocella* (Sakai et al., 2011) generating CH_4. Although in the BH10 column no microorganisms have been identified capable of carrying out anaerobic methane oxidation, this metabolism has been detected in enrichment cultures. However, in the MARTE project it was detected the presence of archaea ANME2c (Puente-Sánchez, 2016), which could support the anaerobic consumption of CH_4 in the IPB subsurface, generating CO_2. The CO_2, in addition, can be fixed by quimiolithoautotrophic microorganisms such as *At. ferrooxidans* or *Acidimicrobium (Am) ferrooxidans* (Hedrich and Johnson, 2013). The organic matter produced by these microorganisms can be degraded again by fermenting microorganisms or by anaerobic respiration, thus closing the carbon

cycle. Finally, the sulfur cycle can be maintained by oxidizing bacteria of reduced sulfur compounds such as *At. ferrooxidans* (Hedrich and Johnson, 2013) or *Sulfobacillus* (Bridge and Johnson, 1998), which couple the reduction of Fe^{3+} to the oxidation of S^0 or $S_4O_6^{2-}$ respectively, and SRB such as *Desulfovibrio* (Barton, 2013) o *Desulfosporosinus* (Pester et al., 2012).

If we consider that cooperation between species is essential for life in underground environments, it would imply that the presence of certain microorganisms (or metabolisms) influences the survival of other microorganisms and, consequently, their distribution.

Furthermore, the biodiversity distribution in the subsurface depends on the energy sources and the physical-chemical characteristics of a given location. The underground environments, being so heterogeneous, are characterized by the possible presence of innumerable different microniches, whose characteristics will be determined both by geohydrology and geochemistry. Thus, the more porous areas or the presence of faults and fractures will allow a greater space for life as well as a greater flow of water (Fredrickson et al., 1997a; Pedersen, 2000) and, therefore, a greater interconnection of microniches. The IPB subsurface is not an exception, since the largest colonies of microorganisms have been detected in depths where fault zones were located. On the contrary, if the porosity is low, the interconnection of microniches diminishes, being able to originate independent and auto-sufficient environments. On the other hand, if we consider that energy sources are endogenous, that is, independent of the surface, minerals would be the main sources of primary energy in the system. Thus, the mineralogy of the system will determine the available electron donors and acceptors and, therefore, the type

of metabolism that can take place in each of these microniches (Rempfert et al., 2017). In fact, the microorganism-mineral interaction is one of the key questions that still need to be resolved to understand the functioning of life in the subsurface, since some studies have shown that, effectively, the type of mineral directly influences the biodiversity of an underground system (Jones and Bennett, 2014).

In the IPB subsurface, as discussed, this issue acquires even greater relevance since the origin of the Río Tinto characteristics is attributed to the microorganism-metal sulfide interaction (Fernández-Remolar et al., 2008a; Fernández-Remolar et al., 2008b). As shown in the incubation experiments of native subsurface samples, the high iron concentration of the Río Tinto is, as predicted, the direct consequence of microbial metabolism. Yet, a thorough analysis is needed to determine which iron-containing minerals are dissolving in these microcosms.

Nevertheless, since pyrite is the main mineral of the IPB (Tornos, 2006), its dissolution in the subsurface could explain the high concentration of iron in the Río Tinto. Although the dissolution of metal sulfides was originally attributed exclusively to the biological iron oxidation in the aerobic or microaerobic zones of the IPB subsurface (Fernández-Remolar et al., 2008b), the role of indirect iron oxidation mediated by nitrate-reducing microorganisms, such as *Acidovorax*, in anaerobic and neutral conditions cannot be ignored. In fact, the Raman-FISH analyzes that have been carried out on native subsurface samples from the IPB, showed that the distribution of *Acidovorax* seems to be associated with the presence of pyrite. We estimate that the *Acidovorax*-mineral interaction, by increasing the pyrite dissolution rate and, therefore, the availability of iron, could satisfy a high demand for it (Klueglein and Kappler, 2013), either as a nutrient or

as an electron donor, by *Acidovorax*. The observation of a greater number of microorganisms attaching to pyrite in the absence of an iron source in solution would support this hypothesis.

As shown, the production of Fe^{3+} with nitrite enhances the dissolution of pyrite. Therefore, any microorganism producing reactive nitrogen species is, in principle, a candidate for dissolving metal sulfides, as indicated by the ability of *T. lapidicaptus* to oxidize Fe^{2+} and the co-localization of both along the BH10 column. The fact that 30% of microorganisms that inhabit the IPB subsurface can carry out the reduction of nitrate allow to suggest that they play a role in the generation of high concentrations of Fe in the anaerobic bioreactor and the source of the Fe detected in the Tinto basin. In addition, the dissolution of pyrite through nitrate-reducing microorganisms, resulting in the generation of iron, sulfur and reduced nitrogen species, as well as the presence of microorganisms in the BH10 column whose metabolisms are based on the oxidation or reduction of these compounds, imply an interconnection of the nitrogen, iron, sulfur and carbon cycles in the IPB subsurface through biolixivation processes (Figure 50).

Despite the numerous open questions that remains, thanks to the IPBSL project we started to understand how the underground ecosystem of the IPB operates. The joint effort of an interdisciplinary team as well as the use of different complementary techniques has been essential for this purpose. Within the techniques used in the subsurface studies, fluorescence microscopy, especially FISH, has proven to be a powerful tool to be considered.

7. Conclusions

1. To facilitate the recognition of authentic fluorescent signals in the study of microorganisms associated with solid mineral substrates, it is advisable to use additional DNA stains and the use of lambda mode available in confocal laser scanning microscopes.

2. Three new specific probes have been designed to detect, by fluorescent *in situ* hybridization, members of the genera *Tessaracoccus* (TESS681 and Tlap1449) and *Rhizobium* (RHI124), which optimal percentage of formamide are 50%, 10% and 50% respectively.

3. The bacteria domain is the most distributed along the BH10 column, highlighting the phyla Proteobacteria, Actinobacteria and Firmicutes. Of these phyla, in turn, highlight the large distribution of the genera *Acidovorax*, *Tessaracoccus* and *Sulfobacillus*.

4. Other phyla very distributed along BH10 column are Chloroflexi and Planctomycetes, as well as the Archaea domain, whose distribution along the IPB subsurface suggests an important role of these microorganisms in the ecosystem.

5. The co-localization of bacteria and archaea as well as the co-localization of microorganisms related to iron and sulfur metabolisms have been detected along borehole BH10. These interactions suggest the existence of an iron cycle and a sulfur cycle operating at the microniche level in the IPB subsurface.

6. The coexistence of microorganisms in multi-species biofilms seems to be a generalized lifestyle in the IPB subsurface, regardless of the depth or porosity that the system presents.

7. The presence of biofilms and the hybridizations carried out with FISH probes indicate that most of the microorganisms in the system are metabolically active.

8. For the detection of intact biofilms and the amplification of the fluorescent signal of the probe, we propose the application of DOPE-FISH probes together with the hybridization buffer developed to carry out geneFISH.

9. The origin of the high concentration of iron in the Rio Tinto basin is due to the metabolic activity of microorganisms that inhabit the IPB subsurface.

10. Both *T. lapidicaptus* and *Acidovorax* are able to oxidize iron through the production of reactive nitrogen species. Both microorganisms, in addition, are carrying out the oxidation of iron in the IPB subsurface.

11. *Acidovorax* BoFeN1 is able to promote the dissolution of pyrite by the oxidation of Fe^{2+} and its adhesion to the mineral at neutral pH.

12. The set of data obtained supports the hypothesis that all denitrifying microorganisms have the capacity to promote the dissolution of metallic sulfides in the IPB susburface.

13. The correlation of fluorescence microscopy and confocal Raman microscopy can be used for the *in situ* study of the distribution of microorganisms according to the mineralogy of the system. In the IPB

subsurface, *Acidovorax* is preferentially attached to pyrite, which seems to determine its distribution along the BH10 column.

14. The use of confocal Raman microscopy has allowed to analyze the surface variations of the native pyrite of the IPB subsurface, which can be associated with the presence of *Acidovorax*.

15. A geomicrobiological model of the IPB subsurface ecosystem has been proposed, highlighting the biogeochemical cycles of iron, sulfur, nitrogen and carbon. In this model, microorganisms form a metabolic network through which they can maximize their energy production through the use of the metabolism products of co-inhabitants of the system.

6. Conclusiones

1. Para facilitar el reconocimiento de auténticas señales fluorescentes en el estudio de microorganismos asociados a sustratos sólidos minerales, es recomendable el uso de tinciones adicionales de DNA y el uso del modo lambda disponible en microscopios de barrido laser confocal.

2. Se han diseñado tres nuevas sondas específicas para detectar mediante hibridación *in situ* fluorescente a miembros de los géneros *Tessaracoccus* (TESS681 y Tlap1449) y *Rhizobium* (RHI124), cuyos porcentajes óptimos de formamida son 50%, 10% y 50% respectivamente.

3. El dominio Bacteria es el más distribuido a lo largo de la columna BH10, destacando los phyla Proteobacteria, Actinobacteria y Firmicutes. De estos phyla, a su vez, destaca la gran distribución de los géneros *Acidovorax*, *Tessaracoccus* y *Sulfobacillus*.

4. Otros phyla muy distribuidos en la columna son Chloroflexi y Planctomycetes, así como el dominio Archaea, cuya gran distribución a lo largo del subsuelo de la FPI sugiere un papel importante en el ecosistema por parte de estos microorganismos.

5. Se ha detectado a lo largo de la columna BH10 la co-localización de bacterias y arqueas así como la co-localización de microorganismos relacionados con un metabolismo del hierro y el azufre. Éstas interacciones sugieren la

existencia de un ciclo del hierro y un ciclo del azufre operativos a nivel de micronicho en el subsuelo de la FPI.

6. La coexistencia de microorganismos en biopelículas multi-especie parece ser un estilo de vida bastante generalizado en el subsuelo de la FPI, independientemente de la profundidad o porosidad que presenta el sistema.

7. La presencia de biopelículas así como las hibridaciones realizadas con sondas de FISH indican que muchos de los microorganismos del sistema se encuentran metabólicamente activos.

8. Para la detección de biopelículas intactas y la amplificación de la señal fluorescente de la sonda, proponemos la aplicación de sondas DOPE-FISH junto con el tampón de hibridación desarrollado para llevar a cabo el genFISH.

9. El origen de la alta concentración de hierro en la cuenca del Río Tinto se debe a la actividad metabólica de microorganismos que habitan en el subsuelo de la FPI.

10. Tanto *T. lapidicaptus* como *Acidovorax* son capaces de oxidar hierro a través de la producción de especies reactivas de nitrógeno. Ambos microorganismos, además, están llevando a cabo la oxidación de hierro en el subsuelo de la FPI.

11. *Acidovorax* BoFeN1 es capaz de promover la disolución de la pirita mediante la oxidación de Fe^{2+} y su adhesión al mineral a pH neutro.

12. El conjunto de datos obtenidos apoya la hipótesis de que todos los microorganismos desnitrificantes poseen la capacidad de promover la disolución de los sulfuros metálicos en el subsuelo de la FPI.

13. La correlación de la microscopía de fluorescencia y la microscopía Raman confocal puede ser utilizado para el estudio *in situ* de la distribución de microorganismos en función de la mineralogía del sistema. En el subsuelo de la FPI, *Acidovorax* se encuentra preferentemente adherido a pirita, la cual parece determinar su distribución a lo largo de la columna BH10.

14. El uso de la microscopía Raman confocal ha permitido analizar las variaciones de la superficie de la pirita nativa del subsuelo de la FPI, las cuales pueden asociarse a la presencia de *Acidovorax*.

15. Se ha establecido de un modelo geomicrobiológico del ecosistema del subsuelo de la FPI en el que destacan los ciclos biogeoquímicos del hierro, azufre, nitrógeno y carbono. En este modelo, los microorganismos forman una red metabólica gracias a la cual pueden maximizar su obtención de energía mediante el uso de los productos del metabolismo de co-habitantes del sistema.

7. Bibliography

Aguilera, A., Gómez, F., Lospitao, E., and Amils, R. (2006) A molecular approach to the characterization of the eukaryotic communities of an extreme acidic environment: methods for DNA extraction and denaturing gradient gel electrophoresis analysis. *Systematic and applied microbiology* **29**: 593-605.

Aguilera, A., Souza-Egipsy, V., Gomez, F., and Amils, R. (2007) Development and structure of eukaryotic biofilms in an extreme acidic environment, Río Tinto (SW, Spain). *Microbial ecology* **53**: 294-305.

Alm, E.W., Oerther, D.B., Larsen, N., Stahl, D.A., and Raskin, L. (1996) The oligonucleotide probe database. *Applied and Environmental Microbiology* **62**: 3557.

Amann, R., and Fuchs, B.M. (2008) Single-cell identification in microbial communities by improved fluorescence in situ hybridization techniques. *Nat Rev Microbiol* **6**: 339-348.

Amann, R., Ludwig, W., Schulze, R., Spring, S., Moore, E., and Schleifer, K.-H. (1996) rRNA-targeted oligonucleotide probes for the identification of genuine and former pseudomonads. *Systematic and applied microbiology* **19**: 501-509.

Amann, R.I., Ludwig, W., and Schleifer, K.-H. (1995) Phylogenetic identification and in situ detection of individual microbial cells without cultivation. *Microbiological reviews* **59**: 143-169.

Amann, R.I., Binder, B.J., Olson, R.J., Chisholm, S.W., Devereux, R., and Stahl, D.A. (1990) Combination of 16S rRNA-targeted oligonucleotide probes with flow cytometry for analyzing mixed microbial populations. *Applied and environmental microbiology* **56**: 1919-1925.

Amaral-Zettler, L.A., Gómez, F., Zettler, E., Keenan, B.G., Amils, R., and Sogin, M.L. (2002) Microbiology: eukaryotic diversity in Spain's River of Fire. *Nature* **417**: 137-137.

Amend, J.P., and Teske, A. (2005) Expanding frontiers in deep subsurface microbiology. *Palaeogeography, Palaeoclimatology, Palaeoecology* **219**: 131-155.

Amend, J.P., Rogers, K.L., Shock, E.L., Gurrieri, S., and Inguaggiato, S. (2003) Energetics of chemolithoautotrophy in the hydrothermal system of Vulcano Island, southern Italy. *Geobiology* **1**: 37-58.

Amils, R., González-Toril, E., Fernández-Remolar, D., Gómez, F., Rodríguez, N., and Durán, C. (2002) Interaction of the sulfur and iron cycles in the Tinto River ecosystem. *Reviews in Environmental Science and Biotechnology* **1**: 299-309.

Amils, R., González-Toril, E., Aguilera, A., Rodrıguez, N., Fernández-Remolar, D., Gómez, F. et al. (2011) From rıo tinto to Mars: the terrestrial and extraterrestrial ecology of acidophiles. *Adv Appl Microbiol* **77**: 41-70.

Amils, R., Fernández-Remolar, D., Parro, V., Rodríguez-Manfredi, J.A., Timmis, K., Oggerin, M. et al. (2013) Iberian Pyrite Belt Subsurface Life (IPBSL), a drilling project of biohydrometallurgical interest. In *Advanced Materials Research*: Trans Tech Publ, pp. 15-18.

Anderson, C., Pedersen, K., and Jakobsson, A.-M. (2006a) Autoradiographic Comparisons of Radionuclide Adsorption Between Subsurface Anaerobic Biofilms and Granitic Host Rocks. *Geomicrobiology Journal* **23**: 15-29.

Anderson, C.R., James, R.E., Fru, E.C., Kennedy, C.B., and Pedersen, K. (2006b) In situ ecological development of a bacteriogenic iron oxide-producing microbial community from a subsurface granitic rock environment. *Geobiology* **4**: 29-42.

Apps, J.A., and van de Kamp, P.C. (1993) Energy gases of abiogenic origin in the Earth's crust. *US Geol Surv Prof Paper* **1570**: 81-132.

Barrero-Canosa, J., Moraru, C., Zeugner, L., Fuchs, B.M., and Amann, R. (2017) Direct-geneFISH: a simplified protocol for the simultaneous detection and quantification of genes and rRNA in microorganisms. *Environmental microbiology* **19**: 70-82.

Barton, H., Taylor, N., Lubbers, B., and Pemberton, A. (2006) DNA extraction from low-biomass carbonate rock: an improved method with reduced contamination and the low-biomass contaminant database. *Journal of microbiological methods* **66**: 21-31.

Barton, L.L. (2013) *Sulfate-reducing bacteria*: Springer Science & Business Media.

Barton, L.L., and Tomei, F.A. (1995) Characteristics and activities of sulfate-reducing bacteria. In *Sulfate-reducing bacteria*: Springer, pp. 1-32.

Basso, O., Lascourreges, J.-F., Le Borgne, F., Le Goff, C., and Magot, M. (2009) Characterization by culture and molecular analysis of the microbial diversity of a deep subsurface gas storage aquifer. *Research in microbiology* **160**: 107-116.

Bastin, E.S., Greer, F.E., Merritt, C., and Moulton, G. (1926) The presence of sulphate reducing bacteria in oil field waters. *Science* **63**: 21-24.

Beaty, P.S., and McInerney, M.J. (1989) Effects of organic acid anions on the growth and metabolism of Syntrophomonas wolfei in pure culture and in defined consortia. *Applied and environmental microbiology* **55**: 977-983.

Behrens, S., Fuchs, B.M., Mueller, F., and Amann, R. (2003) Is the in situ accessibility of the 16S rRNA of Escherichia coli for Cy3-labeled oligonucleotide probes predicted by a three-dimensional structure model of the 30S ribosomal subunit? *Applied and environmental microbiology* **69**: 4935-4941.

Benz, M., Brune, A., and Schink, B. (1998) Anaerobic and aerobic oxidation of ferrous iron at neutral pH by chemoheterotrophic nitrate-reducing bacteria. *Archives of Microbiology* **169**: 159-165.

Björnsson, L., Hugenholtz, P., Tyson, G.W., and Blackall, L.L. (2002) Filamentous Chloroflexi (green non-sulfur bacteria) are abundant in wastewater treatment processes with biological nutrient removalc. *Microbiology* **148**: 2309-2318.

Blanco, Y., Prieto-Ballesteros, O., Gómez, M.J., Moreno-Paz, M., García-Villadangos, M., Rodríguez-Manfredi, J.A. et al. (2012) Prokaryotic communities and operating metabolisms in the surface and the permafrost of Deception Island (Antarctica). *Environmental microbiology* **14**: 2495-2510.

Blanchard, M., Alfredsson, M., Brodholt, J., Price, G.D., Wright, K., and Catlow, C.R.A. (2005) Electronic structure study of the high-pressure vibrational spectrum of FeS2 pyrite. *The Journal of Physical Chemistry B* **109**: 22067-22073.

Blodau, C. (2006) A review of acidity generation and consumption in acidic coal mine lakes and their watersheds. *Science of the total environment* **369**: 307-332.

Boetius, A., Ravenschlag, K., Schubert, C.J., Rickert, D., Widdel, F., Gieseke, A. et al. (2000) A marine microbial consortium apparently mediating anaerobic oxidation of methane. *Nature* **407**: 623-626.

Bohorquez, L.C., Delgado-Serrano, L., López, G., Osorio-Forero, C., Klepac-Ceraj, V., Kolter, R. et al. (2012) In-depth characterization via complementing culture-independent approaches of the microbial community in an acidic hot spring of the Colombian Andes. *Microbial ecology* **63**: 103-115.

BOJA (2005) DECRETO 558/2004, de 14 de diciembre, por el que se declara el Paisaje Protegido de Río Tinto. In. Junta de Andalucía: Boletín Oficial de la Junta de Andalucía, Conserjería de Medio Ambiente, pp. 24-55.

Bomberg, M., Nyyssönen, M., Pitkänen, P., Lehtinen, A., and Itävaara, M. (2015) Active microbial communities inhabit sulphate-methane interphase in deep bedrock fracture fluids in Olkiluoto, Finland. *BioMed research international* **2015**.

Bomberg, M., Nyyssönen, M., Nousiainen, A., Hultman, J., Paulin, L., Auvinen, P., and Itävaara, M. (2014) Evaluation of molecular techniques in characterization of deep terrestrial biosphere. *Open Journal of Ecology* **4**: 468.

Bond, P., and Banfield, J. (2001) Design and performance of rRNA targeted oligonucleotide probes for in situ detection and phylogenetic identification of microorganisms inhabiting acid mine drainage environments. *Microbial ecology* **41**: 149-161.

Bonnissel-Gissinger, P., Alnot, M., Ehrhardt, J.-J., and Behra, P. (1998) Surface oxidation of pyrite as a function of pH. *Environmental Science & Technology* **32**: 2839-2845.

Borgonie, G., García-Moyano, A., Litthauer, D., Bert, W., Bester, A., van Heerden, E. et al. (2011) Nematoda from the terrestrial deep subsurface of South Africa. *Nature* **474**: 79-82.

Bosch, J., Lee, K.-Y., Jordan, G., Kim, K.-W., and Meckenstock, R.U. (2012) Anaerobic, nitrate-dependent oxidation of pyrite nanoparticles by Thiobacillus denitrificans. *Environmental science & technology* **46**: 2095-2101.

Bottrell, S., Parkes, R.J., Cragg, B.A., and Raiswell, R. (2000) Isotopic evidence for anoxic pyrite oxidation and stimulation of bacterial sulphate reduction in marine sediments. *Journal of the Geological Society* **157**: 711-714.

Boxer, S.G., Kraft, M.L., and Weber, P.K. (2009) Advances in Imaging Secondary Ion Mass Spectrometry for Biological Samples. *Annual Review of Biophysics* **38**: 53-74.

Brazelton, W.J., Nelson, B., and Schrenk, M.O. (2012) Metagenomic evidence for H2 oxidation and H2 production by serpentinite-hosted subsurface microbial communities. *Frontiers in microbiology* **2**: 268.

Breuker, A., Köweker, G., Blazejak, A., and Schippers, A. (2011) The deep biosphere in terrestrial sediments in the Chesapeake Bay area, Virginia, USA. *Frontiers in microbiology* **2**.

Bridge, T.A., and Johnson, D.B. (1998) Reduction of soluble iron and reductive dissolution of ferric iron-containing minerals by moderately thermophilic iron-oxidizing bacteria. *Applied and environmental microbiology* **64**: 2181-2186.

Brierley, C.L., and Brierley, J.A. (2013) Progress in bioleaching: part B: applications of microbial processes by the minerals industries. *Applied microbiology and biotechnology* **97**: 7543-7552.

Briggs, B., Pohlman, J., Torres, M., Riedel, M., Brodie, E., and Colwell, F. (2011) Macroscopic biofilms in fracture-dominated sediment that anaerobically oxidize methane. *Applied and environmental microbiology* **77**: 6780-6787.

Brons, H.J., Hagen, W.R., and Zehnder, A.J. (1991) Ferrous iron dependent nitric oxide production in nitrate reducing cultures of Escherichia coli. *Archives of microbiology* **155**: 341-347.

Bryant, R.N., Pasteris, J.D., and Fike, D.A. (2018) Variability in the Raman Spectrum of Unpolished Growth and Fracture Surfaces of Pyrite Due to Laser Heating and Crystal Orientation. *Applied spectroscopy* **72**: 37-47.

Buczolits, S., Denner, E.B., Kämpfer, P., and Busse, H.-J. (2006) Proposal of Hymenobacter norwichensis sp. nov., classification of 'Taxeobacter ocellatus','Taxeobacter gelupurpurascens' and 'Taxeobacter chitinovorans' as Hymenobacter ocellatus sp. nov., Hymenobacter gelipurpurascens sp. nov. and Hymenobacter chitinivorans sp. nov., respectively, and emended description of the genus Hymenobacter Hirsch et al. 1999. *International journal of systematic and evolutionary microbiology* **56**: 2071-2078.

Cael, S., Koenig, J., and Blackwell, J. (1973) Infrared and Raman spectroscopy of carbohydrates: part III: Raman spectra of the polymorphic forms of amylose. *Carbohydrate research* **29**: 123-134.

Caldeira, C., Ciminelli, V., Dias, A., and Osseo-Asare, K. (2003) Pyrite oxidation in alkaline solutions: nature of the product layer. *International Journal of Mineral Processing* **72**: 373-386.

Carareto Alves, L.M., de Souza, J.A.M., Varani, A.d.M., and Lemos, E.G.d.M. (2014) The Family Rhizobiaceae. In *The Prokaryotes: Alphaproteobacteria and Betaproteobacteria*. Rosenberg, E., DeLong, E.F., Lory, S., Stackebrandt, E., and Thompson, F. (eds). Berlin, Heidelberg: Springer Berlin Heidelberg, pp. 419-437.

Carlson, H.K., Clark, I.C., Blazewicz, S.J., Iavarone, A.T., and Coates, J.D. (2013) Fe (II) oxidation is an innate capability of nitrate-reducing bacteria that involves abiotic and biotic reactions. *Journal of bacteriology* **195**: 3260-3268.

Cavalazzi, B., Barbieri, R., Cady, S.L., George, A.D., Gennaro, S., Westall, F. et al. (2012) Iron-framboids in the hydrocarbon-related Middle Devonian Hollard Mound of the Anti-Atlas mountain range in Morocco: Evidence of potential microbial biosignatures. *Sedimentary Geology* **263**: 183-193.

Cockell, C.S., Gronstal, A.L., Voytek, M.A., Kirshtein, J.D., Finster, K., Sanford, W.E. et al. (2009) Microbial abundance in the deep subsurface of the Chesapeake Bay impact crater: Relationship to lithology and impact processes. *Geological Society of America Special Papers* **458**: 941-950.

Cockell, C.S., Voytek, M.A., Gronstal, A.L., Finster, K., Kirshtein, J.D., Howard, K. et al. (2012) Impact disruption and recovery of the deep subsurface biosphere. *Astrobiology* **12**: 231-246.

Coombs, P., Wagner, D., Bateman, K., Harrison, H., Milodowski, A., Noy, D., and West, J. (2010) The role of biofilms in subsurface transport processes. *Quarterly Journal of Engineering Geology and Hydrogeology* **43**: 131-139.

Corliss, J.B., Dymond, J., Gordon, L.I., Edmond, J.M., von Herzen, R.P., Ballard, R.D. et al. (1979) Submarine thermal sprirngs on the galapagos rift. *Science* **203**: 1073-1083.

Coyte, K.Z., Tabuteau, H., Gaffney, E.A., Foster, K.R., and Durham, W.M. (2016) Microbial competition in porous environments can select against rapid biofilm growth. *Proceedings of the National Academy of Sciences*: 201525228.

Crocetti, G., Murto, M., and Björnsson, L. (2006) An update and optimisation of oligonucleotide probes targeting methanogenic Archaea for use in fluorescence in situ hybridisation (FISH). *Journal of microbiological methods* **65**: 194-201.

Czamara, K., Majzner, K., Pacia, M.Z., Kochan, K., Kaczor, A., and Baranska, M. (2015) Raman spectroscopy of lipids: a review. *Journal of Raman Spectroscopy* **46**: 4-20.

Chakraborty, A., and Picardal, F. (2013) Induction of nitrate-dependent Fe (II) oxidation by Fe (II) in Dechloromonas sp. strain UWNR4 and Acidovorax sp. strain 2AN. *Applied and environmental microbiology* **79**: 748-752.

Chakraborty, A., Roden, E.E., Schieber, J., and Picardal, F. (2011) Enhanced growth of Acidovorax sp. strain 2AN during nitrate-dependent Fe (II) oxidation in batch and continuous-flow systems. *Applied and environmental microbiology* **77**: 8548-8556.

Chandra, A.P., and Gerson, A.R. (2010) The mechanisms of pyrite oxidation and leaching: a fundamental perspective. *Surface Science Reports* **65**: 293-315.

Chapelle, F.H., O'neill, K., Bradley, P.M., Methé, B.A., Ciufo, S.A., Knobel, L.L., and Lovley, D.R. (2002) A hydrogen-based subsurface microbial community dominated by methanogens. *Nature* **415**: 312-315.

Chivian, D., Brodie, E.L., Alm, E.J., Culley, D.E., Dehal, P.S., DeSantis, T.Z. et al. (2008) Environmental genomics reveals a single-species ecosystem deep within Earth. *Science* **322**: 275-278.

D'Hondt, S., Rutherford, S., and Spivack, A.J. (2002) Metabolic activity of subsurface life in deep-sea sediments. *Science* **295**: 2067-2070.

D Hondt, S., Smith, D., and Spivack, A. (2002) *Exploration of the marine subsurface biosphere*.

Daims, H., Brühl, A., Amann, R., Schleifer, K.-H., and Wagner, M. (1999) The Domain-specific Probe EUB338 is Insufficient for the Detection of all Bacteria: Development and Evaluation of a more Comprehensive Probe Set. *Systematic and Applied Microbiology* **22**: 434-444.

Daniel, R.M., Limmer, A., Steele, K., and Smith, I. (1982) Anaerobic growth, nitrate reduction and denitrification in 46 Rhizobium strains. *Microbiology* **128**: 1811-1815.

Darwin, C. (1839) Voyages of the adventure and beagle, volume III–Journal and remarks, 1832–1836. *Henry Colburn, London*.

Davis Jr, R., Welty, A., Borrego, J., Morales, J., Pendon, J., and Ryan, J.G. (2000) Rio Tinto estuary (Spain): 5000 years of pollution. *Environmental Geology* **39**: 1107-1116.

De Faria, D., and Lopes, F. (2007) Heated goethite and natural hematite: can Raman spectroscopy be used to differentiate them? *Vibrational Spectroscopy* **45**: 117-121.

De Faria, D., Venâncio Silva, S., and De Oliveira, M. (1997) Raman microspectroscopy of some iron oxides and oxyhydroxides. *Journal of Raman spectroscopy* **28**: 873-878.

Dieing, T., Hollricher, O., and Toporski, J. (2011) *Confocal raman microscopy*: Springer Science & Business Media.

Direito, S.O., Marees, A., and Röling, W.F. (2012) Sensitive life detection strategies for low-biomass environments: optimizing extraction of nucleic acids adsorbing to terrestrial and Mars analogue minerals. *FEMS microbiology ecology* **81**: 111-123.

Domaille, D.W., Que, E.L., and Chang, C.J. (2008) Synthetic fluorescent sensors for studying the cell biology of metals. *Nature chemical biology* **4**: 168.

Dong, Y., Sanford, R.A., Locke, R.A., Cann, I.K., Mackie, R.I., and Fouke, B.W. (2014a) Fe-oxide grain coatings support bacterial Fe-reducing metabolisms in 1.7– 2.0 km-deep subsurface quartz arenite sandstone reservoirs of the Illinois Basin (USA). *Frontiers in microbiology* **5**: 511.

Dong, Y., Kumar, C.G., Chia, N., Kim, P.J., Miller, P.A., Price, N.D. et al. (2014b) Halomonas sulfidaeris-dominated microbial community inhabits a 1.8 km-deep subsurface Cambrian Sandstone reservoir. *Environmental microbiology* **16**: 1695-1708.

dos Santos, A.M., Vieira, K.R., Sartori, R.B., dos Santos, A.M., Queiroz, M.I., Zepka, L.Q., and Jacob-Lopes, E. (2017) Heterotrophic cultivation of cyanobacteria: study of effect of exogenous sources of organic carbon, absolute amount of nutrients, and stirring speed on biomass and lipid productivity. *Frontiers in bioengineering and biotechnology* **5**.

Edwards, K.J., and Rutenberg, A.D. (2001) Microbial response to surface microtopography: the role of metabolism in localized mineral dissolution. *Chemical Geology* **180**: 19-32.

Edwards, K.J., Bond, P.L., Gihring, T.M., and Banfield, J.F. (2000) An archaeal iron-oxidizing extreme acidophile important in acid mine drainage. *Science* **287**: 1796-1799.

Edwards, K.J., McCollom, T.M., Konishi, H., and Buseck, P.R. (2003) Seafloor bioalteration of sulfide minerals: results from in situ incubation studies. *Geochimica et Cosmochimica Acta* **67**: 2843-2856.

Egland, P.G., Palmer, R.J., and Kolenbrander, P.E. (2004) Interspecies communication in Streptococcus gordonii–Veillonella atypica biofilms: signaling in flow conditions requires juxtaposition. *Proceedings of the National Academy of Sciences of the United States of America* **101**: 16917-16922.

El-Naggar, M.Y., Wanger, G., Leung, K.M., Yuzvinsky, T.D., Southam, G., Yang, J. et al. (2010) Electrical transport along bacterial nanowires from Shewanella oneidensis MR-1. *Proceedings of the National Academy of Sciences* **107**: 18127-18131.

Escudero-Sanz, I., Ahlers, B., and Courreges-Lacoste, G.B. (2008) Optical design of a combined Raman–laser-induced-breakdown-spectroscopy instrument for the European Space Agency ExoMars Mission. *Optical Engineering* **47**: 033001-033001-033011.

Escudero, C., Vera, M., Oggerin, M., and Amils, R. (2018) Active microbial biofilms in deep poor porous continental subsurface rocks. *Scientific Reports* **8**: 1538.

Essalhi, M., Sizaret, S., Barbanson, L., Chen, Y., Lagroix, F., Demory, F. et al. (2011) A case study of the internal structures of gossans and weathering processes in the Iberian Pyrite Belt using magnetic fabrics and paleomagnetic dating. *Mineralium Deposita* **46**: 981-999.

Eydal, H.S., Jägevall, S., Hermansson, M., and Pedersen, K. (2009) Bacteriophage lytic to Desulfovibrio aespoeensis isolated from deep groundwater. *The ISME journal* **3**: 1139-1147.

Fernández-Remolar, D.C., Morris, R.V., Gruener, J.E., Amils, R., and Knoll, A.H. (2005) The Río Tinto Basin, Spain: mineralogy, sedimentary geobiology, and implications for interpretation of outcrop rocks at Meridiani Planum, Mars. *Earth and Planetary Science Letters* **240**: 149-167.

Fernández-Remolar, D.C., Gómez, F., Prieto-Ballesteros, O., Schelble, R.T., Rodríguez, N., and Amils, R. (2008a) Some ecological mechanisms to generate habitability in planetary subsurface areas by chemolithotrophic communities: The Río Tinto subsurface ecosystem as a model system. *Astrobiology* **8**: 157-173.

Fernández-Remolar, D.C., Prieto-Ballesteros, O., Rodríguez, N., Gómez, F., Amils, R., Gómez-Elvira, J., and Stoker, C.R. (2008b) Underground habitats in the Río Tinto basin: a model for subsurface life habitats on Mars. *Astrobiology* **8**: 1023-1047.

Fernández-Remolar, D.C., Rodriguez, N., Gómez, F., and Amils, R. (2003) Geological record of an acidic environment driven by iron hydrochemistry: The Tinto River system. *Journal of Geophysical Research: Planets* **108**.

Finster, K., Cockell, C., Voytek, M., Gronstal, A., and Kjeldsen, K.U. (2009) Description of Tessaracoccus profundi sp. nov., a deep-subsurface actinobacterium isolated from a Chesapeake impact crater drill core (940 m depth). *Antonie van Leeuwenhoek* **96**: 515-526.

Flemming, H.-C., and Wingender, J. (2010) The biofilm matrix. *Nature Reviews Microbiology* **8**: 623-633.

Flemming, H.-C., Wingender, J., Szewzyk, U., Steinberg, P., Rice, S.A., and Kjelleberg, S. (2016) Biofilms: an emergent form of bacterial life. *Nature Reviews Microbiology* **14**: 563-575.

Flemming, H.C. (2011) The perfect slime. *Colloids Surf B Biointerfaces* **86**: 251-259.

Fowler, T., Holmes, P., and Crundwell, F. (2001) On the kinetics and mechanism of the dissolution of pyrite in the presence of Thiobacillus ferrooxidans. *Hydrometallurgy* **59**: 257-270.

Fredrickson, J., McKinley, J., Bjornstad, B., Long, P., Ringelberg, D., White, D. et al. (1997a) Pore-size constraints on the activity and survival of subsurface bacteria in a late cretaceous shale-sandstone sequence, northwestern New Mexico. *Geomicrobiology Journal* **14**: 183-202.

Fredrickson, J.K., and Balkwill, D.L. (2006) Geomicrobial processes and biodiversity in the deep terrestrial subsurface. *Geomicrobiology Journal* **23**: 345-356.

Fredrickson, J.K., McKinley, J.P., Bjornstad, B.N., Long, P.E., Ringelberg, D.B., White, D.C. et al. (1997b) Pore-size constraints on the activity and survival of subsurface bacteria in a late cretaceous shale-sandstone sequence, northwestern New Mexico. *Geomicrobiology Journal* **14**: 183-202.

French, S., Puddephatt, D., Habash, M., and Glasauer, S. (2013) The dynamic nature of bacterial surfaces: implications for metal–membrane interaction. *Critical reviews in microbiology* **39**: 196-217.

Fry, J.C., Parkes, R.J., Cragg, B.A., Weightman, A.J., and Webster, G. (2008) Prokaryotic biodiversity and activity in the deep subseafloor biosphere. *FEMS Microbiology Ecology* **66**: 181-196.

Fry, N.K., Fredrickson, J.K., Fishbain, S., Wagner, M., and Stahl, D.A. (1997) Population structure of microbial communities associated with two deep, anaerobic, alkaline aquifers. *Applied and Environmental Microbiology* **63**: 1498-1504.

Fuerst, J.A. (2005) Intracellular compartmentation in planctomycetes. *Annu Rev Microbiol* **59**: 299-328.

Fuerst, J.A., and Sagulenko, E. (2011) Beyond the bacterium: planctomycetes challenge our concepts of microbial structure and function. *Nature Reviews Microbiology* **9**: 403-413.

Fuerst, J.A., and Sagulenko, E. (2013) Planctomycetes: Their Evolutionary Implications for Models for Origins of Eukaryotes and the Eukaryote Nucleus and Endomembranes. In *Planctomycetes: Cell Structure, Origins and Biology*: Springer, pp. 243-270.

Fukuda, A., Hagiwara, H., Ishimura, T., Kouduka, M., Ioka, S., Amano, Y. et al. (2010) Geomicrobiological properties of ultra-deep granitic groundwater from the Mizunami Underground Research Laboratory (MIU), central Japan. *Microbial ecology* **60**: 214-225.

Gantner, S., Schmid, M., Dürr, C., Schuhegger, R., Steidle, A., Hutzler, P. et al. (2006) In situ quantitation of the spatial scale of calling distances and population density-independent N-acylhomoserine lactone-mediated communication by rhizobacteria colonized on plant roots. *FEMS microbiology ecology* **56**: 188-194.

García-Moyano, A., González-Toril, E., and Amils, R. (2009) Characterization of the anoxic sediments of Rio Tinto: biohydrometallurgical implications. In *Advanced Materials Research*: Trans Tech Publ, pp. 109-112.

García-Moyano, A., González-Toril, E., Aguilera, A., and Amils, R. (2007) Prokaryotic community composition and ecology of floating macroscopic filaments from an extreme acidic environment, Rio Tinto (SW, Spain). *Systematic and Applied Microbiology* **30**: 601-614.

García-Moyano, A., Gonzalez-Toril, E., Aguilera, Á., and Amils, R. (2012) Comparative microbial ecology study of the sediments and the water column of the Río Tinto, an extreme acidic environment. *FEMS microbiology ecology* **81**: 303-314.

García Moyano, A.J. (2007) Fisiología y ecología del género Leptospirillum, responsable de las condiciones extremas de Río Tinto. *Dissertation Thesis, UAM*.

Garrido, P., González-Toril, E., García-Moyano, A., Moreno-Paz, M., Amils, R., and Parro, V. (2008) An oligonucleotide prokaryotic acidophile microarray: its validation and its use to monitor seasonal variations in extreme acidic environments with total environmental RNA. *Environmental microbiology* **10**: 836-850.

Gehrke, T., Telegdi, J., Thierry, D., and Sand, W. (1998) Importance of extracellular polymeric substances from Thiobacillus ferrooxidans for bioleaching. *Applied and Environmental Microbiology* **64**: 2743-2747.

Georgellis, D., Kwon, O., and Lin, E.C. (2001) Quinones as the redox signal for the arc two-component system of bacteria. *Science* **292**: 2314-2316.

Ghiorse, W.C., and Wilson, J.T. (1988) Microbial ecology of the terrestrial subsurface. *Advances in applied microbiology* **33**: 107-172.

Gich, F., Garcia-Gil, J., and Overmann, J. (2001) Previously unknown and phylogenetically diverse members of the green nonsulfur bacteria are indigenous to freshwater lakes. *Archives of microbiology* **177**: 1-10.

Gihring, T., Moser, D., Lin, L.-H., Davidson, M., Onstott, T., Morgan, L. et al. (2006) The distribution of microbial taxa in the subsurface water of the Kalahari Shield, South Africa. *Geomicrobiology Journal* **23**: 415-430.

Glöckner, F.O., Amann, R., Alfreider, A., Pernthaler, J., Psenner, R., Trebesius, K., and Schleifer, K.-H. (1996) An In Situ Hybridization Protocol for Detection and Identification of Planktonic Bacteria. *Systematic and Applied Microbiology* **19**: 403-406.

Gold, T. (1992) The deep, hot biosphere. *Proceedings of the National Academy of Sciences* **89**: 6045-6049.

Goldstein, J.I., Newbury, D.E., Michael, J.R., Ritchie, N.W., Scott, J.H.J., and Joy, D.C. (2017) *Scanning electron microscopy and X-ray microanalysis*: Springer.

Goltsman, D.S.A., Denef, V.J., Singer, S.W., VerBerkmoes, N.C., Lefsrud, M., Mueller, R.S. et al. (2009) Community genomic and proteomic analyses of chemoautotrophic iron-oxidizing

"Leptospirillum rubarum"(Group II) and "Leptospirillum ferrodiazotrophum"(Group III) bacteria in acid mine drainage biofilms. *Applied and environmental microbiology* **75**: 4599-4615.

Gómez-Ortiz, D., Fernández-Remolar, D.C., Granda, Á., Quesada, C., Granda, T., Prieto-Ballesteros, O. et al. (2014) Identification of the subsurface sulfide bodies responsible for acidity in Río Tinto source water, Spain. *Earth and Planetary Science Letters* **391**: 36-41.

González-Toril, E., Llobet-Brossa, E., Casamayor, E., Amann, R., and Amils, R. (2003) Microbial ecology of an extreme acidic environment, the Tinto River. *Applied and environmental microbiology* **69**: 4853-4865.

González Toril, E. (2002) Ecología molecular de la comunidad microbiana de un ambiente extremo: el río Tinto. *Dissertation Thesis, UAM*.

Gronstal, A.L., Voytek, M.A., Kirshtein, J.D., Nicole, M., Lowit, M.D., and Cockell, C.S. (2009) Contamination assessment in microbiological sampling of the Eyreville core, Chesapeake Bay impact structure. *Geological Society of America Special Papers* **458**: 951-964.

Haaijer, S.C., Lamers, L.P., Smolders, A.J., Jetten, M.S., and Op den Camp, H.J. (2007) Iron sulfide and pyrite as potential electron donors for microbial nitrate reduction in freshwater wetlands. *Geomicrobiology Journal* **24**: 391-401.

Hafenbradl, D., Keller, M., Dirmeier, R., Rachel, R., Roßnagel, P., Burggraf, S. et al. (1996) Ferroglobus placidus gen. nov., sp. nov., a novel hyperthermophilic archaeum that oxidizes Fe2+ at neutral pH under anoxic conditions. *Archives of microbiology* **166**: 308-314.

Hallberg, K.B., Coupland, K., Kimura, S., and Johnson, D.B. (2006) Macroscopic streamer growths in acidic, metal-rich mine waters in North Wales consist of novel and remarkably simple bacterial communities. *Applied and environmental microbiology* **72**: 2022-2030.

Hao, L., Li, J., Kappler, A., and Obst, M. (2013) Mapping of heavy metal ion sorption to cell-extracellular polymeric substance-mineral aggregates by using metal-selective fluorescent probes and confocal laser scanning microscopy. *Applied and environmental microbiology* **79**: 6524-6534.

Hao, L., Guo, Y., Byrne, J.M., Zeitvogel, F., Schmid, G., Ingino, P. et al. (2016) Binding of heavy metal ions in aggregates of microbial cells, EPS and biogenic iron minerals measured in-situ using metal-and glycoconjugates-specific fluorophores. *Geochimica et Cosmochimica Acta* **180**: 66-96.

Harneit, K., Göksel, A., Kock, D., Klock, J.H., Gehrke, T., and Sand, W. (2006) Adhesion to metal sulfide surfaces by cells of Acidithiobacillus ferrooxidans, Acidithiobacillus thiooxidans and Leptospirillum ferrooxidans. *Hydrometallurgy* **83**: 245-254.

Harz, M., Rösch, P., Peschke, K.-D., Ronneberger, O., Burkhardt, H., and Popp, J. (2005) Micro-Raman spectroscopic identification of bacterial cells of the genus Staphylococcus and dependence on their cultivation conditions. *Analyst* **130**: 1543-1550.

Hedrich, S., and Johnson, D.B. (2013) Aerobic and anaerobic oxidation of hydrogen by acidophilic bacteria. *FEMS microbiology letters* **349**: 40-45.

Hedrich, S., Schlömann, M., and Johnson, D.B. (2011) The iron-oxidizing proteobacteria. *Microbiology* **157**: 1551-1564.

Hoehler, T.M. (2004) Biological energy requirements as quantitative boundary conditions for life in the subsurface. *Geobiology* **2**: 205-215.

Hoehler, T.M., and Jorgensen, B.B. (2013) Microbial life under extreme energy limitation. *Nat Rev Micro* **11**: 83-94.

Hoshino, T., Yilmaz, L.S., Noguera, D.R., Daims, H., and Wagner, M. (2008) Quantification of target molecules needed to detect microorganisms by fluorescence in situ hybridization (FISH) and catalyzed reporter deposition-FISH. *Applied and environmental microbiology* **74**: 5068-5077.

Houben, G.J., Sitnikova, M.A., and Post, V.E. (2017) Terrestrial sedimentary pyrites as a potential source of trace metal release to groundwater–A case study from the Emsland, Germany. *Applied Geochemistry* **76**: 99-111.

Huang, W.E., Stoecker, K., Griffiths, R., Newbold, L., Daims, H., Whiteley, A.S., and Wagner, M. (2007) Raman-FISH: combining stable-isotope Raman spectroscopy and fluorescence in situ hybridization for the single cell analysis of identity and function. *Environmental Microbiology* **9**: 1878-1889.

Huang, Y., Li, H., Rensing, C., Zhao, K., Johnstone, L., and Wang, G. (2012) Genome sequence of the facultative anaerobic arsenite-oxidizing and nitrate-reducing bacterium Acidovorax sp. strain NO1. *Journal of bacteriology* **194**: 1635-1636.

Hug, L.A., Thomas, B.C., Sharon, I., Brown, C.T., Sharma, R., Hettich, R.L. et al. (2016) Critical biogeochemical functions in the subsurface are associated with bacteria from new phyla and little studied lineages. *Environmental microbiology* **18**: 159-173.

Hugenholtz, P., Tyson, G.W., and Blackall, L.L. (2002) Design and evaluation of 16S rRNA-targeted oligonucleotide probes for fluorescence in situ hybridization. *Gene Probes: Principles and Protocols*: 29-42.

Hughes, L.D., Rawle, R.J., and Boxer, S.G. (2014) Choose Your Label Wisely: Water-Soluble Fluorophores Often Interact with Lipid Bilayers. *PLoS ONE* **9**: e87649.

Inagaki, F., Takai, K., Hirayama, H., Yamato, Y., Nealson, K.H., and Horikoshi, K. (2003) Distribution and phylogenetic diversity of the subsurface microbial community in a Japanese epithermal gold mine. *Extremophiles* **7**: 307-317.

Ino, K., Konno, U., Kouduka, M., Hirota, A., Togo, Y.S., Fukuda, A. et al. (2016) Deep microbial life in high-quality granitic groundwater from geochemically and geographically distinct underground boreholes. *Environmental microbiology reports* **8**: 285-294.

Ino, K., Hernsdorf, A.W., Konno, U., Kouduka, M., Yanagawa, K., Kato, S. et al. (2017) Ecological and genomic profiling of anaerobic methane-oxidizing archaea in a deep granitic environment. *The ISME Journal*.

Ishii, K., Mussmann, M., MacGregor, B.J., and Amann, R. (2004) An improved fluorescence in situ hybridization protocol for the identification of bacteria and archaea in marine sediments. *FEMS Microbiol Ecol* **50**: 203-213.

Itävaara, M., Nyyssönen, M., Kapanen, A., Nousiainen, A., Ahonen, L., and Kukkonen, I. (2011a) Characterization of bacterial diversity to a depth of 1500 m in the Outokumpu deep borehole, Fennoscandian Shield. *FEMS microbiology ecology* **77**: 295-309.

Itävaara, M., Nyyssönen, M., Bomberg, M., Kapanen, A., Nousiainen, A., Ahonen, L. et al. (2011b) Microbiological sampling and analysis of the Outokumpu Deep Drill Hole biosphere in 2007–2009. *Geol Surv Finland* **51**: 199-206.

Ivleva, N.P., Wagner, M., Horn, H., Niessner, R., and Haisch, C. (2009) Towards a nondestructive chemical characterization of biofilm matrix by Raman microscopy. *Analytical and bioanalytical chemistry* **393**: 197-206.

Iwatsuki, T., Hagiwara, H., Ohmori, K., Munemoto, T., and Onoe, H. (2015) Hydrochemical disturbances measured in groundwater during the construction and operation of a large-

scale underground facility in deep crystalline rock in Japan. *Environmental Earth Sciences* **74**: 3041-3057.

Jagevall, S., Rabe, L., and Pedersen, K. (2011) Abundance and diversity of biofilms in natural and artificial aquifers of the Aspo Hard Rock Laboratory, Sweden. *Microb Ecol* **61**: 410-422.

Jakobsen, R. (2007) Redox microniches in groundwater: a model study on the geometric and kinetic conditions required for concomitant Fe oxide reduction, sulfate reduction, and methanogenesis. *Water resources research* **43**.

Jannasch, H.W., Eimhjellen, K., and Farmanfarmalan, A. (1971) Microbial degradation of organic matter in the deep sea. *Science* **171**: 672-675.

Johnson, D., and Bridge, T. (2002) Reduction of ferric iron by acidophilic heterotrophic bacteria: evidence for constitutive and inducible enzyme systems in Acidiphilium spp. *Journal of applied Microbiology* **92**: 315-321.

Johnson, D.B. (1998) Biodiversity and ecology of acidophilic microorganisms. *FEMS microbiology ecology* **27**: 307-317.

Jones, A.A., and Bennett, P.C. (2014) Mineral Microniches Control the Diversity of Subsurface Microbial Populations. *Geomicrobiology Journal* **31**: 246-261.

Jones, A.A., and Bennett, P.C. (2017) Mineral Ecology: surface specific colonization and geochemical drivers of biofilm accumulation, composition, and phylogeny. *Frontiers in microbiology* **8**.

Jørgensen, B.B., and Boetius, A. (2007) Feast and famine—microbial life in the deep-sea bed. *Nature Reviews Microbiology* **5**: nrmicro1745.

Jørgensen, C., Jacobsen, O.S., Elberling, B., and Aamand, J. (2009) Microbial oxidation of pyrite coupled to nitrate reduction in anoxic groundwater sediment. *Environmental science & technology* **43**: 4851-4857.

Justice, N.B., Norman, A., Brown, C.T., Singh, A., Thomas, B.C., and Banfield, J.F. (2014) Comparison of environmental and isolate Sulfobacillus genomes reveals diverse carbon, sulfur, nitrogen, and hydrogen metabolisms. *BMC genomics* **15**: 1107.

Justice, N.B., Pan, C., Mueller, R., Spaulding, S.E., Shah, V., Sun, C.L. et al. (2012) Heterotrophic archaea contribute to carbon cycling in low-pH, suboxic biofilm communities. *Applied and environmental microbiology* **78**: 8321-8330.

Kallmeyer, J., Pockalny, R., Adhikari, R.R., Smith, D.C., and D'Hondt, S. (2012) Global distribution of microbial abundance and biomass in subseafloor sediment. *Proceedings of the National Academy of Sciences* **109**: 16213-16216.

Kappler, A., Schink, B., and Newman, D.K. (2005) Fe (III) mineral formation and cell encrustation by the nitrate-dependent Fe (II)-oxidizer strain BoFeN1. *Geobiology* **3**: 235-245.

Kapuscinski, J. (1995) DAPI: a DNA-specific fluorescent probe. *Biotechnic & Histochemistry* **70**: 220-233.

Kaspar, H.F. (1982) Nitrite reduction to nitrous oxide by propionibacteria: detoxication mechanism. *Archives of Microbiology* **133**: 126-130.

Kerr, R.A. (2002) Deep life in the slow, slow lane. In: American Association for the Advancement of Science.

Kieft, T. (2010) Sampling the deep sub-surface using drilling and coring techniques. In *Handbook of Hydrocarbon and Lipid Microbiology*: Springer, pp. 3427-3441.

Kieft, T.L. (2016) Microbiology of the Deep Continental Biosphere. In *Their World: A Diversity of Microbial Environments*: Springer, pp. 225-249.

Klueglein, N., and Kappler, A. (2013) Abiotic oxidation of Fe (II) by reactive nitrogen species in cultures of the nitrate-reducing Fe (II) oxidizer Acidovorax sp. BoFeN1–questioning the existence of enzymatic Fe (II) oxidation. *Geobiology* **11**: 180-190.

Klueglein, N., Picardal, F., Zedda, M., Zwiener, C., and Kappler, A. (2015) Oxidation of Fe (II)-EDTA by nitrite and by two nitrate-reducing Fe (II)-oxidizing Acidovorax strains. *Geobiology* **13**: 198-207.

Klueglein, N., Zeitvogel, F., Stierhof, Y.-D., Floetenmeyer, M., Konhauser, K.O., Kappler, A., and Obst, M. (2014) Potential role of nitrite for abiotic Fe (II) oxidation and cell encrustation during nitrate reduction by denitrifying bacteria. *Applied and environmental microbiology* **80**: 1051-1061.

Knittel, K., and Boetius, A. (2009) Anaerobic oxidation of methane: progress with an unknown process. *Annu Rev Microbiol* **63**: 311-334.

Koch, M., Rudolph, C., Moissl, C., and Huber, R. (2006) A cold-loving crenarchaeon is a substantial part of a novel microbial community in cold sulphidic marsh water. *FEMS microbiology ecology* **57**: 55-66.

Koschorreck, M. (2007) Natural alkalinity generation in neutral lakes affected by acid mine drainage. *Journal of environmental quality* **36**: 1163-1171.

Kubota, K. (2013) CARD-FISH for environmental microorganisms: technical advancement and future applications. *Microbes and environments* **28**: 3-12.

Kumar, S., Herrmann, M., Thamdrup, B., Schwab, V.F., Geesink, P., Trumbore, S.E. et al. (2017) Nitrogen loss from pristine carbonate-rock aquifers of the Hainich Critical Zone Exploratory (Germany) is primarily driven by chemolithoautotrophic anammox processes. *Frontiers in microbiology* **8**: 1951.

Kumaraswamy, R., Sjollema, K., Kuenen, G., Van Loosdrecht, M., and Muyzer, G. (2006) Nitrate-dependent [Fe (II) EDTA] 2− oxidation by Paracoccus ferrooxidans sp. nov., isolated from a denitrifying bioreactor. *Systematic and applied microbiology* **29**: 276-286.

Kurakov, A., Lavrent'Ev, R., Nechitailo, T.Y., Golyshin, P., and Zvyagintsev, D. (2008) Diversity of facultatively anaerobic microscopic mycelial fungi in soils. *Microbiology* **77**: 90-98.

Küsel, K., Dorsch, T., Acker, G., and Stackebrandt, E. (1999) Microbial reduction of Fe (III) in acidic sediments: isolation of Acidiphilium cryptum JF-5 capable of coupling the reduction of Fe (III) to the oxidation of glucose. *Applied and Environmental Microbiology* **65**: 3633-3640.

Kyle, J.E., Eydal, H.S., Ferris, F.G., and Pedersen, K. (2008) Viruses in granitic groundwater from 69 to 450 m depth of the Äspö hard rock laboratory, Sweden. *The ISME Journal* **2**: 571-574.

Kyselkova, M., Kopecky, J., Frapolli, M., Defago, G., Sagova-Mareckova, M., Grundmann, G.L., and Moenne-Loccoz, Y. (2009) Comparison of rhizobacterial community composition in soil suppressive or conducive to tobacco black root rot disease. *Isme j* **3**: 1127-1138.

Labonté, J.M., Field, E.K., Lau, M., Chivian, D., Van Heerden, E., Wommack, K.E. et al. (2015) Single cell genomics indicates horizontal gene transfer and viral infections in a deep subsurface Firmicutes population. *Frontiers in microbiology* **6**.

Lack, J., Chaudhuri, S., Chakraborty, R., Achenbach, L., and Coates, J. (2002) Anaerobic biooxidation of Fe (II) by Dechlorosoma suillum. *Microbial ecology* **43**: 424-431.

Langmuir, D., and Whiitemore, D.O. (1971) Variations in the stability of precipitated ferric oxyhydroxides. In: ACS Publications.

Lau, M.C., Cameron, C., Magnabosco, C., Brown, C.T., Schilkey, F., Grim, S. et al. (2014) Phylogeny and phylogeography of functional genes shared among seven terrestrial subsurface metagenomes reveal N-cycling and microbial evolutionary relationships. *Frontiers in microbiology* **5**.

Lau, M.C., Kieft, T.L., Kuloyo, O., Linage-Alvarez, B., Van Heerden, E., Lindsay, M.R. et al. (2016) An oligotrophic deep-subsurface community dependent on syntrophy is dominated by sulfur-driven autotrophic denitrifiers. *Proceedings of the National Academy of Sciences*: 201612244.

Leandro, T., da Costa, M.S., Sanz, J.L., and Amils, R. (2017) Complete Genome Sequence of Tessaracoccus sp. Strain T2. 5-30 Isolated from 139.5 Meters Deep on the Subsurface of the Iberian Pyritic Belt. *Genome announcements* **5**: e00238-00217.

Leblanc, M., Morales, J., Borrego, J., and Elbaz-Poulichet, F. (2000) 4,500-year-old mining pollution in southwestern Spain: long-term implications for modern mining pollution. *Economic Geology* **95**: 655-662.

Lee, J.H., Fredrickson, J.K., Plymale, A.E., Dohnalkova, A.C., Resch, C.T., McKinley, J.P., and Shi, L. (2015) An autotrophic H2-oxidizing, nitrate-respiring, Tc (VII)-reducing Acidovorax sp. isolated from a subsurface oxic-anoxic transition zone. *Environmental microbiology reports* **7**: 395-403.

Lehman, R.M., O'Connell, S.P., Banta, A., Fredrickson, J.K., Reysenbach, A.-L., Kieft, T.L., and Colwell, F.S. (2004) Microbiological comparison of core and groundwater samples collected from a fractured basalt aquifer with that of dialysis chambers incubated in situ. *Geomicrobiology Journal* **21**: 169-182.

Li, H., Chang, J., Liu, P., Fu, L., Ding, D., and Lu, Y. (2015) Direct interspecies electron transfer accelerates syntrophic oxidation of butyrate in paddy soil enrichments. *Environmental microbiology* **17**: 1533-1547.

Li, S., Li, X., and Li, F. (2017) Fe (II) oxidation and nitrate reduction by a denitrifying bacterium, Pseudomonas stutzeri LS-2, isolated from paddy soil. *Journal of Soils and Sediments*: 1-11.

Lin-Vien, D., Colthup, N.B., Fateley, W.G., and Grasselli, J.G. (1991) *The handbook of infrared and Raman characteristic frequencies of organic molecules*: Elsevier.

Lin, L.-H., Hall, J., Onstott, T., Gihring, T., Lollar, B.S., Boice, E. et al. (2006a) Planktonic microbial communities associated with fracture-derived groundwater in a deep gold mine of South Africa. *Geomicrobiology Journal* **23**: 475-497.

Lin, L.-H., Wang, P.-L., Rumble, D., Lippmann-Pipke, J., Boice, E., Pratt, L.M. et al. (2006b) Long-term sustainability of a high-energy, low-diversity crustal biome. *Science* **314**: 479-482.

Lipman, C.B. (1931) Living microörganisms in ancient rocks. *Journal of bacteriology* **22**: 183.

López-Archilla, A., Marín, I., and Amils, R. (2001) Microbial Community Composition and Ecology of an Acidic Aquatic Environment: The Tinto River, Spain. *Microbial ecology* **41**.

López-Archilla, A., González, A., Terrón, M., and Amils, R. (2004) Ecological study of the fungal populations of the acidic Tinto River in southwestern Spain. *Canadian Journal of Microbiology* **50**: 923-934.

Ludwig, W., Strunk, O., Westram, R., Richter, L., Meier, H., Yadhukumar et al. (2004) ARB: a software environment for sequence data. *Nucleic acids research* **32**: 1363-1371.

Luther III, G.W. (1987) Pyrite oxidation and reduction: molecular orbital theory considerations. *Geochimica et Cosmochimica Acta* **51**: 3193-3199.

Llobet-Brossa, E., Rosselló-Mora, R., and Amann, R. (1998) Microbial community composition of Wadden Sea sediments as revealed by fluorescence in situ hybridization. *Applied and environmental microbiology* **64**: 2691-2696.

MacLean, L.C.W., Pray, T.J., Onstott, T.C., Brodie, E.L., Hazen, T.C., and Southam, G. (2007) Mineralogical, Chemical and Biological Characterization of an Anaerobic Biofilm Collected from a Borehole in a Deep Gold Mine in South Africa. *Geomicrobiology Journal* **24**: 491-504.

Magnabosco, C., Ryan, K., Lau, M.C., Kuloyo, O., Lollar, B.S., Kieft, T.L. et al. (2016) A metagenomic window into carbon metabolism at 3 km depth in Precambrian continental crust. *The ISME journal* **10**: 730-741.

Magnabosco, C., Tekere, M., Lau, M.C., Linage, B., Kuloyo, O., Erasmus, M. et al. (2014) Comparisons of the composition and biogeographic distribution of the bacterial communities occupying South African thermal springs with those inhabiting deep subsurface fracture water. *Frontiers in microbiology* **5**.

Malki, M. (2003) Acidithiobacillus ferrooxidans y su papel en la geomicrobiología del ciclo del hierro en el Río Tinto. *Dissertation Thesis, UAM*.

Mannan, R.M., and Pakrasi, H.B. (1993) Dark heterotrophic growth conditions result in an increase in the content of photosystem II units in the filamentous cyanobacterium Anabaena variabilis ATCC 29413. *Plant physiology* **103**: 971-977.

Manz, W., Eisenbrecher, M., Neu, T.R., and Szewzyk, U. (1998) Abundance and spatial organization of Gram-negative sulfate-reducing bacteria in activated sludge investigated by in situ probing with specific 16S rRNA targeted oligonucleotides. *FEMS Microbiology Ecology* **25**: 43-61.

Manz, W., Amann, R., Ludwig, W., Wagner, M., and Schleifer, K.-H. (1992) Phylogenetic oligodeoxynucleotide probes for the major subclasses of proteobacteria: problems and solutions. *Systematic and applied microbiology* **15**: 593-600.

Manz, W., Amann, R., Ludwig, W., Vancanneyt, M., and Schleifer, K.-H. (1996) Application of a suite of 16S rRNA-specific oligonucleotide probes designed to investigate bacteria of the phylum cytophaga-flavobacter-bacteroides in the natural environment. *Microbiology* **142**: 1097-1106.

Maquelin, K., Kirschner, C., Choo-Smith, L.-P., van den Braak, N., Endtz, H.P., Naumann, D., and Puppels, G. (2002) Identification of medically relevant microorganisms by vibrational spectroscopy. *Journal of microbiological methods* **51**: 255-271.

Martino, A.J., Rhodes, M.E., Biddle, J.F., Brandt, L.D., Tomsho, L.P., and House, C.H. (2012) Novel degenerate PCR method for whole-genome amplification applied to Peru Margin (ODP Leg 201) subsurface samples. *Frontiers in microbiology* **3**.

McMahon, S., and Parnell, J. (2014) Weighing the deep continental biosphere. *FEMS microbiology ecology* **87**: 113-120.

Meier, H., Amann, R., Ludwig, W., and Schleifer, K.H. (1999) Specific oligonucleotide probes for in situ detection of a major group of gram-positive bacteria with low DNA G+ C content. *Systematic and Applied Microbiology* **22**: 186-196.

Meisinger, D.B., Zimmermann, J., Ludwig, W., Schleifer, K.H., Wanner, G., Schmid, M. et al. (2007) In situ detection of novel Acidobacteria in microbial mats from a chemolithoautotrophically based cave ecosystem (Lower Kane Cave, WY, USA). *Environmental microbiology* **9**: 1523-1534.

Méndez-García, C., Peláez, A.I., Mesa, V., Sánchez, J., Golyshina, O.V., and Ferrer, M. (2015) Microbial diversity and metabolic networks in acid mine drainage habitats. *Frontiers in microbiology* **6**: 475.

Miot, J., Remusat, L., Duprat, E., Gonzalez, A., Pont, S., and Poinsot, M. (2015) Fe biomineralization mirrors individual metabolic activity in a nitrate-dependent Fe (II)-oxidizer. *Frontiers in microbiology* **6**: 879.

Miyoshi, T., Iwatsuki, T., and Naganuma, T. (2005) Phylogenetic characterization of 16S rRNA gene clones from deep-groundwater microorganisms that pass through 0.2-micrometer-pore-size filters. *Applied and environmental microbiology* **71**: 1084-1088.

Möckl, L., Lamb, D.C., and Bräuchle, C. (2014) Super-resolved Fluorescence Microscopy: Nobel Prize in Chemistry 2014 for Eric Betzig, Stefan Hell, and William E. Moerner. *Angewandte Chemie International Edition* **53**: 13972-13977.

Momper, L., Jungbluth, S.P., Lee, M.D., and Amend, J.P. (2017a) Energy and carbon metabolisms in a deep terrestrial subsurface fluid microbial community. *The ISME journal* **11**: ismej201794.

Momper, L., Reese, B.K., Zinke, L., Wanger, G., Osburn, M.R., Moser, D., and Amend, J.P. (2017b) Major phylum-level differences between porefluid and host rock bacterial communities in the terrestrial deep subsurface. *Environmental microbiology reports*.

Moraghan, J., and Buresh, R. (1977) Chemical Reduction of Nitrite and Nitrous Oxide by Ferrous Iron 1. *Soil Science Society of America Journal* **41**: 47-50.

Moraru, C., Lam, P., Fuchs, B.M., Kuypers, M.M., and Amann, R. (2010) GeneFISH–an in situ technique for linking gene presence and cell identity in environmental microorganisms. *Environmental microbiology* **12**: 3057-3073.

Morita, R.Y. (1999) Is H2 the Universal Energy Source for Long-Term Survival? *Microbial Ecology* **38**: 307-320.

Morris, B.E., Henneberger, R., Huber, H., and Moissl-Eichinger, C. (2013) Microbial syntrophy: interaction for the common good. *FEMS Microbiology Reviews* **37**: 384-406.

Moser, D.P., Onstott, T., Fredrickson, J.K., Brockman, F.J., Balkwill, D.L., Drake, G. et al. (2003) Temporal shifts in the geochemistry and microbial community structure of an ultradeep mine borehole following isolation. *Geomicrobiology Journal* **20**: 517-548.

Moser, D.P., Gihring, T.M., Brockman, F.J., Fredrickson, J.K., Balkwill, D.L., Dollhopf, M.E. et al. (2005) Desulfotomaculum and Methanobacterium spp. dominate a 4-to 5-kilometer-deep fault. *Applied and Environmental Microbiology* **71**: 8773-8783.

Moses, C.O., and Herman, J.S. (1991) Pyrite oxidation at circumneutral pH. *Geochimica et Cosmochimica Acta* **55**: 471-482.

Moses, C.O., Nordstrom, D.K., Herman, J.S., and Mills, A.L. (1987) Aqueous pyrite oxidation by dissolved oxygen and by ferric iron. *Geochimica et Cosmochimica Acta* **51**: 1561-1571.

Moter, A., and Göbel, U.B. (2000) Fluorescence in situ hybridization (FISH) for direct visualization of microorganisms. In: Elsevier.

Muehe, E.M., Gerhardt, S., Schink, B., and Kappler, A. (2009) Ecophysiology and the energetic benefit of mixotrophic Fe (II) oxidation by various strains of nitratereducing bacteria. *FEMS Microbiology Ecology* **70**: 335-343.

Müller, V. (2003) Energy conservation in acetogenic bacteria. *Applied and environmental microbiology* **69**: 6345-6353.

Murakami, Y., Fujita, Y., Naganuma, T., and Iwatsuki, T. (2002) Abundance and viability of the groundwater microbial communities from a borehole in the Tono uranium deposit area, central Japan. *Microbes and environments* **17**: 63-74.

Nealson, K.H., Inagaki, F., and Takai, K. (2005) Hydrogen-driven subsurface lithoautotrophic microbial ecosystems (SLiMEs): do they exist and why should we care? *Trends in microbiology* **13**: 405-410.

Neef, A. (1997) Anwendung der in situ-Einzelzell-Identifizierung von Bakterien zur Populationsanalyse in komplexen mikrobiellen Biozo¨nosen. In. Munich, Germany: Technical University Munich.

Neu, T., and Lawrence, J. (2016) The extracellular matrix: An intractable part of biofilm systems. *The Perfect Slime—Microbial Extracellular Substances; Flemming, H-C, Wingender, J, Neu, TR, Eds*: 25-60.

Neu, T.R., and Lawrence, J.R. (2014) Investigation of microbial biofilm structure by laser scanning microscopy. *Adv Biochem Eng Biotechnol* **146**: 1-51.

Neu, T.R., Swerhone, G.D., and Lawrence, J.R. (2001) Assessment of lectin-binding analysis for in situ detection of glycoconjugates in biofilm systems. *Microbiology* **147**: 299-313.

Neumann, S., Jetten, M.S., and van Niftrik, L. (2011) The ultrastructure of the compartmentalized anaerobic ammonium-oxidizing bacteria is linked to their energy metabolism. In: Portland Press Limited.

Nielsen, A.T., Tolker-Nielsen, T., Barken, K.B., and Molin, S. (2000) Role of commensal relationships on the spatial structure of a surface-attached microbial consortium. *Environmental microbiology* **2**: 59-68.

Nieto, J.M., Sarmiento, A.M., Olías, M., Canovas, C.R., Riba, I., Kalman, J., and Delvalls, T.A. (2007) Acid mine drainage pollution in the Tinto and Odiel rivers (Iberian Pyrite Belt, SW Spain) and bioavailability of the transported metals to the Huelva Estuary. *Environment International* **33**: 445-455.

Nordstrom, D., and Alpers, C. (1999) *Geochemistry of acid mine waters*.

Nordstrom, D.K. (1982) *Aqueous pyrite oxidation and the consequent formation of secondary iron minerals*: Soil Science Society of America.

Nyyssönen, M., Bomberg, M., Kapanen, A., Nousiainen, A., Pitkänen, P., and Itävaara, M. (2012) Methanogenic and sulphate-reducing microbial communities in deep groundwater of crystalline rock fractures in Olkiluoto, Finland. *Geomicrobiology Journal* **29**: 863-878.

Nyyssönen, M., Hultman, J., Ahonen, L., Kukkonen, I., Paulin, L., Laine, P. et al. (2014) Taxonomically and functionally diverse microbial communities in deep crystalline rocks of the Fennoscandian shield. *The ISME journal* **8**: 126-138.

O'hara, G., and Daniel, R.M. (1985) Rhizobial denitrification: a review. *Soil Biology and Biochemistry* **17**: 1-9.

Omelon, S., Georgiou, J., Henneman, Z.J., Wise, L.M., Sukhu, B., Hunt, T. et al. (2009) Control of vertebrate skeletal mineralization by polyphosphates. *PLoS One* **4**: e5634.

Onstott, T., Moser, D.P., Pfiffner, S.M., Fredrickson, J.K., Brockman, F.J., Phelps, T. et al. (2003) Indigenous and contaminant microbes in ultradeep mines. *Environmental Microbiology* **5**: 1168-1191.

Onstott, T., McGown, D.J., Bakermans, C., Ruskeeniemi, T., Ahonen, L., Telling, J. et al. (2009) Microbial communities in subpermafrost saline fracture water at the Lupin Au Mine, Nunavut, Canada. *Microbial ecology* **58**: 786-807.

Orcutt, B.N., Sylvan, J.B., Knab, N.J., and Edwards, K.J. (2011) Microbial ecology of the dark ocean above, at, and below the seafloor. *Microbiology and Molecular Biology Reviews* **75**: 361-422.

Oremland, R.S., Culbertson, C., and Simoneit, B. (1982) Methanogenic activity in sediment from Leg 64, Gulf of California. *Curray, JR, Moore, DG, et al, Init Repts DSDP* **64**: 759-762.

Orphan, V.J. (2009) Methods for unveiling cryptic microbial partnerships in nature. *Current opinion in microbiology* **12**: 231-237.

Osburn, M.R., LaRowe, D.E., Momper, L.M., and Amend, J.P. (2014) Chemolithotrophy in the continental deep subsurface: Sanford Underground Research Facility (SURF), USA. *Frontiers in microbiology* **5**.

Osorio, H., Mangold, S., Denis, Y., Ñancucheo, I., Esparza, M., Johnson, D.B. et al. (2013) Anaerobic sulfur metabolism coupled to dissimilatory iron reduction in the extremophile Acidithiobacillus ferrooxidans. *Applied and environmental microbiology* **79**: 2172-2181.

Paddock, S.W. (1999) Confocal laser scanning microscopy. *Biotechniques* **27**: 992-1007.

Peccia, J., Marchand, E.A., Silverstein, J., and Hernandez, M. (2000) Development and application of small-subunit rRNA probes for assessment of selected Thiobacillus species and members of the genus Acidiphilium. *Applied and environmental microbiology* **66**: 3065-3072.

Pedersen, K. (1997) Microbial life in deep granitic rock. *FEMS Microbiology Reviews* **20**: 399-414.

Pedersen, K. (1999) Subterranean microorganisms and radioactive waste disposal in Sweden. *Engineering Geology* **52**: 163-176.

Pedersen, K. (2000) Exploration of deep intraterrestrial microbial life: current perspectives. *FEMS microbiology letters* **185**: 9-16.

Pedersen, K. (2012) Subterranean microbial populations metabolize hydrogen and acetate under in situ conditions in granitic groundwater at 450 m depth in the Äspö Hard Rock Laboratory, Sweden. *FEMS microbiology ecology* **81**: 217-229.

Pernthaler, A., Pernthaler, J., and Amann, R. (2004) Sensitive multi-color fluorescence in situ hybridization for the identification of environmental microorganisms. In *Molecular Microbial Ecology Manual*. Kowalchuk, G.e.a. (ed). Netherlands: Kluwer Academic Publishers, pp. 711–726.

Pernthaler, A., Preston, C.M., Pernthaler, J., DeLong, E.F., and Amann, R. (2002) Comparison of fluorescently labeled oligonucleotide and polynucleotide probes for the detection of pelagic marine bacteria and archaea. *Applied and Environmental Microbiology* **68**: 661-667.

Pernthaler, J., Glöckner, F.-O., Schönhuber, W., and Amann, R. (2001) Fluorescence in situ hybridization (FISH) with rRNA-targeted oligonucleotide probes. *Methods in microbiology* **30**: 207-226.

Pester, M., Brambilla, E., Alazard, D., Rattei, T., Weinmaier, T., Han, J. et al. (2012) Complete genome sequences of Desulfosporosinus orientis DSM765T, Desulfosporosinus youngiae DSM17734T, Desulfosporosinus meridiei DSM13257T, and Desulfosporosinus acidiphilus DSM22704T. *Journal of bacteriology* **194**: 6300-6301.

Pfiffner, S.M., Cantu, J.M., Smithgall, A., Peacock, A.D., White, D.C., Moser, D.P. et al. (2006) Deep Subsurface Microbial Biomass and Community Structure in Witwatersrand Basin Mines. *Geomicrobiology Journal* **23**: 431-442.

Phelps, T., Murphy, E., Pfiffner, S., and White, D. (1994) Comparison between geochemical and biological estimates of subsurface microbial activities. *Microbial Ecology* **28**: 335-349.

Picardal, F. (2012) Abiotic and microbial interactions during anaerobic transformations of Fe (II) and NOx. *Frontiers in microbiology* **3**: 112.

Pinchuk, G.E., Ammons, C., Culley, D.E., Li, S.-M.W., McLean, J.S., Romine, M.F. et al. (2008) Utilization of DNA as a sole source of phosphorus, carbon, and energy by Shewanella spp.: ecological and physiological implications for dissimilatory metal reduction. *Applied and environmental microbiology* **74**: 1198-1208.

Postma, D., Boesen, C., Kristiansen, H., and Larsen, F. (1991) Nitrate reduction in an unconfined sandy aquifer: water chemistry, reduction processes, and geochemical modeling. *Water Resources Research* **27**: 2027-2045.

Poulsen, L.K., Ballard, G., and Stahl, D.A. (1993) Use of rRNA fluorescence in situ hybridization for measuring the activity of single cells in young and established biofilms. *Applied and environmental microbiology* **59**: 1354-1360.

Probst, A.J., and Moissl-Eichinger, C. (2015) "Altiarchaeales": uncultivated Archaea from the subsurface. *Life* **5**: 1381-1395.

Probst, A.J., Holman, H.-Y.N., DeSantis, T.Z., Andersen, G.L., Birarda, G., Bechtel, H.A. et al. (2013) Tackling the minority: sulfate-reducing bacteria in an archaea-dominated subsurface biofilm. *The ISME journal* **7**: 635-651.

Probst, A.J., Birarda, G., Holman, H.-Y.N., DeSantis, T.Z., Wanner, G., Andersen, G.L. et al. (2014a) Coupling genetic and chemical microbiome profiling reveals heterogeneity of archaeome and bacteriome in subsurface biofilms that are dominated by the same archaeal species. *PloS one* **9**: e99801.

Probst, A.J., Weinmaier, T., Raymann, K., Perras, A., Emerson, J.B., Rattei, T. et al. (2014b) Biology of a widespread uncultivated archaeon that contributes to carbon fixation in the subsurface. *Nature communications* **5**: 5497.

Puente-Sánchez, F. (2016) Microbial ecology of the Iberian Pyrite Belt deep subsurface. *Dissertation Thesis, UAM*.

Puente-Sánchez, F., Sánchez-Román, M., Amils, R., and Parro, V. (2014a) Tessaracoccus lapidicaptus sp. nov., an actinobacterium isolated from the deep subsurface of the Iberian pyrite belt. *International journal of systematic and evolutionary microbiology* **64**: 3546-3552.

Puente-Sánchez, F., Moreno-Paz, M., Rivas, L., Cruz-Gil, P., García-Villadangos, M., Gómez, M. et al. (2014b) Deep subsurface sulfate reduction and methanogenesis in the Iberian Pyrite Belt revealed through geochemistry and molecular biomarkers. *Geobiology* **12**: 34-47.

Purkamo, L., Bomberg, M., Nyyssönen, M., Kukkonen, I., Ahonen, L., and Itävaara, M. (2015) Heterotrophic communities supplied by ancient organic carbon predominate in deep Fennoscandian bedrock fluids. *Microbial ecology* **69**: 319-332.

Purkamo, L., Bomberg, M., Nyyssönen, M., Kukkonen, I., Ahonen, L., Kietäväinen, R., and Itävaara, M. (2013) Dissecting the deep biosphere: retrieving authentic microbial communities from packer-isolated deep crystalline bedrock fracture zones. *FEMS microbiology ecology* **85**: 324-337.

Quast, C., Pruesse, E., Yilmaz, P., Gerken, J., Schweer, T., Yarza, P. et al. (2012) The SILVA ribosomal RNA gene database project: improved data processing and web-based tools. *Nucleic acids research* **41**: D590-D596.

Rajala, P., and Bomberg, M. (2017) Reactivation of deep subsurface microbial community in response to methane or methanol amendment. *Frontiers in Microbiology* **8**.

Rajala, P., Bomberg, M., Kietäväinen, R., Kukkonen, I., Ahonen, L., Nyyssönen, M., and Itävaara, M. (2015) Rapid reactivation of deep subsurface microbes in the presence of C-1 compounds. *Microorganisms* **3**: 17-33.

Raskin, L., Stromley, J.M., Rittmann, B.E., and Stahl, D.A. (1994) Group-specific 16S rRNA hybridization probes to describe natural communities of methanogens. *Applied and environmental microbiology* **60**: 1232-1240.

Read, D., Huang, W., and Whiteley, A. (2010) Raman FISH. In *Handbook of Hydrocarbon and Lipid Microbiology*: Springer, pp. 4027-4038.

Rempfert, K.R., Miller, H.M., Bompard, N., Nothaft, D., Matter, J.M., Kelemen, P. et al. (2017) Geological and geochemical controls on subsurface microbial life in the Samail Ophiolite, Oman. *Frontiers in microbiology* **8**.

Rogers, J., Bennett, P., and Choi, W. (1998) Feldspars as a source of nutrients for microorganisms. *American Mineralogist* **83**: 1532-1540.

Rohwerder, T., Gehrke, T., Kinzler, K., and Sand, W. (2003) Bioleaching review part A: progress in bioleaching: fundamentals and mechanisms of bacterial metal sulfide oxidation. *Appl Microbiol Biotechnol* **63**: 239-248.

Rojas-Chapana, J., and Tributsch, H. (2001) Biochemistry of sulfur extraction in bio-corrosion of pyrite by Thiobacillus ferrooxidans. *Hydrometallurgy* **59**: 291-300.

Roller, C., Wagner, M., Amann, R., Ludwig, W., and Schleifer, K.-H. (1994) In situ probing of Gram-positive bacteria with high DNA G+ C content using 23S rRNA-targeted oligonucleotides. *Microbiology* **140**: 2849-2858.

Rygula, A., Majzner, K., Marzec, K.M., Kaczor, A., Pilarczyk, M., and Baranska, M. (2013) Raman spectroscopy of proteins: a review. *Journal of Raman Spectroscopy* **44**: 1061-1076.

Sahl, J.W., Schmidt, R., Swanner, E.D., Mandernack, K.W., Templeton, A.S., Kieft, T.L. et al. (2008) Subsurface microbial diversity in deep-granitic-fracture water in Colorado. *Applied and environmental microbiology* **74**: 143-152.

Sakai, S., Takaki, Y., Shimamura, S., Sekine, M., Tajima, T., Kosugi, H. et al. (2011) Genome sequence of a mesophilic hydrogenotrophic methanogen Methanocella paludicola, the first cultivated representative of the order Methanocellales. *PLoS One* **6**: e22898.

Sakurai, K., and Yoshikawa, H. (2012) Isolation and identification of bacteria able to form biofilms from deep subsurface environments. *Journal of nuclear science and technology* **49**: 287-292.

Sánchez-Andrea, I., Rodríguez, N., Amils, R., and Sanz, J.L. (2011) Microbial diversity in anaerobic sediments at Rio Tinto, a naturally acidic environment with a high heavy metal content. *Applied and environmental microbiology* **77**: 6085-6093.

Sánchez-Andrea, I., Stams, A.J., Amils, R., and Sanz, J.L. (2013) Enrichment and isolation of acidophilic sulfate-reducing bacteria from Tinto River sediments. *Environmental microbiology reports* **5**: 672-678.

Sand, W., and Gehrke, T. (2006) Extracellular polymeric substances mediate bioleaching/biocorrosion via interfacial processes involving iron (III) ions and acidophilic bacteria. *Research in Microbiology* **157**: 49-56.

Sanhueza, A., Ferrer, I., Vargas, T., Amils, R., and Sánchez, C. (1999) Attachment of Thiobacillus ferrooxidans on synthetic pyrite of varying structural and electronic properties. *Hydrometallurgy* **51**: 115-129.

Sanz, J.L., Rodríguez, N., Díaz, E.E., and Amils, R. (2011) Methanogenesis in the sediments of Rio Tinto, an extreme acidic river. *Environmental microbiology* **13**: 2336-2341.

Sauer, K. (2003) The genomics and proteomics of biofilm formation. *Genome biology* **4**: 219.

Saville, R.M., Rakshe, S., Haagensen, J.A., Shukla, S., and Spormann, A.M. (2011) Energy-dependent stability of Shewanella oneidensis MR-1 biofilms. *Journal of bacteriology* **193**: 3257-3264.

Schaedler, F., Kappler, A., and Schmidt, C. (2017) A revised iron extraction protocol for environmental samples rich in nitrite and carbonate. *Geomicrobiology Journal*: 1-8.

Schaedler, F., Lockwood, C., Lueder, U., Glombitza, C., Kappler, A., and Schmidt, C. (2018) Microbially mediated coupling of Fe and N cycles by nitrate-reducing Fe (II)-oxidizing bacteria in littoral freshwater sediments. *Applied and environmental microbiology* **84**: e02013-02017.

Schimak, M.P., Kleiner, M., Wetzel, S., Liebeke, M., Dubilier, N., and Fuchs, B.M. (2015) MiL-FISH: Multilabeled Oligonucleotides for Fluorescence In Situ Hybridization Improve Visualization of Bacterial Cells. *Appl Environ Microbiol* **82**: 62-70.

Schindelin, J., Arganda-Carreras, I., Frise, E., Kaynig, V., Longair, M., Pietzsch, T. et al. (2012) Fiji: an open-source platform for biological-image analysis. *Nat Meth* **9**: 676-682.

Schippers, A., and Jørgensen, B. (2001) Oxidation of pyrite and iron sulfide by manganese dioxide in marine sediments. *Geochimica et Cosmochimica Acta* **65**: 915-922.

Schippers, A., and Jørgensen, B. (2002) Biogeochemistry of pyrite and iron sulfide oxidation in marine sediments. *Geochimica et Cosmochimica Acta* **66**: 85-92.

Schippers, A., Jozsa, P., and Sand, W. (1996) Sulfur chemistry in bacterial leaching of pyrite. *Applied and Environmental Microbiology* **62**: 3424-3431.

Schippers, A., Hedrich, S., Vasters, J., Drobe, M., Sand, W., and Willscher, S. (2013) Biomining: metal recovery from ores with microorganisms. In *Geobiotechnology I*: Springer, pp. 1-47.

Schmid, G., Zeitvogel, F., Hao, L., Ingino, P., Floetenmeyer, M., Stierhof, Y.D. et al. (2014) 3-D analysis of bacterial cell-(iron) mineral aggregates formed during Fe (II) oxidation by the nitrate-reducing Acidovorax sp. strain BoFeN1 using complementary microscopy tomography approaches. *Geobiology* **12**: 340-361.

Schmid, M., Walsh, K., Webb, R., Rijpstra, W.I., van de Pas-Schoonen, K., Verbruggen, M.J. et al. (2003) Candidatus "Scalindua brodae", sp. nov., Candidatus "Scalindua wagneri", sp.

nov., two new species of anaerobic ammonium oxidizing bacteria. *Systematic and applied microbiology* **26**: 529-538.

Schönhuber, W., Zarda, B., Eix, S., Rippka, R., Herdman, M., Ludwig, W., and Amann, R. (1999) In situ identification of cyanobacteria with horseradish peroxidase-labeled, rRNA-targeted oligonucleotide probes. *Applied and environmental microbiology* **65**: 1259-1267.

Schreiber, L., Holler, T., Knittel, K., Meyerdierks, A., and Amann, R. (2010) Identification of the dominant sulfate-reducing bacterial partner of anaerobic methanotrophs of the ANME-2 clade. *Environmental microbiology* **12**: 2327-2340.

Schulze, R., Spring, S., Amann, R., Huber, I., Ludwig, W., Schleifer, K.-H., and Kämpfer, P. (1999) Genotypic diversity of Acidovorax strains isolated from activated sludge and description of Acidovorax defluvii sp. nov. *Systematic and applied microbiology* **22**: 205-214.

Schuster, K.C., Reese, I., Urlaub, E., Gapes, J.R., and Lendl, B. (2000) Multidimensional information on the chemical composition of single bacterial cells by confocal Raman microspectroscopy. *Analytical chemistry* **72**: 5529-5534.

Schwarzenbach, R.P., Gschwend, P.M., and Imboden, D.M. (2005) Sorption III: Sorption Processes Involving Inorganic Surfaces. In *Environmental Organic Chemistry*: John Wiley & Sons, Inc., pp. 387-458.

Schwientek, M., Einsiedl, F., Stichler, W., Stögbauer, A., Strauss, H., and Maloszewski, P. (2008) Evidence for denitrification regulated by pyrite oxidation in a heterogeneous porous groundwater system. *Chemical geology* **255**: 60-67.

Shelobolina, E., Xu, H., Konishi, H., Kukkadapu, R., Wu, T., Blöthe, M., and Roden, E. (2012) Microbial lithotrophic oxidation of structural Fe (II) in biotite. *Applied and environmental microbiology* **78**: 5746-5752.

Shimizu, S., Akiyama, M., Ishijima, Y., Hama, K., Kunimaru, T., and Naganuma, T. (2006) Molecular characterization of microbial communities in fault-bordered aquifers in the Miocene formation of northernmost Japan. *Geobiology* **4**: 203-213.

Shock, E.L. (2009) Minerals as energy sources for microorganisms. *Economic Geology* **104**: 1235-1248.

Smith, E., and Dent, G. (2013) *Modern Raman spectroscopy: a practical approach*: John Wiley & Sons.

Sohlberg, E., Bomberg, M., Miettinen, H., Nyyssönen, M., Salavirta, H., Vikman, M., and Itävaara, M. (2015) Revealing the unexplored fungal communities in deep groundwater of crystalline bedrock fracture zones in Olkiluoto, Finland. *Frontiers in microbiology* **6**.

Song, L., Hennink, E., Young, I.T., and Tanke, H.J. (1995) Photobleaching kinetics of fluorescein in quantitative fluorescence microscopy. *Biophysical journal* **68**: 2588.

Souza-Egipsy, V., Altamirano, M., Amils, R., and Aguilera, A. (2011) Photosynthetic performance of phototrophic biofilms in extreme acidic environments. *Environmental microbiology* **13**: 2351-2358.

Stahl, D.A., and Amann, R. (1991) *Development and application of nucleic acid probes*. New York: John Wiley & Sons Inc.

Stanley, N.R., and Lazazzera, B.A. (2004) Environmental signals and regulatory pathways that influence biofilm formation. *Molecular microbiology* **52**: 917-924.

Stevens, T., McKinley, J., and Fredrickson, J.K. (1993) Bacteria associated with deep, alkaline, anaerobic groundwaters in southeast Washington. *Microbial Ecology* **25**: 35-50.

Stevens, T.O., and McKinley, J.P. (1995) Lithoautotrophic microbial ecosystems in deep basalt aquifers. *Science* **270**: 450.

Stoecker, K., Dorninger, C., Daims, H., and Wagner, M. (2010) Double labeling of oligonucleotide probes for fluorescence in situ hybridization (DOPE-FISH) improves signal intensity and increases rRNA accessibility. *Appl Environ Microbiol* **76**: 922-926.

Stoker, C., Dunagan, S., Stevens, T., Amils, R., Gomez-Elvira, J., Fernandez, D. et al. (2004) Mars Analog Rio Tinto Experiment (MARTE): 2003 Drilling Campaign to Search for a Subsurface Biosphere at Rio Tinto Spain. In *Lunar and Planetary Science Conference*.

Stoodley, P., Sauer, K., Davies, D., and Costerton, J.W. (2002) Biofilms as complex differentiated communities. *Annual Reviews in Microbiology* **56**: 187-209.

Strąpoć, D., Picardal, F.W., Turich, C., Schaperdoth, I., Macalady, J.L., Lipp, J.S. et al. (2008) Methane-producing microbial community in a coal bed of the Illinois Basin. *Applied and environmental microbiology* **74**: 2424-2432.

Straub, K.L., Benz, M., and Schink, B. (2001) Iron metabolism in anoxic environments at near neutral pH. *FEMS microbiology ecology* **34**: 181-186.

Straub, K.L., Benz, M., Schink, B., and Widdel, F. (1996) Anaerobic, nitrate-dependent microbial oxidation of ferrous iron. *Applied and environmental microbiology* **62**: 1458-1460.

Straub, K.L., Schönhuber, W.A., Buchholz-Cleven, B.E., and Schink, B. (2004) Diversity of ferrous iron-oxidizing, nitrate-reducing bacteria and their involvement in oxygen-independent iron cycling. *Geomicrobiology Journal* **21**: 371-378.

Suzuki, S., Ishii, S.i., Wu, A., Cheung, A., Tenney, A., Wanger, G. et al. (2013) Microbial diversity in The Cedars, an ultrabasic, ultrareducing, and low salinity serpentinizing ecosystem. *Proceedings of the National Academy of Sciences* **110**: 15336-15341.

Suzuki, Y., Konno, U., Fukuda, A., Komatsu, D.D., Hirota, A., Watanabe, K. et al. (2014) Biogeochemical signals from deep microbial life in terrestrial crust. *PloS one* **9**: e113063.

Swanner, E.D., and Templeton, A.S. (2011) Potential for nitrogen fixation and nitrification in the granite-hosted subsurface at Henderson Mine, CO. *Frontiers in microbiology* **2**.

Swanner, E.D., Nell, R.M., and Templeton, A.S. (2011) Ralstonia species mediate Fe-oxidation in circumneutral, metal-rich subsurface fluids of Henderson mine, CO. *Chemical Geology* **284**: 339-350.

Takai, K., Moser, D.P., DeFlaun, M., Onstott, T.C., and Fredrickson, J.K. (2001) Archaeal diversity in waters from deep South African gold mines. *Applied and Environmental Microbiology* **67**: 5750-5760.

Takai, K., Hirayama, H., Sakihama, Y., Inagaki, F., Yamato, Y., and Horikoshi, K. (2002) Isolation and metabolic characteristics of previously uncultured members of the order Aquificales in a subsurface gold mine. *Applied and environmental microbiology* **68**: 3046-3054.

Teira, E., Reinthaler, T., Pernthaler, A., Pernthaler, J., and Herndl, G.J. (2004) Combining catalyzed reporter deposition-fluorescence in situ hybridization and microautoradiography to detect substrate utilization by bacteria and archaea in the deep ocean. *Applied and Environmental Microbiology* **70**: 4411-4414.

Thauer, R.K., Jungermann, K., and Decker, K. (1977) Energy conservation in chemotrophic anaerobic bacteria. *Bacteriological reviews* **41**: 100.

Tiedje, J.M. (1988) Ecology of denitrification and dissimilatory nitrate reduction to ammonium. *Biology of anaerobic microorganisms* **717**: 179-244.

Tornos, F. (2006) Environment of formation and styles of volcanogenic massive sulfides: the Iberian Pyrite Belt. *Ore Geology Reviews* **28**: 259-307.

Torrentó, C., Cama, J., Urmeneta, J., Otero, N., and Soler, A. (2010) Denitrification of groundwater with pyrite and Thiobacillus denitrificans. *Chemical Geology* **278**: 80-91.

Torrentó, C., Urmeneta, J., Otero, N., Soler, A., Viñas, M., and Cama, J. (2011) Enhanced denitrification in groundwater and sediments from a nitrate-contaminated aquifer after addition of pyrite. *Chemical Geology* **287**: 90-101.

Tschech, A., and Pfennig, N. (1984) Growth yield increase linked to caffeate reduction in Acetobacterium woodii. *Archives of Microbiology* **137**: 163-167.

Udaondo, Z., Duque, E., and Ramos, J.L. (2017) The pangenome of the genus Clostridium. *Environmental microbiology* **19**: 2588-2603.

Ushioda, S. (1972) Raman scattering from phonons in iron pyrite (FeS2). *Solid state communications* **10**: 307-310.

Vaclavkova, S., Schultz-Jensen, N., Jacobsen, O.S., Elberling, B., and Aamand, J. (2015) Nitrate-controlled anaerobic oxidation of pyrite by Thiobacillus cultures. *Geomicrobiology Journal* **32**: 412-419.

Van Cleemput, O., and Baert, L. (1983) Nitrite stability influenced by iron compounds. *Soil Biology and Biochemistry* **15**: 137-140.

Van Geen, A., Adkins, J., Boyle, E., Nelson, C., and Palanques, A. (1997) A 120-yr record of widespread contamination from mining of the Iberian pyrite belt. *Geology* **25**: 291-294.

Vera, M., Schippers, A., and Sand, W. (2013) Progress in bioleaching: fundamentals and mechanisms of bacterial metal sulfide oxidation—part A. *Applied microbiology and biotechnology* **97**: 7529-7541.

Vogt, H., Chattopadhyay, T., and Stolz, H. (1983) Complete first-order Raman spectra of the pyrite structure compounds FeS2, MnS2 and SiP2. *Journal of Physics and Chemistry of Solids* **44**: 869-873.

Vreeland, R.H., Piselli Jr, A.F., McDonnough, S., and Meyers, S. (1998) Distribution and diversity of halophilic bacteria in a subsurface salt formation. *Extremophiles* **2**: 321-331.

Wagner, M., Ivleva, N.P., Haisch, C., Niessner, R., and Horn, H. (2009) Combined use of confocal laser scanning microscopy (CLSM) and Raman microscopy (RM): investigations on EPS–matrix. *water research* **43**: 63-76.

Wallner, G., Amann, R., and Beisker, W. (1993) Optimizing fluorescent in situ hybridization with rRNA-targeted oligonucleotide probes for flow cytometric identification of microorganisms. *Cytometry* **14**: 136-143.

Wanger, G., Southam, G., and Onstott, T.C. (2006) Structural and Chemical Characterization of a Natural Fracture Surface from 2.8 Kilometers Below Land Surface: Biofilms in the Deep Subsurface. *Geomicrobiology Journal* **23**: 443-452.

Watling, H., Perrot, F., and Shiers, D. (2008) Comparison of selected characteristics of Sulfobacillus species and review of their occurrence in acidic and bioleaching environments. *Hydrometallurgy* **93**: 57-65.

Weber, K.A., Achenbach, L.A., and Coates, J.D. (2006) Microorganisms pumping iron: anaerobic microbial iron oxidation and reduction. *Nature Reviews Microbiology* **4**: 752.

Weber, K.A., Hedrick, D.B., Peacock, A.D., Thrash, J.C., White, D.C., Achenbach, L.A., and Coates, J.D. (2009) Physiological and taxonomic description of the novel autotrophic, metal oxidizing bacterium, Pseudogulbenkiania sp. strain 2002. *Applied microbiology and biotechnology* **83**: 555-565.

Weidler, G.W., Gerbl, F.W., and Stan-Lotter, H. (2008) Crenarchaeota and their role in the nitrogen cycle in a subsurface radioactive thermal spring in the Austrian Central Alps. *Applied and environmental microbiology* **74**: 5934-5942.

Whelan, J., Oremland, R., Tarafa, M., Smith, R., Howarth, R., and Lee, C. (1986) *Evidence for Sulfate-Reducing and Methane-Producing Microorganisms in Sediments from Sites 618, 619, and 622*.

Whitman, W.B., Coleman, D.C., and Wiebe, W.J. (1998) Prokaryotes: the unseen majority. *Proc Natl Acad Sci U S A* **95**: 6578-6583.

Widdel, F., and Pfennig, N. (1981) Studies on dissimilatory sulfate-reducing bacteria that decompose fatty acids. *Archives of microbiology* **129**: 395-400.

Willems, A. (2014) The family comamonadaceae. In *The prokaryotes*: Springer, pp. 777-851.

Winter, J., and Wolfe, R.S. (1979) Complete degradation of carbohydrate to carbon dioxide and methane by syntrophic cultures of Acetobacterium woodii and Methanosarcina barkeri. *Archives of Microbiology* **121**: 97-102.

Wouters, K., Moors, H., Boven, P., and Leys, N. (2013) Evidence and characteristics of a diverse and metabolically active microbial community in deep subsurface clay borehole water. *FEMS microbiology ecology* **86**: 458-473.

Yan, R., Kappler, A., and Peiffer, S. (2015) Interference of nitrite with pyrite under acidic conditions: implications for studies of chemolithotrophic denitrification. *Environmental science & technology* **49**: 11403-11410.

Yin, J., Hu, Y., and Yoon, J. (2015) Fluorescent probes and bioimaging: alkali metals, alkaline earth metals and pH. *Chemical Society Reviews* **44**: 4619-4644.

Young, J., Kuykendall, L., Martinez-Romero, E., Kerr, A., and Sawada, H. (2001) A revision of Rhizobium Frank 1889, with an emended description of the genus, and the inclusion of all species of Agrobacterium Conn 1942 and Allorhizobium undicola de Lajudie et al. 1998 as new combinations: Rhizobium radiobacter, R. rhizogenes, R. rubi, R. undicola and R. vitis. *International Journal of Systematic and Evolutionary Microbiology* **51**: 89-103.

Zablotowicz, R., Eskew, D., and Focht, D. (1978) Denitrification in Rhizobium. *Canadian journal of microbiology* **24**: 757-760.

Zahran, H.H. (1999) Rhizobium-legume symbiosis and nitrogen fixation under severe conditions and in an arid climate. *Microbiology and molecular biology reviews* **63**: 968-989.

Zelezniak, A., Andrejev, S., Ponomarova, O., Mende, D.R., Bork, P., and Patil, K.R. (2015) Metabolic dependencies drive species co-occurrence in diverse microbial communities. *Proceedings of the National Academy of Sciences* **112**: 6449-6454.

Zhang, G., Dong, H., Xu, Z., Zhao, D., and Zhang, C. (2005) Microbial diversity in ultra-high-pressure rocks and fluids from the Chinese Continental Scientific Drilling Project in China. *Applied and environmental microbiology* **71**: 3213-3227.

Zhang, G., Dong, H., Jiang, H., Xu, Z., and Eberl, D.D. (2006) Unique microbial community in drilling fluids from Chinese continental scientific drilling. *Geomicrobiology Journal* **23**: 499-514.

Zhang, R., Neu, T., Bellenberg, S., Kuhlicke, U., Sand, W., and Vera, M. (2015) Use of lectins to in situ visualize glycoconjugates of extracellular polymeric substances in acidophilic archaeal biofilms. *Microbial biotechnology* **8**: 448-461.

Zhang, Y.-C., Slomp, C.P., Broers, H.P., Passier, H.F., and Van Cappellen, P. (2009) Denitrification coupled to pyrite oxidation and changes in groundwater quality in a shallow sandy aquifer. *Geochimica et Cosmochimica Acta* **73**: 6716-6726.

Zhang, Y.-C., Slomp, C.P., Broers, H.P., Bostick, B., Passier, H.F., Böttcher, M.E. et al. (2012) Isotopic and microbiological signatures of pyrite-driven denitrification in a sandy aquifer. *Chemical Geology* **300**: 123-132.

Zinder, S.H. (1993) Physiological ecology of methanogens. In *Methanogenesis*: Springer, pp. 128-206.

Zinke, L.A., Mullis, M.M., Bird, J.T., Marshall, I.P., Jørgensen, B.B., Lloyd, K.G. et al. (2017) Thriving or surviving? Evaluating active microbial guilds in Baltic Sea sediment. *Environmental Microbiology Reports* **9**: 528-536.

Zobell, C.E. (1938) Studies on the bacterial flora of marine bottom sediments. *Journal of Sedimentary Research* **8**.

ZoBell, C.E., and Anderson, D.Q. (1936) Vertical distribution of bacteria in marine sediments. *AAPG Bulletin* **20**: 258-269.

Appendix

Appendix 1. Deep biodiversity detected by studies carried out in continental subsurface

Subsurface studies	References (see principal text of the thesis)	Phylum	Domain
		Class / Sample	
Lupin Au mine (Canada)	Onsttot et al., 2009	W	Bacteria
Tono uranium mine (Japan)	Murakami et al., 2002; Miyoshi et al., 2005	W	Bacteria
*Sippenauer Moor and Müehlbacher Schwefelquelle (Germany)	Probst et al., 2013, 2014 a, b	B	Bacteria
SURF, South Dakota (EE.UU)	Momperet al., 2017	R+W	Bacteria
The Cedars (EE.UU)	Suzukia et al., 2013	SW	Bacteria
Horonobe area (Japan)	SHIMIZU et al., 2006	W	Bacteria
National Engineering and Environmental Laboratory (EE.UU)	Lehman et al., 2004	R+W	Bacteria
Coalbed, Illinois (EE.UU)	Stra˛poc´, et al., 2008	W	Bacteria
Mt. Simon Sandstone (EE.UU)	Dong et al., 2014ab	W	Bacteria
Hishikari gold mine (Japan)	Takai et al., 2002; Inagaki et al., 2003	W	Bacteria
Samail Ophiolite (Oman)	Rempfert et al., 2017	W	Bacteria
Olkiluoto (Finland)	Bomberg et al., 2014, 2015; Nysoonen et al., 2012	W	Bacteria
Gas storage aquifer (Paris)	Basso *et al.*, 2009; Klouche et al., 2009	W	Bacteria
*Driefontein Consolidated Mine (Sudafrica)	Moser et al., 2005; Gihring et al., 2006; Lau et al., 2014;	W	Bacteria
*Mizunami URL (Japan)	Ino et al., 2016, 2017; Fukuda et al., 2010	W	Bacteria
Chesapeake Bay (EE.UU)	Cockell et al., 2012; Breuker et al., 2011	R	Bacteria
*Outukumpu (Finland)	Itävaara et al., 2011ab; Nyyssönen et al., 2013; Purkamo et al., 2013, 2015	W	Bacteria
Dabie sulu (China)	Zhang et al., 2005; Zhang et al., 2006	R+W	Bacteria

Bacteria: Acidobacteria (Acidobacteriia, Holophagae, Solibacteres); Actinobacteria (Actinobacteria, Coriobacteriia, OPB41 Candidatus, Rubrobacteria, Thermoleophilia); Aquificae (Aquificae); Armatimonadetes (Armatimonadia, Other); Bacteroidetes (Bacteroidetes, Bacteroidia, Chitinophagia, Cytophagia, Flavobacteriia, Saprospiria, Sphingobacteriia); Calditrichaeota (Calditrichae); Candidate Atribacteria; Candidate division FBP; Candidate division GN04; Candidate Phylum BRC1; Candidate phylum NKB19; Candidate phylum SM2F11; Candidate phylum Acetothermia; Candidate Phylum Aminicenantes; Candidate Phylum Atribacteria; Candidate phylum Dependentiae; Candidate phylum Dojkabacteria; Candidate phylum GAL15; Candidate phylum Latescibacteria; Candidate phylum Microgenomates; Candidate phylum MSBL6; Candidate phylum NPL-UPA2; Candidate phylum Omnitrophica; Candidate Phylum Parcubacteria; Candidate phylum Saccharibacteria; Candidate division TA06; Candidate phylum TG1; Candidate Phylum TG3; Candidate phylum WPS-1; Candidate phylum WPS-2; Candidate phylum WS1; Candidate phylum WS2; Candidate phylum WS5; Candidate phylum ZB2; Candidatus Cloacimonetes; Candidatus Latescibacteria; Candidatus Marinimicrobia; Candidatus Poribacteria; Chlamydiae (Chlamydiia); Chlorobi (Chlorobia, Others); Chloroflexi (Anaerolineae, Caldilineae, Chloroflexia, Dehalococcoidia, Ktedonobacteria, Thermomicrobia, Others); Chrysiogenetes (Chrysiogenetes); Cyanobacteria; Deferribacteres (Deferribacteres); Deinococcus-thermus; Dictyoglomia (Dictyoglomia); Elusimicrobia; Fibrobacteres (Fibrobacteria); Firmicutes (Bacilli, Candidate division SASF, Clostridia, Erysipelotrichia, Mollicutes, Negativicutes, SASFG 1, Thermolithobacteria, Tissierellia); Fusobacteria (Fusobacteria); Gemmatimonadetes; Ignavibacteriae; Lentisphaerae; Nitrospirae (Planctomycetia, Others); Planctomycetes; Proteobacteria (Acidithiobacillia, Alfa-proteobacteria, Delta-proteobacteria, Epsilon-proteobacteria, Gamma-proteobacteria, Oligoflexia, Zeta-proteobacteria); Spirochaetes (Spirochaetia, Others); Synergistetes (Synergistetes); Tenericutes (Mollicutes, Others); Thermotogae (Thermotogae); Verrucomicrobia (Verrucomicrobia)

Archaea: Euryarchaeota (Bathyarchaeota; Candidatus Altiarchaeales; Candidatus Korarchaeota; Candidatus Micrarchaeota; Candidatus Parvarchaeota); Crenarchaeota (DSAG/MBG-B; HWCG; MCG; SAGMCG-2; Thermoprotei; TMCG); Euryarchaeota (Archaeoglobi; DHVE-2 group; DHVE-3 group; DHVE-4 group; DHVE-5 group; DSEG; Hadesarchaea; Halobacteria; MBGE; MEG; Methanobacteria; Methanococci; Methanomicrobia; Methanopyri; Thermococci; Thermococcales; Thermoplasmata; TMEG); Korarchaeota; Parvarchaea; Thaumarchaeota; Woesearchaeota

* Studies in which NGS techniques were applied. The microorganisms which showed less hits than the 1% of the maximun hits achived in the study have been ignored

B= biofilm sample

W= water sample

R= rock sample

Appendix 1. Deep biodiversity detected by studies carried out in continental subsurface

Appendix 2. Mineral composition of borehole BH10

	Mineral composition of BH10borehole				
Depth	Minerals	Percentage (%)	Depth	Minerals	Percentage (%)
90 m	Quartz, syn	77	414 m	Quartz/jasper	61,6
	Muscovite	7,7		Dolomite	19,2
	Clinochlore-ferroan	15,4		Mg-calcite	13,7
103.5 m	Muscovite	10,6		Ankerite/siderite	5,5
	Quartz	61,7	415.3 m	Quartz	85
	Jacobsite	17		Dolomite	5
	Pyrite	10,6		Siderite	10
121.8 m	Quartz	88,6	420 m	Quartz	86,2
	Illite	11,4		Clinochlore-ferroan	13,8
130.8 m	Quartz	88,6	426.15 m	Quartz	84
	Illite	11,11		Ca-albite, ordered	2
139.4 m	Quartz	73		Clinochlore-ferroan	14
	Pyrite	8,3	433.32 m	Quartz	71
	Clinoclhore ferroan	18,75		Illite	8,8
206.6 m	Clinoclore	15,25		Clinochlore-ferroan	20
	Pyrite	8,5	450.3 m	Quartz	83,3
	Quartz	76,3		Illite	8,3
228.67 m	Quartz	74,5		Titanomagnetite	8,3
	Pyrite	8,5	468.8 m	Pyrite	10,2
	Clinoclhore ferroan	17,1		Clinochlore-ferroan	15,3
266.3 m	Quartz	67,3		Titanomagnetite	4
	Pyrite	4,8		Quartz	51
	Illite	27,8		Illite	10,2
284 m	Quartz	67,3	477.45 m	quartz	71,4
	Illite	27,8		clinochloro	21,5
	Pyrite	4,8		Illite	7,14
294.65 m	Pyrite	71,4	487.2 m	Quartz	68,8
	Muscovite	28,6		Cookeite-la borian	4,3
304.9 m	Muscovite	7,14		Muscovite	5,4
	Quartz/jaspe	78,5		Illite	21,5
	Clinocholore ferroan	14,3	492.6 m	Quartz	61,15
311.1 m	Pyrite	17		Titanomagnetite	3,18
	Quartz	75,5		Muscovite	10,19
	Jacobsite	3,8		Dolomite	19
	Illite	3,8	496.8 m	Quartz	82
336.5 m	Quartz	81		Pyrite	6,55
	Clinoclhore	18,18		Illite	11,5
352.65 m	Jacobsite	3	519.1 m	Quartz	76,5
	Muscovite	7		Dolomite	11,22
	Quartz	90		Illite	12,24
353.12 m	Quartz	88,8	538.4 m	Jaspe	66
	Titanomagnetite	7,4		Cubanite	5,8
	Muscovite	3,7		Pyrite	4,4
355.7 m	Quartz	92,4		Illite	23,5
	Jacobsite	3,36	544 m	Quartz	66
	Muscovite	4,2		Illite	23,5
392.9 m	Quartz	83,3		Pyrite	4,4
	Albite, ordered	16,6		Cubanite	5,8
411.9 m	Hematite	10,4	568.6 m	ankerite	18,3
	Clinochlore ferroan	12,5		Pyrite	1,3
	Quartz/jasper	62,5		Quartz	79,3
	Albite	14,6		muscovite	1,3
413.3 m	Clinochlore ferroan	8,3	607.6 m	Quartz	62
	Quartz/jasper	83,3		Calcite	31
	Vermiculite	8,3		Dolomite	7
			612.94 m	Chamosite	12,5
				Quartz	76,4
				Illite	11